# University of Alberta


Development of an Enantioselective Two-Dimensional Liquid Chromatography-Atmospheric Pressure Photoionization-Tandem Mass Spectrometry Method for the Analysis of Methylsulfonyl Polychlorinated Biphenyls in Tissue Extracts


by


Victoria Irene Cooper


A thesis submitted to the Faculty of Graduate Studies and Research
in partial fulfillment of the requirements for the degree of


Master of Science


Department of Chemistry

# Abstract

An enantioselective heart-cut two-dimensional liquid chromatography-atmospheric pressure photoionization-tandem mass spectrometry method was developed for the analysis of 25 methylsulfonyl polychlorinated biphenyl metabolites in tissue extracts. Enantioseparation was achieved for 9 out of the 10 chiral analytes in less than 91 minutes, improving upon previous gas chromatography-based methods. Use of a pyrenyl-ethyl silica column in the first dimension enabled separation of all but two pairs of isobaric analytes. Limits of detection of 0.01 to 1.73 ng on-column were achieved. The precision and accuracy were within acceptable limits, but poor sensitivity was achieved for several *meta*-methylsulfonyl-substituted congeners. Despite this limitation, the method was successfully applied to the analysis of Greenland sledge dog (*Canis familiaris*) plasma and adipose tissue extracts. Concentration and enantiomer fraction data are presented. None of the target analytes were detected in Norwegian glaucous gull (*Larus hyperboreus*) plasma extracts.

# Acknowledgements

First and foremost, I would like to express my gratitude to my supervisor, Dr. Charles S. Wong, for his support throughout my graduate program. Thank you for fostering my development as a researcher and for the opportunity to work on a challenging project that has helped me develop many useful and marketable skills. I am particularly grateful for your patience, understanding, advice, and encouragement over the past year. Writing a thesis while working full time is a challenge that you are all too familiar with, and I really appreciate your help in getting me through it.

I am extremely grateful to my family, June, Stephen, and Stephanie Cooper, for their tremendous amount of love, support, and encouragement throughout my graduate studies. Mom and Dad, thank you for always being there when I needed words of wisdom or reassurance and for taking such good care of me while I was writing this summer. I feel truly blessed to have such wonderful, devoted parents. Steph, you are not just my sister, you are a good friend, and I am really thankful for your support and encouragement through this, as well.

I would like to extend a big thank you to Ryan Arnold for his love, support, and patience through everything. Thank you for helping me to see the lighter side and to stop worrying so much. Thank you for comedic relief and for doing your best to be accommodating while I was writing and working this year. I am very appreciative of your understanding, humour, and realism, and I cannot imagine my life without you.

My thanks go out to the entire Arnold family, Maria, Peter, and Laura, for their support and encouragement throughout my graduate program. A special thanks to Peter for countless rides between Calgary and Edmonton over the past few years. It has been so nice getting to know you better, and I really appreciate your help.

I am so fortunate to have many wonderful friends who helped me along the way to completing my Masters. I am very grateful to my good friend, Correne DeCarlo, for her advice, encouragement, and moral support. I am also very thankful for the support of my oldest friend, Sarah Hawkes. Within the Chemistry department, I would like to thank Azeret Zuniga, Avalyn Lewis, and Stephen Kibbee for making those first few months of classes much more enjoyable. I am also grateful to Hayley Wan and Jennifer Landry for their support and advice through some difficult times. Thank you to the members of my soccer and softballs teams at the University of Alberta and the lovely ladies of Cassia United in Calgary for the fun, friendship, and exercise that has helped keep me sane. Thank you to all of my other friends in the department; you know who you are. You have all enriched my life and contributed to my success as a graduate student.

I am enormously grateful to the members of my research group, from whom I learned so much and without whose assistance I could not have gotten through in one piece. Thank you Brian Asher, Derek Bleackley, Sherri MacLeod, Lisa Nikolai, Matthew Ross, Rainie Sharpe and Nicholas Warner for your various contributions. I am particularly grateful to Lisa and Evelyn, who continued to be a

valuable resource for technical advice on mass spectrometry and chiral chromatography upon graduation, and to Matt for data analysis tips that saved me an incredible amount of time. A big thank you to our summer student, Kathy Yackulic, for laboratory assistance and to Matt and Brian and the members of the Winnipeg-based Wong group for assistance with thesis editing and defence preparation. Finally, I cannot begin to express the extent of my gratitude to Sherri, Matt, and Brian, who formed the core of the group at the University of Alberta for the majority of my graduate program. I definitely could not have gotten through without your support, assistance, encouragement, and friendship. Not only have you challenged my knowledge and ideas to help me become a better scientist, you have instilled in me a re-invigorated passion for environmental issues and a new interest in politics. You have made me a more civically responsible, globally aware, and environmentally conscious person, and I will always be grateful for the positive influence you have had on me and the way I live.

I would like to thank the staff of the Alberta Centre for Toxicology for their cooperation while I completed my academic program this year. I am particularly grateful to Lorinda Butlin for her support, flexibility, and understanding. I would also like to extend profound thanks to Amy MacDonald for tea and sympathy, advice, encouragement, and, of course, for help editing my thesis. Finally, I would like to thank my new friend, Erin Johnson, who has been particularly supportive during this time.

There are a number of colleagues, collaborators and staff members that I must thank for their technical and administrative assistance. I am very grateful to

# Table of Contents

# List of Figures

# List of Tables

# List of Abbreviations and Symbols

| | |
|---|---|
| *AF2* | excitation energy |
| **amu** | atomic mass unit |
| **ANOVA** | analysis of variance |
| **APCI** | atmospheric pressure chemical ionization |
| **APPI** | atmospheric pressure photoionization |
| **BAF** | bioaccumulation factor |
| **bp** | percent base peak |
| **C18** | octadecylsilyl silica |
| *C2B* | collar 2 barrier |
| **CAD** | collisionally activated dissociation |
| *CAD* | collisionally activated dissociation gas pressure |
| **CCSP** | Clara cell secretory protein |
| *CE* | collision energy |
| *CEP* | collision cell entrance potential |
| *CES* | collision energy spread |
| **CID MIKE** | collision induced dissociation mass-analyzed ion kinetic energy |
| **CON** | control |
| **cps** | counts per second |
| *CUR* | curtain gas pressure |
| *CXP* | collision cell exit potential |
| **CYP** | cytochrome P450 |
| **DCM** | dichloromethane |

| | |
|---|---|
| *DP* | declustering potential |
| E1 | first eluting enantiomer |
| E2 | second eluting enantiomer |
| ECD | electron capture detection |
| ECNI | electron capture negative ionization |
| EF | enantiomer fraction |
| EI | electron impact ionization |
| *EP* | entrance potential |
| EPI | enhanced product ion |
| ER | enantiomer ratio |
| EROD | 7-ethoxyresorufin *O*-dealkylase |
| ESI | electrospray ionization |
| EXP | exposed |
| F1 | first generation offspring |
| FABP | fatty acid binding protein |
| FIA | flow injection analysis |
| GC | gas chromatography |
| GPC | gel permeation chromatography |
| GR | glucocorticoid receptor |
| GS | glutathionyl group |
| *GS1* | nebulizer gas |
| *GS2* | auxiliary gas |
| GS-PCB | glutathionyl polychlorinated biphenyl |
| HDL | high-density lipoprotein |
| HPLC | high performance liquid chromatography |

| | |
|---|---|
| **i.d.** | internal diameter |
| **IPA** | isopropanol |
| *IS* | ion spray voltage |
| **IS** | internal standard |
| **IT** | ion trap |
| **IUPAC** | International Union of Pure and Applied Chemistry |
| **LC** | liquid chromatography |
| **LC-LC** | heart-cut two-dimensional liquid chromatography |
| **LDL** | low-density lipoprotein |
| *LG* | lamp gas |
| **LIT** | linear ion trap |
| **LOD** | limit of detection |
| **LOEC** | lowest observed effect concentration |
| **log K$_{ow}$** | octanol-water partition coefficient |
| **LOQ** | limit of quantitation |
| **LPDP** | lipoprotein depleted |
| *m/z* | mass-to-charge ratio |
| **MAP** | mercapturic acid pathway |
| **MeOH** | methanol |
| **MeS-CB** | methylthio polychlorinated biphenyl |
| **MeSO$_2$-CB** | methylsulfonyl polychlorinated biphenyl |
| **MLK** | pre-weaning |
| **MLOD** | method limit of detection |
| **MLOQ** | method limit of quantitation |
| **MRM** | multiple reaction monitoring |

| | |
|---|---|
| **MS/MS** | tandem mass spectrometry |
| **MS3** | MS/MS/MS |
| **n** | sample number |
| **n-hexane** | normal hexane, linear hexane |
| **NIST** | National Institute of Standards and Technology |
| **OC** | organic contaminant |
| **OC** | organic contaminant |
| **OH-PCB** | hydroxylated polychlorinated biphenyl |
| **P** | parental generation |
| **PAH** | polyaromatic hydrocarbon |
| **PCB** | polychlorinated biphenyl |
| **PCDD** | polychlorinated dibenzo-$p$-dioxin |
| **PCDF** | polychlorinated dibenzo-$p$-furan |
| **PEEK** | polyether ether ketone |
| **PID** | photoionization detection |
| **PROD** | 7-pentoxyresorufin $O$-dealkylase |
| **PTFE** | polytetrafluoroethylene |
| **PYE** | 1-(2-pyreneyl)ethyldimethylsilyl silica |
| **Q3** | third quadrupole |
| **$r^2$** | correlation coefficient |
| **RRF** | relative response factor |
| **RSD** | relative standard deviation |
| **S/N** | signal-to-noise ratio |
| **SDF** | sledge dog fat |

| | |
|---|---|
| **SDS-PAGE** | sodium dodecyl sulphate-polyacrylamide gel electrophoresis |
| **SRM** | standard reference material |
| **T** | transition |
| ***TEM*** | heated nebulizer temperature |
| ***tert*** | tertiary |
| **THDMS-β-CD** | heptakis(2,3-di-*O*-methyl-*tert*-hexyldimethylsilyl)-β-cyclodextrin |
| **TR** | transition ratio |
| **TSH** | thyroid stimulating hormone |
| **UGT** | uridine diphosphate-glucuronosyltransferase |
| **UV** | ultra-violet |
| **UV-CD** | electronic circular dichroism |
| **v/v** | volume per volume |
| **VCD** | vibrational circular dichroism |
| **VLDL** | very-low-density lipoprotein |
| **w/w** | weight per weight |
| **α** | selectivity factor, separation factor |
| **$\Delta^{\ddagger}G$** | free energy of activation |
| **σ** | Hammett rho constant |

# 1      Methyl sulfone PCBs - Environmental occurrence and analytical strategies

## 1.1      Introduction

Polychlorinated biphenyls (PCBs) are persistent organic pollutants of significant concern. They were used throughout the mid 1900s as coolants, lubricants, hydraulic fluids, and plasticizers. Their thermal and chemical stability led to their extensive application as dielectric fluids in capacitors and other electrical equipment. It is estimated that approximately 635 million kg of PCBs were produced in the United States (US) between 1930 and 1975 and that 1.7 million kg of PCB wastes were released into the environment in the US in the year 1998 alone (Agency for Toxic Substances and Disease Registry 2000). Concern over the use of polychlorinated biphenyls began in the 1960s when reports of their toxic effects and of their occurrence in animal and human tissues in several different countries began to surface (*New Scientist* 1966). Due to their semi-volatile nature, PCBs have the ability to undergo long-range atmospheric transport to remote areas of the globe, including the Arctic and Antarctic. This phenomenon is known as global distillation, sometimes referred to as the "grasshopper effect", as it results from successive volatilization and deposition processes (Wania and Mackay 1993). These compounds are now ubiquitous contaminants that can be detected in the air, water and soil, and in the tissues of humans and many other animal species around the globe.

Initially thought to be innocuous due to their low acute toxicity, PCBs were later discovered to produce many serious toxicological effects upon chronic

exposure, ranging from the dermatological condition chloracne, characterized by inflammation and accumulation of keratin in the hair follicles in animals and humans, to immunotoxic effects such as decreased monocyte counts and increased susceptibility to infectious diseases in humans, as well as decreased antigen responses in animals (Agency for Toxic Substances and Disease Registry 2000). Polychlorinated biphenyls also lead to a range of hepatotoxic effects, including liver enzyme, lipid and cholesterol level changes in humans and hepatomegaly, cellular necrosis and liver cancer in animals (Agency for Toxic Substances and Disease Registry 2000). To make the situation worse, PCBs exhibit a high level of persistence in the environment. They are not readily susceptible to hydrolysis or photolysis, and there are no known organisms that can fully biodegrade them. In addition, PCBs are capable of bioaccumulating up food chains such that the top predators acquire a larger body burden of contaminants than the lower organisms. This poses a concern for the health of higher trophic level organisms, including humans. The discovery of the persistent, toxic and bioaccumulative nature of PCBs throughout the 1960s, in addition to their widespread detection in the environment, led to a ban on their production in North America in the 1970s.

Some higher order organisms, like mammals and birds, have the ability to metabolize PCBs to varying degrees. The major metabolites formed are hydroxyl and methylsulfonyl metabolites, the latter of which will be the focus of the current work. Methyl sulfone PCBs ($MeSO_2$-CBs) were first detected in the blubber of grey seals from the Baltic Sea in 1976 (Jensen and Jansson 1976). Subsequent

studies have determined that these metabolites are only slightly less hydrophobic than their parent compounds and that they also possess the ability to bioaccumulate. They are persistent metabolites that produce some unique toxicological effects compared to their parent compounds. For example, they have the ability to inhibit the cytochrome P450 11B1-dependent synthesis of corticosterone in mouse adrenocortical Y1 cells, whereas parent PCBs do not (Johansson *et al.* 1998a). Many different animal species and tissues have now been tested for $MeSO_2$-CBs, including several types of fish, birds, marine and terrestrial mammals, and humans (Letcher *et al.* 2000). The highest sum concentration of $MeSO_2$-CBs detected to date was 110 μg/g lipid weight in the blubber of a female Baltic grey seal with severe disease symptoms in 1992 (Haraguchi *et al.* 1992).

Like their parent compounds, certain $MeSO_2$-CBs have the potential to be chiral under particular sets of conditions. A chiral molecule exists in two different non-superimposable mirror image forms, known as enantiomers or antipodes. Differences in toxicity between enantiomers can occur because many biological molecules, ranging in size from amino acids to large proteins, are chiral (Davankov 2006, Voet and Voet 2004). In one study of the differential effects of PCB enantiomers on the induction of drug-metabolizing enzymes in rats, it was found that the (+)-enantiomer of PCB 139 was a more potent inducer of aminopyrine *N*-demethylase, aldrin epoxidase and cytochrome P450 enzymes (CYPs) than the (-)-enantiomer or the racemic mixture (Püttmann *et al.* 1989). Another more famous example of this is the drug thalidomide, which was

prescribed as a sleep aid throughout the late 1950s and early 1960s and led to congenital abnormalities in babies born from exposed mothers (Theoret 1962). It was later discovered that the pharmacologically active enantiomer produced the desired effect of somnolence, but, unfortunately, the other enantiomer was teratogenic (Heger *et al.* 1994, Höglund *et al.* 1998). This antipode led to stunted limb growth in the exposed foetuses, resulting in characteristic "flipper-like" appendages (Lenz 1962). While there have not been any single enantiomer exposure studies for MeSO$_2$-CBs to date, these compounds have been detected in high enantiomer excesses in a variety of organisms, including humans (Ellerichmann *et al.* 1998). As a result, the difference in toxicity between enantiomers is of great interest.

## 1.2     General properties of MeSO$_2$-CBs

### *1.2.1   Structure and nomenclature*

Methyl sulfone PCB metabolites encompass the core structure of a polychlorinated biphenyl with the addition of a methylsulfonyl group, –SO$_2$CH$_3$. A sample structure is given in **Figure 1.1** below.
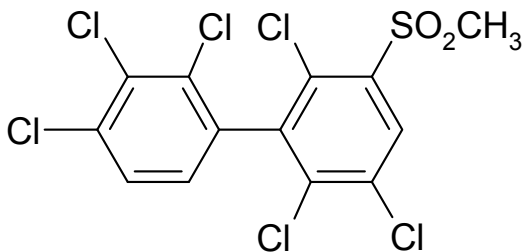


**Figure 1.1: Structure of 5′-MeSO$_2$-CB132**

The condensed nomenclature for these compounds is based upon the numbering system developed for PCBs (Ballschmiter and Zell 1980). The congener is assigned the number of the parent PCB with the same chlorine substitution pattern, and a prefix inserted with a number to indicate the position of the methyl sulfone substituent, e.g. 4-MeSO$_2$-CB91. The nomenclature for these compounds was recently revised, as the previous IUPAC naming system resulted in some ambiguities (Maervoet *et al.* 2004). The latest nomenclature removes this uncertainty by giving priority to the parent PCB structure and by using a prime symbol after the number assigned to the methyl sulfone group to indicate if it is present on the lower priority ring (less chlorinated and/or higher numbers assigned to the chlorine substituents). A list of the complete and abbreviated names of all the environmentally relevant (see **Section 1.4.2** for further discussion) congeners is provided in **Table 1.1** on the following page.

### 1.2.2   Chirality

Methyl sulfone PCB metabolites, like their parent compounds, display a particular type of chirality known as atropisomerism, which arises from hindered rotation about a single bond. In the case of substituted biphenyls, the molecule must also be asymmetrically substituted about the axis of the biphenyl bond in order to be chiral. Since the methylsulfonyl group introduces an element of asymmetry, there are several theoretically possible congeners where the parent PCB is not chiral, but the MeSO$_2$-metabolite is. In total, there are 78 theoretically possible chiral PCBs and 456 chiral MeSO$_2$-CBs (Nezel *et al.* 1997).

**<u>Table 1.1</u>: Nomenclature and abbreviations for environmentally relevant MeSO$_2$-CB congeners**

*Congeners in bold are chiral and stable at environmentally relevant temperatures; congeners in italics are not target analytes in this study.*
*[a]Used throughout text; [b]Used in figures and tables.*

| Full Name | Abbreviation 1[a] | Abbreviation 2[b] |
|---|---|---|
| *3-MeSO$_2$-2,4',5-trichlorobiphenyl* | *3-MeSO$_2$-CB31* | *3-31* |
| *4-MeSO$_2$-2,4',5-trichlorobiphenyl* | *4-MeSO$_2$-CB31* | *4-31* |
| 3'-MeSO$_2$-2,2',4,5'-tetrachlorobiphenyl | 3'-MeSO$_2$-CB49 | 3'-49 |
| 4'-MeSO$_2$-2,2',4,5'-tetrachlorobiphenyl | 4'-MeSO$_2$-CB49 | 4'-49 |
| 3-MeSO$_2$-2,2',5,5'-tetrachlorobiphenyl | 3-MeSO$_2$-CB52 | 3-52 |
| 4-MeSO$_2$-2,2',5,5'-tetrachlorobiphenyl | 4-MeSO$_2$-CB52 | 4-52 |
| *5-MeSO$_2$-2,3,4',6-tetrachlorobiphenyl* | *5-MeSO$_2$-CB64* | *5-64* |
| 4-MeSO$_2$-2,3,4',6-tetrachlorobiphenyl | 4-MeSO$_2$-CB64 | 4-64 |
| 3-MeSO$_2$-2,3',4',5-tetrachlorobiphenyl | 3-MeSO$_2$-CB70 | 3-70 |
| 4-MeSO$_2$-2,3',4',5-tetrachlorobiphenyl | 4-MeSO$_2$-CB70 | 4-70 |
| 3'-MeSO$_2$-2,2',3,4,5'-pentachlorobiphenyl | 3'-MeSO$_2$-CB87 | 3'-87 |
| 4'-MeSO$_2$-2,2',3,4,5'-pentachlorobiphenyl | 3'-MeSO$_2$-CB87 | 3'-87 |
| **5-MeSO$_2$-2,2',3,4,5'-pentachlorobiphenyl** | **5-MeSO$_2$-CB91** | **5-91** |
| **4-MeSO$_2$-2,2',3,4,5'-pentachlorobiphenyl** | **4-MeSO$_2$-CB91** | **4-91** |
| **3'-MeSO$_2$-2,2',3,5',6-pentachlorobiphenyl** | **3'-MeSO$_2$-CB95** | **3'-95** |
| **4'-MeSO$_2$-2,2',3,5',6-pentachlorobiphenyl** | **4'-MeSO$_2$-CB95** | **4'-95** |
| 3'-MeSO$_2$-2,2',4,5,5'-pentachlorobiphenyl | 3'-MeSO$_2$-CB101 | 3'-101 |
| 5-MeSO$_2$-2,3,3',4',6-pentachlorobiphenyl | 5-MeSO$_2$-CB110 | 5-110 |
| 4-MeSO$_2$-2,3,3',4',6-pentachlorobiphenyl | 4-MeSO$_2$-CB110 | 4-110 |
| **5'-MeSO$_2$-2,2',3,3',4,6'-hexachlorobiphenyl** | **5'-MeSO$_2$-CB132** | **5'-132** |
| **4'-MeSO$_2$-2,2',3,3',4,6'-hexachlorobiphenyl** | **4'-MeSO$_2$-CB132** | **4'-132** |
| 3'-MeSO$_2$-2,2',3,4,5,5'-hexachlorobiphenyl | 3'-MeSO$_2$-CB141 | 3'-141 |
| 4'-MeSO$_2$-2,2',3,4,5,5'-hexachlorobiphneyl | 4'-MeSO$_2$-CB141 | 4'-141 |
| **5-MeSO$_2$-2,2',3,4',5',6-hexachlorobiphenyl** | **5-MeSO$_2$-CB149** | **5-149** |
| **4-MeSO$_2$-2,2',3,4',5',6-heptachlorobiphenyl** | **4-MeSO$_2$-CB149** | **4-149** |
| **5'-MeSO$_2$-2,2',3,3',4,5,6'-heptachlorobiphenyl** | **5'-MeSO$_2$-CB174** | **5'-174** |
| **4'-MeSO$_2$-2,2',3,3',4,5,6'-heptachlorobiphenyl** | **4'-MeSO$_2$-CB174** | **4'-174** |

In practicality, atropisomers can be quite stereolabile compounds. Since their chirality is determined by hindered rotation about a single bond, if enough energy is present within the surrounding environment, the free energy barrier to rotation can be surmounted and interconversion between enantiomers can occur. The average rotational barrier for atropisomeric PCBs at room temperature has been estimated by quantum chemical methods to be in the range of 105 to 240 kJ/mol, depending on the chlorine substitution pattern (Kaiser 1974). The rotational barriers have also been measured experimentally using enantioselective gas chromatography with several runs performed at different final temperatures (Krupčík *et al.* 1995) or with an off-column enantiomerization step (Harju and Haglund 1999), and the experimental values agree well with those found using quantum theory. Rotational barriers associated with selected *ortho*-MeSO$_2$-CB congeners with one to three *ortho*-chlorines have been estimated by quantum calculations to be in the range of 86.2 to 168.1 kJ/mol, higher than the corresponding PCB congeners at 67.0 to 155.1 kJ/mol (Nezel *et al.* 1997). However, as discussed more thoroughly in **Section 1.4.2**, the *ortho*-MeSO$_2$-substituted congeners are not of environmental interest. Nonetheless, it can be concluded that the rotational barriers for the *meta*- and *para*-substituted congeners, which are of environmental concern, are expected to be in a similar range to their parent PCBs. A more detailed discussion of atropisomeric rotational barriers can be found at the end of **Section 2.2.3.3**.

As a general rule, in order for asymmetrically substituted MeSO$_2$-CBs or PCBs to have sufficiently high rotational energy barriers to be chiral at

physiological temperatures, they must possess three or four *ortho*-chlorines. As a result, there are only 19 PCB congeners and 10 MeSO$_2$-CB congeners, 5 *meta*- and *para*-MeSO$_2$-substituted pairs, that are considered chiral under environmentally relevant conditions. There are less chiral MeSO$_2$-CBs of environmental interest than chiral PCBs because only certain chlorine substitution patterns are recognized by specific enzymes involved in the biotransformation pathway leading to MeSO$_2$-CBs (see **Section 1.4.2** for further detail). All of the chiral *meta*- and *para*-MeSO$_2$-CBs of environmental interest are derived from chiral parent PCBs. The chiral MeSO$_2$-CB congeners are displayed in bold in **Table 1.1**.

The configurations of the enantiomers of selected chiral MeSO$_2$-CBs have been determined previously using vibrational circular dichroism (VCD) and electronic circular dichroism (UV-CD). These two techniques irradiate the sample with circularly polarized light in the infrared and ultra violet ranges of the spectrum, respectively, and can be used to determine the relative configurations of the enantiomers if pure enantiomer formulations are available. Absolute configurations can also be determined, but this generally requires the aid of complex calculations. These techniques have been applied to the enantiomers of 4-MeSO$_2$-CB149 (Pham-Tuan *et al.* 2004, 2005) and 5-MeSO$_2$-CB149 (Döbler *et al.* 2002, Pham-Tuan *et al.* 2004, 2005), as well as 5′-MeSO$_2$-CB132, 4′-MeSO$_2$-CB132, and 4′-MeSO$_2$-CB174 (Döbler *et al.* 2002). In all of these studies, the enantiomers were separated initially using enantioselective liquid chromatography

with a Nucleodex β-PM column. The absolute structures for the (*R*)-enantiomers

of 5-MeSO$_2$-CB149 and 4-MeSO$_2$-CB149 are presented in **Figure 1.2** below.



5′-MeSO$_2$-CB132                4′-MeSO$_2$-CB132
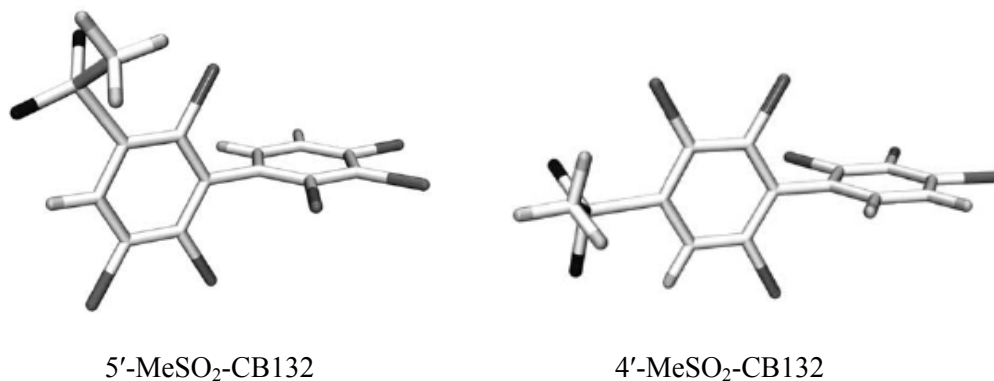
**Figure 1.2: Absolute configurations of single enantiomers of 5′-MeSO$_2$-CB132 and 4′-MeSO$_2$-CB132[1]**

### *1.2.3    Physico-chemical properties*

Methyl sulfone PCBs are solids with melting points in excess of 130°C

under standard conditions (Letcher *et al.* 2000). They are sufficiently volatile to

be easily compatible with gas chromatographic techniques without the need for

derivatization. They are extremely stable and do not break down under strong acid

or strong base conditions. However, they are Lewis bases and can be protonated

under extremely acidic conditions, a characteristic that can be exploited for

sample preparation purposes (Letcher *et al.* 2000). Upon addition of concentrated

sulphuric acid to a mixture of PCBs and MeSO$_2$-CBs in a non-polar solvent like

*n*-hexane, the MeSO$_2$-CBs will be ionized and partition into the acid phase,

whereas the parent PCBs will remain in the organic phase. For the purposes of

---

[1] Reprinted from *Journal of Molecular Structure (Theochem)*, Vol. 586, Döbler, J., Peters, N., Larsson, C., Bergman, Å., Geidel, E., and Hühnerfuss, H., "The absolute structures of separated PCB-methylsulfone enantiomers determined by vibrational circular dichroism and quantum chemical calculations", p. 159-166, Copyright 2002, with permission from Elsevier.

liquid chromatographic separations, methyl sulfone PCBs will not ionize in the

pH range compatible with most liquid chromatography (LC) columns, so

changing the pH of the eluent will have no effect on retention. Due to their

aromatic nature, $MeSO_2$-CBs absorb strongly in the UV region, making them

amenable to UV detection with liquid chromatography. Because of their increased

polarity compared to PCBs, $MeSO_2$-CBs tend to be more soluble in chlorinated

organic solvents than in aliphatic solvents. However, despite their additional polar

functionality, they are only slightly less hydrophobic than their parent

compounds, having log $K_{ow}$ (octanol-water partition coefficient) values in the

range of 4.5 to 6 for congeners with 3 to 6 chlorines (Letcher *et al.* 2000). As a

result, they are considered bioaccumulative contaminants.

## 1.3 Toxicokinetics of $MeSO_2$-CBs

### 1.3.1 *Absorption and disposition*

There are two main sources of $MeSO_2$-CBs in organisms:

biotransformation of PCBs and absorption from the diet. It is difficult to apportion

the body burden of $MeSO_2$-CBs between these two sources accurately, but

estimates can be made using bioaccumulation factors (BAF), usually calculated as

the ratio of the contaminant concentration in the predator to that in the prey, and

by comparing the congener distribution in the organism to that in its diet. A study

of the polar bear food chain in the Canadian Arctic calculated an apparent

bioaccumulation factor of 27.8 from seal to polar bear using the sum $MeSO_2$-CB

concentrations in the adipose tissues of these animals (Letcher *et al.* 1998). Since

this value is greater than one, it is evident that some biotransformation of PCBs must be occurring in the polar bear, hence the label "apparent" BAF. When individual congener concentrations were used, an increase in BAF values was observed with increasing congener chlorination. Upon comparing the congener pattern in polar bear to that in seal, many similarities were revealed. The authors concluded that the congeners 5′-MeSO$_2$-CB132 and 4′-MeSO$_2$-CB132 were completely bioaccumulated in polar bear from seal. It was therefore possible to calculate true BAFs for these congeners of approximately 0.5 and 0.6, respectively. Fifteen other congeners were determined to arise mostly from bioaccumulation and seven others partially from bioaccumulation and partially from PCB biotransformation in polar bear.

Regardless of the source of the methyl sulfone PCBs, dietary absorption or metabolic formation, selective retention occurs in the lungs, liver and adipose tissues, and to a lesser extent in other organs, such as the kidneys. However, the relative accumulation between these tissues varies by congener and by organism, and some structure-activity relationships have been uncovered. For example, it has been found that the retention of *meta*-MeSO$_2$-CBs in rat liver depends largely on the number of *ortho*-chlorines, not on total chlorination (Haraguchi *et al.* 1999). Congeners with more *ortho*-chlorines on the non-MeSO$_2$-substituted ring are more strongly retained, whereas those with more *ortho*-chlorines on the MeSO$_2$-substituted ring are less retained. In mouse kidney, metabolites with larger substituents in the *para*-positions are the most efficiently accumulated, so bis(MeSO$_2$)-metabolites are strongly retained, metabolites with a *para*-MeSO$_2$

11

group and a *para*-chlorine are less retained, and those with a *para*-MeSO$_2$ group and a hydrogen in the other *para*-position are only slightly retained. Highly selective accumulation of either the *meta*- or the *para*-isomer has been observed in many organisms with variations in selectivity between tissues, and this will be discussed further in **Section 1.4.4**. There is also some evidence to suggest that the tissue distribution pattern may be dose-dependent. In mice administered with a low dose of 4,4′-bis(MeSO$_2$)-CB52, the majority of accumulation occurred in the lungs and kidneys (Brandt *et al.* 1985). However, upon high dose administration, the highest concentrations were generally found in the liver and adipose tissue. The authors therefore proposed that the retention mechanisms in the lungs and kidneys are saturable, whereas those in the liver and adipose tissue are not.

In humans, the highest total concentration of MeSO$_2$-CBs is generally found in the liver, followed by the lungs, adipose tissue, and brain (Chu *et al.* 2003b, Covaci *et al.* 2003). The majority of the MeSO$_2$-CBs in human blood plasma are present in the lipoprotein depleted (LPDP) fraction, followed by 15% in both the high-density lipoprotein (HDL) and low-density lipoprotein (LDL) fractions, and 8% in the very-low-density lipoprotein (VLDL) fraction (Norén *et al.* 1999). Of the lipoprotein fractions, it was noted that the congeners 4-MeSO$_2$-CB52 and 4-MeSO$_2$-CB70 accumulated more in the VLDL fraction and the higher chlorinated congeners more in the HDL fraction.

Differences in the tissue distribution of MeSO$_2$-CBs have been observed between rats, mice, hamsters and guinea pigs dosed with 11 mg/kg of PCB 101 or 19 mg/kg of PCB 132 (Haraguchi *et al.* 2005a). In rats and mice, the highest sum

concentration of MeSO$_2$-CBs was detected in the adipose tissue at 1.9 µg/g wet weight, followed by approximately one quarter and one tenth of this level in the lungs and liver, respectively. The concentration of the MeSO$_2$-CB101 metabolites exceeded the concentration of the parent compound remaining in the lungs of rats and mice by factors of 2.4 and 3.2, respectively. Although hamsters produced much lower levels of these metabolites overall, the highest concentration was still observed in the adipose tissue at 0.06 µg/g wet weight, six times higher than that found in the liver. However, much less accumulation was observed in the lungs of hamsters compared to rats and mice, with a total concentration approximately one decade lower in the lung and serum than in the adipose tissue. In guinea pigs, the majority of MeSO$_2$-CB accumulation also occurred in the adipose tissue but with little retention in any other tissues. The sum concentration of MeSO$_2$-CBs in the liver, lung and serum of guinea pigs were all one order of magnitude lower than in the adipose tissue at 0.62 µg/g wet weight. Although the absolute concentration of MeSO$_2$-CBs was low in guinea pig liver at 0.06 µg/g wet weight, the concentration of the MeSO$_2$-CB132 isomers exceeded that of the remaining parent compound by a factor of 1.8.

Investigations into the occurrence of MeSO$_2$-CBs in a variety of species have also been informative as to the tissue distribution of these contaminants. For example, in grey seals (*Halichoerus grypus*) from the Baltic Sea, significantly higher concentrations of MeSO$_2$-CBs were detected in liver compared to lungs and blubber (Larsson *et al.* 2004). The sum MeSO$_2$-CB concentration was three to five times higher in the liver of Swedish harbour porpoises (*Phocoena phocoena*)

compared to the blubber and nuchal fat, and the concentration in muscle tissue was slightly lower than that found in the liver (Karlson *et al.* 2000). The penta-chlorinated congeners were reported to be the most abundant in the livers of grey seals, ringed seals (*Phoca hispida botnica*) and harbour seals (*Phoca vitulina vitulina*) (Haraguchi *et al.* 1992). In polar bears from East Greenland, the highest concentrations were detected in the adipose tissue and the liver, with relatively low and very low concentrations found in the blood and brain, respectively (Gebbink *et al.* 2008a, Gebbink *et al.* 2008b). The sum $MeSO_2$-CB concentrations in adipose tissue and blood have also been compared in Canadian polar bears (Sandala *et al.* 2004). It was found that the adipose tissue contained a two decade higher sum concentration than whole blood when wet weight was used, but a two fold lower concentration when lipid weight was used. The sum $MeSO_2$-CB to sum PCB ratio was an order of magnitude higher in whole blood compared to adipose tissue in this study. The concentrations and congener patterns in polar bear tissues will be discussed in further detail in **Section 2.2.6**.

The time course of $MeSO_2$-CB disposition has been examined in a rat exposure study administering a single 25 mg/kg dose of Clophen A50, a German PCB mixture, and monitoring the tissue concentrations over a period of 8 weeks (Larsson *et al.* 2002). The liver was observed to have the highest concentration of $MeSO_2$-CBs in the first week at approximately 230 ng/g lipid weight. The concentration in this organ decreased over the remainder of the study period but still contained the highest concentration of the tissues examined at the end of the study. The $MeSO_2$-CB concentrations in the adipose and lung tissues increased

over the first two weeks of the study then decreased over time. The gradual

increase in concentration was attributed to their slow formation via the

mercapturic acid pathway in the liver prior to transfer to these organs. At the end

of the study, the lung possessed a sum $MeSO_2$-CB concentration slightly lower

than that in the liver at approximately 25 ng/g lipid weight, while that in the

adipose tissue was approximately one fourth of the liver concentration. Selective

retention in the lungs was attributed to binding to the protein uteroglobin, which

has been reported previously and will be discussed further in the following section

(Larsen *et al.* 1998, Lund *et al.* 1984). In another rat exposure study that was

carried out over a time period of 42 days, the animals were treated with a single

dose of PCBs 101 and 149 at 342 μmol/kg each. The concentrations of the *meta*-

and *para*-$MeSO_2$-substituted metabolites of the parent congeners in the liver,

kidney, and adipose tissue all reached a maximum at day 4 or 8 at approximately

0.1 to 6 nmol/g wet weight and declined slowly thereafter (Haraguchi *et al.* 1999).

The highest concentrations of the *meta*- and *para*-$MeSO_2$ metabolites of PCB 101

detected at the end of the study were in the adipose tissue at 1.12 and 1.32 nmol/g

wet weight. Both of these studies presented evidence that the disposition of

$MeSO_2$-CBs is regioselective, and this will be discussed further in **Section 1.4.4**.

*1.3.1.1 Protein binding*

    Protein binding is suspected to play an important role in the tissue

selective accumulation of $MeSO_2$-CBs. An extensive mammalian protein binding

study has been carried out in male rats, which were dosed with ^{14}C labelled 5-

$MeSO_2$-CB149 (Larsen *et al.* 1998). The proteins were isolated using sodium

dodecyl sulphate polyacrylamide gel electrophoresis (SDS-PAGE) and the percentage of the dose bound to proteins in selected tissues was determined by liquid scintillation counting. It was found that 2.6, 1.1 and 0.2% of the dose accumulated in the liver, lungs and kidneys, respectively. Of the methyl sulfone metabolite detected in the liver, only 1% was unbound to protein. Approximately 0.26% was bound to soluble proteins, including fatty acid binding proteins (FABPs), and the remainder to cellular components. Non-covalent binding of mono- and bis-$MeSO_2$-CBs to FABPs in rat liver, and in chicken liver and intestinal mucosa, respectively, was also observed and characterized by SDS-PAGE and immunoblot assay in two previous studies by these authors (Larsen *et al.* 1991, Larsen *et al.* 1992). In the present study, approximately 0.01% of the dose was detected bound to FABPs in the kidneys, and a 0.20% portion of the dose was bound to a 14 kDa protein in the lungs, which the authors suggested was uteroglobin-like (see following paragraph for further discussion). In bile-duct cannulated rats, 0.7% of the dose was bound to an unidentified 79 kDa protein between 0 and 24 hours. Trace amounts of the $MeSO_2$-CB metabolite were detected bound to albumin in the lungs and kidneys. Binding to albumin has also been suggested in human blood, where 61% of the whole blood sum $MeSO_2$-CB concentration was bound to the lipoprotein depleted (LPDP) fraction, which contains albumin as the most abundant protein (Norén *et al.* 1999).

In a rat and mouse dosing study that investigated lung cytosol protein binding, it was found that radiolabelled 4,4′-bis($MeSO_2$)-CB52, as well as 4′-$MeSO_2$-CB101, 4-$MeSO_2$-CB70, and 4-$MeSO_2$-CB52, all bound to a protein

characterized as uteroglobin-like (Lund *et al.* 1984). Similar findings were described in the work of Larsen *et al.* 1998 above. Using microautoradiography, it was possible for these researchers to localize the majority of the binding and accumulation of the bis-MeSO$_2$-CB to the apical cytoplasm of bronchiolar Clara cells, which are non-ciliated lung epithelium cells. These microautoradiography results have been corroborated elsewhere (Brandt *et al.* 1985), and this protein has been referred to more recently as Clara cell secretory protein (CCSP) (Stripp *et al.* 1996) and PCB binding protein (Bründl and Buff 1993). A small amount of protein binding was also detected in rat kidney, prostate and large intestine cytosol. Subsequently, it has been demonstrated that 4,4′-bis(MeSO$_2$)-CB52 accumulates in the apical cytoplasm of the proximal tubules in the kidney cortex of mice (Brandt *et al.* 1985). Only small amounts of the uteroglobin-like protein are generally present in kidney, so these authors suggested that a different mechanism may be involved in accumulation in this organ. However, more recently, it was found that 4′-MeSO$_2$-CB101 tritium labelled on the methyl sulfone group accumulates in the lungs and kidneys of wild type mice but not in mutant mice lacking the dominant allele for CCSP expression (Stripp *et al.* 1996).

Entero-pulmonary recirculation is expected to play an important role in the persistence of MeSO$_2$-CBs in the lungs. These metabolites have been detected bound to the uterogloblin-like protein in lung lavage fluid at higher concentrations than in the cytosol of mice, suggesting an active excretion process (Brandt *et al.* 1985). It has been proposed that upon excretion from the Clara cells into the

mucous, they may be transported to the pharynx via the mucocilliary escalator then swallowed and re-absorbed (Brandt and Bergman 1987).

### 1.3.2 Metabolism

Phase I biotransformation of PCBs involves oxidation to form hydroxylated metabolites (OH-PCBs) or arene oxide intermediates, as shown in **Figure 1.3**. The hydroxyl metabolite may be formed by direct insertion of a hydroxyl group in the *meta*-position, which may occur spontaneously, or via an arene oxide intermediate. These reactions occur primarily in the liver, particularly in the endoplasmic reticulum (Jerina and Daly 1974). Cytochrome P450 (CYP) enzymes are involved in both reaction pathways, and the isozymes involved depend on the chlorine substitution pattern of the congener and on the animal species. The isozyme CYP1A is generally implicated in the oxidation of PCB congeners with one or fewer *ortho*-chlorines, whereas CYP2B1 and 3A4 are involved for PCB congeners with one or more *ortho* chlorines in rats and humans, respectively. The position of arene oxide formation is also variable and may occur in the *meta-para* position or in the *ortho-meta* position, with the former being more common (Letcher *et al.* 2000). Note that the OH-PCB metabolites may undergo a 1,2-shift with an adjacent hydrogen or chlorine atom (Jerina and Daly 1974), as indicated in **Figure 1.3**. Obviously, this changes the chlorine substitution pattern relative to the parent PCB. However, no 1,2-shift occurs in the pathway leading to the methyl sulfone metabolites, which are known to have the same chlorine substitution pattern as their parent PCBs.

The arene oxide resulting from phase I can undergo a number of different reactions in phase II and III biotransformation. Initially, the arene oxide forms a glutathione conjugate with a hydroxyl group in an adjacent position either spontaneously or enzymatically in the presence of glutathione-S-transferase (Jerina and Daly 1974). Note that this ring opening reaction produces two isomers, one with the glutathionyl (GS) group in the *meta*-position and one with it in the *para*-position. This step provides the basis for the production of *meta*- and *para*-substituted methyl sulfone metabolites later on. At this point, the GS-OH-PCB intermediate can either be dehydrated to form an aromatic GS-PCB conjugate, or it can undergo spontaneous ejection of the glutathionyl group to re-form an OH-PCB, as shown in **Figure 1.3**.

Selected congeners that undergo dehydration to form the GS-PCB conjugate may then enter the mercapturic acid pathway (MAP) (Bakke *et al.* 1982), as shown in **Figure 1.3**. Some of the MAP enzymes are quite selective, and, in general, only PCBs with a 2,5-dichloro or a 2,3,6-trichloro substitution pattern are recognized (Brandt *et al.* 1976). Since this pathway is involved in the production of $MeSO_2$-CBs, the only methyl sulfone metabolites of environmental interest contain one of these two substitution patterns. A list of the environmentally relevant $MeSO_2$-CBs congeners is provided in **Table 1.1**. However, some exceptions exist, and methyl sulfone metabolites that do not contain one of these two substitution patterns have been detected in PCB dosing studies with rats (Darnerud *et al.* 1986, Haraguchi *et al.* 1998, Haraguchi *et al.* 1997). Some other comprehensive studies targeting all of the "environmentally

relevant" methyl sulfone metabolites have also detected unidentifiable $MeSO_2$-CBs in the tissues of wild animals (Letcher *et al.* 1998).

The mercapturic acid pathway leads to the formation of cysteine (Bergman *et al.* 1980a) and mercapturic acid conjugates (Bakke *et al.* 1982), both of which may undergo biliary excretion. In the intestinal tract, these conjugates can then be transformed into thiols via mediation with C-S β-lyase (Bakke *et al.* 1982, Bergman *et al.* 1982a), an enzyme produced by microogranisms that are naturally present in the colon. The thiol metabolite may be glucoronidated (Bakke *et al.* 1982), or it may react with *S*-adenosylmethionine via mediation with *S*-methyltransferase to form a methylthio metabolite (Bergman *et al.* 1980a). Both reactions occur predominantly in the intestines. Finally, the methylthio metabolite may be converted to a methyl sulfone via a two-step oxidation reaction involving CYP enzymes and occurring in the intestines or in the liver after enterohepatic recirculation (Bakke *et al.* 1982). The entire metabolic pathway for the production of $MeSO_2$-CBs is summarized in **Figure 1.3** on the following page.

Congeners that possess a 2,5-dichloro or 2,3,6-trichloro substitution pattern on both rings may form bis-methylsulfonyl metabolites, which have been detected in wildlife (Letcher *et al.* 1998) and in laboratory studies with mice (Bergman *et al.* 1982b), but will not be studied here. This is particularly common in birds and terrestrial mammals, which demonstrate high levels of CYP2B-like activity (Letcher *et al.* 1998). Many types of seals, including arctic ringed seals, possess lower CYP2B-like activity than polar bears, leading to the detection of bis-$MeSO_2$-CBs in bears but not in ringed seals in the Canadian Arctic
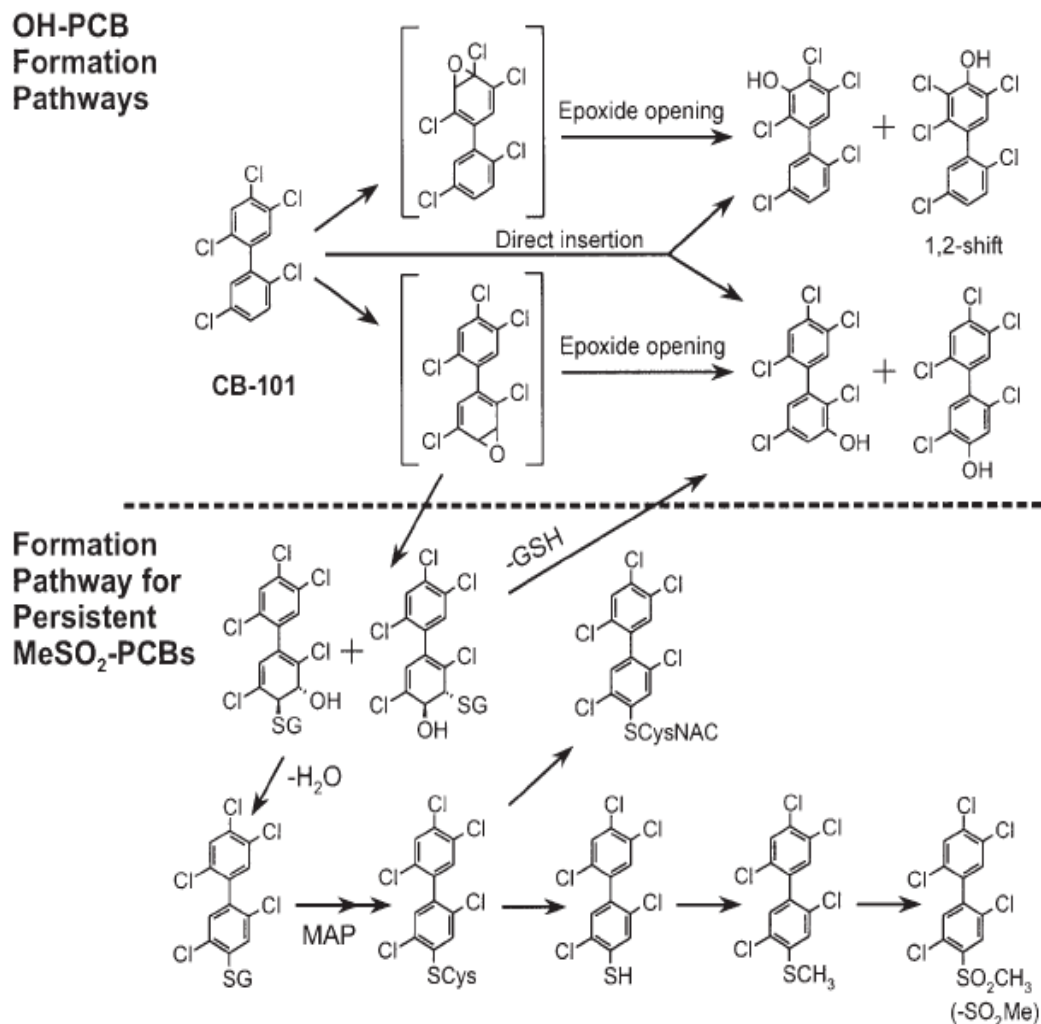
**Figure 1.3: Metabolic pathway for the formation of MeSO₂-CBs from PCBs[2]**

(Letcher *et al.* 1998). Metabolites containing both a methylsulfonyl group and a
hydroxyl group or a methylsulfonyl group and a methylthio group have been
detected in humans (Haraguchi *et al.* 1987a) and rats (Haraguchi *et al.* 1997),
respectively. It has been suggested that congeners with seven chlorines may only
be found in organisms exposed to PCBs for a long period of time, since the

---

[2] Reprinted from Letcher, R.J., Klasson-Wehler, E., and Bergman, Å., **2000**, "Methyl sulfone and
hydroxylated metabolites of polychlorinated biphenyls" in *The Handbook of Environmental
Chemistry*, Paasivirta, J., Ed., Springer-Verlag, Berlin, Germany, Vol. 3, Chap. 11, p. 315-359,
copyright (2000), with permission from Springer-Verlag and the authors.

overall rate for the production of MeSO$_2$-CBs tends to decrease with increasing chlorination (Mizutani *et al.* 1978).

Several species differences in the formation methyl sulfone PCB metabolites have been observed previously. For example, fish generally do not produce significant amounts of MeSO$_2$-CBs because they have low levels of CYP2B-like enzymes, which are required for phase I biotransformation of PCBs (Letcher *et al.* 2000). However, MeSO$_2$-CBs have been detected in deepwater sculpin from Lake Michigan, along with lower than expected concentrations of PCBs, suggesting higher CYP activity in this species than most other fish (Stapleton *et al.* 2001). Among terrestrial mammals, a comparative metabolism study has been carried out where subject animals were dosed with Kanechlor 500 technical PCB mixture (Haraguchi *et al.* 2005b). Higher concentrations of *meta*-substituted MeSO$_2$-CBs were detected in guinea pig liver compared to rats and hamsters, potentially indicating greater selectivity of the CYP isozymes in this organism. In another comparative study by these authors, these three species of animals and mice were dosed with PCBs 101 and 132 and the methylsulfonyl and hydroxyl metabolite levels compared (Haraguchi *et al.* 2005a). It was found that rats and mice produced similar results with the metabolite profile of both PCBs being dominated by methyl sulfones. Guinea pigs and hamsters, on the other hand, demonstrated selective metabolism with MeSO$_2$-CBs formed preferentially from PCB 132 and OH-PCBs formed from PCB 101 in guinea pig, and with OH-PCBs formed preferentially from both parent PCBs in hamsters.

### *1.3.3 Excretion and maternal transfer*

A small amount of methyl sulfone PCBs are excreted in the urine, bile and feces. In a study where rats were dosed with $^{14}C$ labelled 5-$MeSO_2$-CB149, 2.5% of the dose was detected in the 0 to 24 hour urine and 1.0% in the 24 to 48 hour urine (Larsen *et al.* 1998). In bile duct cannulated rats, 10.7% of the dose was detected in the bile collected from 0 to 24 hours post-dose and 4.6% in that collected from 24 to 48 hours. In a separate study where rats were dosed with PCBs 101 and 149 (342 μmol/kg each) and the metabolite levels in the feces measured for ten days after administration, it was estimated that approximately 0.5 and 0.3% of the doses of these PCB congeners, respectively, were excreted as the MeS- and $MeSO_2$-CB metabolites in total (Haraguchi *et al.* 1999). The concentration of both methylsulfonyl metabolites in feces reached a maximum 5 days after administration. Methyl sulfone PCBs have also been detected in rat feces in at least two other studies (Mizutani *et al.* 1978, Norström *et al.* 2006).

Other significant excretion mechanisms for $MeSO_2$-CBs are via lactation in mammals and via ovo deposition in birds. Methyl sulfone PCBs have been detected in white tailed sea eagle (*Haliaetus albicilla*) eggs with a sum concentration three orders of magnitude lower than the sum PCB concentration (Olsson *et al.* 1993). In Norwegian glaucous gulls (*Laurus hyperboreus*), the concentration of the hexachlorinated $MeSO_2$-CBs relative to the sum $MeSO_2$-CB concentration was significantly lower in eggs than in male and female plasma, whereas the relative concentrations of the tetra- and penta-chlorinated congeners was significantly higher (Verreault *et al.* 2005a). The authors reasoned that the

greater persistence of the higher chlorinated congeners decreased the efficiency of maternal transfer to the eggs. In a follow up study, it was determined that laying order had no effect on the concentrations of $MeSO_2$-CBs observed in three egg clutches from Norwegian glaucous gulls (Verreault *et al.* 2006). The sum concentration of $MeSO_2$-CBs detected in these eggs was six times lower than that found in the plasma of the mother birds. In addition, unlike their parent PCBs, the sum $MeSO_2$-CB concentrations in eggs did not correlate well with those in female plasma, suggesting that there are different toxicokinetic mechanisms involved in maternal transfer between these two types of contaminants. The concentrations and congener patterns found in birds and bird eggs will be discussed further in **Section 2.2.5**.

Maternal transfer of $MeSO_2$-CBs has also been observed in humans through an extensive study of human milk conducted in Sweden (Norén *et al.* 1996). The penta- and hexa-chlorinated analytes were the most abundant in the pooled milk samples, unlike bird eggs, where the tetra- and penta-chlorinated analytes were more common, as discussed above. Similar results were also found in a study of human milk in Canada (Newsome and Davies 1996). The sum $MeSO_2$-CB concentrations correlated well with the sum PCB concentrations in the Canadian milk samples. Human cord serum has also been investigated in women from Eastern Slovakia, and it was determined that transplacental transfer of $MeSO_2$-CBs must occur due to the presence of these contaminants in cord serum (Linderholm *et al.* 2007). The lipid normalized sum $MeSO_2$-CB concentration determined in the cord serum was on average approximately 1.5

times lower than that found in the mothers' serum, and the congener patterns were similar. In mice, the methyl sulfone metabolites of PCB 77 have been detected in the soft tissues of foetuses (Darnerud *et al.* 1986), as well as in the yolk sac epithelium and in the uterine fluid of exposed mothers during the mid-gestational period (Brandt *et al.* 1982) . In a mink reproductive study, transfer of $MeSO_2$-CBs from dams to kits was also evident, and similar sum $MeSO_2$-CB concentrations were detected in the muscle tissue of the mothers and of the 5 week old offspring (Lund *et al.* 1999). Similar congener patterns were observed between the dams and kits, suggesting a non-specific transfer process.

### 1.3.4    *Isomer selective toxicokinetics*

Several differences in the concentrations of $MeSO_2$-CB regioisomers and enantiomers have been observed between species, as well as between tissues within a single species. This may be attributable to selective absorption, disposition, metabolism, and/or excretion, but it is generally quite difficult to ascertain which processes are involved. Therefore, the differences in isomer and enantiomer patterns will be discussed below in general terms without attributing a root cause, unless specified by the authors.

#### 1.3.4.1 Regioisomer selectivity

In a feeding study where male Sprague-Dawley rats were exposed to a single dose of Clophen A50 and monitored over a period of 8 weeks, selective retention of the *para*-$MeSO_2$-CB isomers was observed in all tissues, with particularly high selectivity in the lungs and for the congener 4-$MeSO_2$-CB149

(Larsson *et al.* 2002). This was attributed to stronger retention of the *para*-isomers, and/or accelerated excretion or additional metabolism of the *meta*-isomers. In another feeding study where rats were exposed to PCB 132, the *para*-methylsulfonyl metabolite was also found to accumulate in higher concentrations in liver, lungs and adipose tissues (Norström *et al.* 2006). The *meta*-MeSO$_2$ isomer could not be detected in the lungs. Similar results were reported for selected tissues in a third study where rats were dosed with PCBs 101 and 149 (Haraguchi *et al.* 1999). The concentration of 4-MeSO$_2$-CB149 exceeded that of the *meta*-isomer by four to five times in the kidney and blood and by two orders of magnitude in the lungs. Similar results were obtained in the blood for PCB 101, but a slightly higher dominance of the *para*-isomer was observed in the kidney with a concentration ten times higher than that of the *meta*-MeSO$_2$-substituted isomer. However, it is interesting to note that in this case the *meta*- and *para*-isomers were very similar in concentration in the liver and adipose tissue for both the metabolites of PCB 101 and PCB 149, unlike the previous two studies. Fecal excretion was also examined by these workers, and it was noted that the concentrations of the *para*-substituted MeSO$_2$-CB metabolites were approximately 5 times higher than those of the *meta*-isomers.

In a comparative metabolism study involving rats, hamsters and guinea pigs dosed once with 100 mg/kg Kanechlor 500, the guinea pigs were found to selectively form *meta*-MeSO$_2$-CB congeners from parent tetra- to hexa-chlorinated PCBs with a 2,3,6-trichloro substitution pattern (Haraguchi *et al.* 2005b). The concentrations of these congeners detected in guinea pig liver were

in the range of 6 to 130 µg/g wet weight. Rats also formed tetra- to hexa-chlorinated MeSO$_2$-CBs but generally produced approximately equal amounts of the *meta*- and *para*-isomers. That being said, strong retention of an unidentified *para*-MeSO$_2$-metabolite with five chlorines was detected in rat lung, but not in guinea pig or hamster. The hamsters only formed small quantities of MeSO$_2$-metabolites from parent PCBs with a 2,5-dichloro substitution pattern and four or five total chlorines with concentrations in the range of 5 to 42 µg/g wet weight. The hamsters, like the rats, did not display any particular selectivity in terms of *meta*- versus *para*-isomer formation. In a complementary study, a strong preference for retention of 5-MeSO$_2$-CB132 compared to its *para*-substituted analogue was observed in the liver of guinea pigs (Haraguchi *et al.* 2005a). A smaller preference for the accumulation of the *meta*-isomer was found in the adipose tissue, with a *meta*/*para* ratio of only 1.6 compared to 4.2 in the liver.

A strong preference for the accumulation of *meta*-MeSO$_2$ substituted congeners has also been observed in human liver, with the *para*-MeSO$_2$ substituted congeners being observed more frequently in the adipose tissue (Weistrand and Norén 1997), brain and lung (Chu *et al.* 2003b, Covaci *et al.* 2003). The ratio of the sum concentration of the *meta*-isomers to the *para*-isomers in these tissues was reported to be 9.3, 0.3, 0.1 and 0.5, respectively (Chu *et al.* 2003b, Covaci *et al.* 2003). Another study also found that *meta*-MeSO$_2$-isomers were the most abundant in human liver, to the point where only the congeners 5′-MeSO$_2$-CB132 and 5-MeSO$_2$-CB149 were detected (Ellerichmann *et al.* 1998). A slightly higher abundance of the *para*-substituted isomers versus the *meta*-

substituted isomers has been noted in the lipoprotein depleted fraction of human plasma, while the opposite trend was observed in the remaining blood plasma fractions (Norén *et al.* 1999). The most abundant isomers detected in maternal and cord serum in Slovakia were *para*-substituted (Linderholm *et al.* 2007). Higher concentrations of the *para*-substituted isomers compared to their *meta*-counterparts were also reported in human breast milk in Sweden (Norén *et al.* 1996). It therefore appears that regioselective maternal transfer of these metabolites may occur in humans.

Several studies have also been carried out to determine the occurrence of the $MeSO_2$-CB regioisomers in the tissues of various organisms in the wild or in captivity. For example, a small preference for the accumulation of the *meta*-isomer of $MeSO_2$-CB87 has been observed in the liver of polar bears from East Greenland (Gebbink *et al.* 2008b). In contrast, the *para*-isomer was observed in higher abundance in the brain, blood and adipose tissues. In the polar bear food chain in the Canadian Arctic, higher apparent bioaccumulation factors were calculated for the *para*-isomers compared to the *meta*-isomers for certain $MeSO_2$-CBs, indicating a possibility of selective retention in polar bear and/or selective formation or retention in ringed seal (Letcher *et al.* 1998). In mink dosed daily with a mixture of $MeSO_2$-CBs at 0.1 mg/kg for a period of one year, the *meta*-substituted metabolites were selectively accumulated in the liver with 45 and 65 times higher concentrations of the congeners 5′-$MeSO_2$-CB132 (11.8 μg/g wet weight) and 5-$MeSO_2$-CB149 (19.6 μg/g wet weight), respectively, compared to muscle tissue (Lund *et al.* 1999).

*1.3.4.2 Enantiomer selectivity*

Several enantioselective PCB metabolism studies have been carried out in rats. In one feeding study involving exposure to a single dose of Clophen A50, enantioselective retention was observed with an excess of the second eluting enantiomer (E2) of 4-MeSO$_2$-CB149 found in the lungs using a heptakis(2,3-di-*O*-methyl-6-*O*-*tert*-hexyldimethylsilyl)-β-cyclodextrin (THDMS-β-CD; 4:1 in SE52) column (Larsson *et al.* 2002). The first eluting enantiomer (E1) of this congener was observed in excess in the liver and adipose tissues. Meanwhile, E1 of 4′-MeSO$_2$-CB132 and 4-MeSO$_2$-CB91, and E2 of 5′-MeSO$_2$-CB132 and 5-MeSO$_2$-CB149 were the dominant enantiomers in all tissues examined. The enantiomer fraction (EF), or the ratio of the concentration of the first-eluting enantiomer to the sum concentration of the enantiomers (see **Equation 2.1** in **Section 2.1.5**), is the preferred expression of enantiomer excess in environmental disciplines (Harner *et al.* 2000). In this study, all of the measured EFs were different from 0.5, indicating different concentrations of enantiomers, or a non-racemic mixture. An EF of 0.95 was reported for 4′-MeSO$_2$-CB132 in the adipose tissue, and an EF of <0.01 was reported for 5-MeSO$_2$-CB149 in the liver where the first eluting enantiomer was below the detection limit. More intermediate EFs of 0.43 and 0.61 were reported for the latter congener in the lung tissue and for 4-MeSO$_2$-CB91 in lung, but other researchers later commented that the dose used here was quite high, which could have saturated the biotransformation enzymes leading to the presence of both atropisomers (Norström *et al.* 2006). However, the EFs were constant over the 8 week monitoring period of the study.

Another feeding study carried out in rats involved exposure to single enantiomers (1 mg/kg dose) as well as a racemic mixture of PCB 132 (2 mg/kg dose) (Norström *et al.* 2006). The single enantiomer formulations were obtained by separating a racemic mixture using enantioselective liquid chromatography with a Nucleodex β-PM column, and the enantiomers of the methyl sulfone metabolites were analyzed using a THDMS-β-CD chiral selector, like that employed by Larsson and colleagues above, but dissolved 1:1 in OV1701. The (*R*)-enantiomers of the MeSO$_2$-CB metabolites were the only ones observed for the rats exposed to E1 PCB 132, and the concentrations were relatively high, ranging from 45 to 200 ng/g of fat for the *meta*- and *para*-isomers in the liver, lung and adipose tissue. However, in the E2 PCB 132-dosed rats, only the (*S*)-enantiomers of the methyl sulfone PCBs were detected and in comparably lower concentrations, in the range of 2.2 to 23 ng/g of fat. The authors concluded that enantioselective formation of 4′- and 5′-MeSO$_2$-CB132 must have occurred. It was further suggested that these results support a model where one enzyme metabolizes both enantiomers of the parent PCB but with greater specificity for one enantiomer over the other. Only the (*R*)-enantiomer of these congeners was observed in the feces, although the authors pointed out that the limit of detection was quite high for the enantioselective gas chromatography (GC) method employed, so it is possible that the (*S*)-enantiomer was present but could not be detected.

In a rat hepatocyte study, liver cells were exposed separately to 2 mmol/L racemic PCB149 and racemic 5-MeSO$_2$-CB149 for a period of 12 hours

(Hühnerfuss *et al.* 2003). It was observed that the 5-MeSO$_2$-CB149 metabolites were initially formed in nearly racemic proportions upon exposure to PCB 149. However, the concentration of the first eluting enantiomer of 5-MeSO$_2$-CB149 from a heptakis(2,3-di-*O*-methyl-6-*O*-*tert*-butyldimethylsilyl)-β-cyclodextrin stationary phase (dissolved 5:1 in SE52), which is known to be the (*S*)-enantiomer, increased in concentration, while that of the second eluting, (*R*)-enantiomer remained the same in the sample exposed to racemic 5-MeSO$_2$-CB149. The authors concluded that the initial metabolism of this congener is not enantioselective in rat, but further transformation processes occur over a longer time period to produce an excess of the (*S*)-enantiomer.

Several studies have also been carried out to determine the occurrence of the enantiomers of methyl sulfone PCBs in the tissues of various organisms in the wild. For example, in grey seals from the Baltic Sea the first eluting enantiomer dominated in all tissues for 4-MeSO$_2$-CB91, 4-MeSO$_2$-CB149, 4′-MeSO$_2$-CB132, and 4′-MeSO$_2$-CB174 with THDMS-β-CD 1:1 in OV1701 as the stationary phase (Larsson *et al.* 2004). In contrast, the second eluting enantiomers dominated for the corresponding *meta*-substituted isomers, except for 5-MeSO$_2$-CB91, which was not determined because its enantiomers could not be separated. For 5-MeSO$_2$-CB149, E2 is known to correspond to the (+)-enantiomer on this column. No differences in the dominant enantiomer were observed between tissues, unlike a previous rat study (Larsson *et al.* 2002). However, more extreme EFs (i.e. greater than 0.94 and less than 0.09) were observed in this seal species compared to rat. Differences in the metabolism of the enantiomers and/or in their transport

across cell membranes were suggested as potential mechanisms involved in creating this large disparity in the enantiomer concentrations.

A study of $MeSO_2$-CBs in the liver tissue of harbour porpoises (*Phocoena phocoena*) from the Southern North Sea also revealed strong enantiomer excesses (Chu *et al.* 2003a). The second eluting enantiomer from a Chirasil-Dex column dominated for the congeners 5′-$MeSO_2$-CB132, 5-$MeSO_2$-CB149 and 5′-$MeSO_2$-CB174, whereas the second eluting enantiomer dominated for the congeners 4-$MeSO_2$-CB149 and 4′-$MeSO_2$-CB174. This is the opposite trend from that described above for Baltic grey seals, but it is possible that the enantiomer elution order was reversed between the different columns used. It was also found that the EFs were much more pronounced than those found for the parent PCBs in a previous study of the same samples (Chu *et al.* 2003c), and the authors suggested that enantioselective metabolism may be the main cause for the extreme EFs observed for $MeSO_2$-CBs.

Similar trends to those reported in Baltic grey seals were found in a study of ringed seal (*Phoca hispida*) blubber from the Resolute Bay area of the Canadian Arctic, where higher abundances of the first eluting enantiomers of 4-$MeSO_2$-CB91 and 4′-$MeSO_2$-CB132 were found using a BGB-172 column (Wiberg *et al.* 1998). This may indicate that the same elution order was obtained on BGB-172 compared to the handmade column used by Larsson and colleagues (Larsson *et al.* 2004). The enantiomer ratios (E1/E2) in this study were approximately 4 and 3, respectively, corresponding to EFs in the range of 0.2 to 0.4, slightly less dramatic than those found in Baltic grey seals by Larsson *et al*.

2004. Since methyl sulfone PCBs were not detected in a previous study of Arctic

cod (Letcher *et al.* 1998), a major component of the diet of ringed seals, the

authors concluded that enantioselective metabolism or excretion, or a combination

of the two, must have occurred in these seals. Finally, one study examined the

blubber of seals (species not specified) raised in the Prague Zoo using an

enantioselective GC stationary phase consisting of THDMS-β-CD 1:4 in SE52

(Karásek *et al.* 2007). These authors also found similar EF trends to Larsson *et al.*

2004 for 4-MeSO$_2$-CB91, 4′-MeSO$_2$-CB132 and 5-MeSO$_2$-CB149, although the

EFs were also less extreme in this case at 0.76, 0.79 and 0.26, respectively.

However, an entirely different result was obtained for 4-MeSO$_2$-CB149, for

which an approximately racemic EF of 0.53 was measured.

Wiberg and colleagues also examined MeSO$_2$-CB enantiomers in polar

bear adipose tissue from Resolute Bay (Wiberg *et al.* 1998). They found very

dramatic enantiomer excesses in this organism, with only one enantiomer being

detectable in many cases. The enantiomer ratios (ERs) for 4-MeSO$_2$-CB91 and 4′-

MeSO$_2$-CB132 were estimated to be greater than 10, indicating dominance of the

first eluting enantiomer from BGB-172. Since the ERs found in polar bear were

much higher than those found in ringed seal, the main component of the polar

bear diet, it was concluded that enantioselective metabolism must occur in bear.

Chiral methyl sulfone PCBs have also been determined in pooled egg

samples from the Baltic guillemot (*Uria aalge*) using the same handmade

THDMS-β-CD column (1:1 in OV1701) employed by Larsson and colleagues

(2004) for the analysis of Baltic grey seal tissues (Jörundsdóttir *et al.* 2006). A

slight dominance of the first eluting enantiomer was observed for 4-MeSO$_2$-CB91 and 4′-MeSO$_2$-CB132 with EFs of 0.65 and 0.67, respectively, and a slight dominance of the second eluting enantiomer was observed for 5-MeSO$_2$-CB149 and 5′-MeSO$_2$-CB174 with EFs of 0.41 and 0.27, respectively. These trends are similar to those reported by Larsson *et al.* 2004 in Baltic grey seal, however, very different results were obtained for 4-MeSO$_2$-CB149 and 4′-MeSO$_2$-CB174. Nearly racemic EFs were observed for these congeners at 0.52 and 0.56, respectively. Unfortunately, maternal guillemot EFs were not determined in this work, so it could not be ascertained whether enantioselective maternal transfer was occurring. However, a previous study of egg yolks and adult plasma from Norwegian glaucous gulls (*Larus hyperboreus*) found that enantioselective maternal transfer of PCBs and chlordanes does not occur in this species (Ross *et al.* 2008). Very similar EFs to the guillemots were obtained for 4′-MeSO$_2$-CB132, 5-MeSO$_2$-CB149 and 4′-MeSO$_2$-CB174 in the muscle tissue of pelicans raised in the Prague Zoo at 0.68, 0.43 and 0.62, respectively (Karásek *et al.* 2007). Interestingly, these pelicans were fed fish from the same source used to feed the seals examined concurrently in this work (described two paragraphs previous), so it was concluded that the differences in EFs observed were due to differences in metabolism between these two species.

Chiral analysis of MeSO$_2$-CBs has also been performed on some human tissues. Liver samples from German subjects have been examined using a THDMS-β-CD (1:1 in OV1701) enantioselective GC column (Ellerichmann *et al.* 1998). In all of the samples investigated, only the second eluting enantiomers of

5′-MeSO$_2$-CB132 and 5-MeSO$_2$-CB149 were detectable. These authors also attempted to analyze human lung tissues, but all of the MeSO$_2$-CBs examined were below their respective detection limits. This problem was also encountered in study examining human adipose tissues (Karásek *et al.* 2007).

## 1.4    Toxicological effects of MeSO$_2$-CBs

### *1.4.1    Endocrine disruption and enzyme modulation*

Several studies have been carried out to determine the inducing effects of MeSO$_2$-CBs on cytochrome P450 and other drug-metabolizing enzymes in rats. It has been found that several *meta*-substituted MeSO$_2$-CBs, including 3-MeSO$_2$-CB31, 3′-MeSO$_2$-CB49, 3′-MeSO$_2$-CB87, 3′-MeSO$_2$-CB101, 3′-MeSO$_2$-CB141 and 5-MeSO$_2$-CB149, significantly increase the quantities of cytochrome P450 and $b_5$, as well as aminopyrene-$N$-demethylase and benzo[$a$]pyrene hydroxylase, enzymes in liver microsomes from rats administered with a 2 μmol/kg single congener dose via intraperitoneal injection 96 hours prior to the assay (Kato *et al.* 1997). The congeners 3′-MeSO$_2$-CB49, 3′-MeSO$_2$-CB87 and 3′-MeSO$_2$-CB101 were the most potent inducers of total CYP P450s and of CYPs 2B1 and 2B2, in particular. Two 431 μmol/kg doses of phenobarbital administered at 24 hour intervals were required to produce a similar effect to these congeners. The isomers 3-MeSO$_2$-CB52 and 3-MeSO$_2$-CB70 only slightly increased the total CYP and CYP 2B2 levels, as well as aminopyrene-$N$-demethylase for both congeners and benzo[$a$]pyrene hydroxylase for the latter congener. The isomers 3-MeSO$_2$-CB31, 3′-MeSO$_2$-CB49 and 3′-MeSO$_2$-CB101 also led to a small

increase in the activity of aniline hydroxylase, whereas the congeners 5-MeSO$_2$-CB64 and 5-MeSO$_2$-CB110 had no effect and any drug-metabolizing enzymes. Overall, the CYP inducing effects of most of the methyl sulfone PCBs were similar to those of phenobartibal but not of 3-methylchloanthrene, leading to the conclusion that these compounds are phenobartibal-type inducers. In terms of structure-activity relationships, it was found that congeners with strong CYP inducing potential generally possessed a chlorine in the *para*-position of the non-MeSO$_2$-substituted ring, and that the strongest inducers also possessed a chlorine in the *ortho*-position of this ring. The weak inducers generally possessed chlorines in *meta*-position on the non-MeSO$_2$-substituted ring and/or in the *ortho*-position on the opposite ring. The only exception to these rules was 3-MeSO$_2$-CB52, which contains a 2′-chlorine and no 3′- or 6-chlorines, but was a weak inducer.

In a previous study by these authors, the inducing effects of the *meta*- and *para*-substituted isomers of MeSO$_2$-CBs 70, 87, 101 and 141 were studied in rat hepatic microsomes (Kato *et al.* 1995b). It was found that the *para*-MeSO$_2$-CBs had no significant effect on any of the enzyme activities examined. In another earlier study, these authors compared the effects of the *meta*-MeSO$_2$ metabolites to those of their parent PCBs and found that the metabolites produced greater drug metabolizing enzyme induction than the parent compounds (Kato *et al.* 1995a). To produce the same effect on the induction of the phenobarbital-inducible CYPs 2B1, 2B2, 3A6 and 2C6, a 342 μmol/kg dose of PCBs 70, 87, 101, or 141 was required to produce the same effect as a 10 μmol/kg dose of 3-MeSO$_2$-CB70, a 0.5 μmol/kg dose of 3′-MeSO$_2$-CB87 and 3′-MeSO$_2$-CB101, or a

2 μmol/kg dose of 3′-MeSO$_2$-CB141, respectively. In particular, the metabolite 3′-MeSO$_2$-CB101 was a much stronger inducer than PCB 101 for several enzymes, including CYP P450 and $b_5$, aminopyrene-$N$-demethylase, aniline and benzo[$a$]pyrene hydroxylase, and 7-ethoxyresorufin-$O$-dealkylase (EROD).

In a rat exposure study where a 20 μmol/kg dose of one of nine MeSO$_2$-CBs was administered on four consecutive days and hepatic microsomes prepared seven days after the last dose, it was found that all seven of the *meta*-substituted congeners led to a significant increase in total CYP and 7-pentoxyresorufin $O$-dealkylase (PROD), or CYP2B1/2, activity (Kato *et al.* 2000b). There was an approximate 2 fold increase in CYP activity and a 28 to 55 fold increase in PROD activity with these treatments. The congeners 3′-MeSO$_2$-CB87, 3′-MeSO$_2$-CB101 and 5′-MeSO$_2$-CB132 also led to a significant increase in 7-ethoxyresorufin-$O$-dealkylase, EROD or CYP1A1/2, activity. However, neither of the *para*-congeners studied, 4′-MeSO$_2$-CB101 and 4-MeSO$_2$-CB149, had any effect on the drug metabolizing enzymes examined. Increases in PROD activity and progesterone catabolism of greater than 10 times and of 2 times, respectively, have also been observed in liver microsomes prepared from female mink chronically exposed to methyl sulfone PCBs (Lund *et al.* 1999). The five week old offspring of these mink exhibited an average five fold increase in hepatic PROD activity compared to controls.

Aromatase, also known as CYP19, levels are also affected by MeSO$_2$-CBs. Exposure of human mammary fibroblast and adrenocortical carcinoma H295R cells led to a concentration-dependent decrease in aromatase levels upon a

6 or 24 hour exposure to 0.1 to 10 μmol/L of 5′-MeSO$_2$-CB132, 4′-MeSO$_2$-CB132, 4-MeSO$_2$-CB91 or 4-MeSO$_2$-CB149 (Heneweer *et al.* 2005). The IC$_{50}$ values were estimated to be between 1 and 3 μmol/L for 4-MeSO$_2$-CB91 and less than 1 μmol/L for the remaining congeners. The authors did not detect any effect on the aromatase mRNA levels in the 24 hour exposure studies and concluded that these methylsulfonyl PCBs likely decrease enzyme activity by direct catalytic inhibition. No cytotoxicity was observed at the concentration levels employed. The effects of MeSO$_2$-CBs on aromatase activity have also been examined in human placental JEG-3 and JAR choriocarcinoma cell cultures for the *meta-* and *para*-MeSO$_2$ metabolites of PCBs 52, 70, 87 and 101 (Letcher *et al.* 1999). In this study, it was found that 4-MeSO$_2$-CB52 alone caused a dose-dependent decrease in CYP19 activity in JEG-3 cells incubated without serum (serum-free). The lowest observed effect concentration (LOEC) for aromatase activity was 10 μmol/L, but cytotoxicity was observed with cell leakage at 0.001 μmol/L (measured as percent lactate dehydrogenase leakage), and with decreased cell protein content at 0.1 μmol/L. Significant DNA fragmentation was also observed at 10 μmol/L, suggesting an apoptotic mechanism of cellular toxicity. Similar cytotoxic effects were observed in the serum-free JAR cells, but 4-MeSO$_2$-CB52 had no effect of aromatase activity up to 10 μmol/L in this case. For the remaining congeners, no dose-dependent effect on aromatase activity was observed up to 10 μmol/L in serum-free JEG-3 or JAR cells. It was not possible to assess the effects of these congeners above this concentration due to the high level of cytotoxicity

observed, with cell leakage and decreased protein content occurring as low as 0.001 μmol/L, and decreased DNA content occurring as low as 0.01 μmol/L.

The antiestrogenic activity of methyl sulfone PCB metabolites has been probed using *in vitro* bioassays. Estrogen-responsive gene expression was examined using a chemically-activated luciferase expression assay with co-administration of a single MeSO$_2$-CB congener and 17β-estradiol (100 pmol/L) in recombinant human breast adenocarcinoma T47D cells and two types of embryonic kidney cells, one expressing α-estrogen receptors and one expressing β-estrogen receptors (Letcher *et al.* 2002). In a fourth assay, vitellogenin production was monitored in male carp (*Cyprinus carpio*) hepatocytes upon co-administration of an MeSO$_2$-CB congener and 17β-estradiol (20 and 100 nmol/L). In all four bioassays, three of the four MeSO$_2$-CBs examined led to a concentration-dependent inhibition of 17β-estradiol-induced luciferase/vitellogenin production. The congener 4′-MeSO$_2$-CB101 was the most potent 17β-estradiol antagonist, followed by 4′-MeSO$_2$-CB49 and 3′-MeSO$_2$-CB101. The lowest observed effect concentrations were 1.0 μmol/L for 4′-MeSO$_2$-CBs 49 and 101, and 2.5 μmol/L for 3′-MeSO$_2$-CB 101 in the human cell line assays and 2.5 μmol/L for 4′-MeSO$_2$-CBs 49, and 101 and 20 μmol/L for 3′-MeSO$_2$-CBs 101 in the fish hepatocyte assay, approximately 100 to 1000 fold lower than tamoxifen. These congeners also led to greater inhibition in the embryonic estrogen receptor-α cell line than in the estrogen receptor-β cell line, indicating a higher affinity for the α receptors. The congener 3′-MeSO$_2$-CB39 had no antiestrogenic effects in the concentration range examined. No effect, agonistic

or antagonistic, was produced in any of the assay systems by PCB 101. No cytotoxic effects were observed. The authors concluded that the *para*-substituted methylsulfonyl PCB congeners possess greater antiestrogenicity than the *meta*-substituted congeners. Since the level of inhibition increased with concentration, the authors predicted that $MeSO_2$-CBs interact directly with estrogen receptors to competitively inhibit the effects of 17β-estradiol. The interaction of the $MeSO_2$-CBs was also deemed to be reversible, since increasing the concentration of 17β-estradiol led to a restoration of luciferase/vitellogenin production at the lower $MeSO_2$-CB exposure concentrations.

The effects of several $MeSO_2$-CB metabolites on uridine diphosphate-glucuronosyltransferase (UGT), a phase II drug-metabolizing enzyme, in rat liver microsomes has been studied by dosing live rats with 20 μmol/kg of one of nine $MeSO_2$-CBs via intraperitoneal injection on four consecutive days (Kato *et al.* 2000a). On day 7, the response of the prepared rat hepatic microsomes to different UGT test substrates was examined. It was found that the activity of phenobarbital-inducible UGT, or UGT2B1, increased significantly for all of the congeners studied, namely 3′-$MeSO_2$-CB49, 3-$MeSO_2$-CB70, 3′-$MeSO_2$-CB87, 3′-$MeSO_2$-CB101, 4′-$MeSO_2$-CB101, 5′-$MeSO_2$-CB132, 3′-$MeSO_2$-CB141, 5-$MeSO_2$-CB149, and 4-$MeSO_2$-CB149. The activity of 3-methylcholanthrene-inducible UGT, or UGT1A6, increased significantly for all of the congeners studied except for 4-$MeSO_2$-CB149. The same results were observed for the activity of UGT towards thyroxine. Interestingly, all of the congeners led to a decrease in total serum thyroxine levels, including 4-$MeSO_2$-CB149. It was therefore concluded

that most of the MeSO$_2$-CBs decreased serum thyroxine concentrations by increasing UGT activity, but that 4-MeSO$_2$-CB149 did so via a different mechanism.

A reduction in serum thyroxine levels in rats upon treatment with MeSO$_2$-CBs has been observed in two other studies by these authors (Kato *et al.* 1999, 2000b). The same dosing regime as that described in the previous paragraph was employed and blood drawn on days 2, 3, 4 and 7 after the last dose administered. The levels of thyroxine, triiodothyronine and thyroid stimulating hormone (TSH) in serum were measured, and in both studies it was found that all of the MeSO$_2$-CBs investigated led to a significant decrease in thyroxine levels of 16 to 44% at all time points examined. The results for triiodothyronine were much less dramatic and varied more over the time points studied. The levels of TSH were examined on days 3, 4 and 7 only. The only congener that led to a consistent, significant increase in serum TSH over all time points investigated was 3′-MeSO$_2$-CB141. An approximate two fold increase in TSH was also observed at days 3 and 4 for 3′-MeSO$_2$-CB101. Increases were observed on days 3 or 4 for the remaining congeners except for 3-MeSO$_2$-CB70 and 4′-MeSO$_2$-CB101, which had no effect on serum TSH. The concentrations of thyroxine and triiodothyronine were also observed to decrease by 60 to 65% in female mink upon dietary exposure to methylsulfonyl PCBs for a period of one year, although no effect was detected in their kits (Lund *et al.* 1999).

Methyl sulfone PCBs have been demonstrated to bind competitively to human and mouse glucocorticoid receptors (Johansson *et al.* 1998b). Of the 24

MeSO$_2$-CBs studied, it was observed that only the congeners with three *ortho*-chlorines and one *para*-chlorine bound to mouse glucocorticoid receptors (GRs). Stronger binding was observed for the *para*-MeSO$_2$-subsituted congeners compared to the *meta*-congeners, with a four fold lower affinity calculated for 5-MeSO$_2$-CB149 compared to 4-MeSO$_2$-CB149 in mouse liver cytosol. The congeners 5-MeSO$_2$-CB149 and 3′-MeSO$_2$-CB101 competed the most effectively with dexamethasone for binding to human GR. The authors concluded that methylsulfonyl PCBs may have an effect on glucocorticoid homeostasis and further suggested that this may play a role in the disease syndrome described in grey seals from the highly-polluted Baltic Sea. Methyl sulfone PCBs have also been determined to decrease the CYP11B1-dependent production of corticosterone in mouse adrenocortical Y1 cells (Johansson *et al.* 1998a). The *para*-substituted congeners generally led to a greater decrease in corticosterone production (36 to 109% of control) compared to their *meta*-counterparts (60 to 138% of control), with 4-MeSO$_2$-CB64 being the most potent inhibitor. Binding studies suggested a competitive mechanism with an inhibition constant of 4.6 μmol/L for 4-MeSO$_2$-CB64. However, the *para*-congeners also led to cytotoxicity with decreased protein content, whereas no cytotoxicity was observed for the majority of the *meta*-congeners.

## 1.4.2    *Gross pathology, respiratory and reproductive effects*

In the rat exposure studies examining TSH levels described in the previous section, the thyroid gland was weighed, and it was found that treatment with 3′-MeSO$_2$-CB101 and 3′-MeSO$_2$-CB141 led to a significant increase in weight (Kato

*et al.* 1999, 2000b). These congeners also produced the largest and most sustained increase in TSH of the MeSO$_2$-CBs studied, and it was suggested that the increase in thyroid weight was due to hyperplasia (abnormal cell proliferation) and/or hypertrophy (organ/tissue enlargement due to an increase in cell size). A decrease in kidney weight was observed in female mink exposed to an average total dose of 0.1 mg/day of MeSO$_2$-CBs for a period of one year (Lund *et al.* 1999). A two-fold increase in total liver lipids was observed in an acute exposure study where rats were injected with a single 100 mg/kg dose of 4-MeSO$_2$-CB52 (Haraguchi *et al.* 1985). Enlargement of the cortex of the adrenal gland has also been observed in Baltic grey seals, and it has been suggested that the accumulation of MeSO$_2$-CBs, particularly 4-MeSO$_2$-CB64 and 4′-MeSO$_2$-CB101, may be responsible for this gross pathological change (Letcher *et al.* 2000).

In a reproductive study of methyl sulfone PCBs, one year old female mink were dosed three times weekly with a mixture of 15 MeSO$_2$-CB congeners and MeSO$_2$-DDE in their feed, amounting to an average total daily dose of 0.1 mg (Lund *et al.* 1999). This was continued over the course of one year, encompassing one mating period. There was a significant increase in the total and live births for the exposed group, but the birth weight of the kits was significantly reduced. Furthermore, there was a significant decrease in the frequency of survival at 2 weeks after birth for the exposed group. No evidence of toxicity was observed in the dams or the kits, and no malformations occurred in any of the kits. By comparison with previous mink reproductive studies, it was judged that the methyl sulfone metabolites are less toxic than their parent compounds. However,

different findings have been suggested in mice, where the methyl sulfone and hydroxyl metabolites of PCB 77, a congener known to be highly fetotoxic (Brandt and Bergman 1987), have been observed to accumulate selectively in foetal soft tissues from exposed mothers (Darnerud *et al.* 1986). This suggests that the metabolites may be responsible for the fetotoxic effects, not the parent compound.

In 1968 in Yusho, Japan, a batch of rice bran oil was accidentally contaminated with PCBs during production. Many studies have been carried out on the victims of this incident, and symptoms of respiratory distress, including atelectasis (lack of gas exchange in the alveoli due to collapse or fluid accumulation), bronchiolitis (inflammation of the bronchioles) and pneumonia have been observed in approximately one tenth of patients (Shigematsu *et al.* 1978). Expectoration was also encountered in 40% of the non-smoking patients. Similar clinical findings have been reported elsewhere (Nakanishi *et al.* 1985), and the severity of symptoms has been reported to increase with the concentration of PCBs in the blood and sputum (Shigematsu *et al.* 1978). Sixty different $MeSO_2$-CB congeners were detected in the lung tissue of one Yusho victim (Haraguchi *et al.* 1986). It has since been suggested that the respiratory symptoms observed in Yusho patients may be a consequence of toxicity from the methyl sulfone metabolites that have accumulated in their lungs (Brandt and Bergman 1987).

## 1.5    Environmental occurrence of MeSO$_2$-CBs

### 1.5.1    Concentrations and congener patterns in biota

Methyl sulfone PCBs have now been tested in the tissues of a number of different organisms, including various bird species, fish, and marine and terrestrial mammals, including humans (Letcher *et al.* 2000). The concentrations found in fish are generally quite low, whereas higher levels are found in birds, followed by marine and terrestrial mammals, generally following the same trend as CYP activity. The highest sum concentration of MeSO$_2$-CBs recorded to date was 110 µg/g lipid weight in an adult female grey seal (*Halichoerus grypus*) from the Baltic Sea (Haraguchi *et al.* 1992), a region known to be highly contaminated with PCBs and other organohalogen contaminants. Several studies have also been carried on Arctic birds and terrestrial mammals, which will be discussed further in **Sections 2.2.5** and **2.2.6**. A brief summary of the data on the occurrence of these contaminants in human is given below. In all cases, organ tissues were obtained from autopsies of individuals that died of causes unrelated to environmental contamination. A complete review of the environmental occurrence of methyl sulfone PCBs in biota is beyond the scope of this work, but an excellent summary can be found in the *Handbook of Environmental Chemistry* (Letcher *et al.* 2000).

In a study of human tissues from the autopsies of 11 Belgian individuals, average sum MeSO$_2$-CB concentrations of 9.30, 2.72, 1.57 and 0.24 ng/g lipid weight were detected in the liver, lung, adipose tissue and brain, respectively (Chu *et al.* 2003b, Covaci *et al.* 2003). The most commonly detected congener in liver was 5′-MeSO$_2$-CB132, making up approximately 59% of the total MeSO$_2$-

CBs in this tissue. However, the congeners 4′-MeSO$_2$-CB87 and 4′-MeSO$_2$-CB101 were the most common in the lung, adipose and brain tissues, together making up around 60% of the total MeSO$_2$-CBs detected in these tissues. The highest accumulation of MeSO$_2$-CBs relative to PCBs was observed in the liver, followed by the brain and lung, then the adipose tissue. Little variation in the congener pattern was observed between the 11 human subjects studied. Adipose tissue and liver samples from autopsies of 7 Swedish individuals ranging from 47 to 80 years of age contained similar congener patterns but different concentrations of MeSO$_2$-CBs (Weistrand and Norén 1997). The congeners 4′-MeSO$_2$-CB87 and 4-MeSO$_2$-CB149 were the most common in adipose tissue, whereas 5′-MeSO$_2$-CB132 was the most common in liver, making up 61 to 80% of the total MeSO$_2$-CBs in this tissue. A study of a single Belgian individual also found that 4′-MeSO$_2$-CB87 was the most abundant congener in the adipose tissue and 5′-MeSO$_2$-CB132 in the liver with concentrations of approximately 2 and 9 ng/g lipid, respectively (Chu *et al.* 2002). Human liver samples from German individuals contained the congeners 5′-MeSO$_2$-CB132 and 5-MeSO$_2$-CB149 in the highest quantities, with concentrations ranging from 0.3 to 7.8 ng/g lipid and 0.006 to 0.7 ng/g lipid, respectively (Ellerichmann *et al.* 1998). In human adipose tissue of individuals from Prague, the congener 4′-MeSO$_2$-CB101 was one of the most common (Karásek *et al.* 2007). The isomers 3′-MeSO$_2$-CB49 and 5-MeSO$_2$-CB110 were the other two most abundant, but it must be noted that 4′-MeSO$_2$-CB87 was not a target analyte in this work. All of the individual congener concentrations in this study were lower than 5 ng/g lipid weight.

Methyl sulfone PCBs have also been measured in human blood and sum concentrations in the range of 6.5 to 38 ng/L were detected in plasma, approximately two orders of magnitude lower than the sum PCB concentrations (Norén *et al.* 1999). The most abundant congeners detected were the *meta-* and *para*-MeSO$_2$-substituted metabolites of PCBs 149, 87 and 101, similar to lung, adipose and brain tissue, as discussed above. Again, little variation in congener composition was found between samples. The average sum concentration of MeSO$_2$-CBs found in the breast milk of Swedish women between 1972 and 1992 was on the order of 2 to 9 ng/g lipid weight (Norén *et al.* 1996). The major isomers detected were 4′-MeSO$_2$-CB87 and 4-MeSO$_2$-CB149, with average concentrations of 2.13 and 2.00 ng/g lipid in 1972 and 0.33 and 0.35 ng/g lipid in 1992, respectively. Similar concentrations and congener patterns were observed in Canadian mothers' milk, although the congener 4-MeSO$_2$-CB149 was not detected in this case (Newsome and Davies 1996). The predominant congeners detected in maternal serum in Eastern Slovakia were also 4′-MeSO$_2$-CB87, 4′-MeSO$_2$-CB101, 4-MeSO$_2$-CB149 and an unidentified hexa-chlorinated congener, with median sum concentrations of these four isomers estimated at around 1.0 ng/g lipid weight over the entire study group of 1,103 women (Linderholm *et al.* 2007). Similarly, 4′-MeSO$_2$-CB101 and the unidentified hexa-chlorinated isomer were among the most commonly detected in cord serum, although the individual congener and sum concentrations in the 10 samples analyzed were approximately one half of those detected in the corresponding maternal serum samples.

### 1.5.2 Geographical distribution and temporal trends

The geographical distribution of methyl sulfone PCBs has not been thoroughly examined, but one study investigated how the levels in polar bear adipose tissues vary across the western Arctic and Subarctic (Letcher *et al.* 1995). These workers found that the sum $MeSO_2$-CB concentrations were higher in the southern and eastern regions studied, around south Hudson Bay and Baffin Bay, and around Scoresby Sound east of Greenland, respectively. The authors reasoned that these findings were indicative of transportation from the high use areas of North America and Europe, respectively, via air flows. The congener patterns did not vary significantly between regions. However, it was found that the ratio of the sum $MeSO_2$-CB concentration to the sum PCB concentration decreased from west to east. This was attributed to the fact that the most abundant $MeSO_2$-CB congeners produced in polar bears are tetra- and penta-chlorinated and that these precursor PCBs are present in higher proportions in the Aroclor mixtures used in the western hemisphere.

Two other smaller range geographical distribution studies conducted in Eastern Slovakia compared the concentrations of methyl sulfone PCBs in adult male and female serum, and in maternal and cord serum, respectively, between the Svidnik/Stopkov region and the highly contaminated Michalovce region (Hovander *et al.* 2006, Linderholm *et al.* 2007). These workers found that the sum concentration of $MeSO_2$-CBs in the serum samples was two to three times higher in the Michalovce region where the technical PCB mixture, Delor, was manufactured between 1959 and 1984. A similar difference in the concentration

of PCB 153 was observed between these two regions in both studies. The ratio of the sum concentration of $MeSO_2$-CBs to PCBs was lower in the control region than in the contaminated region in the study of adult male and female serum (Hovander *et al.* 2006). In addition, the concentrations of the parent PCBs and their methyl sulfone metabolites were observed to increase with age from 20 to 59 years for both men and women (Hovander *et al.* 2006).

Recently, a couple of studies have been conducted to determine the changes in concentration of methyl sulfone PCB metabolites quantitatively over time. For example, temporal trends in $MeSO_2$-CB concentrations have been studied in Baltic guillemot (*Uria aalge*) eggs between the years 1971 and 2001 (Jörundsdóttir *et al.* 2006). The three congeners 3′-$MeSO_2$-CB101, 4′-$MeSO_2$-CB101 and 4-$MeSO_2$-CB149 were detected in all of the samples analyzed, and their concentrations decreased by 3.5%, 2.4% and 3.4% per year, respectively. It was also noted that the annual decrease in concentration for the former two congeners was much lower than that of their parent PCBs at 11% per year, indicating that these are persistent metabolites that are retained more than their precursor compounds. As a result, the ratio of the concentration of the methyl sulfone metabolites to that of the precursor PCB was found to increase significantly over time.

Another temporal trend study was carried out in humans and examined the milk of breast-feeding mothers from Sweden between the years of 1972 and 1992 (Norén *et al.* 1996). Pooled milk samples from Stockholm women averaging in age between 27 and 29 years were analyzed, and it was found that the sum

concentration of MeSO$_2$-CBs decreased from 9.2 to 1.6 ng/g lipid weight from 1972 to 1992. The congener pattern was not observed to change significantly over time, as in the guillemot study described above. However, unlike the guillemot study, the decrease in the sum MeSO$_2$-CB concentration displayed a strong linear correlation (r$^2$ = 0.95) with the sum PCB concentration, indicating a similar rate of excretion of both compound classes via lactation in humans.

## 1.6      Analytical methods for the determination of MeSO$_2$-CBs

### 1.6.1   Gas chromatographic methods

Many of the previous studies of MeSO$_2$-CBs have employed conventional gas chromatographic techniques with polysiloxane-type columns (Haraguchi *et al.* 2005b, Larsson *et al.* 2002, Larsson *et al.* 2004, Stapleton *et al.* 2001). This technique is quite effective at separating the various congeners from one another. A representative chromatogram is depicted in **Figure 1.4** on the following page. Note that the congeners 3′-MeSO$_2$-CB101 and 4-MeSO$_2$-CB70 partially co-elute, with the latter peak appearing as a shoulder on the right side of the former (Letcher *et al.* 1995). However, since these congeners are penta-chlorinated and tetra-chlorinated, respectively, they could be resolved with the use of mass spectrometry for detection.
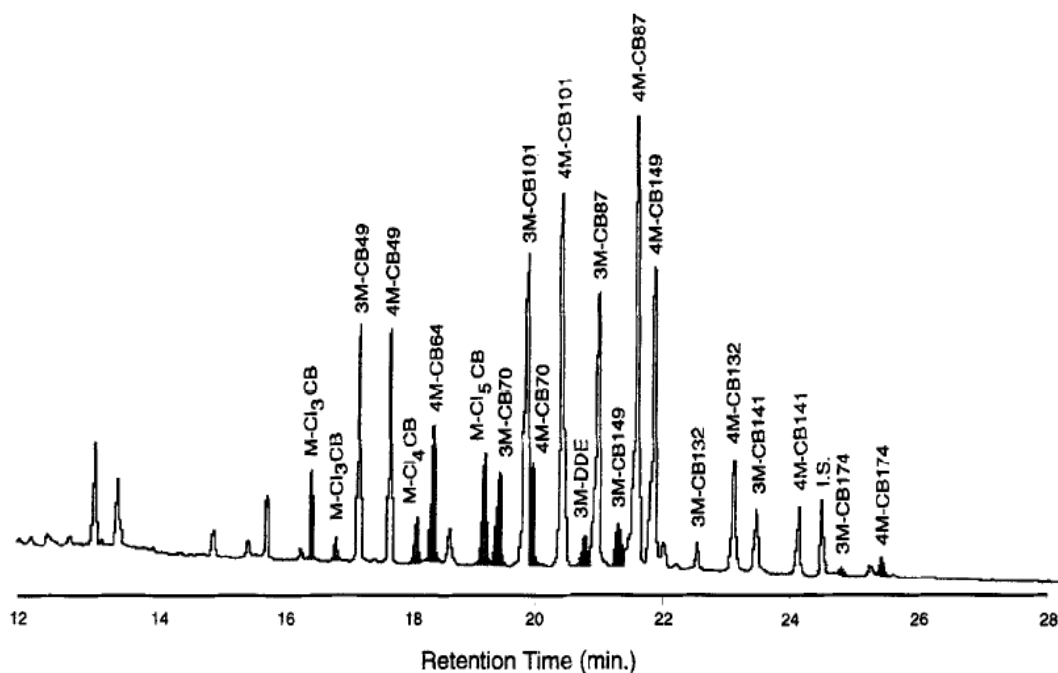
**Figure 1.4: Conventional GC separation of MeSO$_2$-CBs and -DDE in pooled polar bear adipose tissue from the Canadian Arctic[3]**
*GC-ECD chromatogram using a 30 m DB-5 column. DDE: 2,2-bis(4-chlorophenyl)-1,1-dichloro ethene. IS: internal standard, 3-MeSO$_2$-2-Me-2',3',4',5,5'-pentachlorobiphenyl. M-Cl$_x$CB: unidentified congener with x chlorines, as determined by GC-MS. Darkened peaks are congeners not previously identified and/or quantified in Canadian polar bear tissues.*

Enantioselective gas chromatography is by far the dominant separation method used for chiral analysis of MeSO$_2$-CBs and is the only method that has been used for enantiomer quantitation of these contaminants to date. A variety of different derivatized β-cyclodextrin stationary phases have been used to produce successful enantioseparations for some of the chiral MeSO$_2$-CBs, including the commercially available columns BGB-172 (Wiberg *et al.* 1998) and Chirasil-Dex (Chu *et al.* 2003a), as well as two columns handmade by König and coworkers

---

[3] Reprinted from *The Science of the Total Environment*, Vol. 160/161, Letcher, R.J., Norstrom, R.J., and Bergman Å., "Geographical distribution and identification of methyl sulfone PCB and DDE metabolites in pooled polar bear (*Ursus maritimus*) adipose tissue from western hemisphere Arctic and Subarctic regions", p. 409-420, Copyright 1995, with permission from Elsevier.

(König *et al.* 1994): heptakis(2,3-di-*O*-methyl-6-*O*-*tert*-hexyldimethylsilyl)-β-cyclodextrin dissolved 1:1 (w/w) in OV1701 (Ellerichmann *et al.* 1998, Larsson *et al.* 2004) and 1:4 (w/w) in SE52 (Karásek *et al.* 2007, Larsson *et al.* 2002). In one study, five different commercially available enantioselective GC columns were compared, including: BGB-172, β-Dex 120, β-Dex 325, and γ-Dex 325 (Wiberg *et al.* 1998). The only column that gave successful enantioseparation other than BGB-172 was β-Dex 325, which gave resolution 0.7 for 5′-MeSO$_2$-CB174 and 0.5 for 4′-MeSO$_2$-CB174. It was noted that improved resolution was obtained for the *meta*-MeSO$_2$-substituted congeners compared to the *para*-isomers with the BGB-172. Only 5 of the chiral congeners could be separated into their enantiomers on Chirasil-Dex, and the analysis time was extremely long at 300 minutes or 5 hours (Chu *et al.* 2003a). The columns handmade by König and coworkers are by far the most successful, giving baseline or near-baseline resolution for the enantiomers of 8 out of the 10 chiral congeners (Ellerichmann *et al.* 1998). A representative chromatogram of an analytical standard analyzed using the 1:1 (w/w) in OV1701 version of this column is presented in **Figure 1.5** on the following page. The GC-based methodologies suffer from two key disadvantages: long run times, on the order of 2 to 5 hours, and limited or no resolution for some of the chiral congeners. The enantiomers of 3′-MeSO$_2$-CB95 and 4′-MeSO$_2$-CB95 have proven to be particularly difficult to separate. Only a small number of studies have attempted enantioselective GC for the *meta*-(Ellerichmann *et al.* 1998) and *para*-substituted (Ellerichmann *et al.* 1998, Karásek *et al.* 2007, Wiberg *et al.* 1998) forms of this congener relative to the

other chiral analytes, likely due to the fact that analytical standards have only

recently become commercially available. Nonetheless, enantiomer separation of

these compounds remains elusive since none of the studies that have attempted to

separate them have been successful.
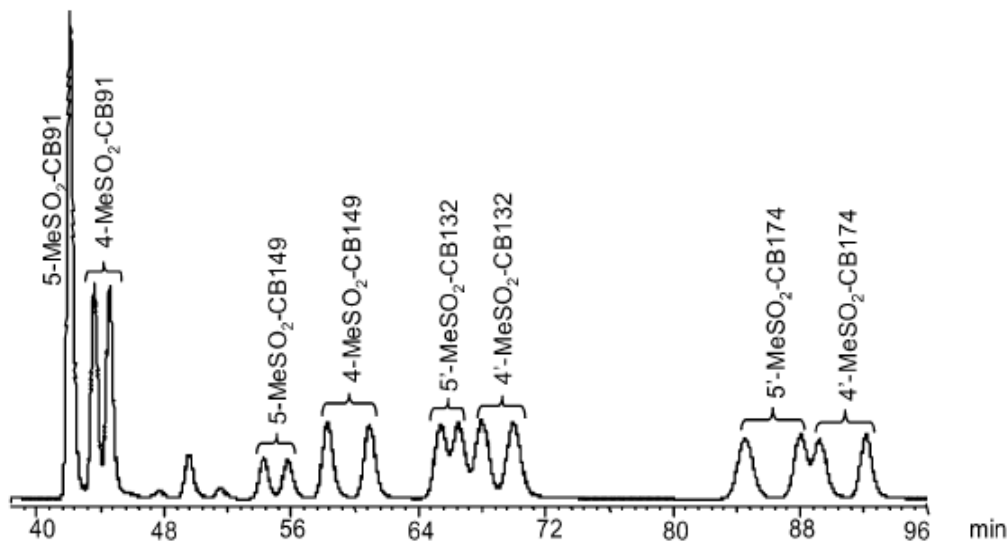


**Figure 1.5: GC-MS enantioseparation of seven chiral MeSO$_2$-CBs[4]**
*GC-ENCI-MS chromatogram of pure analytical standards using a 10 m 1:1 (w/w)
heptakis(2,3-di-O-methyl-6-O-tert-hexyl)-β-cyclodextrin:OV1701 stationary phase.*

## 1.6.2 Liquid chromatographic methods

Liquid chromatography has been used as a sample preparation tool for the

analysis of PCBs in tissue extracts for some time. Both open column and high

performance packed column methods have been explored for fractionating PCBs

from different types of contaminants, including polyaromatic hydrocarbons

---

[4] Adapted with permission from Larsson, C., Norström, K., Athanansiadis, I., Bignert, A., König, W.A., and Bergman, Å., **2004**, "Enantiomeric specificity of methylsulfonyl-PCBs and distribution of bis(4-chlorophenyl) sulfone, PCB, and DDE methyl sulfones in grey seal tissues", *Environmental Science & Technology*, 38: 4950-4955. Copyright 2004 American Chemical Society.

(PAHs) (Jaouen-Madoulet *et al.* 2000), polychlorinated dibenzo-*p*-dioxins

(PCDDs), polychlorinated dibenzo-*p*-furans (PCDFs), and halonapthalenes (Wells

*et al.* 1995), and/or for isolating the low concentration, high toxicity co-planar

congeners from the other PCBs (Haglund *et al.* 1990b). Activated carbon and

porous graphitic carbon were some of the earlier stationary phases used, but these

adsorbents suffer from a number of drawbacks, including very broad, highly

tailed peaks (Haglund *et al.* 1990b), and irreversible adsorption (Ramos *et al.*

1999). One the other hand, solid phase extraction cartridges containing carbon-

based adsorbents have been applied to the fractionation of PCBs, PCDFs and

PCDDs from chicken and pork sausage with good results (Concejero *et al.* 2001).

Packed silica gel-based HPLC columns containing a bonded 2-(1-

pyrenyl)ethyldimethylsilyl stationary phase, more commonly referred to as PYE,

have been applied to the fractionation of PCBs in order to isolate the mono- and

non-*ortho*, coplanar congeners from the di- to tetra-*ortho*-chlorinated, non-

coplanar congeners and other bulk contaminants in Aroclor mixtures and in

marine biota and tissue extracts (Haglund *et al.* 1990a, 1990b, Jaouen-Madoulet *et*

*al.* 2000, Wells *et al.* 1995). In addition, one study used this stationary phase to

separate PCBs into fractions prior to GC analysis (Ramos *et al.* 1999). These

workers found that it was possible to isolate the chiral congeners from several of

the achiral isomers that cause interferences during enantioselective GC with

Chirasil-Dex. In this way, a complete, interference-free analysis of 41 PCBs of

environmental and toxicological importance was achieved by coupling off-line

PYE fractionation with conventional and enantioselective GC methods.

A couple of studies have been carried out to compare the performance of some of these different sorbents and stationary phases for PCB fractionation. For example, the graphitic carbon based adsorbents Amoco PX-21, Carbosphere, and Carbopack B and C, and the silica gel based stationary phase 2-(1-pyrenyl)ethyldimethylsilyl or PYE, were compared for the fractionation of mono- and non-*ortho* PCBs, dioxins and furans from other contaminants (Concejero *et al.* 2001). These workers found that Carbopack B and PYE produced the least background, were the least variable between batches, and the most time- and cost-effective. The PYE column also demonstrated the additional merits of low solvent consumption and the possibility of reutilisation and automation. However, this stationary phase was much more sensitive to the presence of lipids than the other materials examined, a finding that has been corroborated elsewhere (Wells *et al.* 1995). Another study compared various HPLC stationary phases, including monomeric and polymeric C18 phases, as well as PYE and other similar electron donor/acceptor stationary phases, for the purposes of fractionating PCBs, PCDDs and PCDFs (Kimata *et al.* 1997). These researchers found that the PYE stationary phase was one of the best performing both in terms of selectivity and efficiency for PCB fractionation. A coronenylpentylsilyl stationary phase also gave good results with improved planar recognition relative to the PYE column. However, the retention times were longer and the peaks much more tailed. An additional drawback of this material was its lack of commercial availability.

In terms of LC-based enantioselective separations, some preparative scale work has been presented in the literature (Hühnerfuss *et al.* 2002, Pham-Tuan *et*

*al.* 2004, 2005). These studies used 250 x 80 mm Nucleodex β-PM columns, which contain permethylated β-cyclodextrin as the stationary phase, in conjunction with UV detection. The separations were carried out in isocratic elution mode with methanol/water mixtures as the mobile phase at a flow rate of 1.0 to 1.5 mL/min and a column temperature of 5°C. The enantiomers of 5-MeSO$_2$-CB149 (Hühnerfuss *et al.* 2002, Pham-Tuan *et al.* 2004, 2005) and 4-MeSO$_2$-CB149 (Pham-Tuan *et al.* 2004, 2005), as well as 5′-MeSO$_2$-CB132, 4′-MeSO$_2$-CB132 and 5′-MeSO$_2$-CB174 (Hühnerfuss *et al.* 2002) have been resolved on this column to date, and sample chromatograms for selected congeners are presented in **Figure 1.6** on the following page. Interestingly, different enantioselectivity was observed for certain congeners depending on the degree stationary phase methylation (Hühnerfuss *et al.* 2002) (see **Section 2.2.3.1** for further discussion). The enantiomers of 5-MeSO$_2$-CB149 and 4-MeSO$_2$-CB149 were fraction collected and subjected to polarimetry by Pham-Tuan and coworkers (2004, 2005), so the elution order of the enantiomers on Nucleodex β-PM is known to be (+) followed by (-) for both of these congeners. These researchers also subjected the isolated fractions to electronic and vibrational circular dichroism to determine the absolute configurations of the enantiomers. For 5-MeSO$_2$-CB149, the elution order was determined to be (*S*) then (*R*) by UV-CD. For 5-MeSO$_2$-CB149, the elution order was determined to be (*R*) then (*S*) by VCD. The absolute configurations for (*R*)-5-MeSO$_2$-CB149 and (*R*)-5-MeSO$_2$-CB149 are presented in **Figure 1.2** in **Section 1.2.3**.
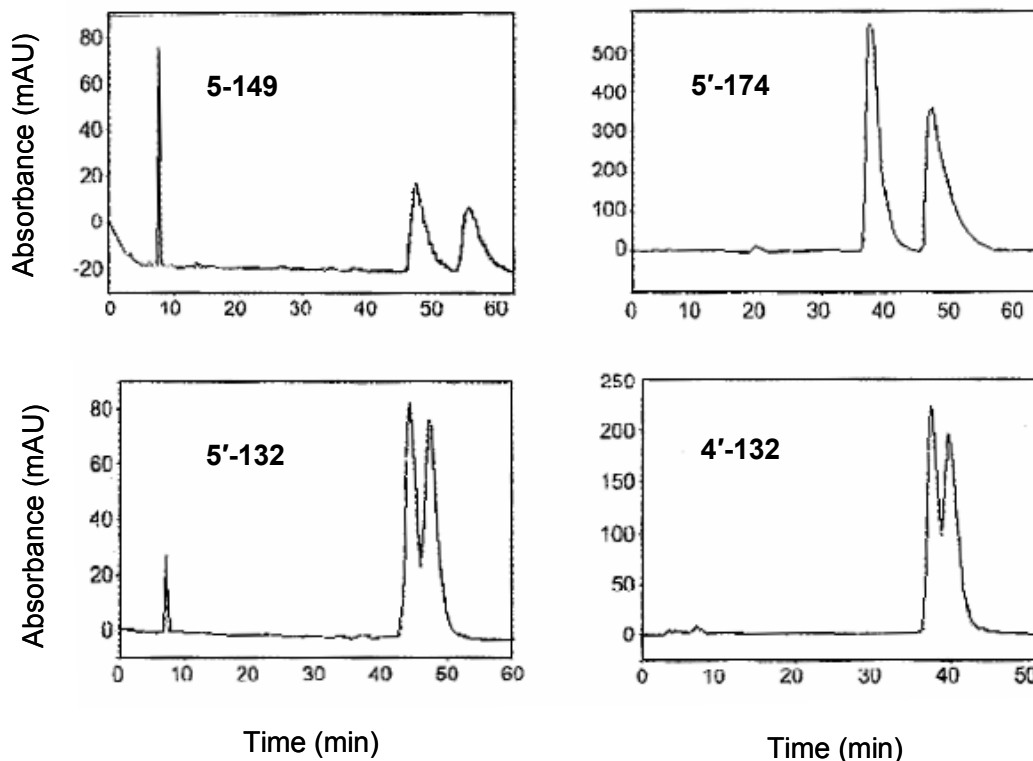
**Figure 1.6:** **Enantioselective HPLC Separation of Selected MeSO$_2$-CBs using a Nucleodex β-PM Column[5]**
*mAU = milli absorbance units*.

Nucleodex β-PM columns are useful for the enantioseparation of several chiral PCB congeners. Baseline resolution has been achieved for PCBs 132 an 174 and partial resolution for PCBs 91 and 95 using this stationary phase (Haglund 1996a). Other workers have obtained baseline enantiomer resolution for PCBs 84, 132, 135, 136, 174 and 175, and partial resolution for PCBs 131, 176, 183 and 196 by optimizing the chromatographic conditions for each congener individually (Reich and Schurig 1999). In this comparative study, ChiraDex and

---

[5] Reprinted with modifications from Hühnerfuss, H., Peters, N., Döbler, J., Larsson, C., Bergman, Å., and Geidel, E., **2002**, "Enantioselective separation of chiral methylsulfonyl-PCB standards by preparative HPLC using methylated cyclodextrin phases", *Organohalogen Compounds*, 59: 287-290, copyright 2002, with permission from the Dioxin International Advisory Board and the authors.

Chirasil-Dex HPLC columns were also investigated. These columns contain native β-cyclodextrin bonded to the silica support via an N-carbamate linker for the former and a permethylated β-cyclodextrin bonded via an eight carbon spacer for the latter. The ChiraDex column gave lower enantiomer resolution for PCBs 84, 136, 176 and 183 compared to the Nucleodex β-PM, but was also able to separate PCBs 45, 91, 95, 139 and 144 with resolution greater than 0.9 for all but PCB 45. The Chirasil-Dex column gave improved enantiomer resolution for PCBs 84 and 132 but worse resolution for PCBs 135, 136, 174 and 176 relative to the Nucleodex β-PM. This column was also able to separate the enantiomers of PCB 91 with similar resolution to the ChiraDex column.

Although derivatized cyclodextrin columns are the only ones that have been investigated for the LC separation of chiral MeSO2-CBs to date, a few other stationary phases have been examined for PCB separations. A polymethacrylate column, Chiralpak OP (+), has been used to separate PCBs 144 and 183 in reversed phase (Harju and Haglund 1999). A triacetylcellulose column has been used previously for the separation of PCB 45 and PCB 91 enantiomers (Püttmann et al. 1986). This stationary phase has also been reported to give improved resolution of the enantiomers of PCBs 88 and 139 compared to Nucleodex β-PM (Haglund 1996a). Carbohydrate-based columns are extremely diverse in the types of compounds they can separate, which include biphenyl derivatives, organometallic compounds, and ketone, amine, acid, alcohol, and ether containing compounds (Okamoto and Kaida 1994). In particular, the tris-(3,5-dimethylphenylcarbamate) derivatives of amylose and cellulose, or Chiralpak AD

and Chiralcel OD, and the tris-(4-methylbenzoate) derivative of cellulose, or

Chiralcel OJ, are known to give very broad enantioselectivity (Perrin *et al.* 2002).

Large selectivity factors are common using these stationary phases, and

separations of flurbiprofen and of amino acid derivatives with distances between

enantiomers on the order of 6 and 3 to 4 baseline peak widths have been

published using supercritical and subcritical fluid chromatography with Chiralpak

AD, respectively (Medvedovici *et al.* 1997, Wenda and Rajendran 2009). The

possibility of using a carbohydrate column for the separation of $MeSO_2$-CBs will

be examined in the current work.

### 1.6.3   *Detection methods*

Electron capture and mass spectrometric detection have been used

extensively in conjunction with gas chromatography for the analysis of $MeSO_2$-

CBs. As with PCBs, electron capture detection (ECD) is more sensitive for the

higher chlorinated congeners than the lower chlorinated isomers. While quite

sensitive, ECD is not a very selective detection method, and thorough sample

preparation must be carried in order to avoid interference from other chlorinated

contaminants. In addition, it is not used for detection with enantioselective gas

chromatography with certain stationary phases due to the interferences that may

arise from column bleed leading to unreliable enantiomer fractions.

The majority of conventional and all enantioselective gas chromatography

methods for the analysis of $MeSO_2$-CBs have employed mass spectrometry (MS)

with electron impact (EI) or electron capture negative ionization (ECNI) for

detection. Single quadrupole mass spectrometry is the most common, but one study has employed GC ion trap-tandem mass spectral (GC-ITMS/MS) detection for the analysis of MeSO$_2$-CBs to date (Wiberg *et al.* 1998). These workers found that two to five times lower detection could be achieved with GC-ECNI-MS compared to GC-EI-ITMS/MS, but improved selectivity was obtained with the latter technique. Electron impact ionization is performed in positive ion mode for MeSO$_2$-CBs, and the positive molecular ion is typically the most abundant. The fragmentation patterns of these compounds with EI have been studied in detail, and the most common fragments for the *meta*- and *para*-MeSO$_2$-substituted congeners involve losses of portions of the methylsulfonyl group (Bergman *et al.* 1980b, Haraguchi *et al.* 1987b) (discussed in greater detail in **Section 2.2.2**). Electron capture negative ionization is more frequently used in recent years due to the 500 to 1000 times greater sensitivity achieved over EI (Haraguchi *et al.* 1993). Pure methane is typically used as the reagent gas, although mixtures of methane and argon have also been employed in order to decrease the amount of hydrocarbons in the background and the abundance of hydrogen inclusion products (Buser *et al.* 1992). This technique is generally used in negative ion mode and the dominant ion produced depends on the quantity of oxygen present within the source. In extremely air-tight systems, the negative molecular ion is the most abundant (Letcher and Norstrom 1997), but in systems where a small amount of oxygen is present, even as little as 100 ppm, the MeSO$_2$-CBs tend to lose a chlorine and gain an oxygen in the source to produce $[M - Cl + O]^-$ ions (Haraguchi *et al.* 1993). Less fragmentation is generally observed with ECNI, but

the most common fragments involve losses of parts of the methylsulfonyl group and/or hydrogen inclusion products, such as $[M - CH_3SO_2 + H]^-$ and $[M - Cl + H]^-$ (Haraguchi *et al.* 1993, Letcher and Norstrom 1997). The sensitivity for the *para*-substituted analytes is much higher than that for the *meta*-substituted analytes by both EI (Bergman *et al.* 1980b, Haraguchi *et al.* 1987b) and ECNI (Letcher and Norstrom 1997). The authors of these studies attributed this phenomenon to the additional resonance structures and therefore stability of the *para*-substituted molecular ions, as shown in **Figure 1.7** on the following page. The mass spectral fragmentation patterns observed for the analysis of MeSO$_2$-CBs with EI and ECNI are discussed in greater detail in **Section 2.2.2**.

As mentioned previously, the only liquid chromatographic studies of methyl sulfone PCBs to date have involved enantiomer fractionation of pure standards using UV detection (Hühnerfuss *et al.* 2002, Pham-Tuan *et al.* 2004, 2005). In this case, a high level of selectivity was not required, so the use of a UV detector was appropriate. However, due to its universality and low selectivity, UV detection is not widely used for environmental analysis due to interference issues. The sensitivity of this method can also be quite low depending on how strongly the analytes absorb in the UV region and on the UV cut-off of the chromatographic solvents. Tandem mass spectral detection (MS/MS), on the other, is a popular detection method for environmental analyses with liquid chromatographic separations due to the combination of high selectivity and sensitivity that can be achieved. The most commonly used ionization sources for small molecule analysis with LC-MS/MS are electrospray ionization (ESI) and
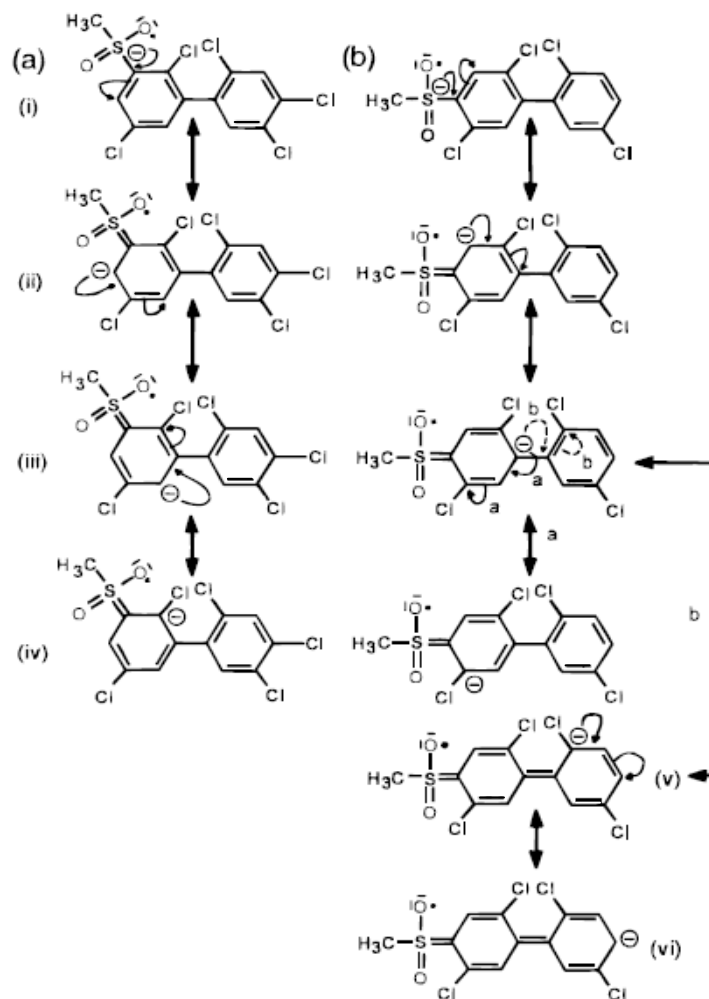
**Figure 1.7: Resonance structures of MeSO$_2$-CB radical anion isomers[6]**
*(a)* meta-*substituted isomer; (b)* para-*substituted isomer.*

atmospheric pressure chemical ionization (APCI). However, these techniques are

generally most effective for moderately to highly polar analytes (Hayen and Karst

2003). That being said, APCI has been employed with some success for the

analysis of non-polar environmental contaminants like PAHs using LC-MS

(Marvin *et al.* 1999, Pérez and Barceló 2001) and PCBs using MS with direct air

---

sampling (Yamada *et al.* 2005). Recently, microchip APCI and APPI sources have been designed for GC-MS, and these have been applied to the analysis of PCBs in soil extracts (Luosujärvi *et al.* 2008). Liquid chromatography-mass spectrometry methods with ESI have also been developed for the analysis of hydroxylated PCB metabolites in the extracted blood plasma of polar bears from the Canadian Arctic (Letcher *et al.* 2005) and eggs of Norwegian birds of prey (Berger *et al.* 2004). In the polar bear study, which employed tandem mass spectral detection, the results of the plasma samples were compared to those obtained by GC-ECD and GC-MS and deemed to be equivalent. The limits of quantitation were also very similar to those obtained by previous GC methods. In the bird of prey study, which employed time of flight mass spectral detection, a GC-high resolution mass spectrometry (HRMS) method was developed simultaneously, and the egg sample results corresponded well between the two methods. However, slightly better limits of detection were achieved with the GC-HRMS method.

In addition to their low ionization efficiency for non-polar analytes, ESI and APCI suffer from a couple of other disadvantages. They are not readily compatible with the highly flammable solvents employed for normal phase LC (i.e. hexane) because of the high voltages applied during ionization (Cai *et al.* 2007a, Chen *et al.* 2005), and they often suffer from matrix effects. A number of studies have explored the sources of matrix effects in LC-MS with ESI and/or APCI. Endogenous compounds present in the sample matrix, such as lipids, proteins and involatile salts, exogenous compounds resulting from sample

preparation and handling, such as polymers extruded from solid phase extraction cartridges, and mobile phase components, such as buffers and ion-pairing agents, are generally agreed to be the main culprits (Annesley 2003, Antignac *et al.* 2005, Mallet *et al.* 2004). A comprehensive study of the mechanisms involved in ion suppression with ESI determined that involatile materials present in the liquid droplets produced during the initial stages of ionization, regardless of their chemical structure or source lead to ion suppression by inhibiting the formation of droplets of decreasing size and, ultimately, analyte ionization (King *et al.* 2000). A number of different strategies for eliminating or decreasing matrix effects during LC-MS analysis with ESI and APCI have been investigated. Thorough sample clean-up is the most reliable (Antignac *et al.* 2005, Mallet *et al.* 2004, Shen *et al.* 2005), although decreasing the LC flow using post-column splitting devices has also proven to be beneficial (Gangl *et al.* 2001, Kloepfer *et al.* 2004). One study that employed both of these strategies along with the use of multiple internal standards structurally similar to the analytes of interest still suffered from matrix effects for the analysis of pharmaceutical compounds in surface water (Van De Steene *et al.* 2006). In this case, it was necessary to use standard addition due to the large variation in matrix effects between samples. Other workers have found that changing the source polarization (i.e. positive versus negative), ion source configuration and/or ion source type can also be beneficial (Antignac *et al.* 2005, Mei *et al.* 2003).

*1.6.3.1 Atmospheric pressure photoionization*

Atmospheric pressure photoionization (APPI) is an alternative ionization source for LC-MS that is becoming increasingly popular due to the wide variety of analytes that can be examined and the typical lack of ion suppression (Bos *et al.* 2006). A diverse array of compounds have been analyzed successfully by LC-APPI-MS, including brominated flame retardants (Debrauwer *et al.* 2005, Lagalante and Oswald 2008, Ross and Wong 2010), estrogenic compounds (Viglino *et al.* 2008), polyaromatic hydrocarbons (Itoh *et al.* 2006), conjugated fatty acid methyl esters (Müller *et al.* 2006), perfluorinated compounds (Chu and Letcher 2008), nitropyrenes (Straube *et al.* 2004), fullerenes (Kawano *et al.* 2006), carbamate pesticides (Takino *et al.* 2004), lipids (Cai *et al.* 2007b, Cai and Syage 2006), and a number of pharmaceutical compounds (Hakala *et al.* 2003, Hsieh *et al.* 2003), including some drug metabolites (Keski-Hynnilä *et al.* 2002, Yang and Henion 2002) and chiral drugs (Cai *et al.* 2007a, Chen *et al.* 2005). This technique was first described as a soft ionization method for LC-MS by Robb and colleagues in 2000 (Robb *et al.* 2000). An orthogonal source design first became commercially available from Syagen Technologies in 2001. Shortly thereafter, in 2002, an axial source design was marketed by Applied Biosystems/MDS Sciex (Wang *et al.* 2005). A schematic of the axial Sciex source configuration, which was used in the current work, is depicted in **Figure 1.8** on the following page. The inlet consists of a stainless steel capillary surrounded by a sheath flow of gas which aids in solvent nebulisation. There is a second inlet with an auxiliary gas flow that may be used for infusion of a dopant. After nebulisation, droplets

containing the analytes, dopant and solvent molecules pass through a heated

quartz tube where desolvation occurs prior to arriving at the ionization region

where they are exposed to photons from a vacuum UV lamp. Finally, any ionized

molecules pass through the orifice at the interface with the mass spectrometer;

any non-ionized species are prevented from entering the orifice by the curtain gas

flow and the entrance potential.
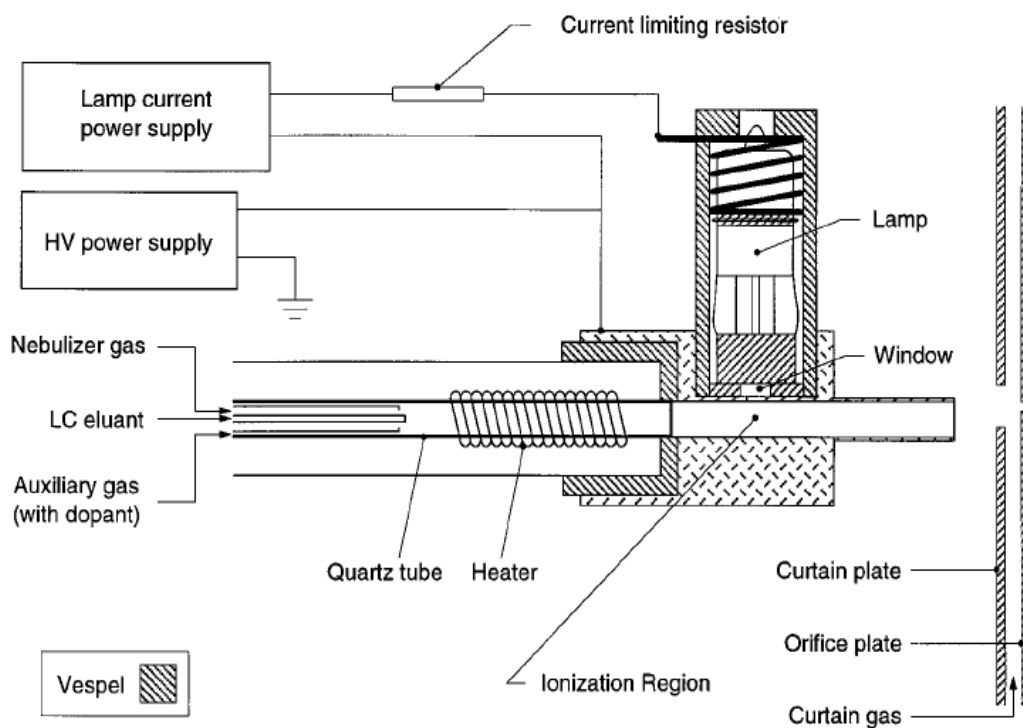


**Figure 1.8:** **Schematic representation of an axial design atmospheric pressure photoionization source**[7]
*Original Applied Biosystems/MDS Sciex APPI source design.*

---

Atmospheric pressure photoionization with LC is quite similar to photoionization detection (PID) with GC, in fact, the same type of gas discharge lamp is used in both (Robb *et al.* 2000). For both GC and LC, the common mobile phase components have fairly high ionization potentials, so the analytes are selectively ionized with little background noise (Robb *et al.* 2000). It was originally assumed that acetonitrile and methanol would not be ionized with APPI, but it has since been discovered that they can react to form isomers, and dimers and trimers in the gas phase, respectively, which are ionizable by the photons emitted by krypton ionization lamps (Marotta *et al.* 2003, Short *et al.* 2007). In fact, these moieties can play an important role as intermediaries between the dopant and the analyte in certain ionization mechanisms (Bos *et al.* 2006, Short *et al.* 2007).

The main ionization mechanisms involved in APPI in positive ion mode are direct photoionization and charge exchange, which produce radical cations, as presented in **Equations 1.1**, and **1.2** to **1.3**, respectively. In addition, proton transfer may occur, which usually involves a sequence of reactions like that presented in **Equations 1.2** to **1.5**, where M is the analyte of interest, D is the dopant, S is the solvent, and *hv* is a photon (Bos *et al.* 2006). Direct photoionization may occur for analytes with low ionization potentials, whereas charge exchange and proton transfer dominate for analytes with high electron affinities and proton affinities relative to the dopant and solvent, respectively (Bos *et al.* 2006). Charge exchange is also favoured when the ionization energy of the analyte is less than that of the dopant (Kauppila and Bruins 2005). It has recently

been demonstrated that neutral radicals of background molecules, including

oxygen, may play an important role in the ionization processes that occur with

APPI (Kersten *et al.* 2009). Note that it is also possible for the analyte molecule to

become photoexcited then undergo a number of de-excitation processes that result

in a neutral analyte molecule, or fragments thereof, such as photodissociation,

radiative decay, and collisional quenching (Raffaelli and Saba 2003).


| | | |
|---|---|---|
| *Direct photoionization* | $M + hv \rightarrow M^{\bullet+}$ | [1.1] |
| *Dopant photoionization* | $D + hv \rightarrow D^{\bullet+}$ | [1.2] |
| *Charge exchange ionization* | $D^{\bullet+} + M \rightarrow D + M^{\bullet+}$ | [1.3] |
| *Solvent protonation* | $D^{\bullet+} + S \rightarrow [D-H]^{\bullet} + [S+H]^{+}$ | [1.4] |
| *Proton transfer* | $[S+H]^{+} + M \rightarrow S + [M+H]^{+}$ | [1.5] |
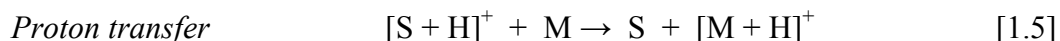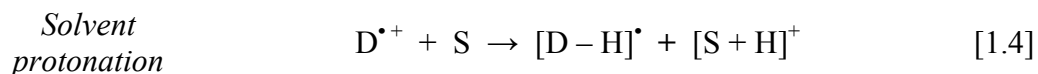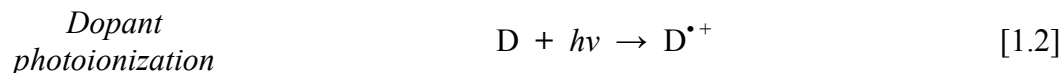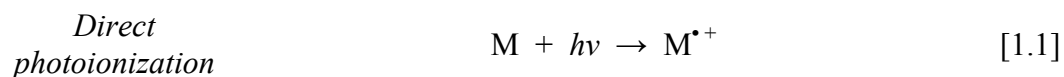

In negative ion mode, mechanisms analogous to those in positive mode are

observed, along with a few additional, unique mechanisms. In all negative ion

reaction mechanisms, the production of free electrons is the first step.

Interestingly, photoionization of the metallic surfaces of the ion source has been

determined to be a significant source of free electrons (Basso *et al.* 2003), as

shown in **Equation 1.6**, where *SS* stands for stainless steel. Photoionization of the

dopant, if used, is also an important source of free electrons (Kauppila *et al.*

2004b), as shown in **Equation 1.7**. Note that the solvent tends to quench free

electrons to produce $S^{\bullet-}$ ions, as shown in **Equation 1.8**. These solvent ions are not known to participate directly in any of the main analyte ionization mechanisms in negative mode.

Charge exchange and proton transfer also occur in negative mode but are sometimes referred to as electron capture and dissociative electron capture, respectively (Song *et al.* 2007). The corresponding reactions are represented in **Equations 1.9**, and **1.12** to **1.14** and are favoured when the analyte has a positive electron affinity in the former case and a low gas phase acidity compared to the solvent and $HO_2^{\bullet}$ in the latter case (Kauppila *et al.* 2004b). Note that charge exchange may also arise from the reaction of the analyte with superoxide radicals, as shown in **Equation 1.10** and **1.11**. This pathway is favoured when the analyte has a higher electron affinity than oxygen (Kauppila *et al.* 2004b). Neutralization of analyte ions by reaction with oppositely charged ions and dissipation due to contact with the source walls are significant loss processes for both negative and positive ion mode APPI (Kauppila and Bruins 2005, Robb and Blades 2005).

One mechanism unique to negative mode is anion attachment, as shown in **Equations 1.15** to **1.17**, where X represents a halogen, most commonly chlorine or bromine (Song *et al.* 2007). This mechanism is only effective for a limited number of analytes, like polyethylenes and polyisobutylene derivatives (Kéki *et al.* 2008a, Kéki *et al.* 2008b), hexabromocyclododecanes (Ross and Wong 2010), and the explosive compounds 1,3,5-trinitroperhydro-1,3,5-triazine (RDX) and 1,3,5,7-tetranitro-1,3,5,7-tetrazocane (HMX) (Song *et al.* 2007), but results in

| | | |
|---|---|---|
| *Production of free electrons* | $SS + h\nu \rightarrow SS + e^-$ | [1.6] |
| *Dopant photoionization* | $D + h\nu \rightarrow D^{\bullet+} + e^-$ | [1.7] |
| *Solvent ionization* | $S + e^- \rightarrow S^{\bullet-}$ | [1.8] |
| *Charge transfer ionization I* | $M + e^- \rightarrow M^{\bullet-}$ | [1.9] |
| *Superoxide ion production* | $O_2 + e^- \rightarrow O_2^{\bullet-}$ | [1.10] |
| *Charge transfer ionization II* | $M + O_2^{\bullet-} \rightarrow M^{\bullet-} + O_2$ | [1.11] |
| *Proton transfer I* | $M + O_2^{\bullet-} \rightarrow [M-H]^- + HO_2^{\bullet}$ | [1.12] |
| *Solvent deprotonation* | $S + O_2^{\bullet-} \rightarrow [S-H]^- + HO_2^{\bullet}$ | [1.13] |
| *Proton transfer II* | $M + [S-H]^- \rightarrow [M-H]^- + S$ | [1.14] |
| *Solvent homolysis* | $S + e^- \rightarrow [S-X]^{\bullet} + X^-$ | [1.15] |
| *Dopant homolysis* | $D + e^- \rightarrow [D-X]^{\bullet} + X^-$ | [1.16] |
| *Anion attachment* | $M + X^- \rightarrow [M+X]^-$ | [1.17] |
| *Substitution /Oxidation* | $M + O_2^{\bullet-} \rightarrow [M-X+O]^- + OX^{\bullet}$ | [1.18] |

excellent sensitivity where applicable. In order to promote these reactions, carbon tetrachloride and dichloromethane were used as the solvents in the two plastic studies conducted by Kéki and coworkers (2008a, 2008b), and 1% methylene chloride in toluene was used as the solvent/dopant in the explosives study carried out by Song and coworkers (2007). The final mechanism encountered in negative ion APPI is substitution. When the reaction involves substitution of an oxygen for an analyte substituent X, typically a halogen or hydrogen, as shown in **Equation 1.18**, it is sometimes referred to as oxidation (Kauppila *et al.* 2002). This ionization mechanism is promoted by the use of air as the nebulising gas rather than nitrogen (Kauppila *et al.* 2002) and has been observed previously for hexachlorobenzene (Kauppila *et al.* 2004b), polybrominated diphenyl ethers (Lagalante and Oswald 2008), tetrabromobisphenol A (Basso *et al.* 2003) and decabromodiphenyl ether (Basso *et al.* 2003, Debrauwer *et al.* 2005), as well as tetra- to octabromodiphenyl ethers (Debrauwer *et al.* 2005). Since these are all halogenated aromatic compounds, PCBs and MeSO$_2$-CBs might be expected to follow this ionization pathway.

One of the most attractive properties of APPI is its general lack of matrix effects. This is partially due to the nature of the analytes for which this ionization source is useful, which is for relatively non-polar compounds. However, it is also partially due to the nature of the ionization process. Several comparative studies have been carried out with ESI, APCI and APPI, and the latter has been demonstrated to have the least problems with matrix effects in many cases. For example, APPI was reported to be more reproducible and to give reduced ion

suppression compared to APCI, in addition to giving 2 to 530 times higher

sensitivity, for the analysis of pharmaceutical compounds by LC-MS (Cai *et al.*

2007a). It has also been demonstrated that significantly reduced matrix effects are

obtained using APPI instead of ESI for the LC-MS analysis of perfluorinated

compounds (Chu and Letcher 2008). An increase in sensitivity of six to eight

times with similar matrix suppression was observed for the analysis of idoxifene

in human plasma with APPI compared to APCI (Yang and Henion 2002).

Improved sensitivity has also been noted for APPI versus APCI for the analysis of

selected pharmaceutical compounds at low solvent flow rates (Hanold *et al.* 2004)

and of pentacyclic triterpenes in positive ion mode (Rhourri-Frih *et al.* 2009).

Improved detection limits were obtained for the analysis of polymer additives

using APPI compared to ESI and APCI as a result of significantly decreased

background noise (Himmelsbach *et al.* 2009). Ionization efficiency with APPI

was not affected by the matrix for the analysis of carbamate pesticides in fruits

and vegetables and gave similar sensitivity to APCI (Takino *et al.* 2004). In

another case, APPI gave similar results to ESI in terms of sensitivity, accuracy

and precision for pharmaceutical analysis (Hakala *et al.* 2003). However, ESI

and/or APCI are typically more effective ionization sources than APPI for polar

compounds. For example, ESI was the most sensitive technique for the analysis of

highly polar drug metabolites, like glucoronides, compared to APCI and APPI

(Keski-Hynnilä *et al.* 2002). Ionspray also gave the best sensitivity for the

analysis of flavonoids compared to APCI and APPI (Rauha *et al.* 2001). Further

discussion of APPI, including mobile phase solvent and flow rate effects, as well as dopant and UV lamp characteristics, is presented in **Section 2.2.1**.

## 1.7    Study objectives

To summarize, although the toxic effects of methyl sulfone PCBs have been well characterized, both for individual congeners and for mixtures, the toxicity of the individual enantiomers remains to be studied. It has been established that high enantiomeric excesses of these compounds are found in the tissues of many organisms, including humans (Ellerichmann *et al.* 1998). In order to investigate the toxicity of the enantiomers and to develop a greater understanding of the enantioselective processes affecting their fate within organisms, an effective chiral analysis method is required. The main technique currently used for this purpose is enantioselective GC. However, there have been some analytical issues with this methodology, including extremely long run times (Chu *et al.* 2003a), and little or no enantioselectivity for some of the chiral congeners, particularly with the use of commercially available columns (Wiberg *et al.* 1998). Some work has been performed using preparative scale enantioselective liquid chromatography to isolate the enantiomers of selected congeners for structural (Pham-Tuan *et al.* 2004, 2005) or toxicological (Hühnerfuss *et al.* 2002) characterization. However, several of the chiral MeSO$_2$-CB congeners have yet to be studied using this technique.

The primary goal of this study is to develop a comprehensive analytical method to separate both the chiral compounds into their enantiomers and the

achiral and chiral congeners from one another and to accomplish this using commercially available columns and with a reduced run time compared to previous enantioselective GC methods. In addition, atmospheric pressure photoionization will be employed due to its efficacy for the ionization of non-polar compounds, its compatibility with a wide variety of solvents, and its lower susceptibility to matrix effects compared to other techniques. Tandem mass spectrometry will be used in order to achieve sufficient sensitivity and selectivity to reliably quantify these analytes in tissue extracts. Finally, the validated method will be applied to the analysis of animal tissue extracts in order to demonstrate its utility for environmental analysis.

## 2 Development of an enantioselective LC-LC-APPI-MS/MS method for the analysis of MeSO$_2$-CBs in tissues

### 2.1 Experimental

#### *2.1.1 Samples*

Norwegian glaucous gull (*Larus hyperboreus*) plasma samples were procured from Drs. Jonathan Verreault and Robert Letcher of Environment Canada (National Water Research Institute, Burlington, ON, Canada) and Dr. Geir Gabrielsen of the Norwegian Polar Institute (Tromsø, Norway). Plasma samples were collected from birds in colonies at Teltvika, Kapp Harry and Glupen along the southern cliffs of Bjørnøya, or Bear Island (74° 22′N, 19° 05′E), a small Arctic island located between mainland Norway and the island of Svalbard. A map of Bear Island is provided in **Figure 2.1** on the following page. The sampling period was from May to June 2002 and 2004. Detailed descriptions of the sampling area and collection methods are provided elsewhere (Verboven *et al.* 2008, Verreault *et al.* 2004).

Greenland sledge dog (*Canis familiaris*) plasma and adipose tissue samples were procured from Environment Canada care of Dr. Robert Letcher. The captive dogs were raised in Aasiaat, a small community located in Disko Bay, central West Greenland, as part of a multi-generational feeding study. A map of Greenland showing the location of Aasiaat is provided in **Figure 2.2**. The study was carried out between the years 2003 and 2005, and full descriptions of the experimental design and tissue collection methods can be found elsewhere (Verreault *et al.* 2009a). Briefly, the parental generation (P) consisted of pairs of
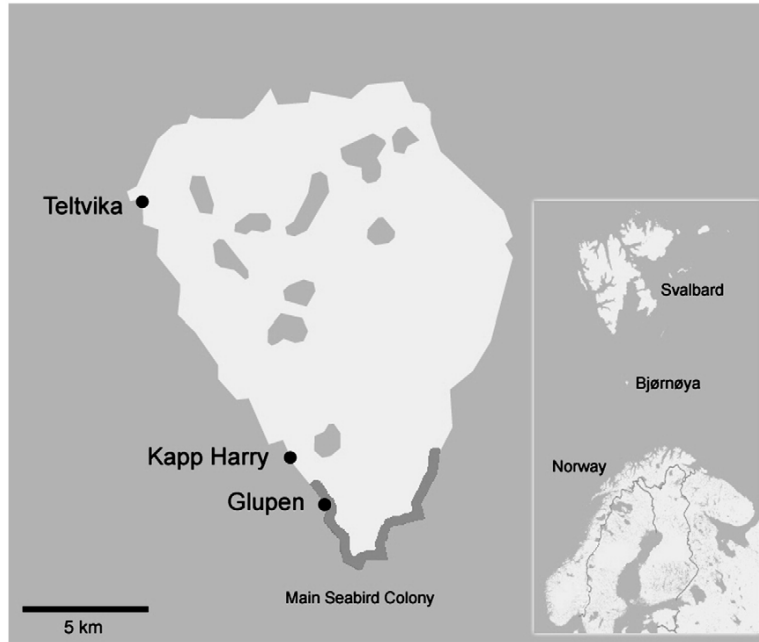
**Figure 2.1:** **Map of Bjørnøya (Bear Island) with the locations of the three glaucous gull study sites and main seabird colony**[8]

sister dogs that were split into two groups, a control group (CON) and an exposure group (EXP). Control group dogs were fed a diet of pork fat known to be low in organic contaminants (OCs), whereas exposure group dogs were fed a diet of Greenland minke whale (*Balaenoptera acutorostrata*) blubber known to be high in OCs. A subset of dogs from the P-CON and P-EXP groups were selected for breeding with a single, control diet-fed male. The dogs were bred on two occasions to produce two generations of male and female offspring, such that the first generation had reached sexual maturity (F1) when the second generation was still pre-weaning (F1-MLK). Both generations of offspring received only milk from their mothers pre-weaning. Therefore, both the F1-EXP and F1-MLK-EXP

---

[8] Reprinted from *Comparative Biochemistry and Physiology Part C*, Vol. 148, Verboven, N., Verreault, J., Letcher, R.J., Gabrielsen, G.W., Evans, N.P., "Maternally derived testosterone and 17β-estradiol in the eggs of Arctic-breeding glaucous gulls in relation to persistent organic pollutants", p. 143-151, Copyright 2008, with permission from Elsevier.

group pups were exposed to OCs through their P-EXP mothers' milk, whereas the

F1-CON and F1-MLK-CON group pups had limited exposure to OCs from their

P-CON mothers. Post-weaning, the F1-CON offspring received a pork fat diet

like their mothers, whereas the F1-EXP offspring received the minke whale

blubber diet, leading to further exposure to OCs.
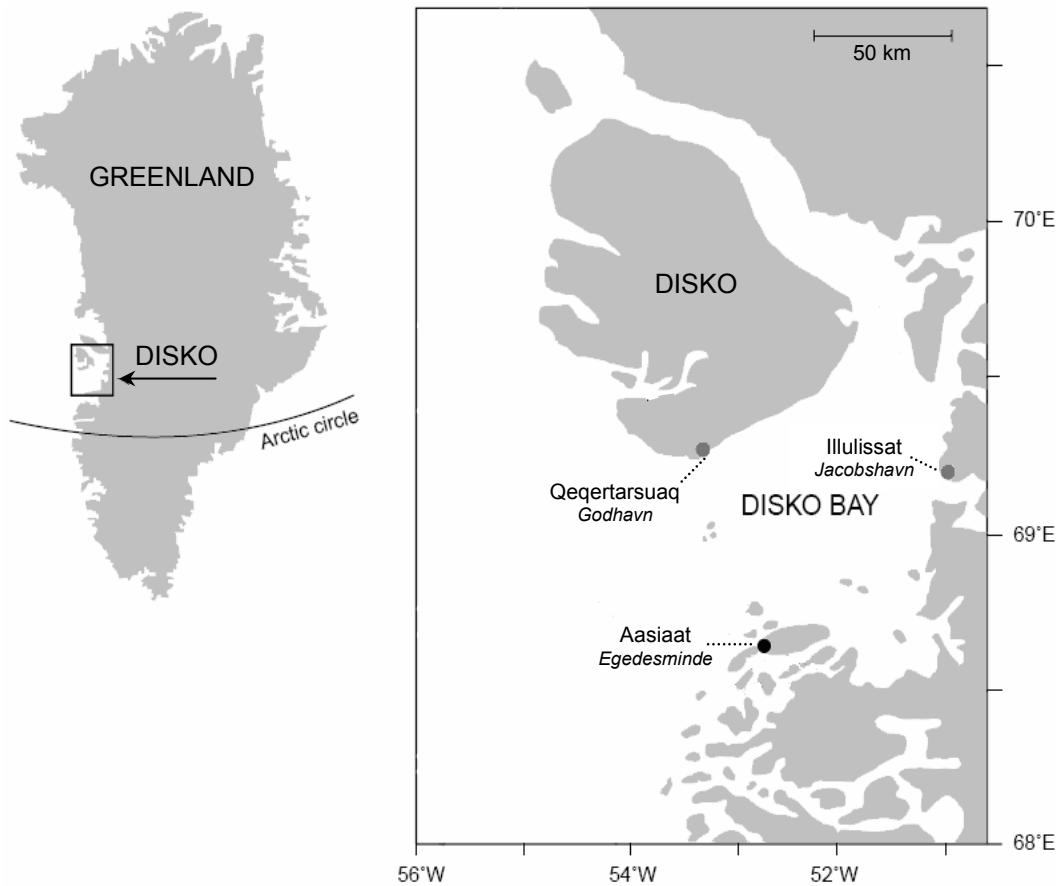


**Figure 2.2:** **Map of Greenland with the location of the sledge dog study site[9]**
*Location of Aasiaat is indicated with a black circle.*

[9] Reprinted with modifications from *Deep-Sea Research I*, Vol. 50, Hansen, A.S., Nielsen, T.G., Levinsen, H., Madsen, S.D., Thingstad, T.F., and Hansen, B.W., "Impact of changing ice cover on pelagic productivity and food web structure in Disko Bay, West Greenland: a dynamic model approach", p. 171-187, Copyright 2003, with permission from Elsevier.

## 2.1.2 Chemicals

High purity analytical standards of 25 *meta-* and *para*-substituted methylsulfonyl polychlorinated biphenyl metabolites (3′-MeSO$_2$-CB49, 4′-MeSO$_2$-CB49, 3-MeSO$_2$-CB52, 4-MeSO$_2$-CB52, 4-MeSO$_2$-CB64, 3-MeSO$_2$-CB70, 4-MeSO$_2$-CB70, 3′-MeSO$_2$-CB87, 4′-MeSO$_2$-CB87, 5-MeSO$_2$-CB91, 4-MeSO$_2$-CB91, 3′-MeSO$_2$-CB95, 4′-MeSO$_2$-CB95, 3′-MeSO$_2$-CB101, 4′-MeSO$_2$-CB101, 5-MeSO$_2$-CB110, 4-MeSO$_2$-CB110, 5′-MeSO$_2$-CB132, 4′-MeSO$_2$-CB132, 3′-MeSO$_2$-CB141, 4′-MeSO$_2$-CB141, 5-MeSO$_2$-CB149, 4-MeSO$_2$-CB149, 5′-MeSO$_2$-CB174 and 4′-MeSO$_2$-CB174) were purchased from AccuStandard (New Haven, CT, USA). A methylated methylsulfonyl polychlorinated biphenyl, 3-MeSO$_2$-4-Me-2′,3′,4′,5,5′-pentachlorobiphenyl, was purchased from Cambridge Isotope Laboratories (Andover, MA, USA) for use as an internal standard. All standards were of 97% purity or greater.

High performance liquid chromatography grade methanol, ethanol, isopropanol, hexanes and heptanes were obtained from Fisher Scientific Inc. (Ottawa, ON, Canada). These solvents were filtered with 2 μm polytetrafluoroethylene (PTFE) membrane filters (Chromatographic Specialties, Hamilton, ON, Canada) prior to use. High purity, HPLC grade toluene was obtained from Sigma-Aldrich (Oakville, ON, Canada) and was also filtered with PTFE membrane filters prior to use. De-ionized water was purified to 18 MΩ using an Ultrapure Nanopore filtration system (Barnsteam/Thermolyne, Dubuque, IA, USA) and was filtered with 2 μm Whatman nylon membrane filters (Whatman Inc., Piscataway, NJ, USA) immediately prior to use. A complete

listing of the materials used for the tissue extractions can be found in Verreault *et al.* 2005 for the glaucous gull samples and in Gebbink *et al.* 2008 for the sledge dog samples.

### 2.1.3 *Sample preparation*

All extracted glaucous gull and sledge dog tissue samples were received in glass vials with PTFE-lined caps and stored at -20°C until analysis. During transportation from the field, the tissue samples were stored below -5°C, then below -20°C in a laboratory freezer prior to extraction. No change in the chiral signature of the parent PCBs or their metabolites is expected during storage of the tissue samples or extracts due to the high rotational barrier (105 to 204 kJ/mol) associated with enantiomerization for these compounds (Eliel and Wilen 1994, Kaiser 1974). In addition, the presence of organic solvents in the extracts would prevent chiral biotransformation by denaturing any residual biological molecules (Wong *et al.* 2001).

Glaucous gull sample extractions were performed by study participants at Environment Canada and the Norwegian Polar Institute. A full description of the extraction method employed can be found elsewhere (Verreault *et al.* 2005a). In short, 2 to 3 g of plasma was isolated and spiked with internal standard, acidified with 1 mL of 6 M hydrochloric acid and diluted with 3 mL of isopropanol. Three liquid-liquid extraction steps were then performed with 6 mL of 50:50 methyl-*tert*-butyl ether:*n*-hexane volume/volume (v/v) and the combined organic layers conserved for further processing. After the bulk of the lipid material was removed

by gel permeation chromatography (GPC), 6 mL of 1 M potassium hydroxide in 50:50 water:ethanol v/v was added in a liquid-liquid partitioning step, with the organic layer containing the $MeSO_2$-CBs. After concentration of the organic layer, a Florisil® (8.0 g magnesium silicate, 60–100 mesh) column deactivated with 1.2% water weight/weight (w/w) was used to fractionate the organic contaminants. Four fractions were collected with the consecutive addition of: 38 mL of *n*-hexane, 34 mL of 15:85 dichloromethane (DCM):*n*-hexane v/v, 54 mL of 50:50 DCM:*n*-hexane v/v, and, finally, 80 mL of 7:93 methanol:DCM v/v. The $MeSO_2$-CBs were contained in fraction four, and the volume of this fraction was reduced to 1 mL by rotary evaporation. Further purification was then achieved using a basic alumina column (3.0 g, Brockman activity grade I, 60–325 mesh, deactivated with 2.3 % water w/w) with 50 mL of 50:50 DCM:*n*-hexane v/v as the eluent. The sample volume was reduced once again, first to 1 mL by rotary evaporation, then to dryness under a stream of nitrogen, followed by reconstitution in 100 µL of isooctane. Before analysis by LC-LC-APPI-MS/MS, the samples were evaporated to dryness under a stream of nitrogen and reconstituted in filtered HPLC grade heptanes.

Sledge dog sample extractions were also performed by study participants at Environment Canada. A complete description of the extraction method employed can be found elsewhere (Gebbink *et al.* 2008b). Briefly, sledge dog adipose tissue (approximately 0.5 g) was homogenized with sodium sulphate and spiked with internal standard prior to extraction with 50:50 DCM:*n*-hexane v/v. Instead of using GPC for lipid removal, concentrated hydrochloric acid was added

in a liquid-liquid partitioning step, and the MeSO$_2$-CB-containing acid fraction reserved. After dilution with an equal volume of water, the MeSO$_2$-CBs were back-extracted into *n*-hexane, then cleaned up using basic silica chromatography (2 g impregnated with 33% 1 M potassium hydroxide w/w) with 50 mL of 50:50 DCM:*n*-hexane v/v as the eluent. The remainder of the extraction procedure was the same as that described above for the glaucous gull plasma samples with Florisil® and alumina clean up chromatographies. Initial treatment of the sledge dog blood samples was similar to that described for the glaucous gull plasma samples, with acidification, followed by extraction with methyl-*tert*-butyl ether and *n*-hexane, and partitioning with potassium hydroxide, except that 2 g of whole blood was used instead of blood plasma. The remainder of the extraction procedure was identical to that described above for the sledge dog adipose tissue samples.

### 2.1.4   Instrumental analysis

*2.1.4.1 Atmospheric pressure photoionization tandem mass spectrometry*

A QTrap® triple quadrupole mass spectrometry system equipped with a first generation PhotoSpray® source (Applied Biosystems/MDS Sciex, Foster City, CA, USA),  integrated syringe pump (Harvard Apparatus, Holliston, MA, USA) and 10-port diverter valve (VICI Valco Instruments Co. Inc., Houston, TX, USA) was employed for detection purposes. The PhotoSpray APPI source was operated in negative ion mode with either a krypton (10.0/10.6 eV, model PKS 100, Heraeus Noblelight GmbH, Hanau, Germany) or an argon (11.8 eV, model

81

FA-737U, Perkin Elmer Optoelectronics, Salem, MA, USA) gas discharge lamp. The lamp current was held constant between 0.70 and 0.85 mA by the APPI source control unit. Dry, purified air and high purity nitrogen (at least 99.5%) were produced on site. In-house shop air was first compressed using a bootstrap compressor (model AA001, Midwest Pressure Systems, Carol Stream, IL, USA) then split into two streams. The first stream was directed to a Parker Balston model N2-14 nitrogen generator to produce high purity nitrogen for use as the lamp and CAD gases, and the second stream passed through a Parker Balston model PB 64-01 membrane air dryer and a HPZA-18000 zero air generator (Parker Hannifin Corp., Haverhill, MA, USA) to produce dry, purified air for use as the curtain, nebulizer and auxiliary gasses. For experiments using argon as the CAD gas, tanks of 99.998% pre-purified argon were used (Praxair, Edmonton, AB, Canada).

Ion source parameters were optimized for each analyte individually by off-column flow injection analysis. The optimized LC mobile phase was delivered at a flow rate of 1.0 mL/min directly to the detector. Individual analyte solutions, 1 μg/mL in hexanes, were analyzed for each set of conditions with an injection volume of 5 μL. Most analyses were carried out in triplicate. Experiments requiring the use of toluene as a dopant employed an external syringe pump (model 11 Plus Advanced, Harvard Apparatus, Holliston, MA, USA) for dopant delivery. The optimized ion source parameters were as follows: curtain gas (*CUR*) 10 psi**,** ion spray voltage (*IS*) -1100 V, nebulizer gas (*GS1*) 90 psi, auxiliary gas (*GS2*) 10 psi**,** interface heater on, probe axial position 2.5 mm, and probe lateral

position 7.0 mm. The remaining parameters varied with the type of gas discharge lamp employed. For the Ar lamp, a lamp gas (*LG*) setting of 3.0 L/min and a heated nebulizer temperature of 250°C with no dopant was optimal. These conditions were employed for all LC-LC-APPI-MS/MS analyses. Conversely, for the Kr lamp, a lamp gas flow of 1.0 L/min and source temperature of 400°C with toluene dopant delivered at 100 μL/min (10% of the LC flow) was deemed optimal, and, unless otherwise stated, these conditions were employed for all flow injection and infusion experiments with this lamp. The results of the ion source optimization experiments are discussed in greater detail in **Section 2.2.1.**

Mass spectral detection parameters were optimized for each congener individually by infusion. Analyte solutions, 1 μg/mL in hexanes, were infused at 10–20 μL/min using the QTrap integrated syringe pump. A mobile phase consisting of 95:2.5:2.5 heptanes:methanol:ethanol was delivered at 0.5 mL/min and the analyte solution infused into the mobile phase stream via a polyether ether ketone (PEEK) T-piece. For all analytes, a collisionally activated dissociation (*CAD*) gas setting of 5 psi was optimal. The remaining multiple reaction monitoring (MRM) parameters, consisting of the various applied potentials (in Volts), including declustering potential (*DP*), entrance potential (*EP*), collision energy (*CE*), collision cell entrance potential (*CEP*) and collision cell exit potential (*CXP*), varied between transitions. A total of 9 MRM transitions were employed in the final method with a dwell time of 100 ms each. The optimal parameters for each transition are summarized in **Table 2.1** on the following page.

**Table 2.1: Optimal tandem mass spectral detection parameters for methylsulfonyl-polychlorinated biphenyl analysis**

*In multiple reaction monitoring mode with atmospheric pressure photoionization source in negative ion mode.*
*[a] All congeners lost a chlorine and gained an oxygen in source leading to a [M – Cl + O]⁻ parent ion.*
*[b] Internal standard: 3-MeSO$_2$-4-Me-2',3',4',5,5'-pentachlorobiphenyl.*

| Parent congener chlorination level | Mass-to-charge ratio (*m/z*, amu) | | | Daughter ion structure | Voltage (V) | | | | |
| --- | --- | --- | --- | --- | --- | --- | --- | --- | --- |
| | Parent molecule | Parent ion[a] | Daughter ion | | *DP* | *EP* | *CE* | *CEP* | *CXP* |
| Tetra | 368 | 349 | 242 | [M – Cl + O – CH$_3$SO$_2$ – CO]⁻ | -50 | -9 | -40 | -21 | -2 |
| Tetra | 368 | 349 | 270 | [M – Cl + O – CH$_3$SO$_2$]⁻ | -55 | -9 | -35 | -21 | -4 |
| Penta | 404 | 385 | 278 | [M – Cl + O – CH$_3$SO$_2$ – CO]⁻ | -50 | -7 | -40 | -14 | -1.5 |
| Penta | 404 | 385 | 306 | [M – Cl + O – CH$_3$SO$_2$]⁻ | -50 | -7 | -40 | -22 | -2 |
| Penta | 418[b] | 399[b] | 320[b] | [M – Cl + O – CH$_3$SO$_2$]⁻ | -60 | -8 | -35 | -22 | -1.5 |
| Hexa | 438 | 419 | 312 | [M – Cl + O – CH$_3$SO$_2$ – CO]⁻ | -45 | -9 | -40 | -14 | -2 |
| Hexa | 438 | 419 | 340 | [M – Cl + O – CH$_3$SO$_2$]⁻ | -45 | -9 | -40 | -23 | -2 |
| Hepta | 472 | 453 | 346 | [M – Cl + O – CH$_3$SO$_2$ – CO]⁻ | -60 | -8 | -30 | -24 | -1.5 |
| Hepta | 472 | 453 | 374 | [M – Cl + O – CH$_3$SO$_2$]⁻ | -60 | -8 | -30 | -24 | -1.5 |

*2.1.4.2 Enantioselective heart-cut two-dimensional liquid chromatography*

Liquid chromatography was performed on an Agilent 1100 (Agilent Technologies, Palo Alto, CA, USA) system equipped with a model G1379A vacuum degasser, G1312A binary pump, G1367A well plate autosampler, G1330B autosampler thermostat, and G1316A column compartment. In order to avoid interference of the achiral $MeSO_2$-CB congeners with the chiral congeners, it was necessary to adopt a heart-cut two-dimensional LC (LC-LC) approach (discussed further in **Section 2.2.3**). In the first dimension of the separation, a Cosmosil™ 5-PYE (PYE) column (2-(1-pyrenyl)ethyl derivatized silica, 4.6 x 250 mm x 5 μm; Nacalai Tesque, Tokyo, Japan) with guard column (4.6 x 10 mm x 5 μm) was used to separate the $MeSO_2$-CBs according to degree of *ortho*-chlorination, such that the chiral congeners with 3 or 4 *ortho*-chlorines were eluted before the achiral congeners with 1 or 2 *ortho*-chlorines (Ramos et al. 1999). In the second dimension of the separation, a Chiralpak® AD-H column (amylose tris-(3,5-dimehtylphenylcarbamate) derivatized silica, 4.6 x 250 mm x 5 μm; Chiral Technologies Inc., West Chester, PA, USA) with guard column (4.0 x 10 mm x 5 μm) was used to perform the enantioselective separation of the chiral congeners. A normal phase solvent system was selected with heptanes (A) and 50:50 methanol:ethanol v/v (B) as the mobile phase components. Isocratic elution was employed with a mobile phase of 95:5 A:B at a flow rate of 1.0 mL/min and temperature of 12.5°C. These conditions were applied to both the Chiralpak AD-H and PYE columns. The autosampler was thermostatted to 4°C, and an injection volume of 20 μL was used for all on-column analyses. An integrated 10-port

diverter valve was employedto change the solvent flow path throughout the chromatographic run, as shown in **Figure 2.3**. In configuration A, the mobile phase was pumped through the PYE column, then through the Chiralpak AD-H and on to the detector. In configuration B, the mobile phase was pumped through the PYE column, which was connected directly to the detector, while the Chiralpak AD-H column was connected to a blocked port, so no solvent passed through it in this configuration. The valve was programmed as follows: 0–14.6 min, A; 14.6–23.8 min, B; 23.8–91 min, A. From 0 to 14.6 min the chiral MeSO2-CBs, which were eluted from the PYE column first, were directed onto the Chiralpak AD-H for enantioselective separation. Note that some achiral congeners eluted in this time frame and were also directed onto the enantioselective column (see Section 2.2.3.4 for further discussion). From 14.6 to 23.8 min, the remaining achiral congeners were eluted from the PYE column and detected immediately. There was no flow through the Chiralpak AD-H during this time frame. At 23.8 min, the flow through the Chiralpak AD-H was resumed, enantioselective separation of the chiral congeners was performed, and all remaining analytes were detected after elution from this second dimension column. This type of column switching set-up with an achiral pre-separation prior to a chiral separation has been employed previously in order to avoid interferences in the chiral separation (Ing-Lorenzini et al. 2009, Lamprecht et al. 2000, Oda et al. 1992).

CONFIGURATION A



CONFIGURATION B
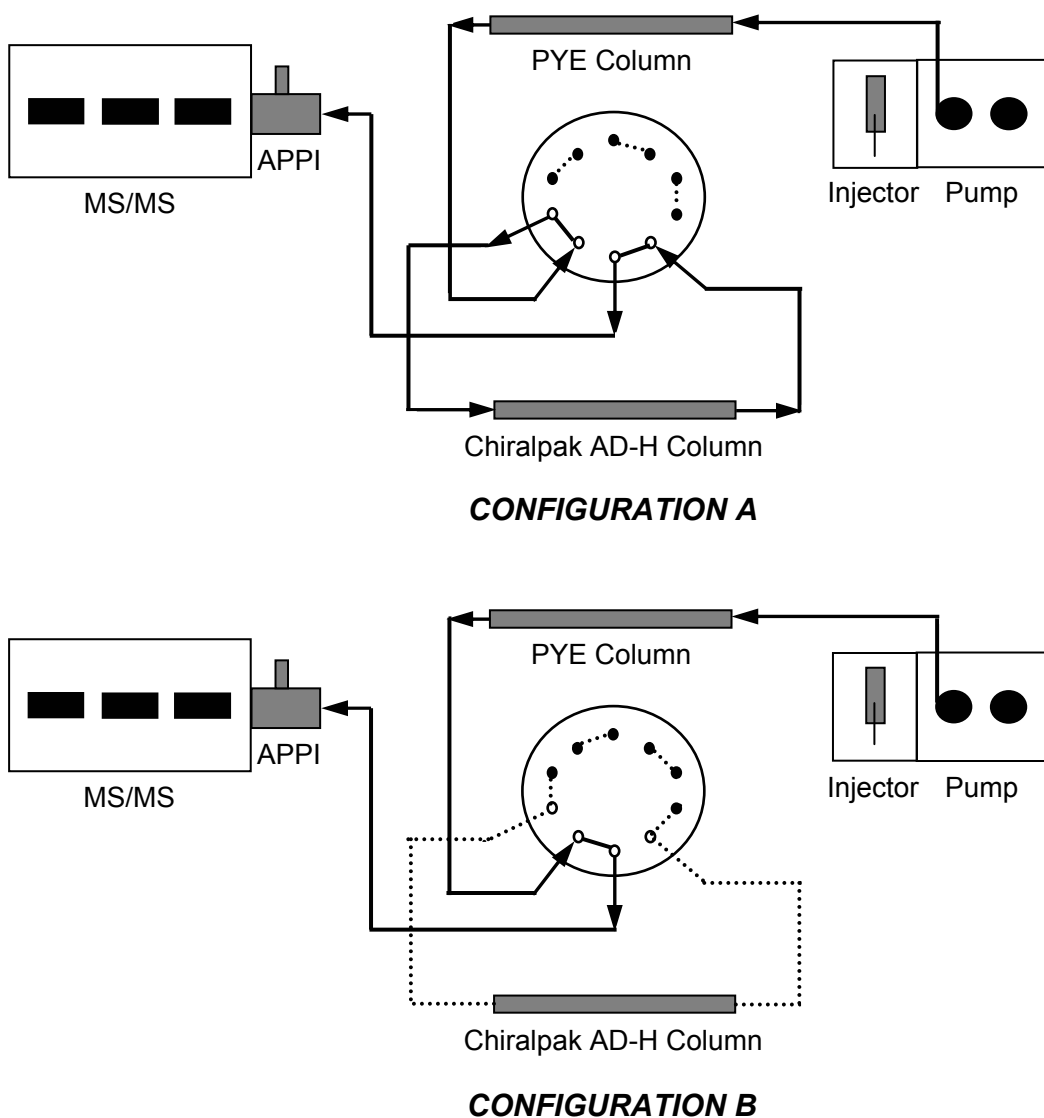
**Figure 2.3: Schematic representation of the 10-port diverter valve connections**

*Solid lines with arrows indicate direction of solvent flow. Dashed lines represent closed loops with no solvent flow. Open circles in valve represent ports connected to tubing. Filled circle in valve represent plugged ports.*

## 2.1.5 *Data analysis and statistical methods*

Peak areas from flow injection analysis experiments were integrated using

Analyst® version 1.4.2 software (Applied Biosystems/MDS Sciex, Foster City,

CA, USA). Peak areas from all chromatographic runs were integrated using PeakFit version 4.06 software (Systat Software, Inc., San Jose, CA, USA). PeakFit software employs mathematical algorithms to fit curve functions of a user-specified type (e.g. exponentially modified Gaussian) to each peak in a chromatogram, such that the addition of the two curves produces the same peak profile as the chromatogram for closely eluting peaks, a process known as deconvolution. In contrast, the "valley-drop method", which is the default method employed by Analyst software, drops a line from the point where two peaks coincide (the "valley") down to the baseline, and assigns the area on the left side to the left hand peak, and vice versa. It has been shown that the deconvolution (i.e. PeakFit) method provides much more accurate results for closely eluting peaks, especially when there is any tailing present (Asher *et al.* 2009), as is often the case with enantioselective LC. For the sake of consistency, all chromatographic peaks, including those that were baseline resolved, were integrated using PeakFit. The exponentially modified Gaussian model was chosen with the "Vary Widths" option turned on. This function is appropriate for modelling peaks with a half-width asymmetry of 0.45-2.225 (SeaSolve Software Inc. 2003), as was the case here. In addition, the various chromatographic peak models were tested against a standard chromatogram, and the exponentially modified Gaussian model gave the best results (highest $r^2$ of the fit). The "Vary Widths" parameter was necessary due to the fact that isocratic elution was employed, so the later eluting peaks were noticeably wider than those the earlier eluting peaks. Enantiomers and co-eluting peaks were fitted together, and no more

than 4 peaks were fitted at a time. Additional peak fitting procedures were carried out as described elsewhere (Asher *et al.* 2009, Ulrich *et al.* 2001).

Enantiomer fractions were calculated using the concentrations of the individual enantiomers as follows (Harner *et al.* 2000):

$$EF = \frac{E1}{E1+E2} \qquad [2.1]$$

$$EF = \frac{(+)}{(+)+(-)} \qquad [2.2]$$

where E1 is the concentration of the first eluting enantiomer, E2 is the concentration of the second eluting enantiomer, (+) is the concentration of the (+)-enantiomer, and (-) is the concentration of the (-)-enantiomer. In this case, the elution order of the (+) and (-) enantiomers was unknown, so **Equation 2.1** was used to calculate EFs. In order to be considered non-racemic, EFs were required to be outside of the range determined by triplicate analyses of racemic analytical standards: $0.487 \pm 0.004$ for 4-MeSO$_2$-CB91, $0.49 \pm 0.01$ for 3′-MeSO$_2$-CB95, $0.53 \pm 0.02$ for 4′-MeSO$_2$-CB95, $0.48 \pm 0.01$ for 4′-MeSO$_2$-CB132, $0.518 \pm 0.007$ for 4-MeSO$_2$-CB149, and $0.541 \pm 0.005$ for 4′-MeSO$_2$-CB174 (refer to **Section 2.2.4.2** for further discussion). Enantioseparation was achieved for all but one congener. However, 5′-MeSO$_2$-CB132, 5-MeSO$_2$-CB149, and 5′-MeSO$_2$-CB174 could not be analyzed due to extremely poor sensitivity (see **Section 2.2.2** for further discussion). No enantioseparation was achieved for 5-MeSO$_2$-CB91, so EFs could not be determined for this analyte.

Any congeners present in the tissue extracts with peak areas below the limit of quantitation were excluded from the sum MeSO$_2$-CB concentration calculations. However, congeners present with peak areas below the limit of quantitation but above the limit of detection were included in the calculations of percent detection. In a few instances, the peak area of the internal standard was below the limit of quantitation, and any congeners present could not be quantified. These analytes were therefore excluded from the sum concentration of MeSO$_2$-CB calculations. However, they were included in the calculations of percent detection provided the peak area exceed the limit of detection.

Statistical analyses were carried out using Prism version 4.00 software (GraphPad Software, Inc., San Diego, CA). One-way analyses of variance (ANOVAs) with Tukey's honestly significant difference post-hoc tests were performed on the APPI-MS optimization data where the results of three or more settings were being compared for each congener. For the matrix effect data and the APPI-MS optimization data where only two settings were being compared, two-tailed Student's $t$-tests were employed. Kruskal-Wallis tests were used in the sledge dog data set to compare concentrations between treatment groups for individual congeners and the sum concentration of MeSO$_2$-CBs. A significance level of 0.05 was used for all statistical analyses.

### 2.1.6 Quality control

Quality control measures included analysis of a 100 ng/mL mixed standard solution every 10 samples to monitor for signal loss or changes in

retention times, and analysis of a solvent blank every 20 samples to monitor for sample carryover and changes in background noise. The ion source, gas discharge lamp window, and the curtain plate of the mass spectrometer were cleaned every 25 samples and the orifice plate and sampling cone of the mass spectrometer cleaned every 50 samples.

Prior to sample analysis, three solvent blanks were analyzed consecutively after a high concentration mixed standard (5 μg/mL) to determine if any carryover was occurring, and none was observed. Reproducibility was assessed by analyzing a mixed standard solution three times consecutively, and the relative standard deviation in the calculated concentrations for each congener was less than 11%. This data was also used to assess the reproducibility of EFs for the chiral congeners, and the relative standard deviation was less than 3% in all cases. Accuracy was assessed by analyzing extracted US National Institute of Standards and Technology standard reference material (SRM) 1945 (Organics in Whale Blubber; Gaithersburg, MD, USA) and comparing the calculated concentrations to those determined in a previous study (Hoekstra *et al.* 2003). The percent difference in concentration was less than 30% for all of the congeners that could be directly compared between the two methods. Three extraction blanks were analyzed for the sledge dog fat and glaucous gull plasma samples and one for the sledge dog plasma samples. No $MeSO_2$-CBs were detected, so there was no background contamination introduced during the extraction procedure. The method precision and accuracy will be discussed further in **Section 2.2.4**.

Retention times were required to be within 2% of the nearest standard run in a batch in order to be accepted. For congeners where two transitions, T1 and T2, were detectable, the transition ratio was calculated as a percentage of the base peak (% bp) using peak areas as shown in Equation 2.3 below:

$$\text{TR (\% bp)} = \frac{\text{T2}}{\text{T1}} \times 100 \qquad\qquad [2.3]$$

where T1 is the peak area of the higher intensity transition and T2 is the peak area of the lower intensity transition. The transition ratio tolerance varied with the relative intensities of the two peaks according to European Union guidelines for LC-MS/MS analyses (The Commission of the European Communities Decision 2002/657/EC 2002) as follows: 30% tolerance for 10% < TR (% bp) ≤ 20%, 25% tolerance for 20% < TR (% bp) ≤ 50%, and 20% tolerance for TR (% bp) > 50%. The only exception to these rules was the congener 4′-MeSO$_2$-CB87, which had an intrinsically large variation in transition ratio due to the fact that it co-eluted closely with the much larger 3′-MeSO$_2$-CB87 + 4-MeSO$_2$-CB110 peak. In order to determine an acceptable range for this analyte, the transition ratio was calculated from replicate analyses of an analytical standard run over a period of several days. The relative standard deviation was 25%, and this value was set as the required transition ratio accuracy for this congener instead of the European Union guideline value of 20%. The retention times, transitions, transition ratios and corresponding accuracy required are presented for each of the achiral congeners in **Table 2.2** and for each of the chiral congeners in **Table 2.3** on the

following pages. Note that for several congeners a low intensity second transition

could be detected in the product ion scans but not in the final chromatographic

method. The transition ratios from the chromatographic method are presented in

the tables below.

**Table 2.2: Summary of retention times and transitions for the analysis of target achiral MeSO$_2$-CBs by LC-LC-APPI-MS/MS**
*Dashes indicate lack of a second transition for confirmation and calculation of a transition ratio.*
*[a]Transition ratio (% base peak) = peak area of low intensity transition/peak area of high intensity transition ×100.*
*[b]As per: The Commission of the European Communities Decision 2002/657/EC 2002.*
*[c]Internal standard: 3-MeSO$_2$-4-Me-2',3',4',5,5'-pentachlorobiphenyl.*

| Congener | Retention Time (min) | Quantitation Transition | Confirmation Transition | Transition Ratio (% base peak)[a] | Transition Ratio[a] Tolerance (%)[b] |
|---|---|---|---|---|---|
| 3'-49 | 44.2 | 349→270 | - | - | - |
| 4'-49 | 58.6 | 349→242 | 349→270 | 90.9 | 20 |
| 3-52 + 4-64 | 55.0 | 349→242 | 349→270 | 28.6 | 25 |
| 4-52 | 69.6 | 349→242 | 349→270 | 66.7 | 20 |
| 3-70 | 18.5 | 349→270 | 349→242 | 76.9 | 20 |
| 4-70 | 19.2 | 349→242 | 349→270 | 30.3 | 25 |
| 3'-87 + 4-110 | 15.0 | 385→278 | 385→306 | 28.6 | 25 |
| 4'-87 | 16.8 | 385→278 | 385→306 | 66.7 | 25 |
| 3'-101 | 50.0 | 385→306 | - | - | - |
| 4'-101 | 85.8 | 385→278 | 385→278 | 47.6 | 25 |
| 5-110 | 16.3 | 385→306 | - | - | - |
| 3'-141 | 15.2 | 419→340 | 419→312 | 23.8 | 25 |
| 4'-141 | 19.0 | 419→312 | 419→340 | 27.8 | 25 |
| IS[c] | 20.4 | 399→320 | - | - | - |

**Table 2.3: Summary of retention times and transitions for the analysis of chiral target MeSO$_2$-CBs by LC-LC-APPI-MS/MS**

*Dashes indicate lack of a second transition for confirmation and calculation of a transition ratio.*
*[a]Transition ratio (% base peak) = peak area of low intensity transition/peak area of high intensity transition ×100.*
*[b]As per: The Commission of the European Communities Decision 2002/657/EC 2002.*
*[c]Internal standard: 3-MeSO$_2$-4-Me-2',3',4',5,5'-pentachlorobiphenyl.*

| Congener | Retention Time (min) | Quantitation Transition | Confirmation Transition | Transition Ratio (% base peak)[a] | Transition Ratio[a] Tolerance (%)[b] |
|---|---|---|---|---|---|
| E1+E2 5-91 | 51.7 | 385→306 | 385→278 | 10.2 | 30 |
| E1 4-91 | 37.2 | 385→278 | 385→306 | 25.0 | 25 |
| E2 4-91 | 38.4 | 385→278 | 385→306 | 25.0 | 25 |
| E1 3′-95 | 33.1 | 385→306 | - | - | - |
| E2 3′-95 | 35.6 | 385→306 | - | - | - |
| E1 4′-95 | 50.5 | 385→306 | 385→278 | 62.5 | 20 |
| E2 4′-95 | 60.5 | 385→306 | 385→278 | 62.5 | 20 |
| E1 5′-132 | 35.5 | 419→340 | - | - | - |
| E2 5′-132 | 41.5 | 419→340 | - | - | - |
| E1 4′-132 | 39.5 | 419→312 | 419→340 | 27.8 | 25 |
| E2 4′-132 | 40.2 | 419→312 | 419→340 | 26.3 | 25 |
| E1 5-149 | 31.8 | 419→340 | - | - | - |
| E2 5-149 | 33.3 | 419→340 | - | - | - |
| E1 4-149 | 37.9 | 419→312 | 419→340 | 31.3 | 25 |
| E2 4-149 | 45.7 | 419→312 | 419→340 | 29.4 | 25 |
| E1 5′-174 | 31.3 | 453→374 | - | - | - |
| E2 5′-174 | 32.5 | 453→374 | - | - | - |
| E1 4′-174 | 40.7 | 453→346 | 453→374 | 66.7 | 20 |
| E2 4′-174 | 56.8 | 453→346 | 453→374 | 71.4 | 20 |

## 2.2    Results and discussion

### 2.2.1   *Optimization of APPI conditions*

Infusion experiments were carried out to find the most intense parent ions using a first quadrupole full scan (Q1). A sample Q1 mass spectrum for 4-MeSO$_2$-CB149 using 50:50 methanol:water as the mobile phase and toluene as the dopant is presented in **Figure 2.4** on the following page. Note that the presence of multiple chlorine atoms leads to a characteristic chlorine isotope pattern, as depicted in the figure inset. The highest intensity peak in this isotope pattern corresponds to $[M - {}^{35}Cl + O]^-$, which was used as the parent ion for all of the congeners studied. No analyte ionization was observed with APPI in positive ion mode. Atmospheric pressure chemical ionization (APCI) was also assessed in positive and negative ion mode for the congener 5′-MeSO$_2$-CB132 under the same conditions as those used for APPI. Once again, no analyte ionization was observed in positive mode. However, a similar spectrum was obtained with $[M - Cl + O]^-$ as the dominant parent ion in negative mode (not shown), but the sensitivity was much lower. The Q1 parent ion intensity was two orders of magnitude lower using APCI, so this technique was abandoned and all future experiments performed using APPI.

Note the plethora of background ions observed in **Figure 2.4**, especially at low *m/z*. Many of these ions have been reported previously. For instance, the background ions at *m/z* 60 and 61 amu have been attributed to $[(N_2)O_2]^-$ and $CO_3^-$, respectively (Kauppila *et al.* (Song *et al.* 2007), and those at 59, 77, 93, 107, and
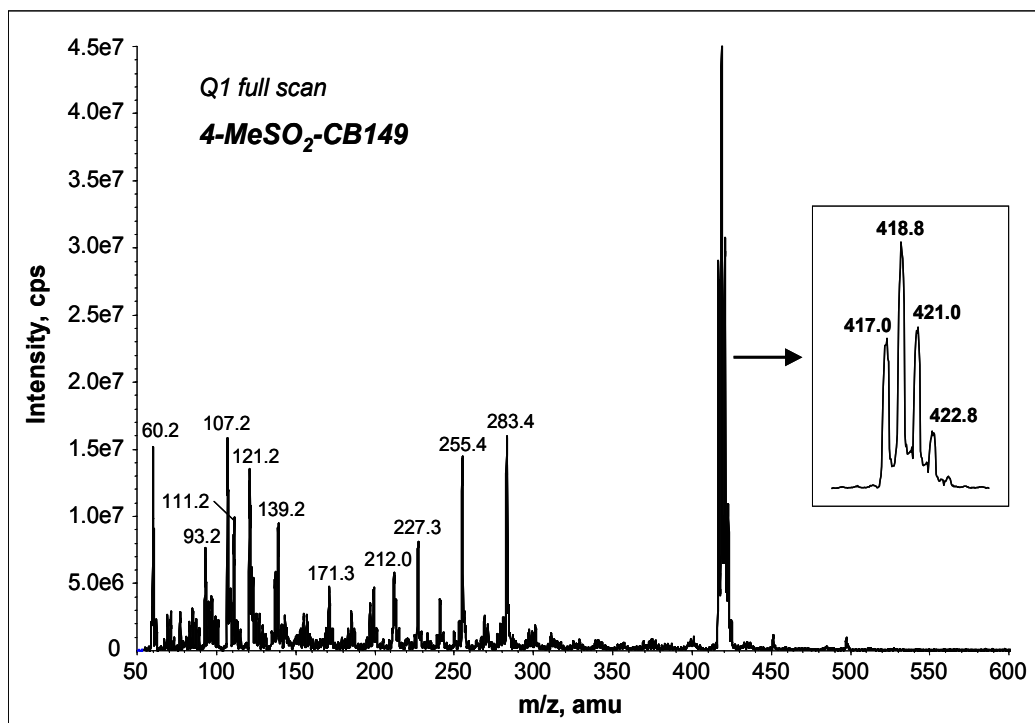
**Figure 2.4: First quadrupole full scan mass spectrum of 4-MeSO₂-CB149 with atmospheric pressure photoionization**

*Analyte solution, 1μg/mL in MeOH, infused via syringe pump at 10 μL/min. Mobile phase 50:50 MeOH:H₂O, flow rate 0.2 mL/min. APPI source temperature 300°C. Krypton lamp with toluene dopant infused at 20 μL/min. Scan time 1.0 min.*

121 amu have been attributed to $CH_3COO^-$, $[(O_2)HCOO]^-$, $C_6H_5O^-$, $CH_3C_6H_4O^-$ and $C_6H_5COO^-$, respectively, in negative ion APPI-MS with water/methanol mixtures as the mobile phase and toluene as the dopant (Song *et al.* 2007). Additional ions at *m/z* 75, 76, 95, 96, 111 and 137 amu (Kauppila *et al.* 2002), and at 212 and 255 amu (Song *et al.* 2007) have also been observed under these conditions, but have not been positively identified. There are a few other high intensity background ions present in **Figure 2.4**, for example at 139, 227, 241 and 283.4 amu, which have not been reported previously. These are likely attributable to clusters forming between solvent and dopant molecules, which have been observed in positive ion mode for methods utilizing methanol (Short *et al.* 2007)

and water (Kauppila *et al.* 2002) as the mobile phases and using toluene as the dopant (Tubaro et al. 2003).

All of the MeSO2-CBs lost a chlorine and gained an oxygen in the APPI source to produce $[M - X + O]^-$ parent ions; no $M^{\bullet-}$ ions were detected. As discussed previously in Section 1.6.3.1, phenoxide ions of this type, where X represents chlorine or bromine, have been reported previously for the analysis of a variety of halogenated aromatic compounds (Basso et al. 2003, Debrauwer et al. 2005) by negative ion LC-APPI-MS, including hexachlorobenzene (Kauppila et al. 2004b). These ionization products have also been observed for the analysis of $MeSO_2$-CBs by GC-MS with electron capture negative ionization (Haraguchi *et al.* 1993) and for trichloro- to hexachloro-substituted benzenes and biphenyls by direct insertion atmospheric pressure ionization mass spectrometry (API-MS) with 0.75 mC $^{63}$Ni foil as the primary source of electrons (Dzidic *et al.* 1975). It has been proposed that this ionization mechanism proceeds via an ipso-substitution with $[M + O_2]^{\bullet-}$ as the intermediate radical anion (Carroll *et al.* 1981).

All of the $MeSO_2$-CBs produced similar response levels in the first quadrupole under the conditions specified in **Figure 2.4**. Some congeners appeared to ionize slightly better than others, but no association could be made with chlorination level, position of the methylsulfonyl group, or chlorine substitution pattern. Similar responses between congeners ranging from tri- to tetrachlorinated have also been reported for the analysis of $MeSO_2$-CBs by GC-ECNI-MS (Haraguchi *et al.* 1993).

Dzidic and coworkers reported an increase in the ratio of phenoxide ions to M⁻ ions with increasing oxygen content of the carrier gas and with increasing chlorination of the parent compound for polychlorobenzenes and biphenyls (Dzidic *et al.* 1975). This trend was attributed to an increase in the electron affinity of the phenoxide ion and in the gas phase acidity of the corresponding phenol (Dzidic *et al.* 1975). However, phenoxide ions were also observed as the predominant product for *para*-chloronitrobenzene, despite its low level of chlorination. In contrast, no phenoxide ions could be observed for 1,2-dichlorobenzene, even with the use of air as the carrier gas. It appears that the presence of a highly electron withdrawing substituent, like a nitro group with Hammet constant $\sigma = 0.81$ or a methylsulfonyl group with $\sigma = 0.79$ (March 1992), also favours the formation of phenoxide ions. In light of these findings, the observation of $[M - Cl + O]^-$ ions as the sole product of ionization for tetra- to hepta-MeSO$_2$-CBs by APPI is anticipated.

Although *ortho*- and *para*-chloronitrobenzene form phenoxide ions easily by API, this is not the case for the *meta*-isomer, which forms mostly $M^{\bullet-}$ ions (Dzidic *et al.* 1975). Because of its substitution pattern, this isomer cannot undergo the requisite ipso-substitution reaction to form a phenoxide ion directly; it undergoes electron attachment to form a parent radical anion instead (Carroll *et al.* 1981), which can then react with oxygen to form phenoxide ions to a certain extent (Dzidic *et al.* 1975). However, it has also been found that ionization of 2,3-dichloronitrophenol by API leads to the sole production of phenoxide ions (Dzidic *et al.* 1975). This suggests that when multiple chlorine substituents are present in

an aromatic system, if at least one is on the same ring and in a position *ortho* or

*para* to the electron withdrawing group, phenoxide ions will be the sole product.

Due to the selectivity of the CYP enzymes that metabolize PCBs, all MeSO$_2$-CBs

of environmental interest possess either 2,5-dichloro or 2,5,6-trichloro

substitution on the MeSO$_2$-containing ring (Brandt *et al.* 1976), and therefore

possess one chlorine substituent *ortho* to the methylsulfonyl group in the former

case and one *ortho* and one *para* to it in the latter case. This is consistent with the

observation of phenoxide ions as the sole product of photoionization for MeSO$_2$-

CBs of environmental concern in the current work.

Once the mass-to-charge ratio of the parent ion was identified,

optimization experiments were undertaken to maximize the response. The first

parameter tackled was the type of ionization lamp. Krypton gas discharge lamps

have been used in the vast majority of APPI studies, but there are two other lamps

types with different fill gases that have been investigated: argon (Cai *et al.* 2007a,

Short *et al.* 2007) and xenon (Short *et al.* 2007). Each of these lamps emits

photons with different energies: 10.0 and 10.6 eV (1:4) for krypton, 11.7 eV for

argon, and 8.4 eV for xenon (Short *et al.* 2007). For the current work, both argon

and krypton lamps were assessed. An argon lamp was of interest because it was

reported to produce less background noise than a krypton lamp in positive ion

mode with methanol as the solvent (Short *et al.* 2007). This was attributed to a

decrease in solvent adduct formation. In addition, these workers found that the

optimal flow rate with the argon lamp (0.5 mL/min) was higher than that with the

krypton lamp (0.3 mL/min) for the analysis of benzo(*a*)pyrene, a definite

advantage for high throughput analysis. However, the argon lamp does suffer from a couple of disadvantages relative to the krypton lamp, namely increased cost and decreased lifetime. In order to fairly compare the ability of these lamps to promote the ionization of MeSO$_2$-CBs, it was first necessary to optimize the source conditions for each in turn. Preliminary infusion experiments suggested that the lamp type had little impact on several of the ion source parameters. However, this was not the case for the dopant use, source temperature and lamp gas flow rate, which will be discussed in turn below.

Although toluene is the most commonly used dopant for APPI, there are a variety of other solvents that have been employed, including acetone (Cai *et al.* 2007a, Himmelsbach *et al.* 2009, Robb *et al.* 2000, Takino *et al.* 2004)**,** anisole (Kauppila *et al.* 2004a, Smith *et al.* 2009) and bromobenzene (Robb *et al.* 2008, Smith *et al.* 2009), as well as THF (Cai *et al.* 2005) and a number of other benzene derivatives (Robb *et al.* 2008). In the current study, the former three dopants, as well as toluene, methylene chloride, and 1% 1,3-dibromobutane in toluene, were assessed for their ability to promote the ionization of MeSO$_2$-CBs in conjunction with a krypton gas discharge lamp and the optimized LC normal phase solvent composition (95:2.5:2.5 heptanes:methanol:ethanol). Infusion experiments were carried out with 3-MeSO$_2$-CB70 as the analyte and with a mobile phase flow rate of 0.5 mL/min. The dopants were delivered at a flow rate of 50 μL/min using an external syringe pump, and the analyte signal was monitored in Q1 in duplicate scans, one in positive ion mode and one in negative ion mode. Toluene and anisole were the only effective dopants. Not only did the

chlorinated and brominated dopants fail to ionize the analyte, they effectively quenched all ionization processes within the source. No analyte signal and only a few very low intensity background ions could be observed. These types of dopants can be effective in negative ion mode for compounds that can undergo anion attachment to produce $[M + X]^-$ ions, where X is a halogen (Kéki *et al.* 2008a, Kéki *et al.* 2008b, Ross and Wong 2010, Song *et al.* 2007), as discussed in **Section 1.6.3.1**. However, for analytes that undergo electron capture, proton transfer or oxidation reactions in negative ion mode, these halogenated dopants generally act as quenching agents, reacting with any thermal electrons present within the source due to their high electron affinities (Kauppila *et al.* 2002). This suppresses analyte ionization, for which all three of these mechanisms require thermal electrons and/or superoxide anions as reactants.

Acetone gave similarly poor results. Acetone is an effective dopant in positive ion mode only for analytes with high proton affinity (Robb *et al.* 2000), so it seems logical that it would not produce good results for $MeSO_2$-CBs which do not ionize by proton transfer. Anisole did lead to some analyte ionization, but the signal intensity was about five times less than that found with toluene. Anisole can be a more effective dopant than toluene for low polarity, low proton affinity analytes in positive ion mode (Kauppila *et al.* 2004a), but to our knowledge, there have been no reports of this dopant being used in negative ion mode. Our results suggest that it may not be as effective as toluene for oxygen substitution mechanisms in negative ion mode, or at least not for $MeSO_2$-CBs. Although these experiments were not repeated with the argon lamp, the same results would be

anticipated. The chlorinated and brominated dopants would be easily ionized by the higher energy photons of the argon lamp and therefore still lead to ion quenching. Furthermore, anisole would not be expected to produce any improvement in signal intensity with the argon lamp since it gave poorer results than toluene with the krypton lamp, and toluene, in turn, had no impact on signal intensity with the argon lamp, as discussed below.

Next, the dopant flow rate was optimized for the krypton lamp using infusion experiments. An increase in signal of approximately two fold was observed with the use of toluene as the dopant at a flow rate of up to 10% of the mobile phase flow in both normal and reversed phase. Increasing the toluene flow above 10% gave no additional benefit, a phenomenon that has been observed previously (Robb and Blades 2006b) and attributed to an increase in dopant neutralization reactions at higher dopant flow rates (Robb and Blades 2005). Interestingly, most of the previous studies employing normal phase solvent systems and a krypton lamp for detection with APPI have found no benefit to using a dopant (Cai *et al.* 2007a, Martens-Lobenhoffer *et al.* 2007, Wang *et al.* 2005). Alkanes, which are used in high proportions in normal phase chromatography, generally have lower ionization energies than most reversed phase solvents and than the photons emitted by krypton ionization lamps. As a result, using these solvents typically avoids the need for a dopant, an effect known as "self-doping" (Wang *et al.* 2005). That being said, one study found that using a dopant increases sensitivity for the analysis of aminonitro- and dinitropyrene with normal phase solvents and a krypton ionization lamp (Straube *et al.* 2004). The

$M^{\bullet -}$ ion of dinitropyrene was examined in this study, and a dopant is generally

beneficial in facilitating ionization in negative ion mode due to the increase in

availability of free electrons (Kauppila *et al.* 2002). Electrons are required to

participate directly in analyte ionization or indirectly by producing other reactive

species in all negative mode APPI mechanisms, as discussed in **Section 1.6.3.1**.

However, the $[M + H]^+$ ion of aminonitropyrene was monitored, and in the other

three normal phase positive mode APPI studies, which also examined $[M + H]^+$

ions, a dopant had no effect on ionization efficiency. The ionization potentials and

proton affinities of the mobile phase components, analytes and dopants, where

applicable, all play an important role in determining the ionization efficiency for

analytes that undergo proton transfer in positive ion mode APPI (Cai *et al.*

2007a). In comparing the conditions used by Straube and coworkers to those used

in the other three studies, the only factor that can explain this difference is the

proton affinity of the analyte. In the latter cases, polar drugs such as cyclosporin

A (Wang *et al.* 2000), naringenin (Cai *et al.* 2007a), and omeprazole (Martens-

Lobenhoffer *et al.* 2007) were studied, and these compounds would presumably

have higher proton affinities than aminonitropyrene, which is a relatively non-

polar molecule by comparison. As a result, less efficient proton transfer with the

solvent would be expected for this compound, and a dopant would increase

sensitivity by increasing the supply of protonated solvent molecules required for

analyte ionization (see **Equation 1.4** and **1.5** in **Section 1.6.3.1**). This suggests

that dopant usage may be beneficial under certain circumstances when employing

APPI with normal phase solvents and a krypton ionization lamp and should be assessed on a case by case basis.

Although a dopant was useful with the krypton lamp, this was not the case with the argon lamp. In order to determine if a dopant was necessary with the argon lamp, flow injection analysis (FIA) experiments were carried out for selected analytes with no dopant then with toluene as the dopant at a flow rate of 10% of the mobile phase flow using the same normal phase solvent system described above. The results are presented in **Figure 2.5** on the following page. No significant difference was observed between the "no dopant" and "with dopant" data sets for 5-MeSO$_2$-CB91 or 4-MeSO$_2$-CB91 by two-tailed Student's $t$-test, but a significant difference was observed for 4′-MeSO$_2$-CB174. In this case, the runs performed with dopant gave a significantly higher signal-to-noise ratio ($S/N$), but the absolute difference between the average signal-to-noise ratios for the "no dopant" and "with dopant" data sets was fairly small, less than 350. In order to conserve solvent and to avoid extending analyses to refill the toluene syringe several times a day, it was elected not to use a dopant for future analyses with this lamp.

Another ion source parameter that differed in its optimal value between the two lamps was the source temperature. For the krypton lamp, manual infusion experiments revealed that a temperature of 400°C was optimal. However, for the argon lamp, there was not as much room for experimentation with the source temperature, owing to the fact that these lamps possess a relatively low
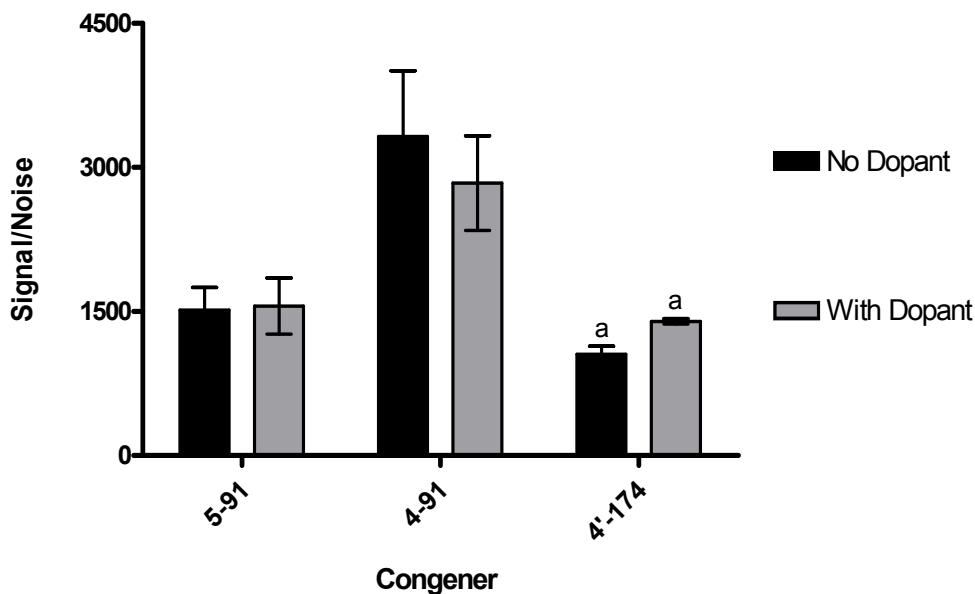
**Figure 2.5:** **Effect of toluene dopant use on the photoionization of MeSO$_2$-CBs by APPI with argon lamp**

*Flow injection analysis with 5 μL injections of individual analyte solutions, 1μg/mL in hexanes. Mobile phase 95:2.5:2.5 heptanes:methanol:ethanol, flow rate 1.0 mL/min. APPI source temperature 250°C. Argon lamp with toluene dopant infused at 100 μL/min for "With Dopant" runs. Error bars indicate maxima and minima of triplicate analyses (n = 3) with average at the midpoint. Letters above error bars indicate a significant difference (P<0.05) between variables for a given analyte by two-tailed Students' t-test.*

temperature tolerance. The window material for argon photoionization lamps is

lithium fluoride, and the manufacturer recommends that this lamp not be heated

above room temperature in order to prevent degradation of the lamp window by

any moisture that may be present in the operating environment (PerkinElmer

Optoelectronics 2008). That being said, this type of lamp has been used in some

reversed phase LC-MS applications requiring a detector temperature of 400°C or

more (Cai *et al.* 2007a). In the current study, the source temperature for the argon

lamp was optimized using infusion experiments to as low a value as possible in

order to extend the lifetime of the lamp. The temperature was increased in 50°C

increments starting at 100°C, and the instrument response increased steadily with no observable changes in noise level up to 250°C. When the source temperature was raised to 300°C, some signal instability and a doubling of the noise level was observed, possibly a result of lamp window degradation. Therefore, a source temperature of 250°C was selected as the final temperature setting. Although a high flow rate of 1.0 mL/min was employed, this relatively low temperature appeared to be sufficient for vaporization of the high-alkane content mobile phase, and no condensation was observed within the source.

The final parameter that differed in its optimal value between the two lamps was the lamp gas flow rate. For the krypton lamp, manual infusion experiments revealed that a lamp gas setting of 1.0 L/min gave the best sensitivity for all analytes. However, for the argon lamp, it was of critical importance to optimize the flow rate to the highest possible value without a significant loss in sensitivity in order to keep the lamp window cool. Flow injection analysis experiments were carried out to this end, varying the lamp gas flow in 1.0 L/min increments. The results are depicted in **Figure 2.6** on the following page. In general, there appeared to be an increase in signal-to-noise ratio from the lowest setting of 1 L/min up to an intermediate setting of 2 or 3 L/min, followed by a decrease in $S/N$ up to the maximum setting of 4 L/min. The only exception to this trend was 4′-MeSO$_2$-CB132, for which 4 L/min was the most favourable. For both 4-MeSO$_2$-CB91 and 5-MeSO$_2$-CB91, 2 L/min was optimal, whereas 3 L/min was slightly better for 4′-MeSO$_2$-CB174. The only significant differences in $S/N$ observed were between the 1 L/min and the 2 and 3 L/min settings for 4-MeSO$_2$-

CB91. Either 2 or 3 L/min was optimal for most of the congeners, so a final flow rate of 3 L/min was selected in order to provide more protection for the argon lamp window.
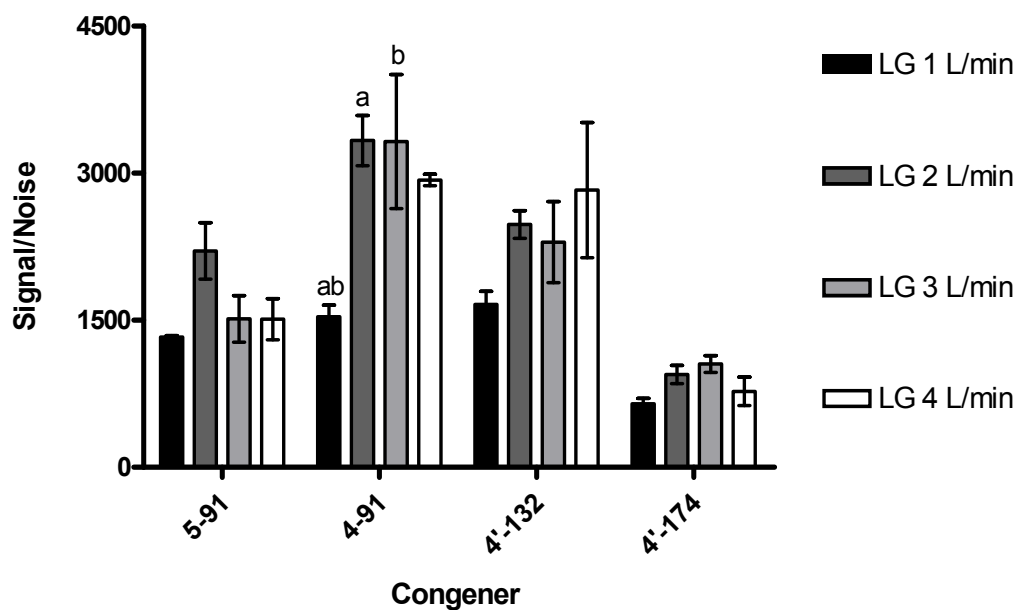


**Figure 2.6:** **Effect of lamp gas flow on the photoionization of MeSO$_2$-CBs with an argon lamp**

*Flow injection analysis with 5 μL injections of individual analyte solutions, 1μg/mL in hexanes. Mobile phase 95:2.5:2.5 heptanes:methanol:ethanol, flow rate 1.0 mL/min. APPI source temperature 250°C. Argon lamp, no dopant. Error bars indicate maxima and minima of triplicate analyses (n = 3) with average at the midpoint. Letters above error bars indicate a significant difference (P<0.05) between lamp gas settings for a given analyte by one-way ANOVA with Tukey's honestly significant difference test.*

Once the conditions had been optimized for each lamp, it was possible to compare their performances to see which gave the best results overall. Flow injection analysis experiments were carried out for each lamp with their respective optimal settings, and the results are presented in **Figure 2.7** on the following page. For both analytes depicted, the *S/N* was significantly higher for the argon lamp (P<0.01 for 4′-MeSO$_2$-CB174). These results were corroborated

by infusion experiments performed with other congeners. It is possible that the higher energy argon lamp led to increased ionization of the heptane-based mobile phase and, therefore, of the analyte due to the self-doping effect. As a result of the improved sensitivity achieved without the need for a dopant, the argon lamp was chosen for use in the remaining optimization experiments and in the final analytical method.
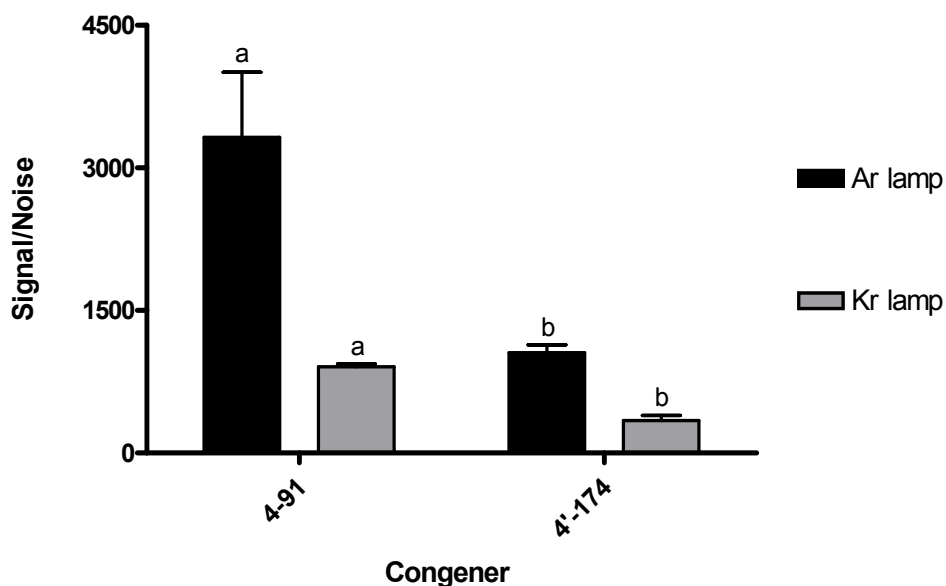


**Figure 2.7:** **Effect of lamp type on the photoionization of MeSO$_2$-CBs**
*Flow injection analysis with 5 μL injections of individual analyte solutions, 1μg/mL in hexanes. Mobile phase 95:2.5:2.5 heptanes:methanol:ethanol, flow rate 1.0 mL/min. "Krypton lamp": APPI source temperature 400°C, lamp gas 1 L/min, toluene dopant infused at 50 μL/min. "Argon lamp": APPI source temperature 250°C, lamp gas 3 L/min, no dopant. Error bars indicate maxima and minima of triplicate analyses (n = 3) with average at the midpoint. Letters above error bars indicate a significant difference (P<0.05) between lamps for a given analyte by two-tailed Student's* t-test.

The remaining ion source conditions were then optimized using the argon lamp with a lamp gas setting of 3 L/min and without the use of a dopant. Although it was possible to set up different time windows employing different ion

source conditions with the version of Analyst software employed, this was not a feasible option since multiple analytes of differing transitions co-eluted during several time frames. As a result, it was necessary to compromise and find ion source parameters that gave acceptable responses for all of the analytes of interest.

For the ion source potential (*IS*, **Figure 2.8 A**), the majority of the analytes demonstrated a trend of increasing *S/N* with increasingly negative ion source potential. However, the only significant difference observed was between *IS* -1050 V and *IS* -1150 V for 5-MeSO$_2$-CB91. Interestingly, it was obvious from the results of manual infusion experiments that the *meta*-substituted congeners did not follow the same trend. The *S/N* for these analytes at *IS* -1100 V was at least twice that at *IS* -1150 or -1050 V. In light of this, a final *IS* setting of -1100 V was chosen in order to increase the response for these lower sensitivity congeners.

For the curtain gas setting (*CUR*, **Figure 2.8 B**), a trend of decreasing *S/N* with increasing curtain gas pressure was observed for all analytes examined. The decrease in noise *S/N* was most pronounced between the minimum pressure of 10 psi and the intermediate pressure of 30 psi where the *S/N* was cut in half for most analytes. There was a significant difference in *S/N* by one-way ANOVA between the 10 psi and the 30 and 50 psi settings for all congeners (P<0.01 for 4′-MeSO$_2$-CB174). A final curtain gas pressure of 10 psi was selected, since this gave the best results for all of the analytes.

**A**



**B**
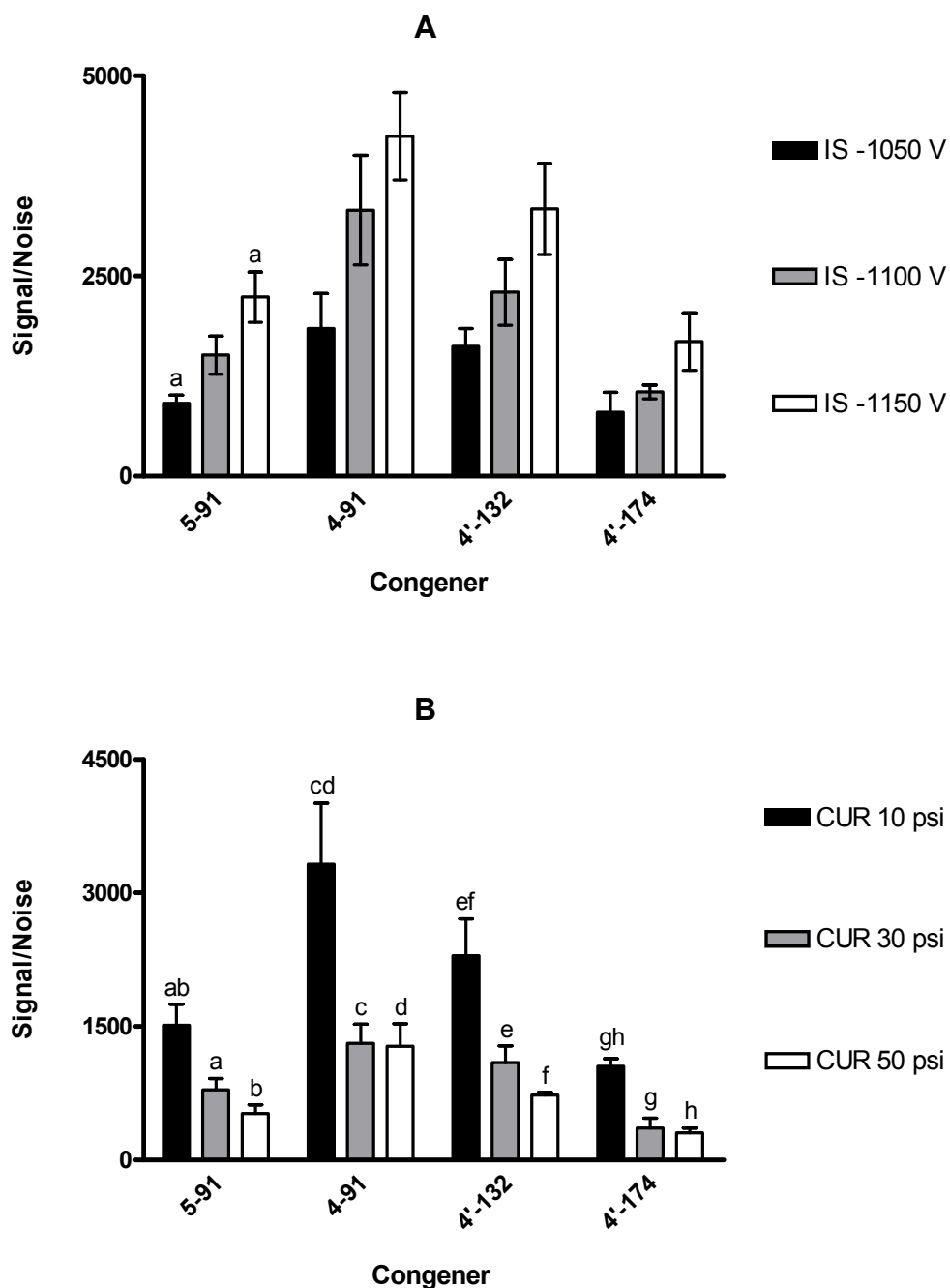
**Figure 2.8:** **Effect of ion spray voltage and curtain gas pressure on the photoionization of MeSO$_2$-CBs**

*IS: ion spray voltage, CUR: curtain gas pressure. Flow injection analysis with 5 μL injections of individual analyte solutions, 1μg/mL in hexanes. Mobile phase 95:2.5:2.5 heptanes:methanol:ethanol, flow rate 1.0 mL/min. APPI source temperature 250°C. Argon lamp, no dopant. Error bars indicate minima and maxima of triplicate analyses (n = 3) with average at the midpoint. Letters above error bars indicate a significant difference (P<0.05) between settings for a given analyte by one-way ANOVA with Tukey's honestly significant difference test.*

For the nebulisation gas (*GS1*, **Figure 2.9 A**), there was a general trend of increasing *S/N* with increasing pressure. There was a significant difference between the 10 psi setting and each of the other *GS1* settings for 4′-MeSO$_2$-CB132 ($P<0.01$ between 10 and 90 psi) and between the 90 psi and the 10 and 30 psi settings for 4-MeSO$_2$-CB91. For 4′-MeSO$_2$-CB174, there was a significant difference between the 10 and 90 psi settings. A one quarter to one third drop in *S/N* was observed going from 90 psi down to 60 psi for all analytes but 5-MeSO$_2$-CB91. For this congener, 60 psi was slightly better, although not significantly. In the end, a nebulisation gas pressure of 90 psi was chosen, as this seemed to be the most favourable value overall.

For the auxiliary gas pressure (*GS2*, **Figure 2.9 B**), the general trend observed was an increase in *S/N* from the minimum setting of 10 psi up to an intermediate setting of 30 or 60 psi, and then a decrease in *S/N* with increasing pressure up to the maximum setting of 90 psi. The *GS2* pressure giving the highest *S/N* was 30 psi for 5-MeSO$_2$-CB91, 4-MeSO$_2$-CB91 and 4′-MeSO$_2$-CB132, and 60 psi for 4′-MeSO$_2$-CB174. However, the difference between the 30 and 60 psi settings was quite minimal for this last congener. No significant differences in *S/N* were detected by one-way ANOVA for any of the congeners in this data set. A final auxiliary gas pressure of 30 psi was selected, since this value was optimal for the majority of the congeners.
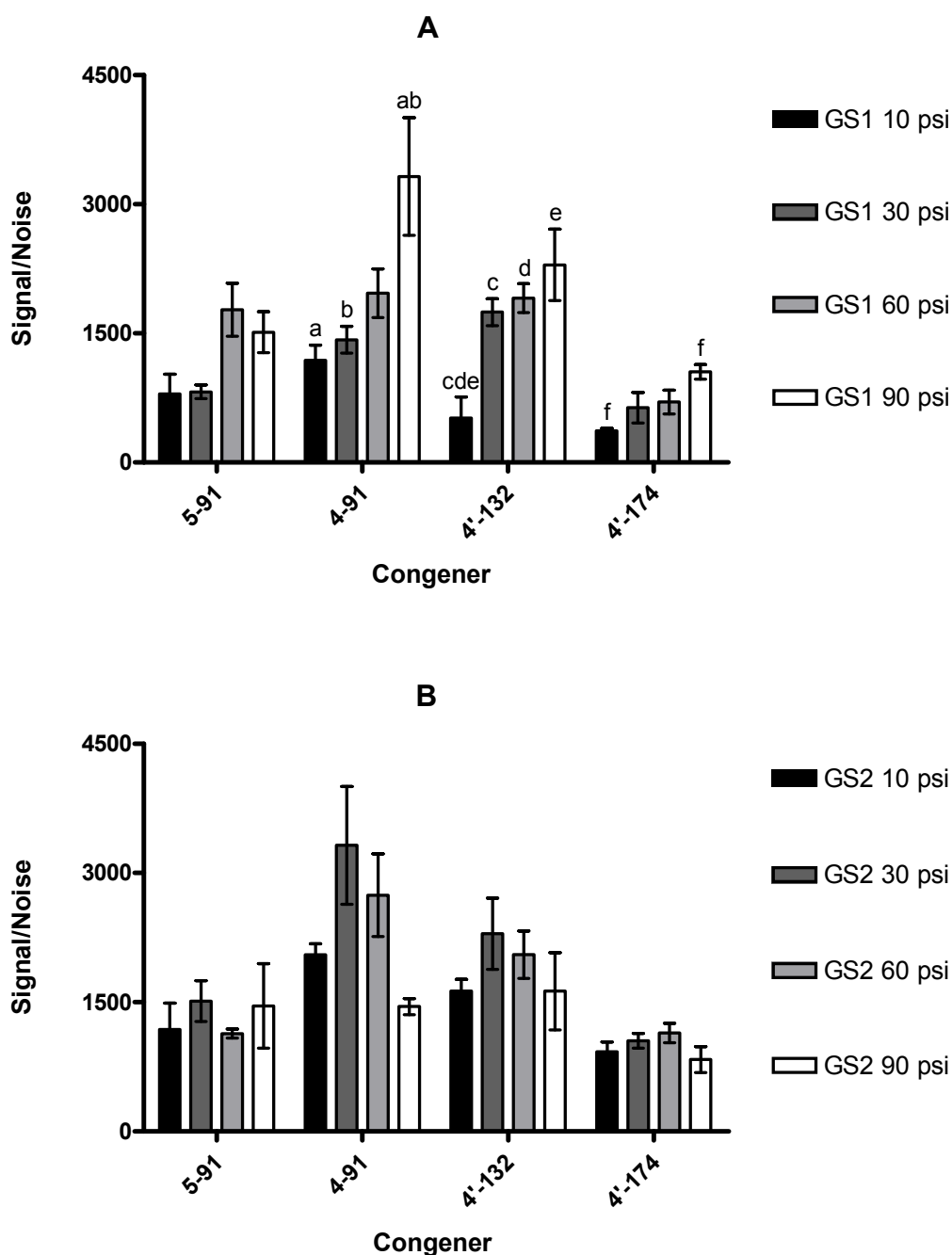
**Figure 2.9: Effect of nebulisation and auxiliary gas pressures on the photoionization of MeSO₂-CBs**

*GS1: nebulisation gas pressure, GS2: auxiliary gas pressure. Flow injection analysis with 5 µL injections of individual analyte solutions, 1µg/mL in hexanes. Mobile phase 95:2.5:2.5 heptanes:methanol:ethanol, flow rate 1.0 mL/min. APPI source temperature 250°C. Argon lamp, no dopant. Error bars indicate minima and maxima of triplicate analyses (n = 3) with average at the midpoint. Letters above error bars indicate a significant difference (P<0.05) between gas pressures for a given analyte by one-way ANOVA with Tukey's honestly significant difference test.*

A summary of the final APPI conditions chosen is presented in **Table 2.4** below.

**Table 2.4:** **Optimal atmospheric pressure photoionization source conditions for MeSO$_2$-CB analysis**

| APPI source parameter | Optimal condition |
|---|---|
| *Lamp type* | Argon |
| *Lamp gas, LG* | 3 L/min |
| *Nebulisation gas, GS1* | 90 psi |
| *Auxiliary gas, GS2* | 30 psi |
| *Curtain gas, CUR* | 10 psi |
| *Ion spray voltage, IS* | -1100 V |
| *Heated nebulizer temperature* | 250°C |
| *Dopant* | None |

Other than the lamp gas flow rate, these conditions were also optimal for the krypton lamp, which was used for the majority of the method development in this study. As expected, the optimal temperature was affected by the mobile phase composition, but none of the other parameters varied with types or ratios of solvents used. That being said, some changes in response were observed with variations in mobile phase. For instance, in reversed phase, acetonitrile was observed to give approximately a ten-fold lower response compared to methanol as the organic modifier. Similar effects have been observed previously in positive ion mode for the analysis of lipids (Cai and Syage 2006) and 9-methylanthracene (Robb and Blades 2005). In addition, methanolic solvents have been found to

increase ionization efficiency of oxidation reactions in negative ion mode

compared to acetonitrile, which tends to favour the production of analyte radical

anions (Kauppila *et al.* 2002). Introduction of 2 mM ammonium acetate as a

buffer in reversed phase produced such a significant decrease in sensitivity that

the signal was almost completely lost, even with the use of a dopant. This

phenomenon has been documented previously for several other buffers in

negative ion mode and attributed to consumption of free electrons needed for

analyte ionization (Kauppila *et al.* 2002).

Ionization efficiency was observed to increase by approximately three-fold

upon switching the polar modifier from pure ethanol to pure methanol in both

reversed phase and normal phase. However, a 50:50 mixture of these solvents

produced a level of sensitivity similar to that found with methanol alone in normal

phase. A small decrease in ionization efficiency was also noted with increasing

alcohol content in normal phase. A similar effect has been observed previously

for the enantioselective LC-APPI-MS analysis of the pharmaceutical compound,

propranolol, where the analyte response decreased with increasing ethanol content

of the mobile phase when isooctane was used as the alkane (Chen *et al.* 2005).

These factors were taken into account during HPLC method development, and the

use of acetonitrile, ethanol, and buffers was limited or avoided in both normal and

reversed phase in order to maximize sensitivity.

Atmospheric pressure photoionization is generally most sensitive at flow

rates between 0.1 and 0.5 mL/min. For example, Robb and Blades observed a

decrease in the abundance of the $M^{\bullet+}$ ion of 9-methylanthracene with solvent flow

using methanol/water as the mobile phase (Robb and Blades 2006a). A significant decrease in analyte ion abundance was also observed by Kauppila and coworkers at higher flow rates using chloroform as the solvent for the model compound 2-ethylnaphthalene, which undergoes charge exchange ionization to form $M^{\bullet +}$ ions (Kauppila and Bruins 2005). The ionization efficiency increased with flow rate up to 0.5 mL/min using a Sciex model APPI source, then decreased gradually up to 1.0 mL/min. When the source temperature and nebulisation gas flow were maximized, this effect was still observed, although to a lesser degree, so the authors concluded that the decrease in sensitivity could not explained by a lack of nebulisation and desolvation alone. Instead, they attributed the decrease in analyte ion abundance to a decrease in the concentration of dopant radical cations at higher flow rates due to neutralization processes and increased photon absorption by the solvent. In the current work, the optimal flow rate for flow injection analysis was 0.2 mL/min, and the ionization efficiency decreased proportionally with flow rate thereafter. However, during chromatographic method development, the increase in sensitivity at low flow rate had to be balanced against the increase in run time and band broadening, which will be discussed further in **Section 2.2.3.5**.

### 2.2.2   *Optimization of MS/MS conditions*

The most abundant fragments produced from the $[M - Cl + O]^-$ parent ions of the MeSO$_2$-CBs resulted from the loss of the methylsulfonyl group forming a $[M - Cl + O - CH_3SO_2]^-$ daughter ion, and from the loss of a carbonyl group in addition to this forming a $[M - Cl + O - CH_3SO_2 - CO]^-$ ion. Although

these compounds have not been analyzed by LC-MS/MS previously, they have

been examined using GC-MS/MS. In a study by Wiberg and colleagues using ion

trap GC-EI-MS/MS in positive ion mode, $M^{\bullet +}$ parent ions were observed to

produce $[M - CH_3SO]^+$ and $[M - CH_3SO - CO]^+$ as the predominant fragments

(Wiberg *et al.* 1998). Some ions analogous to the former, only negatively charged,

were observed in the current work, although these were typically less abundant

than the two major fragments mentioned above. No structure was suggested for

the $[M - CH_3SO - CO]^+$ ion in the study by Wiberg and coworkers. However, a

previous investigation of $[C_6H_5SO]^-$ fragmentation using collision induced

dissociation mass-analyzed ion kinetic energy (CID MIKE) demonstrated that

successive losses of S then CO, or vice versa, occur producing cyclopentadienyl

anions (Bowie and Stringer 1985). It therefore seems possible that the daughter

ions observed by Wiberg *et al.*, as well as the $[M - Cl + O - CH_3SO_2 - CO]^-$ ions

noted in the current work, might possess a chlorinated cyclopentadienyl ring

connected by a carbon-carbon bond to a chlorinated benzene ring.

Similar products have also been observed from in-source fragmentation

during the analysis of MeSO_2-CBs by GC-EI-MS (Bergman *et al.* 1980b, Buser *et

al.* 1992, Jensen and Jansson 1976). The reaction involved in the loss of a –

$CH_3SO$ group is known to proceed via rearrangement to a methanesulfinate ion

(Baarschers and Krupay 1973, Pratanata *et al.* 1974). In fact, it has been

suggested that the loss of $CH_3SO_2$ from methyl phenyl sulfone derivatives,

including MeSO_2-CBs, may be a two step process rather than a single bond

cleavage reaction due to the concurrent observation of $[M - CH_3]^+$ ions by EI-MS

(Baarschers and Krupay 1973, Haraguchi *et al.* 1987b). The negatively charged analogue of this fragment ion was observed in low relative abundance (<3%) in the present study. However, a peak was also visible at 79 amu in some of the product ion scans, corresponding to the intact, ionized methyl sulfone group. It therefore appears that there may be two competing fragmentation pathways for the loss of the methyl sulfone group for the analysis of $MeSO_2$-CBs by APPI-MS/MS.

The loss of $-CH_2SO$ is also commonly encountered in positive mode EI-MS (Bergman *et al.* 1980b, Haraguchi *et al.* 1987b), but this product was not observed in the current work. However, a small peak (<1% relative abundance) corresponding to the loss of water was visible for many analytes. This type of fragment has not been reported previously for $MeSO_2$-CBs but has been observed during the analysis of $[C_6H_5CH_2SO]^-$ ions by CID MIKE (Bowie and Stringer 1985). This may suggest that a rearrangement would be required in order for this fragment to be produced from the $MeSO_2$-CB parent ions.

Ions reported from in-source fragmentation during GC-ECNI-MS include $[M-CH_3SO_2 + H]^-$ (Haraguchi *et al.* 1993, Letcher and Norstrom 1997) and $[M - 2Cl + 2H]^-$ (Buser *et al.* 1992, Letcher and Norstrom 1997). In ECNI, hydrogen inclusion products are common due to the use of methane as a reagent gas. Upon irradiation with electrons, methane decomposes to produce reactive hydrogen atoms that bind to the metal surfaces of the source, catalyzing hydrogenation reactions (Sears and Grimsrud 1989). Due to the use of nitrogen as an inert collision gas in the current work and to the different fragmentation environment

117

where contact with the quadrupole walls generally leads to neutralization and loss of ions, hydrogenation products were not anticipated. Nonetheless, [M – Cl + O – 2Cl + 2H]⁻ ions were observed for the tetra-chlorinated congeners and were the most abundant daughter ions for 3′-MeSO$_2$-CB49 and 3-MeSO$_2$-CB52. Interestingly, these ions were produced in greater relative abundance for the higher chlorinated analytes during ECNI (Letcher and Norstrom 1997) but were only observed for the lower chlorinated analytes in the current work. The tetrachlorinated congeners were also noted to produce the most fragmentation of all the MeSO$_2$-CBs with a plethora of low abundance (≤10% relative intensity), low *m/z* products observed. It is conceivable that collisions between parent ions and hydrogen containing fragments could have led to [M – Cl + O – 2Cl + 2H]⁻ hydrogen-inclusion products. This would explain why these daughter ions were only observed for the tetrachlorinated compounds, since the higher chlorinated analytes produced very few detectable low *m/z* fragments. This is logical since higher chlorinated phenols are known to be stronger gas phase acids (Dzidic *et al.* 1975), so their corresponding phenoxide ions are more stable.

Product ion scans were acquired and compared between congeners in order elucidate any trends in the relative abundances of the major fragment ions. Since comparing the intensities of ions containing different numbers of chlorine atoms based on a single isotopic peak is biased (Letcher and Norstrom 1997), product ion scans for two major parent isotopic peaks were acquired under the same conditions for the tetra-chlorinated congeners and three for the penta- to hepta-chlorinated congeners. The intensities of the isotopic peaks from these

product ion scans were then added for each type of fragment ion detected. Summaries of the different fragment ions observed and their relative abundances for the chiral and achiral analytes are presented in **Tables 2.5** and **2.6** on the following pages.

For the majority of the analytes, the $[M - Cl + O]^-$ parent ion was the base peak in the product ion scans. With a few exceptions, the $[M - Cl + O - CH_3SO_2]^-$ daughter ion was the highest in relative abundance for the *meta*-substituted congeners, while the $[M - Cl + O - CH_3SO_2 - CO]^-$ daughter ion was highest for the *para*-congeners. Interestingly, the opposite trend was observed for the analysis of methoxychlorobiphenyls by GC-EI-MS (Jansson and Sundström 1974). In this case, it was found that the *para*-substituted congeners formed significant $[M - CH_3]^+$ ions, while the *meta*-substituted congeners fragmented further to form $[M - CH_3 - CO]^+$ ions. This was attributed to the enhanced stability of the *para*-congeners due to the availability of a quinoid-type resonance structure. Although rearrangement of the methyl sulfone group may occur during the fragmentation of MeSO$_2$-CBs, the observation of a peak at 79 amu in some of the product ion scans suggests that the entire functional group is lost, leaving the oxygen added during primary ionization behind. As discussed in the previous paragraph, this loss can also occur in two steps. Either way, the remaining oxygen would obviously be in a different position than that of the corresponding methoxy metabolite, leading to different trends. The fact that the opposite trend is observed may suggest that the oxygen remains in the *ortho* or *para* position for the *meta*-MeSO$_2$-substituted congeners and in the *meta* position for the *para*-MeSO$_2$-congeners. Furthermore,

119

**Table 2.5: Summary of fragment ions and their relative abundances for the analysis of chiral MeSO$_2$-CBs by APPI-MS/MS**

*Relative abundances calculated based on the sum of intensities of the three major isotopic peaks observed in the product ion scans for each fragment. Only ions with a relative abundance greater than 1% are shown, and only losses of $^{35}$Cl are considered. Analyte solutions, 1µg/mL in MeOH, infused individually via syringe pump at 10 µL/min. Mobile phase 50:50 methanol:water at 0.2 mL/min. APPI source temperature 300°C. Krypton lamp with toluene dopant infused at 20 µL/min. Scan time 2.0 min for 5-149 and 5'174, and 1.0 min for all other congeners.*

| Congener | Relative abundance (%) | | | | |
|---|---|---|---|---|---|
| | M–19 [M – Cl + O]$^-$ | M–82 [M – Cl + O – CH$_3$SO]$^-$ | M–87 [M – Cl + O – 2Cl + 2H]$^-$ | M–98 [M – Cl + O – CH$_3$SO$_2$]$^-$ | M–126 [M – Cl + O – CH$_3$SO$_2$ – CO]$^-$ |
| 5-91 | 100 | 6 | - | 68 | 4 |
| 4-91 | 38 | 13 | - | 34 | 100 |
| 3'-95 | 100 | - | - | 48 | 15 |
| 4'-95 | 100 | 24 | - | 29 | 16 |
| 5'-132 | 100 | - | - | 27 | 10 |
| 4'-132 | 74 | 12 | - | 19 | 100 |
| 5-149 | 100 | - | - | 56 | 34 |
| 4-149 | 100 | 8 | - | 29 | 85 |
| 5'-174 | 100 | - | - | 11 | 10 |
| 4'-174 | 100 | 6 | - | 50 | 95 |

**Table 2.6: Summary of fragment ions and their relative abundances for the analysis of achiral MeSO$_2$-CBs by APPI-MS/MS**

*Relative abundances calculated based on the sum of intensities of the two major isotopic peaks for the tetra-chlorinated congeners, three for the pentas and hexas, observed in the product ion scans for each fragment. Only ions with a relative abundance greater than 1% are shown and only losses of $^{35}$Cl are considered. Analyte solutions, 1μg/mL in MeOH, infused individually via syringe pump at 10 μL/min. Mobile phase 50:50 methanol:water at 0.2 mL/min. APPI source temperature 300°C. Krypton lamp with toluene dopant infused at 20 μL/min. Scan time 1.0 min.*

| Congener | Relative abundance (%) | | | | |
|---|---|---|---|---|---|
| | M–19 [M – Cl + O]$^-$ | M–82 [M – Cl + O – CH$_3$SO]$^-$ | M–87 [M – Cl + O – 2Cl + 2H]$^-$ | M–98 [M – Cl + O – CH$_3$SO$_2$]$^-$ | M–126 [M – Cl + O – CH$_3$SO$_2$ – CO]$^-$ |
| 3'-49 | 100 | - | 52 | 17 | 2 |
| 4'-49 | 100 | 44 | 29 | 57 | 54 |
| 3-52 | 100 | - | 18 | 7 | - |
| 4-52 | 100 | 49 | 5 | 67 | 83 |
| 4-64 | 47 | 9 | 3 | 44 | 100 |
| 3-70 | 62 | 28 | 16 | 52 | 100 |
| 4-70 | 100 | 13 | 41 | 64 | 40 |
| 3'-87 | 100 | 2 | - | 37 | 12 |
| 4'-87 | 100 | 23 | - | 33 | 35 |
| 3'-101 | 100 | - | - | 41 | 8 |
| 4'-101 | 50 | 34 | - | 54 | 100 |
| 5-110 | 100 | 12 | - | 48 | 6 |
| 4-110 | 79 | 48 | - | 10 | 100 |
| 3'-141 | 100 | - | - | 76 | 26 |
| 4'-141 | 55 | - | - | 34 | 100 |

since the oxygen is known to add via an ipso substitution mechanism involving an unconjugated intermediate with chlorine and peroxide groups attached to the same carbon atom (Dzidic *et al.* 1975), the oxygen must add at the site of a chlorine substituent. If these are assumed not to migrate during ionization or fragmentation (discussed further below), this would mean that the *para*-MeSO$_2$-substituted congeners would undergo oxygen substitution at the *meta* position and the *meta*-MeSO$_2$ congeners at the *ortho* position due to the 2,5-dichloro or 2,3,6-trichloro substitution pattern present in all environmentally relevant MeSO$_2$-CBs (Brandt *et al.* 1976). Steric hindrance would therefore arise due to interactions between the oxygen in the *ortho* position and the other *ortho* substituents for the parent compounds with *meta*-MeSO$_2$-substitution, making them less stable. This may partially explain the lower sensitivity observed for the *meta*-substituted congeners.

The relative abundance of the low intensity [M − Cl + O − CH$_3$SO]$^-$ daughter ions was also higher for the *para*-substituted congeners, while that of the [M − Cl + O − 2Cl + 2H]$^-$ daughter ions was higher for the *meta*-substituted isomers for all but one congener pair. For the former fragment ion, if, as predicted above, the oxygen is added *ortho* to the MeSO$_2$-group during primary ionization, the *meta*-MeSO$_2$-substituted congeners would possess a phenoxide group in the *ortho* position. This would lead to steric hindrance making this isomer less stable and therefore lower in intensity compared to the *para*-MeSO$_2$-substituted parent compound. The hydrogen inclusion product, on the other hand, was only observed for the tetra-chlorinated analytes, which produce a number of low mass fragments

as a result of their decreased stability compared to the higher chlorinated congeners. As discussed previously, these fragments are hypothesized to react with the parent phenoxide ions to produce the hydrogen inclusion species. Since the methyl sulfone group is still present in these fragments, the *meta*-substituted congeners would be less stable due to their lower number of resonance structures and would be expected to produce more low mass fragments and, therefore, $[M - Cl + O - 2Cl + 2H]^-$ ions.

Disparities in the relative abundances of ions between the *meta*- and *para*-isomers have been observed for these analytes in other studies, as well. For example, $[M - CH_3SO]^+$ fragment ions were observed to be slightly higher in abundance for the *para*-substituted congeners compared to the *meta* congeners by GC-EI-MS (Bergman *et al.* 1980b, Haraguchi *et al.* 1987b). Once again, this was attributed to increased stability of the *para*-substituted analogues due to the availability of a quinoid-type resonance structure. A similar observation and justification was made for $M^{\bullet-}$ ions produced during GC-ENCI-MS (Letcher and Norstrom 1997). However, when $MeSO_2$-CBs were analyzed by ion trap GC-EI-MS/MS, the $[M - CH_3SO]^+$ daughter ions were consistently higher in absolute abundance than the $[M - CH_3SO - CO]^+$ fragment ions, regardless of the location of methyl sulfone or chlorine substitution (Wiberg *et al.* 1998). This inconsistency is difficult to explain, but may potentially be attributable to the different types of fragmentation environments proffered by GC-EI-MS and ENCI-MS, LC-MS/MS and GC-EI ion trap MS/MS. The energy applied in the fragmentation environment is known to play an important role in fragmentation. For example, when an

electron energy of 70 eV is used with electron impact ionization, $[CH_3SO]^+$ and

$[CH_3SO_2]^+$ fragment ions are predominant (Bergman *et al.* 1980b), but they are

not detectable when an energy of 20 eV is used (Mizutani *et al.* 1978).

Although the chlorine substituents are known to undergo multiple

positional shifts, otherwise stated as scrambling, during EI ionization of certain

PCB congeners and methoxychlorobiphenyls (Jansson and Sundström 1974), this

has not been reported for the analysis methyl sulfone PCBs using ECNI, a softer

ionization technique that is more similar to APPI than EI. In the current work,

since there were some exceptions to the trends noted above, it is predicted that the

chlorine substitution pattern is conserved and has an impact on the relative and

absolute abundances of the fragment ions. For example, for the *meta*-congeners,

3-MeSO$_2$-CB70 gave a higher relative abundance of $[M - Cl + O - CH_3SO_2]^-$

compared to $[M - Cl + O - CH_3SO_2 - CO]^-$ and vice versa for 4′-MeSO$_2$-CB49,

4-MeSO$_2$-CB70 and 4′-MeSO$_2$-CB95 of the *para*-congeners. These trends are the

opposite of those observed for the remaining congeners. In addition, the relative

abundance of the $[M - Cl + O - 2Cl + 2H]^-$ daughter ion was higher for 4-

MeSO$_2$-CB70 compared to 3-MeSO$_2$-CB70, unlike the remaining tetrachlorinated

congeners. These four analytes all possess 2,5-dichloro substitution on the

MeSO$_2$-containing ring and lack a chlorine at position 5 on the opposite ring. The

only other congeners that satisfy these criteria are 3′- and 4′-MeSO$_2$-CB87, but

these isomers also possess a 2,3,4-trichloro substitution pattern on the non-

MeSO$_2$-CB ring, making them rather unique. Another structural characteristic that

sets 3-MeSO$_2$-CB70 and 4-MeSO$_2$-CB70 apart from all of the other analytes in

this study is that they contain a single *ortho* chlorine. A lower degree of *ortho*

chlorination would allow the adoption of a more planar configuration, which

would increase conjugation and resonance stabilization between the two rings

(Letcher and Norstrom 1997). This could potentially have an effect on the relative

stability of the daughter ions.

The $[M - Cl + O - CH_3SO_2]^-$ fragment ion was also highest in abundance

for the internal standard, 3-MeSO$_2$-4-Me-2',3',4',5,5'-pentachlorobiphenyl.

However, a small fraction of the parent ions of this compound lost the methyl

group within the source, leading to a small peak in the 385.0→306.0 transition.

This necessitated the chromatographic resolution of the internal standard from all

of the other pentachlorinated MeSO$_2$-CBs. No other fragment ions were produced

in significant quantities for the internal standard.

Since the product ion spectra were collected under similar conditions, it

was also possible to compare the absolute intensities between congeners using the

sums of the major isotopic peaks. Tables listing the summed absolute intensities

of the parent and fragment ions are presented in **Table 2.7** for the chiral

congeners and **Table 2.8** for the achiral congeners on the following pages.

Although the relative abundances of certain ions were greater for the *meta*

congeners, the absolute intensities were higher for the *para* congeners for all ions,

parents and fragments, with only a few exceptions. For fragments where the

methyl sulfone group remains intact, this is likely attributable to the greater

number of resonance structures and, therefore, greater stability of the *para*

**Table 2.7:** **Summary of parent and fragment ion absolute intensities and fragmentation efficiencies of *meta-*/*para-* analyte pairs for the analysis of chiral MeSO$_2$-CBs by APPI-MS/MS**

*Absolute intensities presented as the sum of intensities of the three major isotopic peaks observed in the product ion scans for each ion. Fragmentation efficiency calculated as the sum of intensities of the four major fragment ions divided by the parent ion intensity. Analyte solutions, 1 µg/mL in MeOH, infused individually via syringe pump at 10 µL/min. Mobile phase 50:50 methanol:water at 0.2 mL/min. APPI source temperature 300°C. Krypton lamp with toluene dopant infused at 20 µL/min. Scan time 2.0 min for 5-149 and 5'174, and 1.0 min for all other congeners.*

| Congener | Absolute intensity (counts per second) | | | | | Fragmentation efficiency |
|---|---|---|---|---|---|---|
| | M–19 [M – Cl + O]$^-$ | M–82 [M – Cl + O – CH$_3$SO]$^-$ | M–87 [M – Cl + O – 2Cl + 2H]$^-$ | M–98 [M – Cl + O – CH$_3$SO$_2$]$^-$ | M–126 [M – Cl + O – CH$_3$SO$_2$ – CO]$^-$ | |
| 5-91 | $4.42 \times 10^6$ | $2.60 \times 10^5$ | - | $3.01 \times 10^6$ | $1.63 \times 10^5$ | 0.16 |
| 4-91 | $1.28 \times 10^6$ | $4.50 \times 10^5$ | - | $1.15 \times 10^6$ | $3.35 \times 10^6$ | 3.88 |
| 3'-95 | $3.85 \times 10^5$ | - | - | $1.85 \times 10^5$ | $5.75 \times 10^4$ | 0.63 |
| 4'-95 | $4.58 \times 10^6$ | $1.10 \times 10^6$ | - | $1.35 \times 10^6$ | $7.25 \times 10^5$ | 0.69 |
| 5'-132 | $2.46 \times 10^5$ | - | - | $6.60 \times 10^4$ | $2.40 \times 10^4$ | 0.37 |
| 4'-132 | $4.23 \times 10^6$ | $7.00 \times 10^5$ | - | $1.10 \times 10^6$ | $5.70 \times 10^6$ | 1.78 |
| 5-149 | $1.38 \times 10^5$ | - | - | $7.80 \times 10^4$ | $4.70 \times 10^4$ | 0.91 |
| 4-149 | $9.90 \times 10^6$ | $8.00 \times 10^5$ | - | $2.90 \times 10^6$ | $8.40 \times 10^6$ | 1.22 |
| 5'-174 | $5.11 \times 10^5$ | - | - | $5.75 \times 10^4$ | $5.25 \times 10^4$ | 0.27 |
| 4'-174 | $3.58 \times 10^6$ | $3.00 \times 10^4$ | - | $1.80 \times 10^6$ | $3.40 \times 10^6$ | 1.45 |

**Table 2.8:** **Summary of parent and fragment ion absolute intensities and fragmentation efficiencies of *meta-/para-* analyte pairs for the analysis of achiral MeSO$_2$-CBs by APPI-MS/MS**

*Absolute intensities presented as the sum of intensities of the three major isotopic peaks observed in the product ion scans for each ion. Fragmentation efficiency calculated as the sum of intensities of the four major fragment ions divided by the parent ion intensity. Analyte solutions, 1 µg/mL in MeOH, infused individually via syringe pump at 10 µL/min. Mobile phase 50:50 methanol:water at 0.2 mL/min. APPI source temperature 300°C. Krypton lamp with toluene dopant infused at 20 µL/min. Scan time 1.0 min.*

| Congener | Absolute intensity (counts per second) | | | | | Fragmentation efficiency |
|---|---|---|---|---|---|---|
| | M–19 [M – Cl + O]$^-$ | M–82 [M – Cl + O – CH$_3$SO]$^-$ | M–87 [M – Cl + O – 2Cl + 2H]$^-$ | M–98 [M – Cl + O – CH$_3$SO$_2$]$^-$ | M–126 [M – Cl + O – CH$_3$SO$_2$ – CO]$^-$ | |
| 3′-49 | $1.01 \times 10^6$ | - | $5.30 \times 10^5$ | $1.75 \times 10^5$ | $2.00 \times 10^4$ | 0.72 |
| 4′-49 | $1.35 \times 10^6$ | $6.00 \times 10^5$ | $3.90 \times 10^5$ | $7.75 \times 10^5$ | $7.25 \times 10^5$ | 1.84 |
| 3-52 | $1.47 \times 10^6$ | - | $2.70 \times 10^5$ | $1.00 \times 10^5$ | - | 0.25 |
| 4-52 | $1.93 \times 10^6$ | $9.50 \times 10^5$ | $1.00 \times 10^5$ | $1.30 \times 10^6$ | $1.60 \times 10^6$ | 2.05 |
| 4-64 | $2.30 \times 10^6$ | $4.50 \times 10^5$ | $1.25 \times 10^5$ | $2.15 \times 10^6$ | $4.90 \times 10^6$ | 3.32 |
| 3-70 | $1.45 \times 10^6$ | $6.50 \times 10^5$ | $3.75 \times 10^5$ | $1.23 \times 10^6$ | $2.35 \times 10^6$ | 3.17 |
| 4-70 | $2.18 \times 10^6$ | $2.75 \times 10^5$ | $9.00 \times 10^5$ | $1.40 \times 10^6$ | $8.75 \times 10^5$ | 1.58 |
| 3′-87 | $9.90 \times 10^5$ | $2.00 \times 10^4$ | - | $3.70 \times 10^5$ | $1.23 \times 10^5$ | 0.52 |
| 4′-87 | $4.47 \times 10^6$ | $1.05 \times 10^6$ | - | $1.48 \times 10^6$ | $1.58 \times 10^6$ | 0.92 |
| 3′-101 | $1.06 \times 10^6$ | $1.00 \times 10^4$ | - | $4.35 \times 10^5$ | $9.00 \times 10^4$ | 0.51 |
| 4′-101 | $1.17 \times 10^6$ | $7.85 \times 10^5$ | - | $1.25 \times 10^6$ | $2.32 \times 10^6$ | 3.72 |
| 5-110 | $4.53 \times 10^6$ | $5.50 \times 10^5$ | - | $2.18 \times 10^6$ | $2.73 \times 10^5$ | 0.66 |
| 4-110 | $3.68 \times 10^6$ | $4.50 \times 10^5$ | - | $2.25 \times 10^6$ | $4.65 \times 10^6$ | 2.00 |
| 3′-141 | $8.15 \times 10^5$ | - | - | $6.20 \times 10^5$ | $2.15 \times 10^5$ | 1.03 |
| 4′-141 | $1.71 \times 10^6$ | $3.00 \times 10^4$ | - | $1.05 \times 10^6$ | $3.10 \times 10^6$ | 2.45 |

isomers (Bergman *et al.* 1980b, Haraguchi *et al.* 1987b, Letcher and Norstrom 1997). For fragments where the majority or the entirety of the methyl sulfone group is lost, this may be explained by steric effects. As discussed previously, the *meta*-MeSO$_2$ congeners are expected to contain a phenoxide group in the *ortho* position, leading to steric interactions with the other *ortho* substituents, including bulky chlorine atoms, making them less stable. For the chiral pentachlorinated analytes, the congeners 3′-MeSO$_2$-CB95 and 4′-MeSO$_2$-CB95 were noted to give much lower responses than 5-MeSO$_2$-CB91 and 4-MeSO$_2$-91, respectively. The PCB 91 metabolites possess a 2,5,6-trichloro substitution pattern on the MeSO$_2$-containing ring and a chlorine substituent in the *para* position on the opposite ring, unlike the PCB 95 metabolites, which possess 2,5-dichloro substitution on the MeSO$_2$ ring and lack a chlorine at position 4 on the opposite ring. Both of these structural characteristics have previously been suggested to have an effect of the relative abundances of fragment ions using ECNI (Letcher and Norstrom 1997).

The product ion spectra of the chiral pentachlorinated congeners 5-MeSO$_2$-CB91 and 4-MeSO$_2$-CB91 are provided in **Figure 2.10** on the following page. Note the disparity in the intensities of the parent and product ions between the two congeners. Although the spectra shown are for a single parent isotopic peak, the other major isotopes were examined and produced similar intensity ratios for these fragments. The intensity of the parent ion for 4-MeSO$_2$-CB91 was approximately one quarter that of 5-MeSO$_2$-CB91 in these scans, as in the Q1 mass spectra for these analytes (not shown). Also note that these two congeners
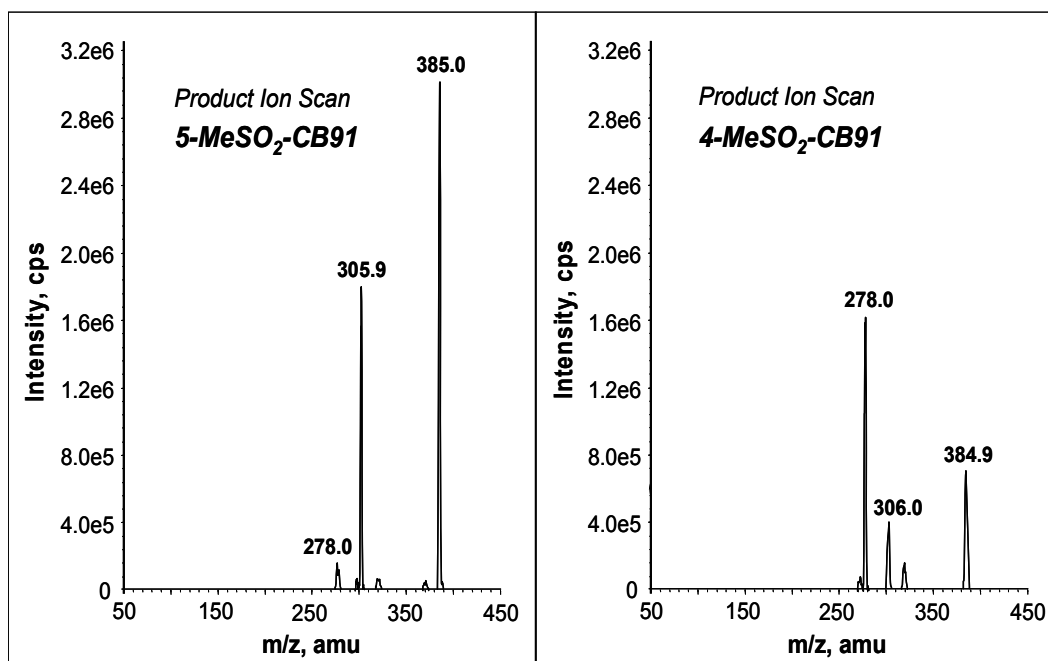
**Figure 2.10:** **Product ion scans of 5-MeSO$_2$-CB91 and 4-MeSO$_2$-CB91**
*Individual analyte solutions, 1μg/mL in MeOH, infused via syringe pump at 10 μL/min.*
*Mobile phase 50:50 MeOH:H$_2$O, flow rate 0.2 mL/min. APPI source temperature 300°C.*
*Krypton lamp with toluene dopant infused at 20 μL/min. Scan time 1.0 min.*

produced different relative abundances of the two predominant daughter ions. The

$[M - Cl + O - CH_3SO_2 - CO]^-$ daughter ion at 278 amu was higher in abundance

than the $[M - Cl + O - CH_3SO_2]^-$ daughter ion at 306 amu for 4-MeSO$_2$-CB91.

The opposite was observed for 5-MeSO$_2$-CB91, so these analytes followed the

general trends in daughter ion relative abundances for *meta* and *para* congeners,

as described above. It is easy to visualize in **Figure 2.10** that the sum of the

intensities of the major product ions for 4-MeSO$_2$-CB91 and 5-MeSO$_2$-CB91 are

similar but the parent ion intensity is much lower for 4-MeSO$_2$-CB91.

Consequently, since the *para* isomer had less parent ions entering the collision

cell but approximately the same amount of fragment ions leaving it, the

fragmentation efficiency for 4-MeSO$_2$-CB91 must have been higher than that of

its *meta* counterpart. The fragmentation efficiency is defined here as the summed intensities of the four major fragment ions and their major isotopes divided by the summed intensity of the parent ion isotopes from product ion scans. This parameter was calculated for all *meta*- and *para*- analyte pairs, and the results are included in **Tables 2.7** and **2.8** above. Note that the fragmentation efficiency was greater for the *para*-substituted analyte for all congeners pairs but the metabolites of PCB 70. As discussed previously, these analytes are unique because they contain a single *ortho* chlorine which could play a role in their deviation from this trend. The fragmentation efficiency was greater than unity for all of the *para* substituted analytes but $4'$-MeSO$_2$-CB95 (0.69) and $4'$-MeSO$_2$-CB87 (0.92), and less than unity for all of the *meta*-substituted analytes but 3-MeSO$_2$-CB70 (3.17) and 3-MeSO$_2$-CB141 (1.03).

Since the *meta*-substituted analytes ionized well but fragmented inefficiently, regardless of the *CAD* and *CE* settings, it was postulated that changing the type of gas used for collisionally activated dissociation might have an effect. It has been observed previously that the use of heavier collision gases leads to improved generation of high *m/z* fragments and transmission of these ions for large protein complexes analyzed using quadrupole time-of-flight mass spectrometry (Lorenzen *et al.* 2007). Although not as frequently used due to its higher cost compared to nitrogen, argon is used as the CAD gas for certain applications (Afonso *et al.* 2005, Headley *et al.* 2001). In a comparative study, argon was reported to give improved fragmentation relative to helium and xenon for the analysis of glycerolipids (Valeur *et al.* 1993). In order to test the

effectiveness of argon as the CAD gas in the current work, a tank of 99.998% argon was procured and attached to the CAD gas inlet of the mass spectrometer. Selected analytes were then analyzed by FIA at a CAD gas pressure of 5 psi. Once complete, the gas lines were switched and the nitrogen generator re-started and left overnight to allow a steady stream of high puritynitrogen to be re-established. The following day, the experiment was repeated using nitrogen as the CAD gas, and the collective results are presented in **Figure 2.11** on the following page. Note that statistical analyses could not be performed on this data set, since only one run was carried out for each combination of analyte and CAD gas type with all other conditions the same. However, some important conclusions could still be drawn. First of all, there was very little difference between the *S/N* calculated with the two different CAD gases for 4′-MeSO$_2$-CB132, 4-MeSO$_2$-CB149 and 4′-MeSO$_2$-CB174. However, there was a very large difference between the two for 5-MeSO$_2$-CB91, the only *meta*-substituted congener studied. In this case, the *S/N* was almost six times higher using nitrogen. Since there was obviously no benefit to the use of argon as the CAD gas, the remaining work was carried out with nitrogen.
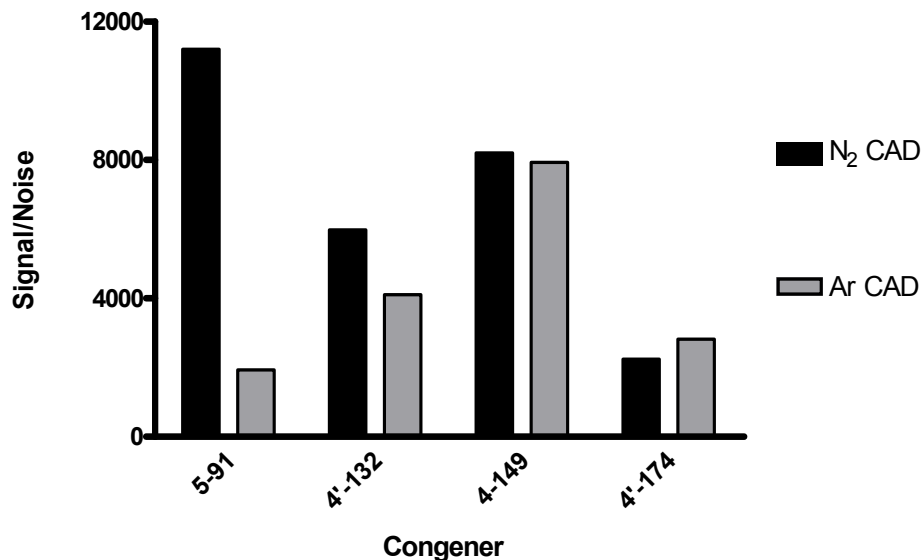
**Figure 2.11:** **Effect of CAD gas type on detection of MeSO$_2$-CBs**
*Flow injection analysis with 10 μL injections of individual analyte solutions, 1μg/mL in hexanes. Mobile phase 95:2.5:2.5 heptanes:methanol:ethanol, flow rate 0.75 mL/min. APPI source temperature 400°C. Krypton lamp, toluene dopant infused at 75 μL/min. CAD gas pressure 3 psi. Results of single analyses.*

Once a the CAD gas type was chosen, the optimal pressure was identified by flow injection analysis in the same manner and using the same representative analytes as described in **Section 2.2.1** for the APPI source parameters. The results of these experiments are presented in **Figure 2.12** on the following page. Although, there were no statistical differences between the *CAD* settings tested for any of the analytes, pressures of 2 and 5 psi appeared to be ideal for the analyte pairs 5-MeSO$_2$-CB91 and 4′-MeSO$_2$-CB132, and 4- MeSO$_2$-CB91 and 4′-MeSO$_2$-CB174, respectively. Manual infusion experiments for the low sensitivity meta-substituted congeners suggested that a CAD gas pressure of 5 psi was preferable, so this was chosen as the final value in order to afford improved detection for these analytes.
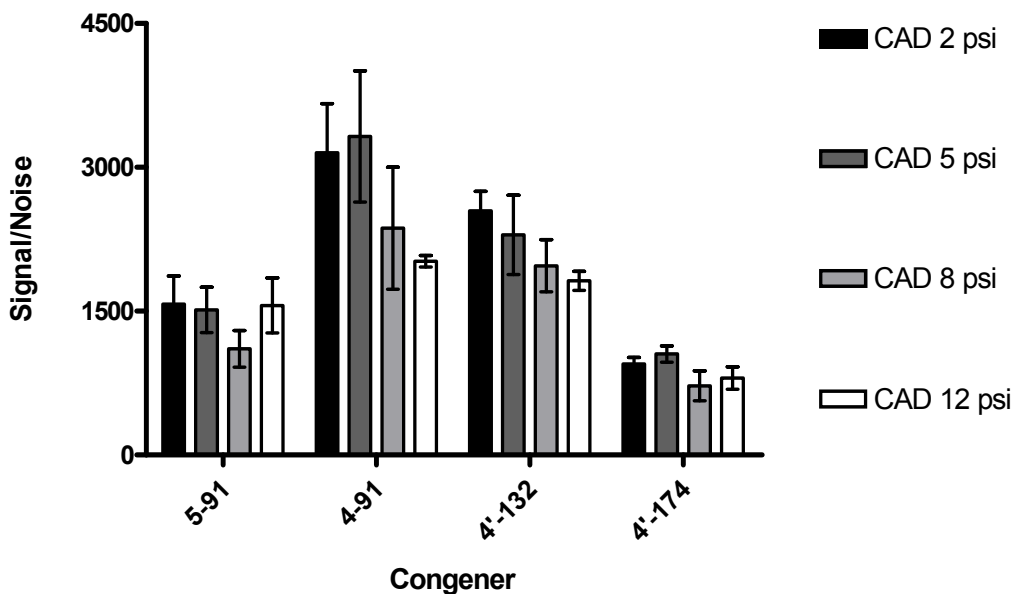
**Figure 2.12:** **Effect of CAD gas pressure on the detection of MeSO$_2$-CBs**
*Flow injection analysis with 5 μL injections of individual analyte solutions, 1μg/mL in hexanes. Mobile phase 95:2.5:2.5 heptanes:methanol:ethanol, flow rate 1.0 mL/min. APPI source temperature 250°C. Argon lamp, no dopant. Error bars indicate maxima and minima of triplicate analyses (n = 3) with average at the midpoint. There were no significant differences between any of the CAD gas pressures for any of the congeners by one-way ANOVA with Tukey's honestly significant difference test.*

In a final effort to improve the sensitivity of tandem mass spectral detection, experiments were performed to compare the different scan types available using the hybrid linear ion trap functionalities of the QTrap to standard multiple reaction monitoring mode. The two ion trap scan types examined were MS3 (MS/MS/MS) and EPI (enhanced product ion scan). In both scan types, the third quadrupole is operated as a quadrupole linear ion trap, capturing ions for a user specified amount of time, then ejecting selected *m/z* or scanning through selected *m/z* ranges, respectively, using radio frequency voltages. The ion trap also acts as a secondary collision cell for the MS3 scan type; resonance excitation is used to produce further fragmentation of the analyte of interest. In the MS3

scan, the masses of the primary and secondary daughter ions are selected by the user, but if no further fragmentation is expected, both can be set to the same value. In this way, the ion trap just acts as a collector for the primary daughter ions. Likewise, with the EPI scan type, the $m/z$ scan ranges can be set to a small span around the desired daughter ions instead of collecting an entire mass spectrum over a wide $m/z$ range. In both scan types, by collecting the ions and releasing them in discrete batches, the amount of ions reaching the electron multiplier tube after each cycle, and therefore the detector sensitivity, is increased. While the ions are being collected in the ion trap, it is also possible to collect the ions entering the first quadrupole simultaneously, referred to as $Q_0$-trapping, which leads to further increases in sensitivity. This strategy has been applied successfully to the quantitation of brominated flame retardants using a 4000 QTrap system with enhanced product ion scanning, which led to improved LODs and similar repeatability and linearity compared to multiple reaction monitoring (Guerra *et al.* 2008). Similar linear calibration ranges, slightly decreased precision and accuracy and similar selectivity have also been achieved using MS3 compared to MRM for the analysis of pharmaceuticals using chip infusion with a 2000 QTrap system (Leuthold *et al.* 2004).

Infusion experiments were performed initially to optimize the linear ion trap parameters. The values did not vary significantly between analytes or scan types (EPI vs. MS3), so the following settings were used for all linear ion trap experiments: LIT fill time 20 ms, scan rate 1000 amu/s, *CAD* medium, Q3 Entry Barrier 8 V, collar 2 barrier (*C2B*) 200 V, collision energy spread (*CES*) 0 V,

134

excitation time 200 ms (MS3 only), excitation energy (*AF2*) 80 V (MS3 only),

and $Q_0$ trapping on. Flow injection analyses were then performed in MRM, MS3

and EPI scan modes with a selected set of analytes, and the results are presented

in **Figure 2.13** on the following page. Note that statistical tests could not be

carried out on this data set since only one data point was collected for each

combination of scan type and analyte with all other conditions constant. However,

some general trends could still be observed. For 4-MeSO$_2$-CB149 and 4′-MeSO$_2$-

CB132, in particular, there was little difference between the various scan types.

The MS3 scan gave the lowest *S/N* for the former, and the EPI scan gave the

lowest *S/N* for the latter, but the other two scan types gave very similar results that

were approximately twice as high as the poorer scan. For 4′-MeSO$_2$-CB174, EPI

gave the best results, followed by MRM with approximately half the *S/N*, and

then MS3 with almost one quarter the *S/N* of EPI. In contrast, the two linear ion

trap scans gave similar results with a *S/N* almost twice that of the MRM scan for

4-MeSO$_2$-CB91. Although these general trends are useful, this figure does not

convey the problems with large noise spikes that were encountered using the

linear ion trap scans. Large time frames, on the order of 20 seconds to 1 minute

exhibited low noise levels in these chromatograms, but then big noise spikes with

peak heights of $10^4$ to $10^5$ cps, compared to analyte peak heights of $10^5$ to $10^8$ cps,

would appear intermittently. The chromatograms were generally noisier compared

to MRM. This led to inconsistent results and made quantitation difficult. These

noise spikes could be due to space charging, which occurs in ion trap mass

spectrometers when too many ions are held close together. However, the typical

manifestations of space charging are increased mass spectral band broadening and shifting to greater apparent mass (Hager 2002). In an effort to reduce the noise spikes, $Q_0$ trapping was turned off, the dynamic fill time feature turned on (stops infiltration of ions into the trap when a threshold ion flux is reached), and the amount of material injected during FIA decreased, but this led to little improvement. This likely indicates that space charging was not the cause. Another possibility is that the ion trap voltages selected were not optimal and somehow led to this intermittent, random ejection of ions. However, the parameters were re-optimized several times by infusion and FIA experiments to no avail. Due to the difficulties with noise spikes and unreliable quantitation, these scan types were abandoned, and MRM was used for all further experimentation.
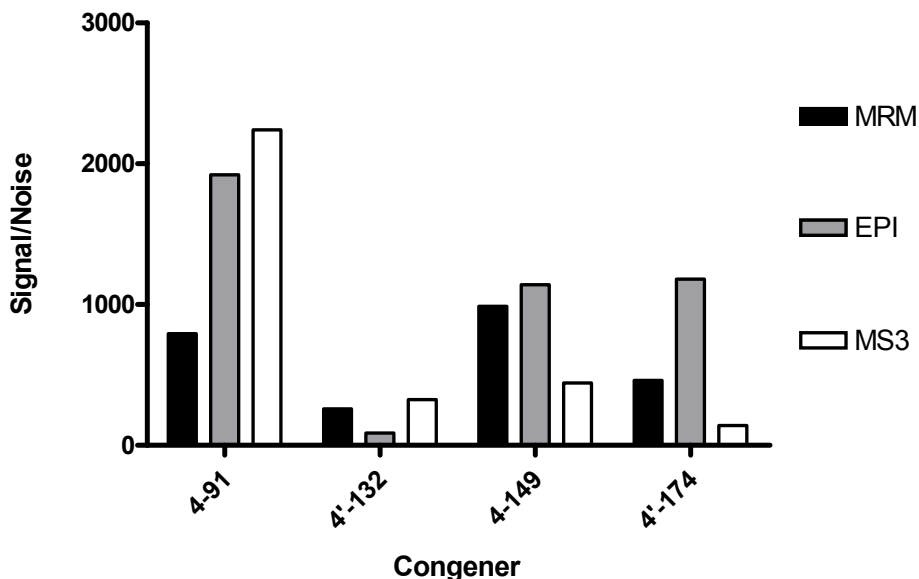


**Figure 2.13:** **Comparison of triple quadrupole and ion trap scan types for the detection of MeSO$_2$-CBs**
*MRM: multiple reaction monitoring; EPI: enhanced product ion scan; MS3: MS/MS/MS. Flow injection analysis with 10 μL injections of individual analyte solutions, 1μg/mL in hexanes. Mobile phase 95:5 heptanes:methanol, flow rate 0.4 mL/min. APPI source temperature 400°C. Krypton lamp, toluene dopant infused at 50 μL/min. Results of single analyses.*

The remaining conditions for tandem mass spectral detection using multiple reaction monitoring were then optimized by manual infusion for each analyte. The following parameters were optimized by ramping the voltage over the applicable range and selecting a value in the high plateau region of the resulting curve: declustering potential (*DP*), entrance potential (*EP*), collision cell entrance potential (*CEP*), collision energy (*CE*) and collision cell exit potential (*CXP*). Traces of selected curves for a representative set of analytes are depicted in **Figure 2.14** on the following page. Unlike the APPI source and CAD gas settings, these parameters could be set to different values for each transition. However, since there were several analytes being monitored by each transition, and dynamic MRM could not be employed with the version of the acquisition software used, it was necessary to compromise and find values for these parameters which produced an acceptable response for each analyte of the same mass. Fortunately, the optimal ranges for these parameters were generally quite similar between isobaric analytes. For instance, the declustering and collision cell exit potentials reached optimal values in similar ranges for all compounds within a given transition, as exemplified below for 5-MeSO$_2$-CB91, 4-MeSO$_2$-CB91, 3′-MeSO$_2$-CB87 and 4′-MeSO$_2$-CB87, as did the entrance potential (not shown). However, the optimal collision energy varied slightly between the *meta-* and *para*-substituted isomers, being slightly higher for the latter by about 5 volts for the pentachlorinated analytes. An intermediate collision energy of 40 volts was therefore selected for the 385.0→306.0 transition. However, a collision energy of 35 volts is recommended
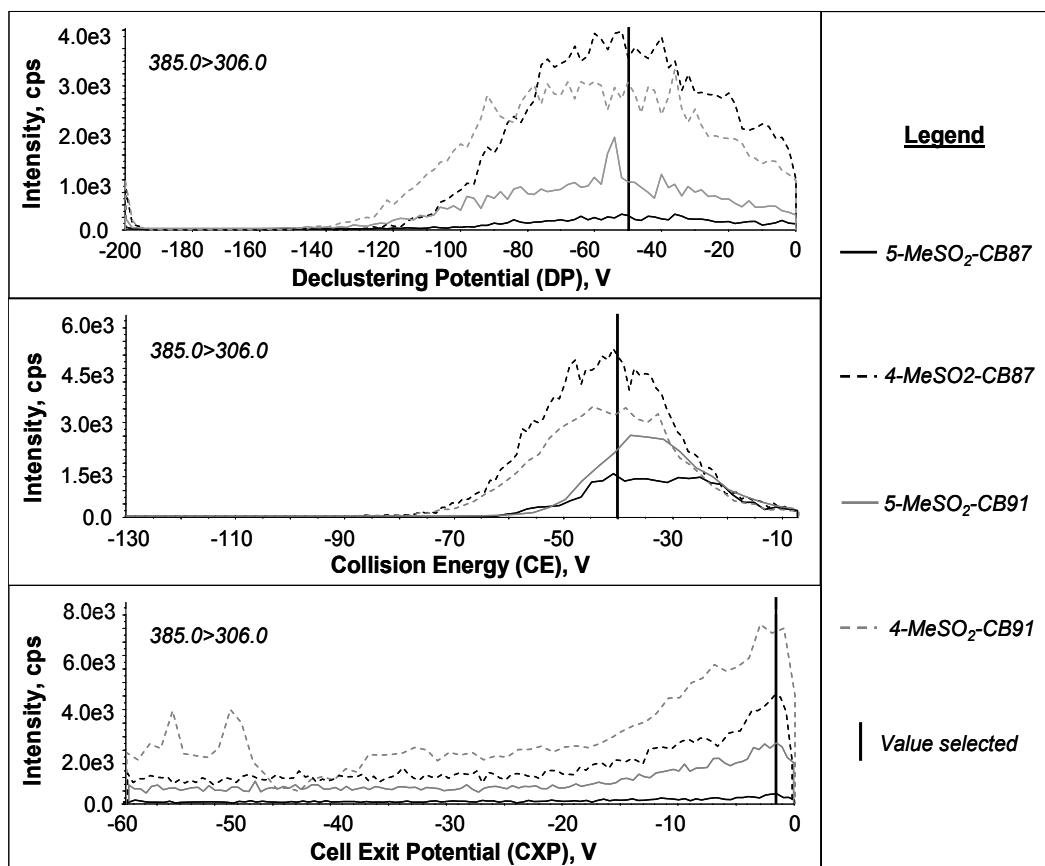
**Figure 2.14: Effect of selected MS/MS potential settings on the detection of MeSO$_2$-CBs**
*Analyte solutions, 1μg/mL in methanol, infused individually via syringe pump at 10 μL/min. Mobile phase 50:50 methanol:water, flow rate 0.2 mL/min. APPI source temperature 300°C. Krypton lamp with toluene dopant infused at 20 μL/min. Multiple reaction monitoring mode.*

for this transition in any future work, since this value is at the apex of the curves

for the *meta* analytes, which suffer from low sensitivity and for which this is the

quantitative transition. Previous analysis of MeSO$_2$-CBs by ion trap GC-EI-

MS/MS has shown that the optimal CID excitation amplitude increases with

increasing chlorination of the congeners (Wiberg *et al.* 1998), but a similar trend

was not observed for collision energy in the current work. The optimal parameters

for the other transitions were selected in a similar fashion, and a summary of the

MRM parameters used in the final method is presented in **Table 2.1** in **Section**

**2.1.4**. The default values assigned by the mass spectrometer software were selected for the collision cell entrance potential (*CEP*).

### *2.2.3 Optimization of liquid chromatographic conditions*

*2.2.3.1 Reversed phase enantiomer separations*

As discussed in detail in **Section 1.6.1**, gas chromatography using derivatized β-cyclodextrin stationary phases is the only separation method that has been applied to the quantitation of $MeSO_2$-CBs to date (Chu *et al.* 2003a, Ellerichmann *et al.* 1998, Karásek *et al.* 2007, Larsson *et al.* 2002, Larsson *et al.* 2004, Wiberg *et al.* 1998). However, the GC-based methodologies suffer from two key disadvantages: long run times and limited or no enantiomer resolution for some of the chiral congeners. Preliminary work towards the development of LC-based enantioselective separations has been presented in the literature (Hühnerfuss *et al.* 2002, Pham-Tuan *et al.* 2004, 2005). These studies used Nucleodex β-PM columns, which contain permethylated β-cyclodextrin as the stationary phase, with methanol/water mobile phases at sub-ambient temperatures in conjunction with UV detection.

Since these reports demonstrated good enantioselectivity for $MeSO_2$-CBs, these conditions were used as a starting point in method development. An analytical size Nucleodex β-PM column (4.6 mm x 250 mm x 5 μm, Macherey Nagel, Bethlehem, PA, USA) was tested using several different methanol/water mixtures and column temperatures in both isocratic and gradient mode. A gradient separation from 70:30 to 100:0 methanol:water over 30 minutes with a flow rate

139

of 0.4 mL/min at ambient temperature gave the best separation for all congeners. However, even under these conditions, only six out of the ten chiral congeners could be partially separated into their enantiomers: 3′-MeSO$_2$-CB95, 5′-MeSO$_2$-CB132, 4′-MeSO$_2$-CB132, 4-MeSO$_2$-CB149, 5′-MeSO$_2$-CB174, and 4′-MeSO$_2$-CB174. The corresponding chromatograms are presented in **Figure 2.15** on the following page. Note that the peaks are quite fronted, so the first eluting enantiomer appears larger than the second eluting enantiomer for several of the analytes, especially for those with limited resolution. This is likely a result of the gradient method employed, since this peak shape was not observed in the isocratic runs.

The remaining congeners did not show any indication of enantioselective separation under the conditions tested, including 5-MeSO$_2$-CB149. This congener has been separated into its enantiomers previously on a partially methylated Nucleodex β-PM column (Hühnerfuss *et al.* 2002), so the lack of separation in the current work may indicate that the stationary phase was fully permethylated. Although 5′-MeSO$_2$-CB174 was resolved, the separation factor (α) was lower (1.02) than that achieved by Hühnerfuss and coworkers (1.41) on their partially permethylated column when the same separation conditions were employed. The separation factors for 5′- and 4′-MeSO$_2$-CB132 (1.02 each), on the other hand, were much more similar to the results of these researchers (1.06 each) who found that enantioseparation of these congeners was best accomplished on a fully permethylated column. Limited separation of 4′-MeSO$_2$-CB174 (α = 1.01) and good separation of 3′-MeSO$_2$-CB95 (α = 1.04) were also achieved in the

current work, and, to our knowledge, there are no published enantioselective LC

separations for either of these congeners, and no GC separation for 3'-MeSO$_2$-

CB95.
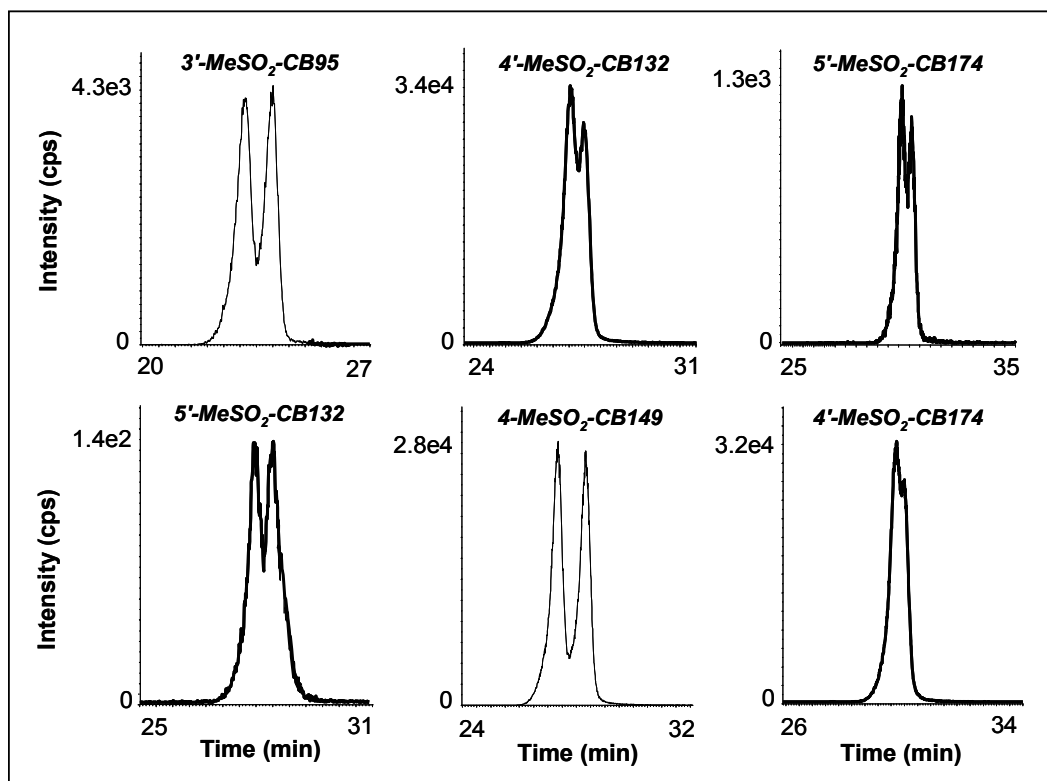


**Figure 2.15:** **Enantioselective separation of chiral MeSO$_2$-CBs on a reversed phase permethylated β-cyclodextrin column**
*Nucleodex β-PM 250 x 4.6 mm x 5 μm. Gradient elution: 0 min, 70:30 MeOH:H$_2$O; 30 min, 100:0 MeOH:H$_2$O; 35 min 100:0 MeOH:H$_2$O. Flow rate 0.3 mL/min, ambient temperature. Mixed standard solution, 1 μg/mL in MeOH, 25 μL injection. Extracted ion chromatograms.*

Although the Nucleodex β-PM produced some encouraging results in

terms of enantioselectivity, the separation of congeners of the same mass from

one another was decidedly poor. This was problematic since the congeners with

the same parent mass yielded daughter ions with the same mass and therefore

could not be distinguished by tandem mass spectrometry. As evidenced by the

retention times in **Figure 2.15**, E1 4-MeSO$_2$- CB149 co-eluted with E2 5-MeSO$_2$-CB149, E2 4-MeSO$_2$-CB149 with E1 5′- MeSO$_2$-CB132, and E1 4′-MeSO$_2$-CB174 with E2 5′-MeSO$_2$-CB174. Although not shown, the combined enantiomers of 4′-MeSO$_2$-CB95 also eluted in the same time window as E1 and E2 3′-MeSO$_2$-CB95, completely obscuring these lower abundance peaks. Various gradient separations were investigated in an effort to increase the separation between congeners, but to no avail.

Since the options for improving the Nucleodex β-PM separation had been exhausted, a number of other reversed phase enantioselective columns were tested in the hopes of simultaneously improving the enantiomer resolution and the separation between congeners. First, an (R,R)-Whelk-O1 Pirkle-type column (150 x 4.6 mm x 5 μm; Regis Technologies, Inc., Morton Grove, IL, USA), which is compatible with both normal and reversed phase solvents, was assessed. This sort of column has been used in normal phase to separate a wide variety of organic atropisomers (Pirkle *et al.* 1996), including some methyl sulfone compounds (Casarini *et al.* 1995, Villani and Pirkle 1995) and some chlorinated diarylmethyl esters (Job *et al.* 2004), which closely resemble PCBs. Unfortunately, despite the promising applications found in the literature, no enantiomer separation of any of the chiral analytes was achieved in reversed phase.

The next column examined was a Chirobiotic V (250 x 2.1 mm x 5 μm; Advanced Separation Technologies, Inc., Whippany, NJ, USA), which comprises a bonded stationary phase based on the macrocylic antibiotic vancomycin. This column has been applied to the separation of a wide variety of chiral

pharmaceuticals, including the non-steroidal anti-inflammatory drugs flurbiprofen and ketoprofen (Péhourcq *et al.* 2001), which contain a biphenyl moiety and a derivatized diphenyl ketone, respectively, making them structurally similar to PCBs. Unfortunately, there was no enantiomer resolution and very little retention for the chiral MeSO$_2$-CBs on this column. In an ambient temperature isocratic run with 80:20 methanol:water as the mobile phase at a flow rate of 0.2 mL/min, all of the analytes were eluted in under 5 minutes.

*2.2.3.2 Reversed Phase Fractionation*

The Nucleodex β-PM was the only enantioselective LC column that gave any enantioseparation for the chiral MeSO$_2$-CBs, but the lack of separation between congeners of the same mass remained a problem. A potential solution to this was to use a non-enantioselective pre-column to separate the MeSO$_2$-CBs from one another before executing the chiral separation. Various mixtures of PCBs have been separated using C18 stationary phases, for example, the congeners of Clophen A 30 and Clophen A 60 using a Nucloesil 100-5 C18 column (Brodsky and Ballschmiter 1988, 1989). In order to explore this option, a variety of different C18 stationary phases were screened. There was a noticeable correlation between retention and chlorination level, with the tetrachlorinated congeners generally eluting first, followed by the penta-, then the hexa-, and finally the heptachlorinated congeners. This was also observed by Brodsky and Ballschmiter in their PCB separations on Nucleosil 100-5.

No correlation between retention and position of MeSO$_2$-substitution was observed. However, some interesting differences in selectivity were seen with varying temperature and type of organic solvent. The separation between the penta-chlorinated congeners improved with decreasing temperature on all columns tested, giving the best separation at 5°C. In general, shape selectivity of C18 stationary phases increases at sub-ambient temperatures due to greater ordering of the brush-like stationary phase, as demonstrated by Sander and Wise using test mixtures of PAHs (Sander and Wise 1993). The *meta-* and *para*-MeSO$_2$ substituted analogues of PCB 95 proved the most difficult to separate. Using methanol as the organic solvent, it was only possible to separate these congeners using one of the five different C18 columns tested with methanol as the organic modifier: a Waters Symmetry Shield C18 (150 x 4.6 mm x 3.5μm; Waters Corporation, Milford, MS, USA) using 80:20 methanol:water as the mobile phase with a column temperature of 5°C. However, these congeners were also separated on a Restek Ultra C18 (150 x 4.6 mm x 5 μm; Restek, Bellefonte, PA, USA) when the organic solvent was switched from methanol to ethanol. The best separation in this case was achieved using 72:25 ethanol:water and a temperature of 5°C. Previously, a comparison of methanol, ethanol and acetonitrile as organic solvents for reversed phase HPLC on various C18 columns concluded that ethanol gives slightly enhanced shape selectivity (Sander and Wise 1993).

Overall, the Waters Symmetry Shield gave the most successful C18 separation for the chiral congeners. A sample chromatogram is depicted in **Figure 2.16** on the following page. The enhanced shape selectivity of this column may be

attributable to the presence of carbamate polar embedded groups in the stationary

phase (Euerby and Petersson 2003). The rest of the columns tested were

endcapped, but did not contain any such groups. This could be confirmed

experimentally by comparing separations acquired under the same conditions on

all columns. The Waters Symmetry Shield exhibited lower retention than all of

the others, which is typical for the separation of non-polar compounds on C18

columns containing polar embedded groups (Euerby and Petersson 2003, Rafferty

*et al.* 2008).
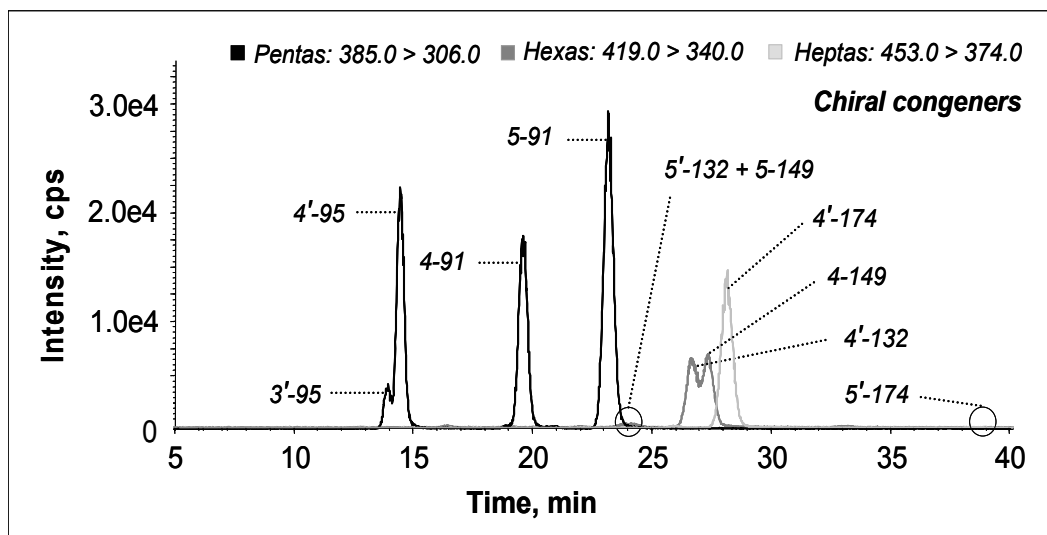


**Figure 2.16: Separation of chiral MeSO$_2$-CBs on an octadecylsilyl column**
*Waters Symmetry Shield C18 150 x 4.6 mm x 3.5 μm. Isocratic elution: 80:20
MeOH:H$_2$O. Flow rate 0.4 mL/min, temperature 15°C. Mixed standard solution,
1 μg/mL in MeOH, 15 μL injection. Extracted ion chromatograms. Low intensity peaks
are circled.*

Unfortunately, a number of co-elutions between the penta- and hexa-

chlorinated congeners resulted when the achiral congeners were introduced, as

shown in **Figure 2.17** on the following page. In order to determine if the

combined retention of the Waters Symmetry Shield C18 and the Nucleodex β-PM

145

could lead to adequate separation overall, the columns were connected in series, but there were still a number of interferences. It was concluded that while some level of separation between MeSO$_2$-CBs could be achieved on a C18 stationary phase, the selectivity was insufficient to allow for resolution of the majority of the target analytes either individually, or in conjunction with a Nucledoex β-PM column.
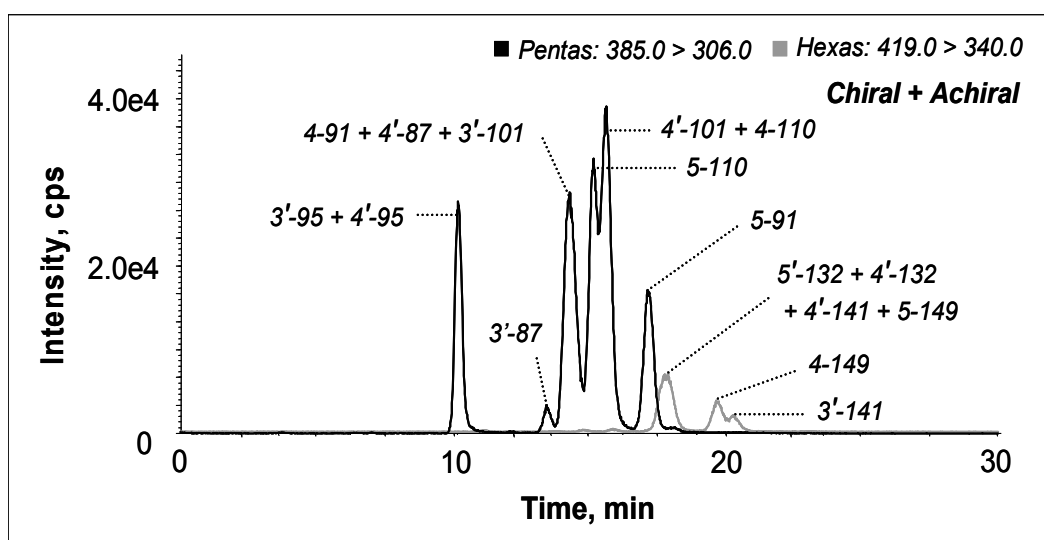


**Figure 2.17:** **Separation of selected achiral and chiral MeSO$_2$-CBs on a reversed phase octadecylsilyl column**
*Restek Ultra C18 150 x 4.6 mm x 5 μm. Isocratic elution: 85:15 MeOH:H$_2$O. Flow rate 0.4 mL/min, ambient temperature. Mixed standard solution, 1 μg/mL in MeOH, 15 μL injection. Extracted ion chromatograms.*

Cyano columns provide quite different selectivity from C18 stationary phases, and differences in elution order are frequently observed upon changing from one stationary phase to the other. Cyano columns have been investigated previously for the separation of PCBs in reversed phase, and reportedly give enhanced separation between congeners with zero or one *ortho* chlorine compared to C18 stationary phases (Brodsky and Ballschmiter 1989). In order to probe the

146

selectivity of this phase towards MeSO$_2$-CBs, some separations were carried out on a Luna cyano column (150 x 2 mm x 5 μm; Phenomenex, Torrance, CA, USA) in reversed phase. Unfortunately, very little selectivity or retention could achieved. In a room temperature isocratic separation with a mobile phase of 80:20 methanol:water and a flow rate of 0.2 mL/min, all of the 10 chiral congeners eluted as one or two broad peaks within 4 minutes. Brodsky and Ballschmiter also found a significant decrease in retention upon switching from a C18 to a cyano phase, with approximately a forty percent difference between run times of the optimized separations.

A ZirChrom CARB (150 x 4.6 mm x 3 μm; ZirChrom Separations, Inc., Anoka, MN, USA) column, consisting of a graphitic carbon stationary phase coated onto zirconia particles, was tested next. This column seemed like a promising candidate, as this type of stationary phase interacts strongly with polar functionalities and aromatic groups and displays excellent stereoselective properties (ZirChrom Separations, Inc. 2004). In addition, Aroclor separations have been carried out on porous silica substrates coated with graphitic carbon (Hanai and Walton 1977) and on porous graphitic carbon substrates (Creaser and Al-Haddad 1989) with some success. Unfortunately, there was far too much retention on this column. Even with the use of 100% ethanol, an elevated column temperature of 50°C, and a flow rate of 0.5 mL/min, it took over two hours for any of the congeners to be eluted. Irreversible adsorption is known to be problem for the separation of aromatic compounds on porous graphitic carbon stationary phases (Ramos *et al.* 1999), so these results are not surprising.

*2.2.3.3 Normal phase enantiomer separations*

Since many options had been explored in reversed phase with limited results, the next logical step was to move to normal phase chromatography. Some enantioselective LC columns are compatible with both reversed phase and normal phase solvents, including Chirobiotic V and (*R,R)*-Whelk-O1, so these columns were re-assessed with an alkane and an alcohol as the mobile phase components. Switching to normal phase did not lead to any improvement for the Chirobiotic V. There was still no enantiomer resolution and very little retention. However, there was a vast improvement for the (*R,R*)-Whelk-O1. With a mobile phase consisting of 97:3 hexanes:isopropanol, a temperature of 5°C, and a flow rate of 0.4 mL/min, it was possible to achieve enantiomer separation for 4-MeSO$_2$-CB91 ($\alpha = 1.03$), 5′-MeSO$_2$CB132 ($\alpha = 1.09$), 4′-MeSO$_2$-CB132 ($\alpha = 1.04$), 5-MeSO$_2$-CB149 ($\alpha = 1.02$), and 5′-MeSO$_2$-CB174 ($\alpha = 1.05$). A very limited amount of enantioseparation was also observed for 4-MeSO$_2$-CB149 under these conditions, although difficult to quantify. As is often the case with enantioselective LC, the resolution was improved by decreasing the column temperature (Snyder *et al.* 1997). Compared to the Nucleodex β-PM, similar enantiomer resolution was achieved for 5′-MeSO$_2$CB132, 4′-MeSO$_2$-CB132, and 5′-MeSO$_2$-CB174, but less for 4-MeSO$_2$-CB149. However, the (*R,R*)-Whelk-O1 column proved unable to separate 3′-MeSO$_2$-CB95 or 5-MeSO$_2$-CB149 much like the Nucleodex β-PM. In addition, separation between congeners with the same mass remained a problem with this Pirkle-type column. All of the chiral penta- and hepta-chlorinated

congeners co-eluted, and the *meta-* and *para-*congener pairs co-eluted for the hexa-chlorinated analytes. The peaks produced were also quite tailed.

While the enantioselectivity achieved in normal phase with the (*R,R*)-Whelk-O1 was encouraging, it was still desirable to resolve the enantiomers of more of the chiral analytes and to separate the congeners of the same mass from one another. Method development was continued to this end, and a Chiralpak AD column (250 x 4.6 mm x 10 µm, Chiral Technologies Inc., West Chester, PA, USA) was tested in normal phase. This column contains a 3,5-dimethylphenylcarbamate derivatized amylose stationary phase and belongs to the general class of carbohydrate columns, which are extremely diverse in the types of compounds they can separate (Okamoto and Kaida 1994). Initial method development on this column was performed in isocratic mode using a mixture of hexanes and isopropanol (IPA). With all combinations of percent isopropanol (1% to 15%) and temperature (5°C to 25°C) evaluated, the enantiomers of 4′-MeSO$_2$-CB95, 5′-MeSO$_2$-CB174 and 4′-MeSO$_2$-CB174 were separated with baseline resolution. Resolution of approximately 0.8 or greater for the enantiomers 4-MeSO$_2$-149 was also achieved under all conditions tested. However, for the remaining congeners, there were some trade offs, and it was not possible to achieve enantiomer separation of more than 7 congeners with resolution greater than about 0.8 simultaneously in one isocratic run. The two sets of conditions where enantioseparation of 7 congeners was possible were: mobile phase 85:15 hexanes:IPA and column temperature 5°C, and 90:10 hexanes:IPA and temperature 10°C. Higher temperatures (15°C to 25°C) favoured the separation of

4-MeSO$_2$-CB91 and 5′-MeSO$_2$-CB132, whereas lower temperatures ($\leq 10$°C) favoured the separation of 3′-MeSO$_2$-CB95, 4′-MeSO$_2$-CB132, and 5-MeSO$_2$-CB149. A higher quantity of hexanes (95% to 99%) favoured the separation of 4-MeSO$_2$-CB91, 5′-MeSO$_2$-CB132, 4′-MeSO$_2$-CB132, and 5-MeSO$_2$-CB149, whereas a lower quantity (85% to 90%) was preferable for 3′-MeSO$_2$-CB95. These trends were generally consistent regardless of the solvents used, and a summary of the optimal separation conditions for each congener are presented in **Table 2.9** below. Note that it was not possible to separate 5-MeSO$_2$-CB91 under any of the conditions tested.

**<u>Table 2.9</u>: Variation in optimal conditions between chiral MeSO$_2$-CB congeners for enantioselective separation on Chiralpak AD or AD-H**
[1]*Any % polar modifier in the range of 3-15%.*
[2]*Any column temperature in the range of 5-25°C.*
[a]*Not separated under any conditions tested.*

| Chiral congener | Optimal % polar modifier | Optimal column temperature, °C |
|---|---|---|
| 5-MeSO$_2$-CB91[a] | - | - |
| 4-MeSO$_2$-CB91 | $\geq 5$ | $\geq 20$ |
| 3′-MeSO$_2$-CB95 | $\geq 10$ | $\leq 10$ |
| 4′-MeSO$_2$-CB95 | Any[1] | Any[2] |
| 5′-MeSO$_2$-CB132 | $\leq 10$ | $\leq 10$ |
| 4′-MeSO$_2$-CB132 | Any[1] | $\leq 10$ |
| 5-MeSO$_2$-CB149 | $\geq 5$ | $\leq 10$ |
| 4-MeSO$_2$-CB149 | $\leq 10$ | $\leq 10$ |
| 5′-MeSO$_2$-CB174 | Any[1] | Any[2] |
| 4′-MeSO$_2$-CB174 | Any[1] | Any[2] |

These initial results were very promising. The Chiralpak AD was able to separate all of the congeners resolved by the Nucleodex β-PM and by the (*R,R*)-

Whelk-O1 with greatly improved resolution, although not in a single run. The enantiomers of 4′-MeSO$_2$-CB95 were also separated, which could not be accomplished with either of the latter two columns, and the number of co-elutions between congeners of the same mass were reduced. However, co-elution of the congeners 5′-MeSO$_2$-CB132 and 4-MeSO$_2$-CB149 remained a problem. In an effort to improve the Chiralpak AD separation further, different polar modifiers were assessed. Ethanol was tested first, and this polar modifier allowed for enantiomer separation of 9 out the 10 chiral analytes with near baseline resolution for all but 4′-MeSO$_2$-CB132 (resolution approximately 0.8) with 95:5 hexanes:ethanol as the mobile phase at 20°C. No single previously published method has achieved enantioseparation of more than 8 out of the 10 chiral congeners. Although there were some changes in elution order with this polar modifier, there were still problems with co-elutions between congeners of the same mass, so experimentation with mobile phase components was continued.

It is possible to use methanol as a polar modifier with hexanes but only in a quantity of 5% or less, as immiscibility can become an issue at higher proportions. Some experiments were carried out using mixtures of methanol and hexanes but with limited success. Even when less than 5% methanol was used, the column took a long time to equilibrate (greater than 1 hour at 1.0 mL/min), especially at decreased temperature. It is known that the polar modifier becomes incorporated into the chiral stationary phase, and the amount reaches a threshold level at approximately 5%. Below this quantity of polar modifier, irreproducible separations have been observed due to slow mass transfer of the polar modifier

between the mobile phase and the stationary phase (Stringham 2006). This phenomenon may have contributed to the slow equilibration and unstable separations observed here. It was also noted that if the flow through the column stopped for any reason, it took a long time to re-establish equilibrium.

For the few runs where equilibration was achieved, the peaks were still quite broad and the retention times not very reproducible. In order to avoid these problems, a 1:1 mixture of methanol and ethanol was assessed, and this gave the best results of any of the polar modifiers investigated without the issues accompanying the use of methanol alone. It has been suggested previously that if the separation is improved by the use of ethanol over isopropanol, it is likely that further improvement may be achieved by the addition of methanol to ethanol for chiral separations on polysaccharide stationary phases (Stringham 2006). The enantiomers of 9 out of the 10 chiral congeners were separated at 10°C with 90:5:5 hexanes:methanol:ethanol as the mobile phase, and all enantiomers were baseline resolved except for 4-MeSO$_2$-CB149, for which the resolution was approximately 0.8. The elution order for the penta-chlorinated congeners changed with this polar modifier, and the number of co-elutions between congeners of the same mass was reduced but not eliminated. Another benefit of adding methanol to the polar modifier was that the analysis time was decreased at the same modifier strength compared to ethanol. In addition, enantiomer resolution was increased compared to the ethanol and isopropanol separations. Interestingly, the reverse effect has been observed previously for the separation of chiral esters on Chiralpak OD (Snyder *et al.* 1997). In this case, the enantiomer resolution

increased with increasing weight of the alcohol with *tert*-butanol giving the best separation. Clearly, the analyte and stationary phase substituents play an important role in determining enantioselectivity.

As a final attempt to improve the separation and minimize the number of co-elutions, the alkane was switched to heptanes. Although not used as commonly, it has been suggested that changing the alkane from hexane(s) to heptane(s) can lead to subtle changes in selectively (*Chiral Technologies Inc.* 2001). Heptanes are also less volatile and less toxic than hexanes, and are therefore safer to handle. This mobile phase indeed lead to a subtle change in selectivity and helped reduce the number of co-elutions while maintaining the quality of the enantiomer separations. With heptanes, it was finally possible to resolve the second eluting enantiomer of 3′-MeSO$_2$-CB95 from the first eluting enantiomer of 4-MeSO$_2$-CB91, which was not achieved with any other mobile phase combination. Some changes in elution order occurred once again upon switching mobile phases. The sensitivity of carbohydrate columns to mobile phase composition has been documented previously and may be attributable to changes in the three dimensional structure of the polymeric stationary phase with changes in solvent (Rousell *et al.* 2004, Stringham 2006). A reversal in elution order for the enantiomers of a variety of compounds has also been observed with changing mobile phase components for carbohydrate columns (Balmér *et al.* 1992, Gaffney *et al.* 1989, Wang *et al.* 2000). It is therefore possible that changes in enantiomer elution order contributed to the overall changes in elution order between congeners in the current work.

Note that the initial method development on this stationary phase was performed on a Chiralpak AD (10 μm particles), and the final phase of method development and all sample analyses were performed on a Chiralpak AD-H (5 μm particles). The Chiralpak AD-H had improved chemical stability and gave improved efficiency over the 10 micron particle column. The peak widths were noticeably reduced and the resolution therefore improved. Subtle selectivity differences were also evident between the two columns. The distance between the second eluting enantiomer of 3′-MeSO$_2$-CB95 and the first eluting enantiomer of 4-MeSO$_2$-CB91 increased, so that these two peaks were no longer overlapping slightly as with the Chiralpak AD. While the elution order remained the same for the hexa-chlorinated congeners, the resolution of 4-MeSO$_2$-CB149 improved to about 0.8 versus 0.6 with the Chiralpak AD.

The chromatographic conditions that gave the best results with the Chiralpak AD-H were a mobile phase of 90:5:5 heptanes:methanol:ethanol and a temperature of 15°C, or 95:2.5:2.5 heptanes:methanol:ethanol and 10°C. The former separation is presented in **Figure 2.18** on the following page. Note that there were still a few co-elutions between congeners of the same mass that could not be avoided. The first enantiomer of 5′-MeSO$_2$-CB132 co-eluted with that of 5-MeSO$_2$-CB 149. Also, when the achiral congeners were introduced, 3′-MeSO$_2$-CB101, 5-MeSO$_2$-CB110, and 4-MeSO$_2$-CB110 all co-eluted with E1+ E2 5-MeSO$_2$-CB91. Also problematic was the interference of the internal standard with the second eluting enantiomer of 3′-MeSO$_2$-CB95. Although there was a dedicated transition for the internal standard where no other congeners could be
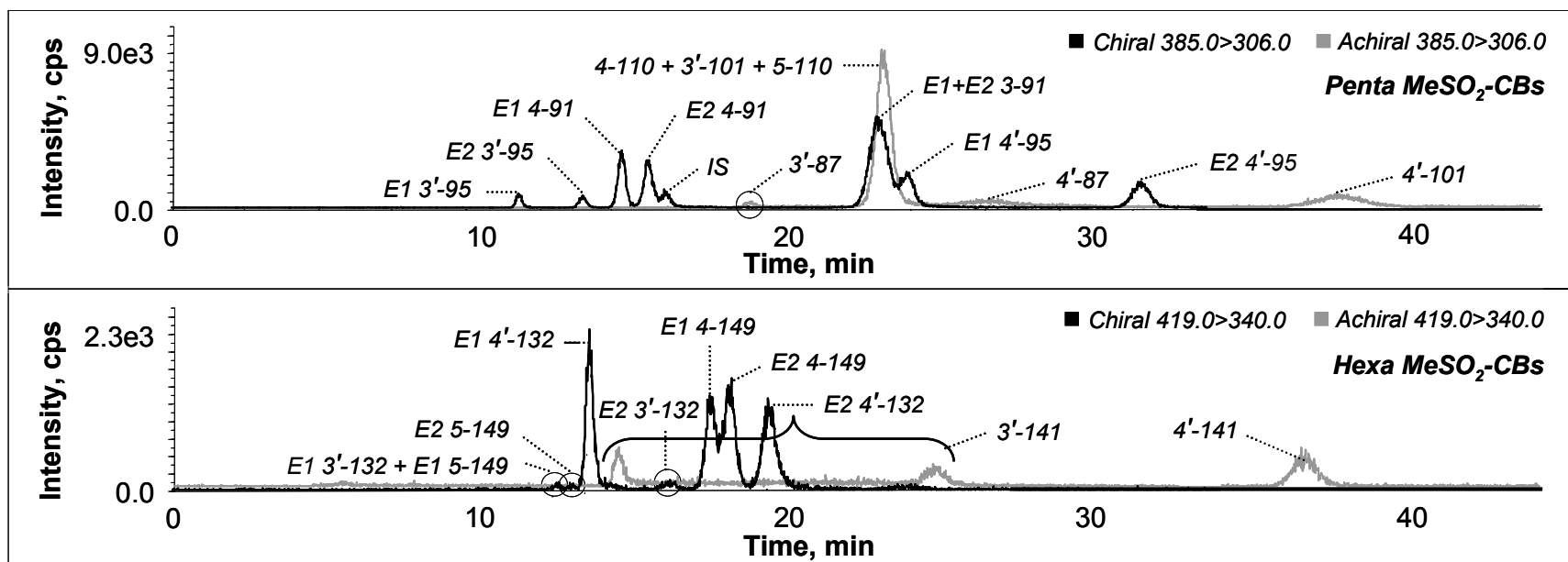
**Figure 2.18:** Separation of achiral and chiral MeSO$_2$-CBs on an enantioselective derivatized amylose column in normal phase
*Chiralpak AD-H 250 x 4.6 mm x 10 μm. Isocratic elution: 90:5:5 heptanes:methanol:ethanol. Flow rate 0.75 mL/min, temperature 15°C. Mixed standard solution, 1 μg/mL in heptanes, 10 μL injection. Extracted ion chromatograms. Low intensity peaks are circled. Bracket indicates bimodal elution profile of 3'-MeSO$_2$-CB141. IS: internal standard, 3-MeSO$_2$-4-Me-2',3',4',5,5'-pentachlorobiphenyl.*

detected, the methyl group dissociated in the ionization source to a certain extent, leading to a small amount of signal for the internal standard in both of the pentachloro transitions. The 385.0→278.0 transition was 2.4% of the base peak and the 385.0→306.0 transition 2.2% of the base peak compared to the internal standard quantifying transition (399.0→320.0).

Some general trends in terms of elution order were observed throughout the method development process with this stationary phase. For instance, the *meta*-substituted congeners were less retained than the *para* congeners under all separation conditions. The only exceptions to this rule were the metabolites of PCBs 91 and 110. For the former, the *meta* congener eluted first only when mixtures of isopropanol and hexanes were used as the mobile phase. For all other solvent combinations tested, the enantiomers of *para* congener eluted first. The achiral congeners 4-MeSO$_2$-CB110 and 5- MeSO$_2$-CB110 co-eluted under many of the sets of conditions employed, but, when they were successfully resolved from one another, the *para*-substituted congener eluted first.

An interesting chromatographic phenomenon was also detected for some of the achiral *meta*-substituted congeners. For example, in **Figure 2.18**, the hexa-chlorinated congener 3′-MeSO$_2$-CB141 is obviously spread out into two peaks with a plateau in between. This was problematic because the plateau region, which had a height on the order of several thousand counts per second, interfered with several of the chiral hexa-chlorinated congeners, including the low intensity peak E2 5′-MeSO$_2$-CB132, which was completely masked. Although not obvious

in this particular chromatogram, this phenomenon was also noted for 5-MeSO$_2$-CB110 and possibly for 3′-MeSO$_2$-CB87 under various conditions. Sample chromatograms for 5-MeSO$_2$-CB110 and 3′-MeSO$_2$-CB141 are displayed in **Figure 2.19** on the following page. The same peak shape was retained when the injection volume was decreased from 25 to 15 μL, so column overloading is not suspected. Unfortunately, it was difficult to obtain a convincing chromatogram for 3′-MeSO$_2$-CB87 due to its poor response. However, two low intensity peaks with a noisier region in between could often be detected for this congener, so it is believed to exhibit the same behaviour.

The peak shapes shown in **Figure 2.19** are curiously similar to those of a chiral compound undergoing enantiomerization during a chromatographic run, which can be observed when the interconversion between enantiomers is relatively slow on the timescale of the separation (D'Acquarica et al. 2006, Trapp et al. 2001, Wolf 2005). This type of behaviour has been observed previously for hindered naphthyl sulfone derivatives upon separation at decreased temperatures on Pirkle-type stationary phases (Casarini *et al.* 1995, Villani and Pirkle 1995). It also has been noted for the separation of PCB 40, which is a di-*ortho*, di-*meta* chlorinated congener, on a Nucleodex β-PM column using a methanol:water mobile phase and a temperature of 0°C (Haglund 1996a). Interestingly, none of the other achiral congeners produced these characteristic chromatograms under any of the conditions tested. The three congeners involved all possessed di-*ortho* chlorine and *meta*-MeSO$_2$ substitution along with asymmetrical substitution about the axis of the biphenyl bond. They also all contained a chlorine substituent in the
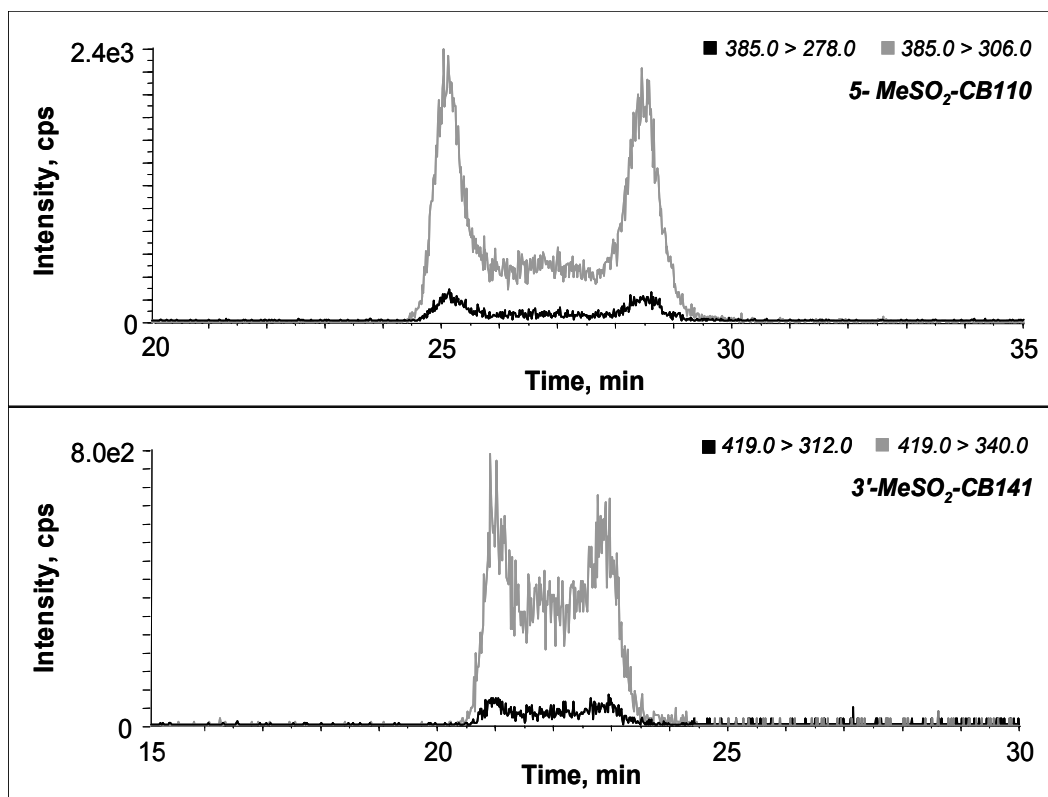
**Figure 2.19:** Separation of achiral *meta*-MeSO$_2$-CBs on an enantioselective derivatized amylose column in normal phase – unusual peak shapes observed for selected congeners

*Chiralpak AD 250 x 4.6 mm x 10 μm. Isocratic elution: 90:10 hexanes:isopropanol. Flow rate 0.4 mL/min, temperature 10°C. Individual standard solutions, 1 μg/mL in hexanes, 25 μL injections. Extracted ion chromatograms.*

*meta*-position adjacent to one of the *ortho* chlorines. None of the other achiral analytes satisfied all four of these criteria. Also of interest is that the distance between the two peaks and the ratio of the height of the first peak to that of the second peak was observed to increase with decreasing temperature and percent polar modifier, and with increasing overall retention on the column, regardless of the solvent system used. Similar changes in the elution profile with changing temperature have been documented previously (D'Acquarica *et al.* 2006, Wolf 2005). Similar findings in terms of changes in solvent composition have also been

reported previously from investigations of pharmaceutical compounds using a ChiraDex column in reversed phase (Cabrera *et al.* 1996). In this work, the authors noted that previous studies employing the same stationary phase but a more highly aqueous, and therefore weaker, mobile phase found lower enantiomerization rate constants for the compounds they investigated.

As mentioned previously, in order for a PCB to be chiral under physiological conditions, it must possess 3 or 4 *ortho* chlorines, as well as asymmetrical substitution about the biphenyl bond (Kaiser 1974). However, atropisomeric compounds, such as PCBs and their metabolites, are stereolabile and their stability to enantiomerization is very much temperature dependent. So long as the congeners are asymmetrically substituted, they have the potential to be exhibit chirality at certain temperatures. The rotational free energy barriers have been predicted or measured for several PCBs using quantum calculations and/or chromatographic techniques, and the Gibbs free energies of activation, $\Delta^{\ddagger}G$, for rotation about the biphenyl bond are generally agreed to be in the range of 80 kJ/mol for di-*ortho* PCBs, 145 to 185 kJ/mol for tri-*ortho* PCBs, and 210 to 250 kJ/mol for tetra-*ortho* PCBs (Harju and Haglund 1999, Kaiser 1974, Nezel *et al.* 1997, Schurig *et al.* 1995). In addition, an average increase in the rotational barrier of 6.4 kJ/mol has been reported for tri-*ortho* PCB congeners with one chlorine substituent in the *meta*-position (Harju and Haglund 1999), a phenomenon referred to as the buttressing effect (Eliel and Wilen 1994). Although PCB 40 exhibited on-column enantiomerization, Haglund (1996a) was able to completely resolve the enantiomers of several other di-*ortho,* di-*meta*

PCBs on a Nucleodex β-PM column. However, PCBs 16 and 180, which are di-*ortho*, mono-*meta* chlorinated congeners, could not be resolved, and a single peak was observed. The author attributed this to a lower enantiomerization barrier due to the lack of a second buttressing *meta*-chlorine substituent.

The rotational barriers for selected methylsulfonyl PCB metabolites have also been estimated using semi-empirical and *ab initio* quantum calculations and compared to the parent compounds (Nezel *et al.* 1997). The presence of the methyl sulfone group in the *ortho* position led to an increase in the rotational barrier of approximately 13 kJ/mol for 2-MeSO$_2$-2′,6′-trichlorobiphenyl compared to 2,2′,6′-trichlorobiphenyl by AM1 calculations. Although the *ortho*-MeSO$_2$-CB congeners were not of interest here, this suggests that the buttressing effect may be increased for congeners with the MeSO$_2$ group in the *meta* position. Since the analytes displaying this unusual chromatographic behaviour possessed both a *meta*-MeSO$_2$ and a *meta*-Cl substituent, the combined buttressing effects may have led to an increase in the rotational barrier over the other achiral analytes. This increase could have been significant enough to allow the enantiomerization barriers of these three congeners to enter into the range that can be explored by dynamic HPLC in the accessible temperature range of 5 to 20°C. Dynamic HPLC has been applied to the analysis of compounds with enantiomerization $\Delta^{\ddagger}G$ values of 60 to 120 kJ/mol (Wolf 2005), which is in the expected range for di-*ortho*-MeSO$_2$-CBs. It is likely that similar effects could be observed for the other achiral analytes if the temperature could be decreased further. Many dynamic HPLC experiments are carried out at temperatures as low as -80°C (Wolf 2005).

*2.2.3.4 Normal phase fractionation*

Although an excellent enantiomer separation had been achieved using the Chiralpak AD-H, there were still some co-elution issues hampering the method. In an effort to circumvent these problems, non-enantioselective columns that could be used as a first dimension pre-separation were investigated once again, only in normal phase this time as opposed to reversed phase. First, the Luna cyano column discussed previously for reversed phase separations in **Section 2.2.3.2** was examined in normal phase and greatly improved separation was achieved compared to reversed phase. A sample chromatogram is presented in **Figure 2.20** on the following page. Although the separation was satisfactory for the hexa-chlorinated congeners, there were still many interferences for the penta-chlorinated congeners. When a trial run was performed with the cyano column connected in series to the Chiralpak AD-H, the situation did not improve and there were still many interferences between achiral and chiral analytes. This was difficult to avoid because of the large plateaus created by the introduction of certain achiral congeners onto the enantioselective column, as discussed above.

Finally, a rather unique stationary phase was encountered in the literature. Pyrenyl ethyl silica (PYE) has been used as a sample preparation tool for the fractionation of PCBs prior to analysis using GC-based methodologies (Haglund *et al.* 1990b, Jaouen-Madoulet *et al.* 2000, Ramos *et al.* 1999, Wells *et al.* 1995). Although this column is marketed mainly for reversed phase separations, it is also compatible with normal phase solvents. In one comparative study, different reversed phase and normal phase solvents were examined for the separation of
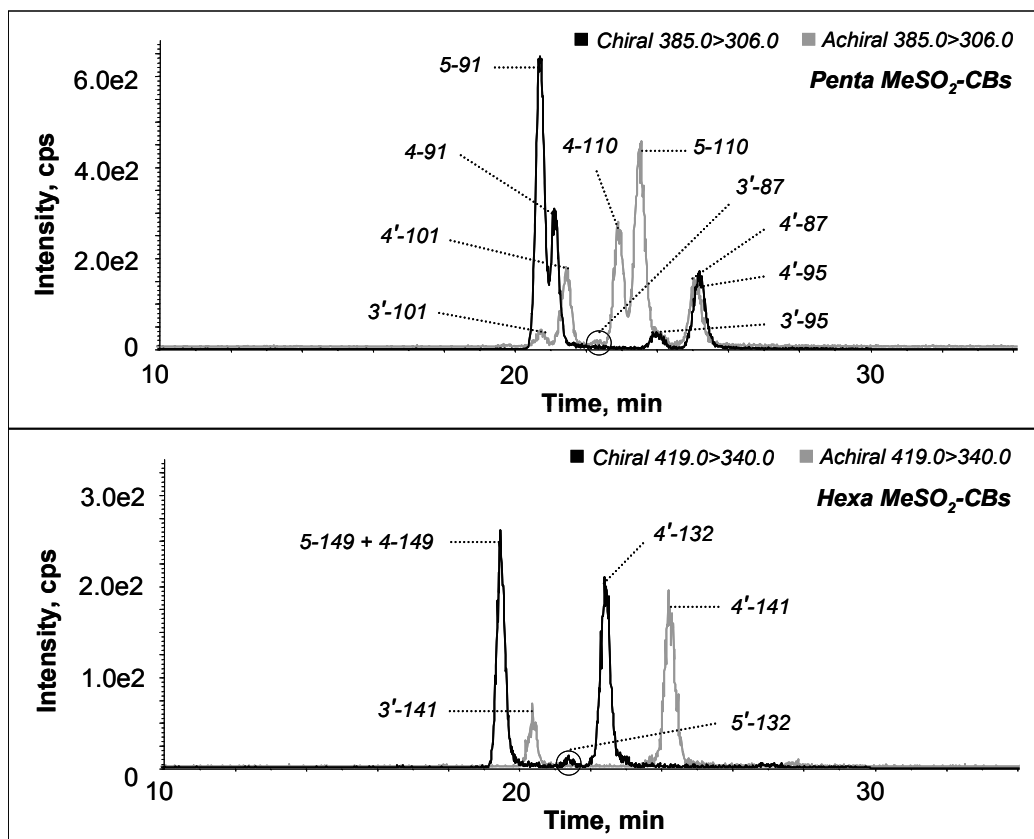
**Figure 2.20:** **Separation of selected achiral and chiral MeSO$_2$-CBs on a cyano column in normal phase**
*Luna Cyano 250 x 4.6 mm x 5 μm. Isocratic elution: 95:2.5:2.5 hexanes:methanol:ethanol. Flow rate 0.4 mL/min, temperature 20°C. Mixed standard solution, 1 μg/mL in hexanes, 25 μL injection. Extracted ion chromatograms. Low intensity peaks are circled.*

PCDDs and hexachloronapthalenes, and the reversed phase solvents gave the best results for all of the isomer pairs examined (Kimata *et al.* 1997). The column was received in a reversed phase solvent, so an initial separation was carried out with 100% methanol in order to allow for a performance comparison with later normal phase runs. The selectivity for the penta and heptachlorinated congeners was quite similar to that achieved in normal phase, but, interestingly, the selectivity for the hexachlorinated congeners was significantly decreased. Excellent separation between 4′-MeSO$_2$-CB132 and 4-MeSO$_2$-CB149 could be achieved under all of

162

the normal phase conditions tested, but in polar organic mode, these two congeners eluted very closely. The resolution was quite poor with a selectivity factor ($\alpha$) of only 1.02 compared to 1.30 with 95:2.5:2.5 heptanes:methanol:ethanol at the same column temperature and flow rate.

To the best of our knowledge, all of the previously reported PCB separations using this column have been performed in normal phase, mostly commonly with 100% hexane, but also with 100% *n*-octane and isooctane (Kimata *et al.* 1997). Some separations were carried out with 100% HPLC grade hexanes as the mobile phase in the current work, but the retention times were excessively long and the resulting peaks extremely broad. The retention time for the last eluting congener was approximately 83 minutes and the peak was over 5 minutes wide, not desirable for a quantitative method. In this case, it was found that introducing a small amount of polar modifier, even as little as 0.5 %, led to much more reasonable retention times and peak widths without sacrificing much in the way of selectivity.

A number of different normal phase solvent combinations and column temperatures were tested. The retention times decreased slightly as the polarity of the alcohol increased from isopropanol to ethanol to 50:50 methanol:ethanol. This is expected, since the eluent strength of lower alcohols as polar modifiers in normal phase chromatography is known to increase with polarity from isopropanol to methanol (Snyder 1978). There were also several changes in elution order noted for the penta-chlorinated congeners with changes in solvent type, composition, and column temperature. Significantly longer retention times

were observed when methanol alone was used as the modifier, accompanied by increased band broadening and peak tailing, as well as large retention time shifts upon repeated runs. This problem was also encountered with the Chiralpak AD and is likely a result of solvent immiscibility. Analyte retention decreased slightly upon changing the alkane from hexanes to heptanes. This was accompanied by a small decrease in selectivity for the penta-chlorinated congeners. Hexanes and isopropanol generally gave the best selectivity overall, but heptanes with 50:50 methanol:ethanol was selected as the mobile phase in the end, simply because this was the optimal mobile phase for the chiral separation. This method could not be performed online unless the same mobile phase could be used in both columns, otherwise a second pump and a complex valve and back-flushing set up would be required. Fortunately, the selectivity achieved on the PYE column with this mobile phase was sufficient for the intended purpose, which was to improve the separation between the chiral congeners and to avoid interferences of the achiral congeners with the chiral targets, which were the main focus of this study.

A chromatogram depicting the separation of the chiral and achiral $MeSO_2$-CBs on the PYE column is presented in **Figure 2.21** on the following page. The chiral congeners with three *ortho*-chlorines eluted first from 9 to 17.5 minutes, followed by the achiral congeners with one or two *ortho*-chlorines from 13 to 24 minutes. Note that there was a region of overlap from 13 to 17.5 minutes where some chiral tri-*ortho* substituted and some achiral di-*ortho* substituted congeners eluted. The achiral congeners that eluted in this region were mostly the lower
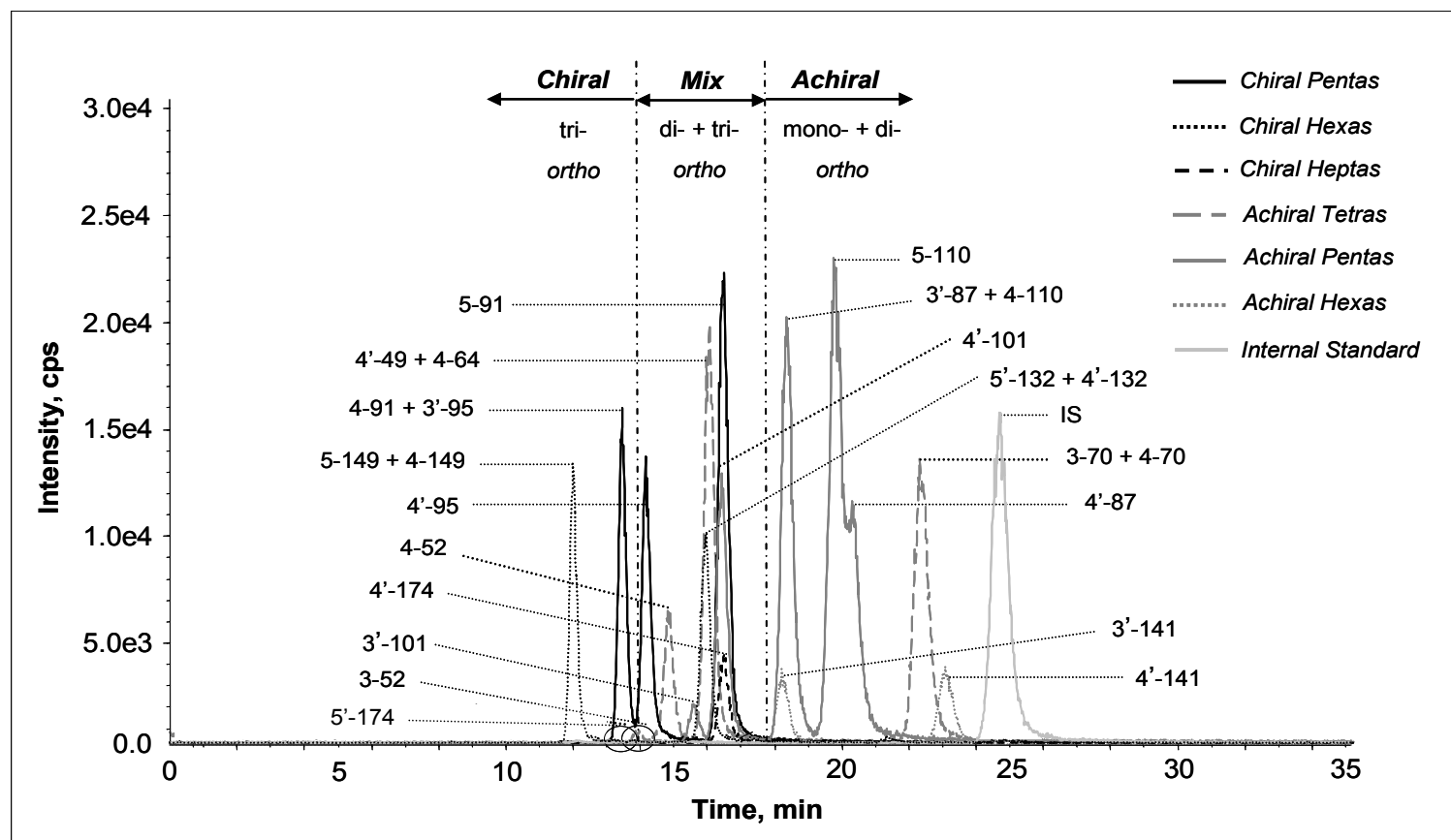
**Figure 2.21:** Separation of MeSO$_2$-CBs on a pyrenyl ethyl silica column in normal phase

*Cosmosil 5-PYE 250 x 4.6 mm x 5 μm. Isocratic elution: 95:2.5:2.5 heptanes:methanol:ethanol. Flow rate 0.85 mL/min, temperature 12.5°C. Mixed standard solution, 1 μg/mL in heptanes, 10 μL injection. Extracted ion chromatograms. Low intensity peaks are circled. IS: internal standard, 3-MeSO$_2$-4-Me-2',3',4',5,5'-pentachlorobiphenyl.*

chlorinated isomers, with four tetras and a single penta-chlorinated congener. The methylated penta-MeSO$_2$-CB internal standard was most retained, likely a result of increased hydrophobic interactions with the stationary phase. The *meta*-substituted congeners were generally less retained than their corresponding *para*-isomers. This may be attributable to the increased rotational barrier of the *meta*-MeSO$_2$ congeners compared to their *para* counterparts as a result of having a larger substituent in the *meta*-position, a phenomenon known as the buttressing effect (Eliel and Wilen 1994), leading to decreased interaction with the planar stationary phase. There were a couple of exceptions to this rule, however, namely for the isomers of MeSO$_2$-CBs 91 and 110, which eluted in the opposite order. These were the only penta-chlorinated analytes with a 2,5,6-trichloro substitution pattern on the MeSO$_2$-containing ring. The only hexa-chlorinated analytes containing this substitution pattern, MeSO$_2$-CBs 132 and 149, produced co-eluting isomers on this column. The isomers of MeSO$_2$-CB70 also overlapped, and these were the only analytes with a single *ortho*-chlorine, making them the most planar. As can be observed in **Figure 2.21**, this led to a significant increase in retention relative to the other tetra-chlorinated compounds and may have made the isomers more difficult to differentiate.

The separation mechanism for the fractionation of PCBs on the PYE stationary phase has been described in detail by Haglund (Haglund *et al.* 1990b). The separation is based primarily on $\pi$-$\pi$ interactions, so as the *ortho*-chlorination of a PCB increases, the angle of declination between the two benzene rings increases, and interaction with the stationary phase decreases. The retention for a

given number of *ortho*-chlorines also increases with total chlorination of PCB congeners due to electrostatic interactions between the high electron affinity chlorines and the strongly electron donating pyrene moiety of the stationary phase. These trends were also observed here for the separation of MeSO$_2$-CBs. Within the groups of congeners with the same level of *ortho*-chlorination, there was some dependence of elution order on total chlorination. For example, for the chiral analytes, the hepta-chlorinated congener 4′-MeSO$_2$-CB174 was one of the last to elute. For the achiral analytes, several of the tetra-chlorinated congeners eluted first, and the hexa-chlorinated congener 4′-MeSO$_2$-CB141 eluted last. However, the level of *ortho*-chlorination was the primary determinant of elution order, as found previously for their parent compounds by Haglund and coworkers (1990).

To unveil further structure-retention relationships, several congener pairs with the same chlorine substitution pattern on the non-MeSO$_2$-substituted ring were compared: 4-MeSO$_2$-CB49 vs. 5- and 4-MeSO$_2$-CB91, 3- and 4- MeSO$_2$-CB70 vs. 3- and 4-MeSO$_2$-CB110, 3- and 4-MeSO$_2$-CB87 vs. 3- and 4-MeSO$_2$-CB132, and 3- and 4-MeSO$_2$-CB101 vs. 3- and 4- MeSO$_2$-CB149. Note that one congener from each pair had a 2,5-dichloro substitution pattern on the MeSO$_2$-containing ring and the other had a 2,5,6-trichloro substitution pattern on the methyl sulfone ring. In almost all cases both the *meta*- and *para*-isomers of the 2,5-dichloro congener eluted first, even though this was the less chlorinated analyte. The only exception was for the isomers of MeSO$_2$-CBs 49 and 91. In this case the elution order was: 4-MeSO$_2$-CB91, 4-MeSO$_2$-CB49, then 5-MeSO$_2$-

CB91. Unfortunately the *meta* isomer of $MeSO_2$-49 could not be detected for comparison.

The elution order also closely followed the trends in chlorine substitution pattern described for PCBs by Haglund and coworkers (Haglund *et al.* 1990b), at least under the conditions presented in **Figure 2.21**. These researchers found that for congeners with the same substitution pattern on one ring, the elution order was as follows if two chlorine substituents were present on the other ring: $2,6 < 2,5 \approx 2,4 < 2,3 \leq 3,5 \ll 3,4$. If three chlorine substituents were present on the other ring, the elution order was: $2,4,6 < 2,3,6 \leq 2,3,5 < 2,4,5 < 2,3,4 \ll 3,4,5$. All $MeSO_2$-CB congeners with the same chlorination level and the same substitution pattern on the $MeSO_2$-containing ring were compared to this pattern. All but one of the tetra-chlorinated congeners possessed the same substitution pattern on the $MeSO_2$-containing ring and contained two chlorines on the opposite ring. The elution order for these congeners was: 3- and 4-$MeSO_2$-CB52 (2,5-dichloro on non-$MeSO_2$ ring) $\approx$ 4′-$MeSO_2$-CBs 49 (2,4) $\ll$ 3- and 4-$MeSO_2$-CBs 70 (3,4), which is right in line with the results found for PCBs. Unfortunately, the peak for 3′-$MeSO_2$-CB49 could not be detected. For the penta-chlorinated congeners with two chlorines on the non-$MeSO_2$ ring, the elution order was: 5- and 4-$MeSO_2$-CB91 (2,4) $\ll$ 5- and 4-$MeSO_2$-CB110 (3,4). For the penta-chlorinated congeners with three chlorine substituents on the methyl sulfone free ring the elution order was: 3′- and 4′-$MeSO_2$-CB95 (2,3,6) < 3′- and 4′-$MeSO_2$-CB101 (2,4,5) < 3′- and 4′-$MeSO_2$-CB87 (2,3,4). Finally, for the hexa-chlorinated congeners with three chlorines on the methyl sulfone free ring the order was: 5- and 4-$MeSO_2$-CB149

(2,4,5) < 5′- and 4′-MeSO$_2$-CB132 (2,3,4). Note that in all cases where both the

*meta-* and *para-*isomers of a given congener were detectable, they both eluted

before those of the next congener in the elution series. These results compare very

well to those published for PCBs by Haglund and coworkers (1990).

*2.2.3.5 Two-dimensional liquid chromatography*

Column switching liquid chromatography employing a conventional

reversed phase column in the first dimension and an enantioselective column in

the second dimension has been employed previously for the enantioseparation of

a variety of pharmaceutical compounds to prevent interferences from biological

matrix components (Cass *et al.* 2003, Ing-Lorenzini *et al.* 2009, Lamprecht *et al.*

2000, Muth *et al.* 1996, Oda *et al.* 1992). However, in these studies two LC

pumps were employed, whereas only one was used in the current work, since it

was possible to optimize a single mobile phase that gave good selectivity in both

dimensions of the separation. Once the PYE and Chiralpak AD-H columns were

connected in series, some small adjustments were made to achieve the final

method. The final conditions that gave the best overall separation were 95:2.5:2.5

heptanes:methanol:ethanol, 12.5°C, and 1.0 mL/min. There were some trade-offs

in resolution between the 10°C and 15°C runs, with better resolution between E1

4′-MeSO$_2$-CB95 and 3-MeSO$_2$-CB91 at 10°C but worse resolution between E1

and E2 4′-MeSO$_2$-132 at 15°C and vice versa. A temperature of 12.5°C provided

a nice balance and gave acceptable resolution in both cases. However, for future

analyses, a temperature of 15°C is recommended to improve the resolution of 4′-

MeSO$_2$-CB132, since this congener is generally detected much more frequently in the environment than 5-MeSO$_2$-CB91 or 4′-MeSO$_2$-CB 95 (Letcher *et al.* 2000).

The initial column switching times were decided from the PYE chromatograms and then fine-tuned once the two columns were set up in series with all of the connecting tubing required. The switching times were selected such that after elution from the PYE column, all of the chiral analytes and a small number of co-eluting achiral analytes were directed onto the chiral column. Then the remaining achiral analytes were directed to the detector, and, finally, the chiral analytes were eluted from the chiral column to the detector (see **Section 2.1.4.2** for a more detailed explanation). As noted previously, during the phase where the achiral analytes were directed from the PYE column to the detector, there was no solvent flow through the chiral column. The peak widths of the analytes held on the chiral column were compared to those from a chromatogram where the analytes were passed directly through both columns with no stop in flow, and there was no noticeable increase in peak width observed. Under stopped flow conditions, longitudinal molecular diffusion is the main contributor to band broadening. According to the Wilke-Chang model, the molecular diffusion coefficient, D, increases directly with temperature, *T*, and with the square root of the solute molecular weight, *M*, and the solvent association parameter, $\chi$, and decreases directly with solute molal volume, *V*, and solution viscosity, $\eta$, as shown in **Equation 2.4** below (Wilke and Chang 1955):

$$D = 7.4 \times 10^{-8} \times \frac{(\chi \cdot M)^{1/2} T}{\eta \cdot V^{0.6}}$$ [2.4]

In the current work, the use of a sub-ambient temperature (i.e. 12.5°C) and a mobile phase high in heptane (i.e. 95%), which has a low solvent association parameter of 1 (Wilke and Chang 1955), likely helped to keep molecular diffusion to a minimum during stopped flow. The relatively small molecular weight of the analyte also would have contributed to the low quantity of longitudinal diffusion and therefore band broadening. Estimating a solute molal volume similar to bromonaphthalene at 180 $cm^2$/g·mol (Wilke and Chang 1955), and using a viscosity of 0.409 cP for heptane (Will and Leipertz 1997), and a solute molecular weight of 402 g/mol (penta-MeSO$_2$-CB), a molecular diffusion coefficient of 4.60 x $10^{-5}$ $cm^2$/s is calculated for the chromatographic conditions of interest. Upon multiplying by the stopped flow time of 9.2 minutes, a diffusion area of 0.025 $cm^2$ is obtained. Dividing by $\pi$, taking the square root, and multiplying by two gives a diffusion diameter, or length, of 0.18 cm. The first eluting peak in the chromatogram was 1.0 minutes wide, which amounts to an elution plug volume of 1.0 mL at a flow rate of 1.0 mL/min. If this is divided by the cross-sectional area of the column, which was 4.6 mm in internal diameter, this gives an elution plug width of 6.0 cm. Therefore the increase in width of the analyte plug due to molecular diffusion during stopped flow is approximately 3.0%, which is negligible. Obviously, this is an oversimplification because the effects of the additional mobile phase components and the chemical interactions of the solute with the stationary phase are ignored, but it is a reasonable approximation. More

importantly, obstruction due to the column packing was ignored, but this would tend to decrease the extent of molecular diffusion, making the above calculation an over-estimation.

The final, optimized separation is presented in **Figure 2.22** on the following page. Note that all of the chiral congeners could be separated without interferences from the achiral congeners. The only instances where baseline resolution was not achieved was between E1 and E2 $4'$-MeSO$_2$-CB132, and between E1 $4'$-MeSO$_2$-CB95 and E1+E2 5-MeSO$_2$-CB 91. However, in the latter case, the $385.0 \rightarrow 278.0$ transition was quite high for $4'$-MeSO$_2$-CB95 and quite low (barely visible in this chromatogram) for 5-MeSO$_2$-CB91, so in instances where both compounds were detected, this transition could be used to allow for better quantification of $4'$-MeSO$_2$-CB95. This was not necessary in this study since neither compound was detected in any of the samples tested. Also note that the internal standard was fully resolved from all of penta-chlorinated congeners, and many of the achiral congeners were resolved, making this a comprehensive method for MeSO$_2$- CB analysis. The total run time was 93 minutes, which is a reduction in run time of approximately one third compared to the fastest (Ellerichmann *et al.* 1998) and of greater than three times compared to the slowest published enantioselective GC methods (Chu *et al.* 2003a).
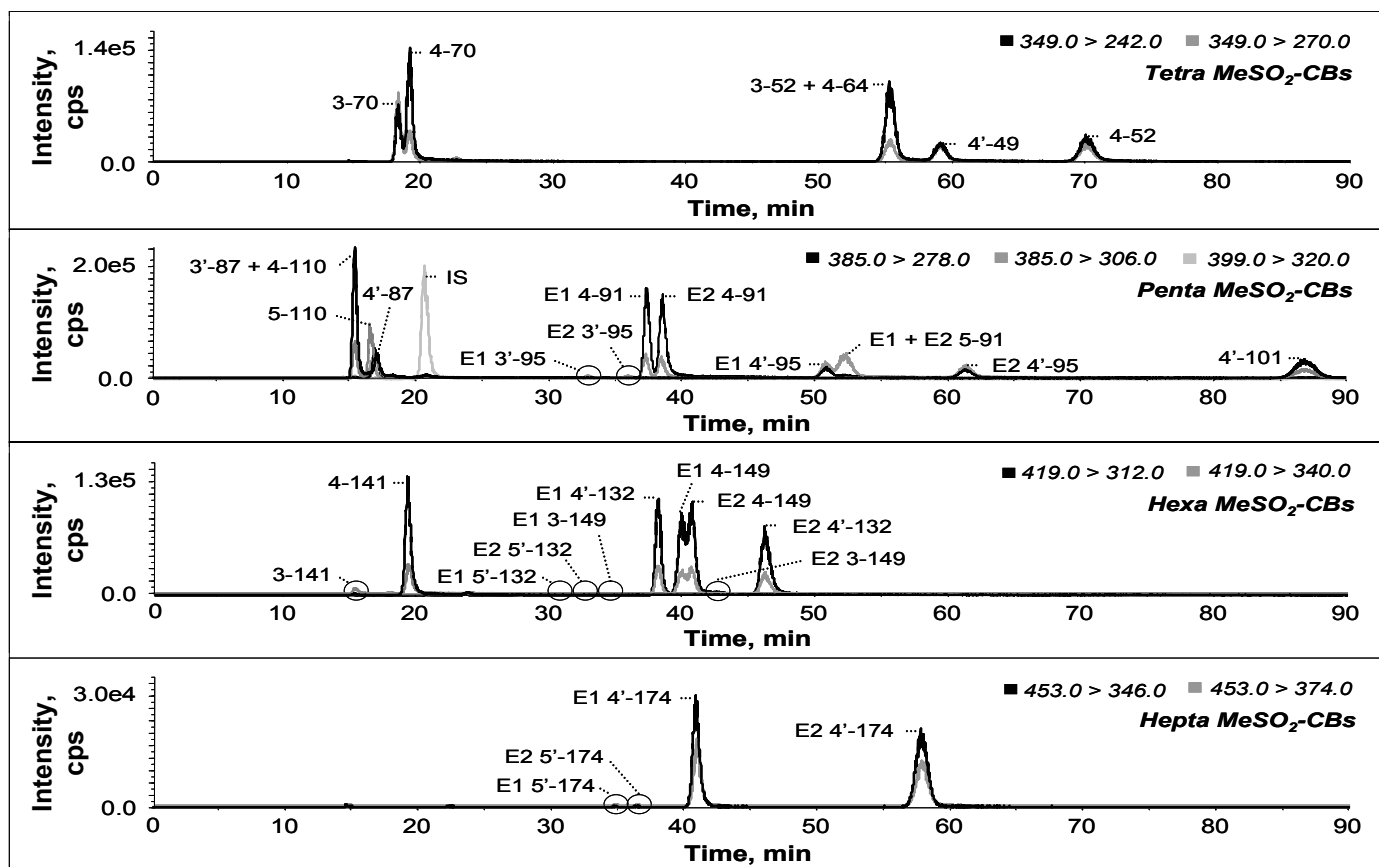
**Figure 2.22:** **Separation of MeSO₂-CBs by stopped-flow enantioselective heart-cut two-dimensional HPLC**

*Cosmosil 5-PYE connected in series with Chiralpak AD-H. Isocratic elution: 95:2.5:2.5 heptanes:methanol:ethanol. Flow rate 1.0 mL/min, temperature 12.5°C. Mixed standard solution, 5 μg/mL in heptanes, 20 μL injection. Diverter valve program: 0-14.6 min, position A; 14.6-23.8 min, position B; 23.8-91 min, position A. Extracted ion chromatograms. Low intensity peaks are circled. IS: internal standard, 3-MeSO₂-4-Me-2',3',4',5,5'-pentachlorobiphenyl.*

### 2.2.4   Method performance

#### 2.2.4.1 Limits of detection, quantitation and linearity

Relative response factors and limits of detection and quantitation were calculated manually using the methods described by Loconto (Loconto 2006). First, to determine the relative response factor for each analyte, a series of solutions were analyzed where the concentrations of the analytes varied from 5 ng/mL to 5000 ng/mL, but the internal standard concentration remained constant at 1000 ng/mL. The peak area of the analyte, $A_{analyte}$, over the peak area of the internal standard, $A_{IS}$, was then plotted versus the concentration of analyte, $C_{analyte}$. The resulting slope of the linear regression line was equal to the relative response factor, RRF, over the concentration of internal standard, $C_{IS}$, as shown in **Equations 2.5** and **2.6**. Since the internal standard concentration was held constant, the slope of linear regression line, m, was simply multiplied by this concentration in order to determine the RRF for each analyte, as shown in **Equations 2.7** and **2.8**. A table summarizing the relative response factors for each analyte is presented in **Appendix A**. Since all of the target analytes gave lower sensitivity than the internal standard, all of the RRFs were smaller than unity.

$$y \quad = \quad m \quad \times \quad x \qquad\qquad [2.5]$$

$$\frac{A_{analyte}}{A_{IS}} \quad = \quad \frac{RRF}{C_{IS}} \quad \times \ C_{analyte} \qquad\qquad [2.6]$$

174

$$m = \frac{A_{analyte}}{A_{IS}} \times \frac{1}{C_{analyte}} \qquad [2.7]$$

$$RRF = m \times C_{IS} \qquad [2.8]$$

Knowing the relative response factor and the concentration of the internal standard in the extracted tissue samples, the concentration of analyte could then be determined using the peak areas of the internal standard and of the analyte, as shown in **Equation 2.9**.

$$C_{analyte} = \frac{A_{analyte}}{A_{IS}} \times \frac{C_{IS}}{RRF} \qquad [2.9]$$

For a given analyte, $i$, the signals associated with the method limit of detection, $S_{MLOD}^{i}$, and method limit of quantitation, $S_{MLOQ}^{i}$, were defined as the average noise in the retention time window of analyte $i$ over three solvent blank runs, $S_{blank}^{i}$, plus 3 times the standard deviation of the noise, $s_{blank}^{i}$, for the method limit of detection, and 10 times the standard deviation of the noise for the method limit of quantitation, as represented in **Equation 2.10** and **2.11** below, respectively.

$$S_{MLOD}^{i} = S_{blank}^{i} + 3 \times s_{blank}^{i} \qquad [2.10]$$

$$S_{MLOQ}^{i} = S_{blank}^{i} + 10 \times s_{blank}^{i} \qquad [2.11]$$

In order to convert the signal levels into concentrations, a calibration curve was established by analyzing a series of mixed standards of varying concentrations. Six levels were selected to span the plausible range of analyte

concentrations in environmental samples: 5 ng/mL, 10 ng/mL, 50 ng/mL, 100 ng/mL, 1000 ng/mL, and 5000 ng/mL. The calibration curves are depicted in **Figures 2.23** and **2.24** on the following pages. Note that the following analytes were excluded from the calibration curves and from future analyses because they could not be detected at any of the concentration levels examined: E1 and E2 5′-MeSO$_2$-CB132, 5-MeSO$_2$-CB149, and 5′-MeSO$_2$-CB174.

For all analytes, a high level of linearity was observed in the concentration range examined, with the majority of the linear regression correlation coefficients falling between 0.9906 to 0.9999. For these analytes, the limit of linearity was determined to be 5000 ng/mL. The only exceptions were 3′-MeSO$_2$-CB141 and the peak corresponding to 3′-MeSO$_2$-CB87 + 4-MeSO$_2$-CB110. When the 5000 ng/mL data point was included for these peaks, the correlation coefficients were 0.9669 and 0.9762, respectively. However, when this point was eliminated, the correlation coefficients increased to 0.9921 and 0.9999, respectively, suggesting that 5000 ng/mL slightly exceeded the linear calibration range. As a result, the limit of linearity for these peaks was determined to be 1000 ng/mL, the concentration of the next highest calibrator.

The method limit of detection (MLOD) and the method limit of quantitation (MLOQ) for each analyte in terms of concentration was then calculated by subtracting the average noise, $S^i_{blank}$, from the analyte signal at the limit of detection, $S^i_{MLOD}$, or limit of quantitation, $S^i_{MLOQ}$, then dividing by the
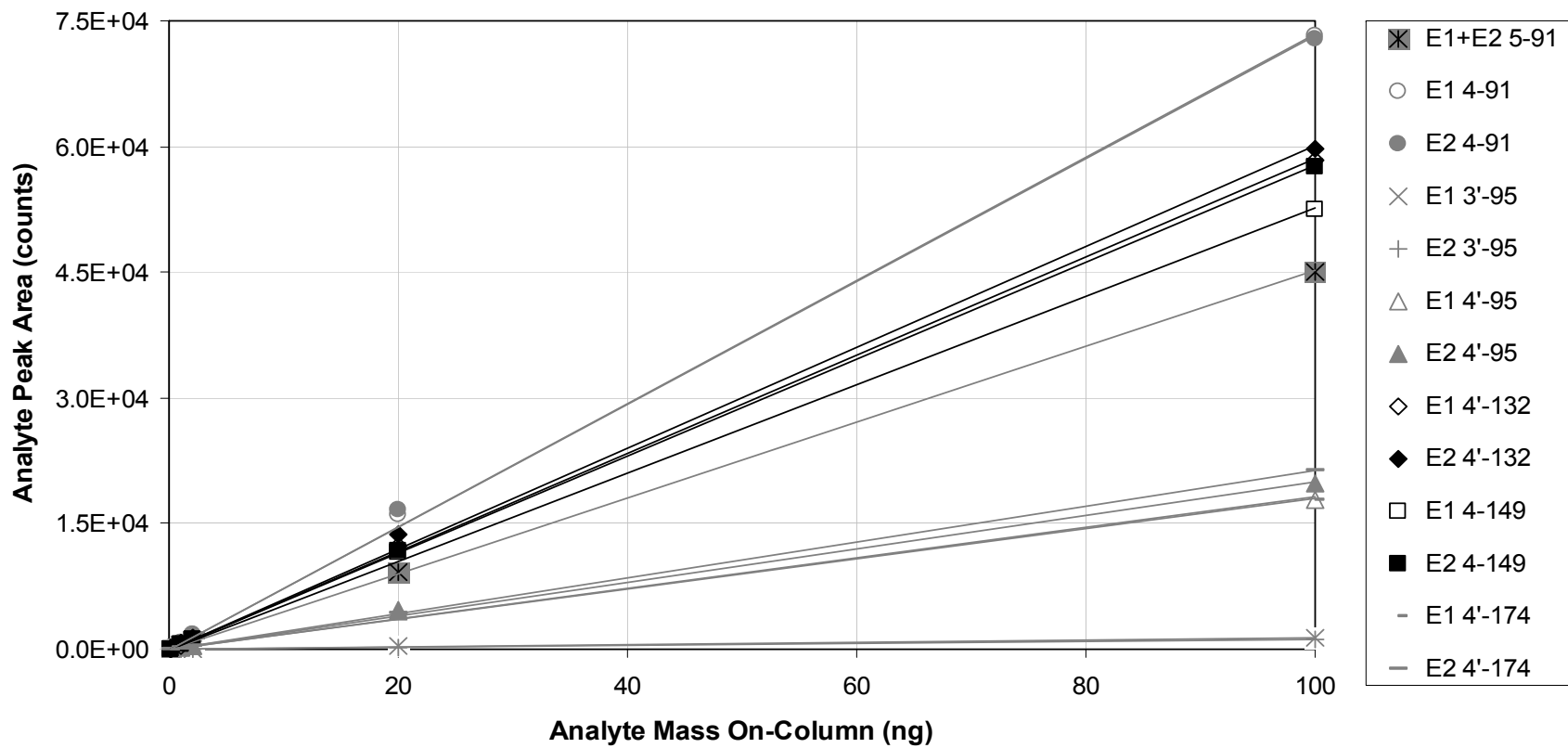
**Figure 2.23:** Calibration curve for the analysis of chiral MeSO$_2$-CBs by LC-LC-APPI-MS/MS

*Analyte mass on-column corresponds to a 20 µL injection of a 5, 10, 50, 100, 1000 or 5000 ng/mL mixed standard solution.*
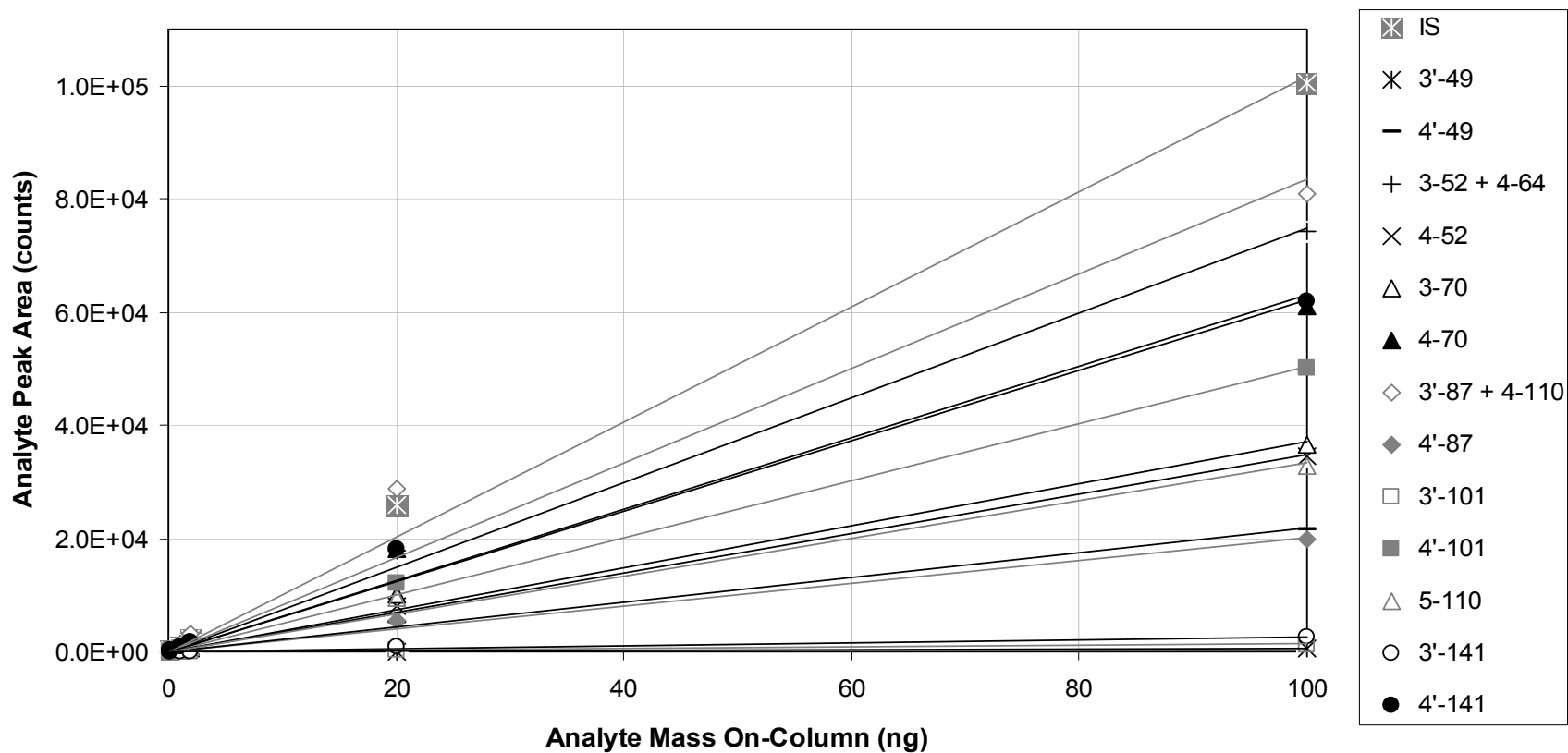
**Figure 2.24: Calibration curve for the analysis of achiral MeSO$_2$-CBs by LC-LC-APPI-MS/MS**
*Analyte mass on-column corresponds to a 20 μL injection of a 5, 10, 50, 100, 1000 or 5000 ng/mL mixed standard solution.*
*IS: internal standard, 3-MeSO$_2$-4-Me-2',3',4',5,5'-pentachlorobiphenyl.*

slope of the slope of the calibration curve, $m^i$, as shown in **Equation 2.12** and **2.13**. The concentration levels for the MLOD and MLOQ for each analyte are summarized in **Table 2.10** on the following page.

$$\text{MLOD}^i \; = \; \frac{S^i_{\text{MLOD}} - S^i_{\text{blank}}}{m^i} \qquad\qquad [2.12]$$

$$\text{MLOQ}^i \; = \; \frac{S^i_{\text{MLOQ}} - S^i_{\text{blank}}}{m^i} \qquad\qquad [2.13]$$

*2.2.4.2 Precision and Accuracy*

Precision was assessed by analyzing a 100 ng/mL mixed standard solution three times consecutively for the majority of the congeners. However, precision was assessed at 5000 ng/mL for the analytes 3′-MeSO$_2$-CB49, 3′-MeSO$_2$-CB95, 3′-MeSO$_2$-CB101, and 3′-MeSO$_2$-CB141, due to the low sensitivity achieved for these congeners. The percent relative standard deviation (%RSD) for each analyte was less than 11%, except for 3-MeSO$_2$-CB49, as shown in **Table 2.10** on the following page. The %RSD was quite high for 3-MeSO$_2$-CB49 at 38.1% because the peaks in the precision runs were just above the LOD and were quite small and broad and therefore difficult to quantify. A %RSD this high is not altogether unusual when precision is measured near the LOD. However, since 5000 ng/mL is at the upper limit of the expected concentration range for environmental samples, this congener was not analyzed in the animal tissue samples due to insufficient precision at the concentration level of interest. Due to the low sensitivity for this analyte, it is highly unlikely that it would have been detected anyway.

**Table 2.10: Summary of LC-LC-APPI-MS/MS method performance characteristics for target MeSO$_2$-CBs and their enantiomers**

*IS: internal standard, 3-MeSO$_2$-4-Me-2',3',4',5,5'-pentachlorobiphenyl.*
*%RSD: percent relative standard deviation; r$^2$: linear regression correlation coefficient.*
[a]*Numbers in subscript are not significant.*
[b]*Within day precision.*

| Congener | Method limit (ng on-column)[a] | | | r$^2$ | Precision[b] (%RSD) |
|---|---|---|---|---|---|
| | Detection | Quantitation | Linearity | | |
| 3'-49 | 1.73$_9$ | 5.79$_7$ | 100 | 0.9986 | 38.1 |
| 4'-49 | 0.04$_8$ | 0.16$_2$ | 100 | 0.9982 | 2.75 |
| 3-52 + 4-64 | 0.01$_4$ | 0.04$_7$ | 100 | 0.9982 | 5.03 |
| 4-52 | 0.03$_1$ | 0.10$_4$ | 100 | 0.9986 | 4.89 |
| 3-70 | 0.03$_3$ | 0.11$_3$ | 100 | 0.9906 | 2.64 |
| 4-70 | 0.02$_3$ | 0.08$_0$ | 100 | 0.9921 | 10.31 |
| 3'-87 + 4-110 | 0.03$_0$ | 0.10$_4$ | 20 | 0.9939 | 2.89 |
| 4'-87 | 0.11$_4$ | 0.38$_6$ | 100 | 1.0000 | 1.87 |
| E1+E2 5-91 | 0.03$_1$ | 0.10$_2$ | 100 | 0.9996 | 2.95 |
| E1 4-91 | 0.02$_8$ | 0.09$_3$ | 100 | 0.9991 | 3.86 |
| E2 4-91 | 0.03$_0$ | 0.10$_1$ | 100 | 0.9956 | 4.87 |
| E1 3'-95 | 0.93$_8$ | 3.12$_7$ | 100 | 0.9982 | 4.74 |
| E2 3'-95 | 1.11$_8$ | 3.72$_6$ | 100 | 0.9987 | 7.20 |
| E1 4'-95 | 0.07$_8$ | 0.06$_7$ | 100 | 0.9993 | 6.33 |
| E2 4'-95 | 0.06$_7$ | 0.02$_6$ | 100 | 0.9979 | 2.95 |
| 3'-101 | 0.99$_8$ | 3.29$_5$ | 100 | 0.9969 | 2.19 |
| 4'-101 | 0.02$_9$ | 0.09$_6$ | 100 | 0.9911 | 0.96 |
| 5-110 | 0.05$_4$ | 0.18$_2$ | 100 | 0.9999 | 6.26 |
| E1 4'-132 | 0.03$_7$ | 0.12$_3$ | 100 | 0.9991 | 4.40 |
| E2 4'-132 | 0.03$_5$ | 0.11$_8$ | 100 | 0.991 | 1.95 |
| 3'-141 | 0.41$_5$ | 1.38$_3$ | 20 | 0.9999 | 2.85 |
| 4'-141 | 0.03$_5$ | 0.11$_8$ | 100 | 0.9996 | 1.51 |
| E1 4-149 | 0.04$_4$ | 0.14$_8$ | 100 | 1.0000 | 2.25 |
| E2 4-149 | 0.03$_8$ | 0.12$_8$ | 100 | 0.9992 | 1.46 |
| E1 4'-174 | 0.02$_2$ | 0.07$_5$ | 100 | 1.0000 | 5.61 |
| E2 4'-174 | 0.02$_1$ | 0.07$_1$ | 100 | 0.9965 | 3.69 |
| IS | 0.03$_7$ | 0.12$_3$ | 100 | 0.9982 | - |

The EF precision was also assessed for the chiral congeners in these runs, and the relative standard deviation was less than 3% in all cases. In order to be considered non-racemic, sample EFs were required to be outside of the range determined in this experiment: $0.487 \pm 0.004$ for 4-MeSO$_2$-CB91, $0.49 \pm 0.01$ for 3′-MeSO$_2$-CB95, $0.53 \pm 0.02$ for 4′-MeSO$_2$-CB95, $0.48 \pm 0.01$ for 4′-MeSO$_2$-CB132, $0.518 \pm 0.007$ for 4-MeSO$_2$-CB149 and $0.541 \pm 0.005$ for 4′-MeSO$_2$-CB174. The standard EFs for 4′-MeSO$_2$-CB95, and 4′-MeSO$_2$-CB174 were the furthest away from 0.500. This is likely attributable to the large enantiomer separation factors achieved for these congeners, with approximately 10 and 18 minutes, respectively, between peaks. Since isocratic elution was used, the second eluting enantiomer peak was significantly broader and shorter than the first, leading to a decrease in detectability and therefore peak area relative to E1 and an increase in the EF. There are methods of correcting for standard EFs that are different from 0.500 (Macleod and Wong 2010), however, this was not deemed necessary in the current work since the EFs were expected to be either very near or very different from 0.500 due to the high level of enantioselective metabolism and/or retention and/or excretion observed for certain MeSO$_2$-CBs (refer to **Section 1.3.4.2**).

Accuracy was assessed by extracting and analyzing US National Institute of Standards and Technology (NIST) Standard Reference Material (SRM) 1945 (Organics in Whale Blubber; Gaithersburg, MD, USA) and comparing the concentrations of the individual congeners to those determined by GC-ECD in a previous study (Hoekstra *et al.* 2003). Unfortunately, due to differences in the

target analytes selected and in co-elutions of congeners between the two methods, only three congeners could be directly compared: 4-MeSO$_2$-CB64, 3-MeSO$_2$-CB70, and 4-MeSO$_2$-CB70. The percent difference in calculated concentration between the two methods was 4.9% for 4-MeSO$_2$-CB 64, 6.4% for 3-MeSO$_2$-CB70, and 27.7% for 4-MeSO$_2$-CB 70. At first glance, the difference for 4-MeSO$_2$-70 appeared quite large, but it is actually reasonable considering the errors in the respective measurements, which were 22.8% for the current analysis and 7.1% for the method of Hoekstra and coworkers. These two percent errors add up to 29.9%, suggesting that the percent difference of 27.7% calculated between the two methods for 4-MeSO$_2$-CB70 could easily be attributed to variation in instrumental response.

*2.2.4.3 Matrix effects*

In order to identify the presence any possible matrix effects, extracted NIST SRM 1945 (Organics in whale blubber) was analyzed in two different experiments. In the first experiment, the matrix was extracted in a similar manner (Morrissey *et al.* 2007) to the sledge dog and glaucous gull samples, but the PCB methyl sulfone fraction was not collected. Instead, the chlorinated pesticide fraction was analyzed. This fraction was selected because it required a slightly polar solvent to be eluted in the clean-up chromatography steps, polar enough to allow for the collection of similar matrix components, but not so polar as to elute any interfering MeSO$_2$-CBs that may have been present. Analyses of a 100 ng/mL MeSO$_2$-CB mixed standard, the blank extracted matrix, and a matrix spike at 100 ng/mL were each performed in triplicate. The analyte masses calculated from the

peak areas of the standard runs were then compared to those of the matrix spikes. As expected, no $MeSO_2$-CBs were detected in the blank extracted matrix. The results of this experiment are represented for each quantifiable analyte in **Figure 2.25** on the following page. Note that $3'$-$MeSO_2$-CB95 and $3'$-$MeSO_2$-CB141 were not included because they were not detectable at the concentration level used. In addition, 4-$MeSO_2$-CB101 was excluded because the peak was truncated in some of the runs and could not be reliably quantified.

A two-tailed Student's *t*-test with a significance level of 0.05 was used to compare the masses of the analytes on-column in the solvent standard and spiked matrix samples. The only significant differences found between the two groups were for 4-$MeSO_2$-CB52 (P = 0.0026), 4-$MeSO_2$-CB64 (P = 0.0362), $3'$-$MeSO_2$-CB87 + 4-$MeSO_2$-CB110 (P = 0.0008), 5-$MeSO_2$-CB110 (P = 0.0240), E2 $4'$-$MeSO_2$-CB132 (P = 0.0034), and $4'$-$MeSO_2$-CB141 (P<0.0001). However, the percent relative standard deviation encompassing both groups was 15.2% for 5-$MeSO_2$-CB110 and less than 9.3% for the remaining analytes. The percent relative standard deviation in analyte mass on-column determined in the precision experiments was around 11%, so the variation observed here could be attributable to variation in instrumental response. Although the %RSD for 5-$MeSO_2$-CB110 was slightly higher than this, 15% was deemed a pretty typical error for this type of measurement.
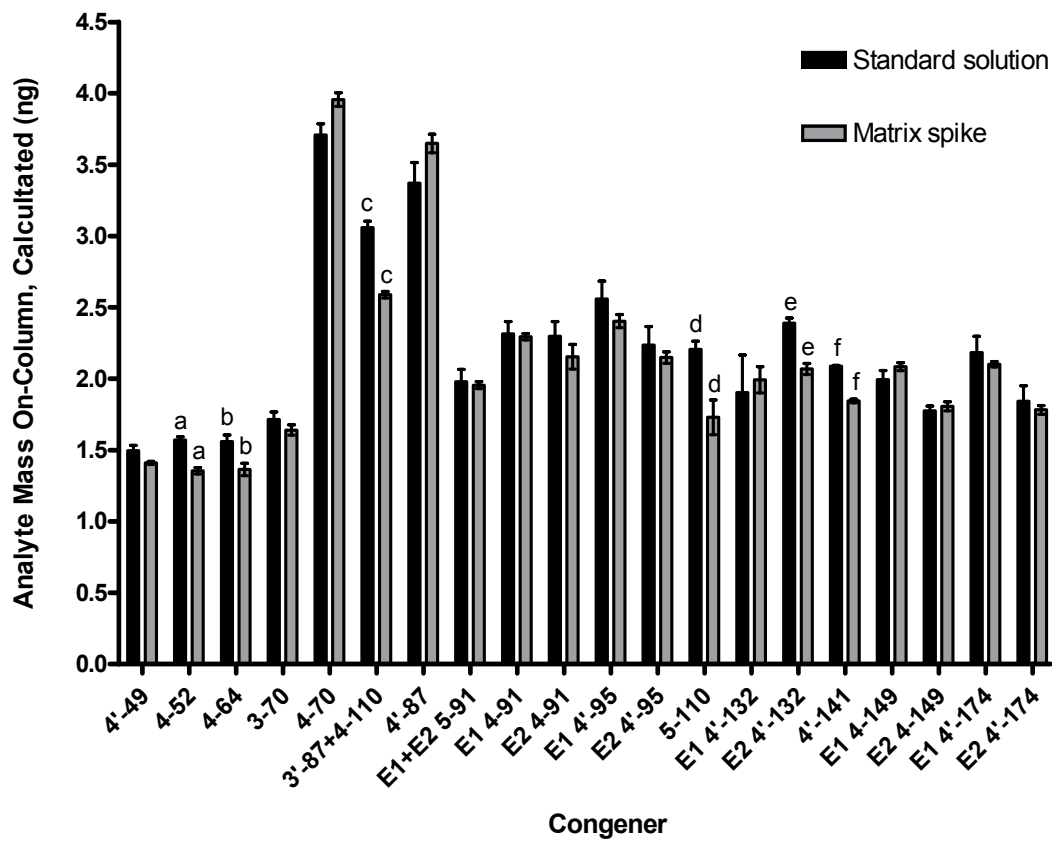
**Figure 2.25: Comparison of standard solutions and spiked matrix samples for the detection of MeSO$_2$-CBs by LC-LC-APPI-MS/MS**

*Mixed standard/spiked matrix solutions 200 ng/mL in heptanes for 4-MeSO$_2$-CB70 and 4'-MeSO$_2$-CB87, 100 ng/mL for all other analytes, 20 $\mu$L injections. Matrix: extracted NIST SRM 1945. Letters above error bars indicate a significant difference (P<0.05) between measurements for a given congener or enantiomer by two-tailed Students' t-test.*

The EFs of the chiral congeners were also compared in this experiment.

The percent relative standard deviation between the standard solutions and the

spiked matrix samples was less than 3% for most congeners. The %RSD

determined in the EF precision experiment was also around 3%, so the variation

observed here is within the expected range. The only exception to this was 4'-

MeSO$_2$-CB132, for which the %RSD was 6.7%. PeakFit gives the best results

when the percent valley between the peaks is 10% or greater, which could not be

achieved for this congener. The resolution achieved in the precision experiment with standard solutions was still sufficient to allow reliable determination of EF, with a %RSD less than 3%. However, when the matrix spiked samples were analyzed, a small increase in noise was observed. This was enough to decrease the resolution of these enantiomers to the point where EF determination became difficult, and the %RSD increased. That being said, the %RSD in this experiment was largely biased by a single run, and when this data point was excluded, it decreased to 3.7%, which was deemed acceptable.

### 2.2.5  *Analysis of MeSO$_2$-CBs in glaucous gull plasma*

Unfortunately, no MeSO$_2$-CBs were detectable in any of the 49 glaucous gull (*Larus hyperboreus*) plasma samples analyzed. The internal standard was quantifiable in the vast majority of the samples, so loss during transportation and/or storage is not suspected to be the main cause. These same samples have been analyzed for 16 MeSO$_2$-CBs previously using conventional GC-MS, and the concentrations of the individual congeners studied ranged from less than 0.62 ng/g lipid weight for 3-MeSO$_2$-CB70 up to 612 ng/g lipid weight for 4-MeSO$_2$-CB70 in one sample, with mean concentrations ranging from zero up to 110 ng/g lipid weight for 5′-MeSO$_2$-CB132 (Verreault *et al.* 2005a). The most abundant congeners were an unidentified hexa-chlorinated metabolite, followed by 5′-MeSO$_2$-CB132, 4′-MeSO$_2$-CB49, and 5-MeSO$_2$-CB149. Unfortunately, extremely poor sensitivity was achieved in the current work for the congeners 5′-MeSO$_2$-CB132 and 5-MeSO$_2$-CB149, so it is not surprising that they could not be detected.

Several bird species have come under scrutiny over the past half century due to observed population declines. These declines have been attributed mostly to a thinning of the egg shells caused by exposure to chlorinated hydrocarbons, including DDTs and PCBs (Risebrough *et al.* 1968). The concentrations and effects of other chlorinated compounds in birds, including PCB metabolites, continue to be of interest. Methyl sulfone PCBs have been measured in several bird species to date, and the levels in their tissues are generally lower than those detected in mammals. This indicates differences in toxicokinetic processes, and it has been suggested that birds may have a lower metabolic capacity for PCB biotransformation than mammals, or that they can excrete these contaminants more efficiently (Jörundsdóttir *et al.* 2006, Klasson-Wehler *et al.* 1998). Methyl sulfone metabolites have been investigated in the eggs of Norwegian glaucous gulls from Bear Island, the same study site as for the plasma samples described above (Verreault *et al.* 2005a). The penta-chlorinated congeners 3′- and 4′-$MeSO_2$-CB101 were observed to be the most abundant in eggs with concentrations in the range of 5 to 38 ng/g lipid weight. These congeners accounted for, on average, 33% of the sum $MeSO_2$-CB concentration of 92 ng/g lipid weight, which is approximately four times lower than that found in the plasma of the adults. These two congeners and 4-$MeSO_2$-CB149 were the most commonly detected in Baltic guillemot (*Uria aalge*) eggs, with individual congener concentrations ranging from 13 to 72 ng/g lipid weight (Jörundsdóttir *et al.* 2006). Total $MeSO_2$-CB concentrations in the range of 10.6 to 77.4 ng/g lipid weight have been detected in the liver of Laysan albatross (*Diomedea*

186

*immutabilis*) from Midway Atoll in the North Pacific Ocean, quite a bit lower than the levels found in glaucous gull and guillemot eggs (Klasson-Wehler *et al.* 1998). The most abundant congeners detected in the albatross study were 3-MeSO$_2$-CB70, 3′-MeSO$_2$-CB87, 3′-MeSO$_2$-CB101 and 4′-MeSO$_2$-CB101. The *meta-* and *para*-isomers of MeSO$_2$-CBs 49, 64 and 141 were also detected at lower levels, along with 4-MeSO$_2$-CB70 and 4′-MeSO$_2$-CB87. The average sum MeSO$_2$-CB concentration detected in the adipose tissue of cormorant chicks from two colonies in The Netherlands were 30 and 70 ng/g lipid weight (de Voogt *et al.* 1996), similar to the levels found in Laysan albatross liver by Klasson-Wehler and colleagues. The most commonly detected congeners in this study were 4-MeSO$_2$-CB149 followed by 5-MeSO$_2$-CB149, amounting to 20 to 50% of the sum MeSO$_2$-CB concentration. The *meta-* and *para-* isomers of MeSO$_2$-CBs 49, 87, 101 and 149 were also detected. Overall, the *meta-* and *para*-isomers of MeSO$_2$-CBs 101 and 149 appear to be the most commonly detected in birds. However, the concentrations and minor congeners detected can vary significantly with geographic location and species.

As discussed in **Section 1.3.4.2**, enantioselective analysis of chiral methyl sulfone PCBs has been performed on pooled egg samples from the Baltic guillemot, *Uria aalge* (Jörundsdóttir *et al.* 2006), and on muscle tissue from pelicans raised in the Prague Zoo (Karásek *et al.* 2007). The EFs reported in these two studies were quite similar, suggesting that the enantioselective toxicokinetics of MeSO$_2$-CBs are similar among bird species. For example, for the congeners 4′-MeSO$_2$-CB132, 5-MeSO$_2$-CB149, and 4′-MeSO$_2$-CB174, EFs of 0.67 and 0.68,

0.41 and 0.43, and of 0.56 and 0.62 were reported, respectively. These results also suggest that the same enantiomer elution order was obtained between the two analytical methods, which is expected since enantioselective GC columns with the same chiral selector were employed. However, Jörundsdóttir and colleagues were also able to quantify the enantiomers of 4-MeSO$_2$-CB91, 4-MeSO$_2$-CB149, and 5′-MeSO$_2$-CB174 and obtained EFs of 0.65, 0.52, and 0.27, respectively, in their pooled guillemot egg samples. The results of both studies indicate that enantioselective toxicokinetic processes occurring for methyl sulfone PCBs in birds are congener-dependent, with the first eluting enantiomer being more abundant for some congeners, the second eluting enantiomer being more abundant for others, and with nearly equal proportions of the two for yet other congeners. Similar EF trends have been reported in Baltic grey seals (Larsson *et al.* 2004), however, the absolute values of the EFs reported in mammals, including humans, are generally more extreme (i.e. greater than 0.94 or less than 0.09) than those reported in birds (Chu *et al.* 2003a, Ellerichmann *et al.* 1998, Wiberg *et al.* 1998).

### 2.2.6  *Analysis of MeSO$_2$-CBs in sledge dog plasma and adipose tissue*

In the four sledge dog plasma samples examined, two control adult and two exposed adult, five methyl sulfone PCB congeners were detected but only one was present above its limit of quantitation. The congeners detected were: 4-MeSO$_2$-CB70 in one sample, and 3′-MeSO$_2$-CB87 + 4-MeSO$_2$-CB110 and the enantiomers of 4-MeSO$_2$-CB149 in all four samples. The enantiomer peak areas for 4-MeSO$_2$-CB149 were very similar to one another in all four samples, so the average EF for this congener is expected to be around 0.5, or racemic. However,

this cannot be stated with confidence since the peak areas were below the LOQ. The congener 4-MeSO$_2$-CB64 was also detected in all four samples with a peak area exceeding the limit of quantitation, but, unfortunately, the internal standard was below LOQ in all samples, so the concentration could not be calculated with confidence. In addition, the qualifying transition was not detectable in any sample for this congener due to its low response relative to the base peak. Using the LODs and LOQs for each congener in nanograms on-column, it was possible to estimate a concentration range for each isomer by dividing these values by the corresponding sample weight (1.02 to 1.14 g wet weight) and percent lipid (0.58% to 1.01%). The concentration of 4-MeSO$_2$-CB64 was greater than 0.0168 ng/g lipid weight in the three samples where its signal was above the LOQ. For the remaining congeners, the peak areas were greater than the LOD but less than the LOQ. The resulting concentration ranges were: 0.0001 to 0.0353 ng/g lipid weight for 4-MeSO$_2$-CB70, 0.0002 to 0.459 ng/g lipid weight for 3′-MeSO$_2$-CB87 + 4-MeSO$_2$-CB110, 0.0002 to 0.0656 ng/g lipid weight for E1 4-MeSO$_2$-CB149, and 0.0002 to 0.0569 ng/g lipid weight for E2 4-MeSO$_2$-CB-149. Low concentrations of these contaminants were expected in blood, since they tend to accumulate to a greater extent in adipose tissue and/or liver in most organisms, including polar bears (Gebbink *et al.* 2008b).

A total of 13 different methyl sulfone PCB congeners were quantified in the 38 sledge dog fat samples analyzed. The sample mass ranged from 1.01 to 1.73 g wet weight and the percent lipid from 70.20 to 98.37%. In 14 samples, the internal standard and all of the MeSO$_2$-CB congeners were below the limit of

detection and sample loss during transportation and/or storage is suspected. These samples were excluded from the final data set. In two other samples, the internal standard was below the limit of quantitation, but several congeners were present with peak areas in excess of their respective LODs. Individual congener and sum MeSO$_2$-CB concentrations could not be calculated for these samples, but they were included in the percent detection calculations. In all samples, congeners with peak areas above the LOD were included in the calculations of percent detection, the results of which are presented in **Table 2.11** on the following page. As described in **Section 2.1.1**, the sledge dog samples consisted of an exposed group (EXP) fed a diet of whale blubber, and a control group (CON) fed a diet of pork fat. Both exposure groups contained adult females (P), which were bred on two occasions with a single control diet fed male to produce two litters of male and female pups (F1 for first litter and F1-MLK for second litter). Unfortunately, information as to which pups belonged to which litter and their sexes was not available, so all of the pups were grouped together and will be referred to collectively as the F1 generation in the data that follows. However, it should be noted that this is a potential confounding factor, since the adult females that had F1-MLK pups and were still nursing at the end of the study had comparably lower sum PCB concentrations than the adult females with F1 pups that had reached maturity by study end (Verreault *et al.* 2009a).

**Table 2.11:** **Percent detection of MeSO$_2$-CBs in sledge dog adipose tissue samples**

*CON: control, EXP: exposed, P: parental generation, F1: first generation offspring.*

| Congener | % Detection | | | | | | | | TOTAL All Dogs |
|---|---|---|---|---|---|---|---|---|---|
| | CON | | EXP | | SUB-TOTALS | | | | |
| | P | F1 | P | F1 | CON | EXP | P | F1 | |
| 4′-49 | 17 | 89 | 67 | 100 | 60 | 82 | 42 | 93 | 70 |
| 3-52 + 4-64 | 17 | 89 | 100 | 100 | 60 | 100 | 50 | 93 | 78 |
| 4-52 | 17 | 89 | 17 | 40 | 60 | 27 | 17 | 71 | 40 |
| 3-70 | 17 | 89 | 100 | 100 | 60 | 100 | 50 | 93 | 78 |
| 4-70 | 17 | 89 | 100 | 100 | 60 | 100 | 50 | 93 | 78 |
| 3′-87 + 4-110 | 17 | 89 | 100 | 100 | 60 | 100 | 50 | 93 | 78 |
| 4′-87 | 17 | 89 | 67 | 80 | 60 | 73 | 42 | 86 | 67 |
| 5-91 | 0 | 0 | 0 | 0 | 0 | 0 | 0 | 0 | 0 |
| 4-91 | 0 | 0 | 67 | 60 | 0 | 63 | 33 | 29 | 15 |
| 3′-95 | 0 | 0 | 0 | 0 | 0 | 0 | 0 | 0 | 0 |
| 4′-95 | 0 | 0 | 0 | 0 | 0 | 0 | 0 | 0 | 0 |
| 3′-101 | 0 | 0 | 0 | 0 | 0 | 0 | 0 | 0 | 0 |
| 4′-101 | 17 | 89 | 100 | 100 | 60 | 100 | 50 | 93 | 78 |
| 5-110 | 17 | 89 | 50 | 60 | 60 | 55 | 33 | 79 | 59 |
| 4′-132 | 0 | 22 | 100 | 80 | 13 | 91 | 50 | 50 | 44 |
| 3′-141 | 0 | 0 | 67 | 20 | 0 | 45 | 33 | 14 | 22 |
| 4′-141 | 0 | 0 | 0 | 0 | 0 | 0 | 0 | 0 | 0 |
| 5-149 | 0 | 11 | 0 | 0 | 0 | 9 | 0 | 7 | 4 |
| 4-149 | 17 | 89 | 83 | 80 | 60 | 82 | 50 | 86 | 67 |
| 4′-174 | 0 | 0 | 0 | 0 | 0 | 0 | 0 | 0 | 0 |
| *# of samples* | *6* | *10* | *6* | *5* | *16* | *11* | *13* | *14* | *27* |

The majority of the achiral congeners were detected in at least one sample with the exceptions of 3′-MeSO$_2$-CB101 and 4′-MeSO$_2$-CB141, which were not observed. Conversely, the only chiral congeners detected in any of the samples were 4-MeSO$_2$-CB91, 4′-MeSO$_2$-CB132, 5-MeSO$_2$-CB149, and 4-MeSO$_2$-CB149. The congener patterns were quite similar between the various sample groups. The only differences were that 4-MeSO2-CB91 and 3′-MeSO$_2$-CB141 were only detected in the exposed dogs (adults and pups) and 5-MeSO$_2$-CB149 in one exposed pup. In addition, 4′-MeSO$_2$-CB142 was detected in all sample groups but the control adults. The detection frequencies were the same for all of the congeners in the control adult group at 17% since there was only one sample where any MeSO$_2$-CBs were detected. The detection frequencies were almost five times higher for the control pups, for which only two samples out of nine were devoid of methylsulfonyl PCBs. The percent detection was also the same for all congeners in this group, except for 5-MeSO$_2$-CB149 and 4′-MeSO$_2$-CB132, which were only detected in one and two samples, respectively. It is plausible that the differences in congeners detected between the control and exposed dogs were simply a function of the higher concentrations of MeSO$_2$-CBs found in the latter group (see below for further discussion of concentrations), which made the detection of minor isomers possible. However, another explanation is that the differences in congener profiles resulted from induction of CYP enzymes in the exposed group. This was suggested as the mechanism leading to different PCB congener patterns between the exposed and control dogs in a complementary study (Verreault *et al.* 2009b) and is supported by the finding of higher EROD

and epoxide hydroxylase activities in the exposed sledge dogs compared to controls (Verreault *et al.* 2009c).

There was more variability in the frequencies of detection between congeners in the exposed dogs. In both the exposed adults and pups, the congeners $3\text{-MeSO}_2\text{-CB52}$ + $4\text{-MeSO}_2\text{-CB64}$, $3\text{-MeSO}_2\text{-CB70}$, $4\text{-MeSO}_2\text{-CB70}$, $3'\text{-MeSO}_2\text{-CB87}$ + $4\text{ MeSO}_2\text{-CB110}$, and $4'\text{-MeSO}_2\text{-CB101}$ were detected in 100% of the samples. In addition, the congener $3'\text{-MeSO}_2\text{-CB49}$ was detected in all of the F1-EXP dogs, whereas $4'\text{-MeSO}_2\text{-CB132}$ was detected in all of the P-EXP dogs. Similar detection frequencies (i.e. $\leq 10\%$ difference) were observed between the exposed adults and pups for $4\text{-MeSO}_2\text{-CB91}$, $5\text{-MeSO}_2\text{-CB110}$, and $4\text{-MeSO}_2\text{-CB149}$. However, higher (i.e. $\geq 10\%$ difference) detection frequencies were observed in the exposed pups for $4\text{-MeSO}_2\text{-CB52}$ and $4'\text{-MeSO}_2\text{-CB87}$, whereas a higher frequency was observed in the exposed adults for $3'\text{-MeSO}_2\text{-CB141}$. Overall, the methyl sulfone PCBs were observed in higher frequencies for the exposed dogs (adults and pups) compared to the control dogs for all congeners but $4\text{-MeSO}_2\text{-CB52}$ and $5\text{-MeSO}_2\text{-CB110}$. Higher frequencies of detection were also calculated for the pups (exposed and control) compared to the adults for all but $4\text{-MeSO}_2\text{-CB91}$, $4'\text{-MeSO}_2\text{-CB132}$, and $3'\text{-MeSO}_2\text{-CB141}$. The most frequently detected congeners over all samples were the tetrachlorinated analytes $3\text{-MeSO}_2\text{-CB52}$ + $4\text{-MeSO}_2\text{-CB64}$, $3\text{-MeSO}_2\text{-CB70}$ and $4\text{-MeSO}_2\text{-CB70}$, and the pentachlorinated analytes $3'\text{-MeSO}_2\text{-CB87}$ + $4\text{-MeSO}_2\text{-CB110}$ and $4'\text{-MeSO}_2\text{-CB101}$, all at 78% detection.

Note that the congeners observed in the pups and adults were the same within each exposure group, with the exception of 5-MeSO$_2$-CB149, which was detected in one control pup but not in any of the control adults. This may indicate that maternal transfer in sledge dogs is non-selective. Similar congener patterns of methyl sulfone PCBs have previously been reported between maternal and cord serum in humans (Linderholm *et al.* 2007) and between maternal and offspring muscle tissue in mink (Lund *et al.* 1999). However, slightly different congener patterns of other organohalogen contaminants, including PCBs, were detected between the F1-MLK and the F1 and P sledge dogs in both the control and exposed groups in these samples, which is suggestive of selective maternal transfer (Verreault *et al.* 2009a). It is therefore possible that the inability to differentiate the F1-MLK and F1 dogs in the current work confounded the results and masked a potentially different congener pattern in the pre-weaning pups. As pointed out by Verreault and coworkers (2009a), the mature pups would be expected to exhibit a congener pattern similar to their mothers because they were fed the same diet post-weaning. Further investigations would be necessary to confirm or deny if selective maternal transfer occurs for methyl sulfone PCBs in sledge dogs.

Interestingly, there were three unknown congeners that were detected in the majority of the exposed sledge dog samples. One was a tetrachlorinated congener that eluted at 23 minutes, one was a pentachlorinated congener that eluted at 40 minutes, and the other was a hexachlorinated congener that eluted at 17 minutes. These retention times did not correspond to any of the target analytes.

However, small peaks at these retention times were detected in the high

concentration (5000 ng/mL) standard runs, and with smaller peak areas in the 100

ng/mL standard runs, where they were barely detectable. The fact that the peak

areas in the standard runs varied directly with concentration likely indicates that

they were present as trace impurities in the analytical standards. As mentioned

previously, no MeSO$_2$-CBs were detected in any of the solvent or extraction

blanks and no carryover was observed in the solvent blanks analyzed after the

highest concentration standard. Therefore, these unknown compounds are likely

methyl sulfone PCBs present in the samples and in trace quantities in the

standards, not artefacts of the analytical method. Twelve unknown tri- to

hexachlorinated MeSO$_2$-CB congeners have previously been detected in Canadian

ringed seal blubber and four in polar bear fat in a comprehensive study targeting

25 of the 28 congeners considered "environmentally relevant" using GC/MS

(Letcher *et al.* 1998). Since the majority of the MeSO$_2$-CB congeners typically

considered environmentally relevant possess a chlorine substituent in the *para*-

position on the non-MeSO$_2$-susbtituted ring as well as a 2,5-dichloro or 2,3,6-

trichloro substitution pattern on the MeSO$_2$-containing ring, these authors

suggested that the unknown congeners may possess the latter structural

characteristic, but not the former. However, PCB feeding studies performed on

rats have revealed that methyl sulfone metabolites may also be formed for certain

PCB congeners lacking a 2,5-dichloro or 2,3,6-trichloro substitution pattern

(Darnerud *et al.* 1986, Haraguchi *et al.* 1998, Haraguchi *et al.* 1997).

Furthermore, it has been established that beagle dogs have the capacity to form

arene oxide intermediates from PCBs deficient of adjacent chlorine unsubstituted *ortho*/*meta* or *meta*/*para* sites (Ariyoshi *et al.* 1992, Ariyoshi *et al.* 1993).

The $MeSO_2$-CB concentration distributions in the sledge dog adipose tissue samples are presented in a censored box and whisker plot in **Figure 2.26** on the following page, where the LOQs for each congener are represented by horizontal dotted lines. Note that only concentrations in excess of the LOQ were used to construct this figure, unlike **Table 2.11** where concentrations above the LOD were used to calculate the detection frequencies. As a result, there is only one bar for the exposed pups for 4-$MeSO_2$-CB91 in **Figure 2.26**, since this congener was only quantifiable in this one group. It was detectable in 67% of the exposed adults and 60% of the exposed pups, but at concentrations below the LOQ in all but one sample. By comparing the data presented in **Table 2.11** above to that presented in **Figure 2.26** on the following page, it is evident that the congeners with the highest detection frequencies were generally the ones found in the highest concentrations. The most notable feature of **Figure 2.26** is that the highest concentrations and greatest variation between samples were observed in the exposed adults, as evidenced by the large spread and high-reaching whiskers for most of the congeners in this data set. This trend is particularly obvious for 3-$MeSO_2$-CB52 + 4-$MeSO_2$-CB64, 4-$MeSO_2$-CB70, 3′-$MeSO_2$-CB87 + 4-$MeSO_2$-CB110, 4′-$MeSO_2$-CB101, and 4-$MeSO_2$-CB149, as well as the sum concentration of $MeSO_2$-CBs. It is also evident, although slightly less pronounced, for the congeners 3-$MeSO_2$-CB70, 4′-$MeSO_2$-CB132, and 3′-$MeSO_2$-CB141. For 4′-$MeSO_2$-CB49, 4-$MeSO_2$-CB52, and 5-$MeSO_2$-CB110,
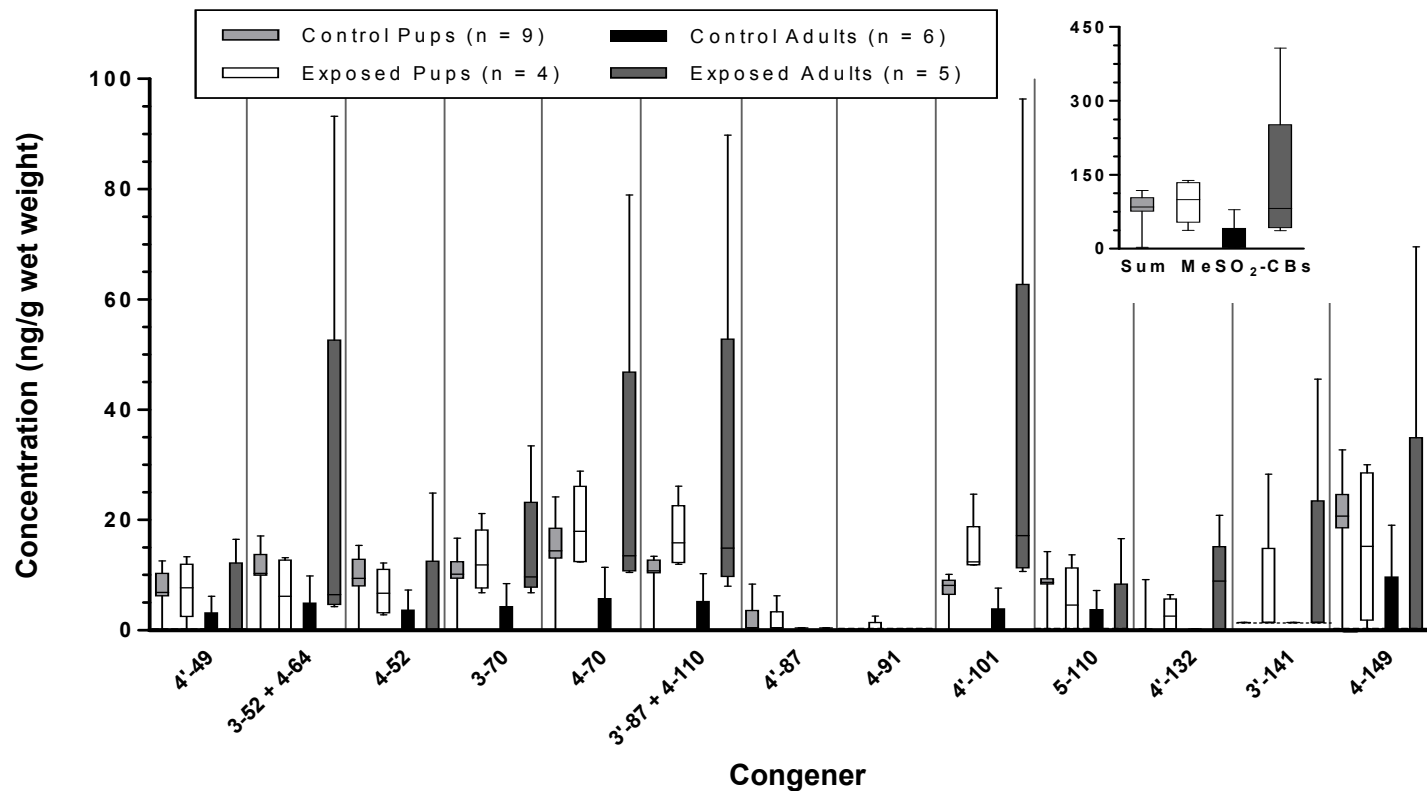
**Figure 2.26:** **Distribution of MeSO$_2$-CBs detected in Greenland sledge dog adipose tissue samples**

*Censored box and whisker plots. Top and bottom of boxes represent 25th and 75th percentiles, respectively. Hash marks inside boxes represent medians, and error bars represent the spread of the data. Horizontal dotted lines indicate LOQs for each congener; not visible for some congeners on this scale. Median for control adults at LOQ for all congeners and the sum concentration of MeSO$_2$-CBs. Sample number indicated in legend. Sum concentration of enantiomers presented for the chiral congeners: 4-91, 4'-132, and 4-149. Sum concentration of MeSO$_2$-CBs presented in figure inset in ng/g wet weight.*

the maximum concentration indicated by the height of the top whisker is still equal to or higher than that of the other groups, but the spread between the 25th and 75th percentiles is more similar. Curiously, although the highest 75th and 100th percentile concentrations were observed for the exposed adults, the median was only highest for the congeners 4′-MeSO$_2$-CB101 and 4′-MeSO$_2$-CB132. For all of the remaining congeners and the sum concentration of MeSO$_2$-CBs, the median concentration was equal to or less than that of the exposed pups or the control pups. The exposed pups demonstrated the highest median concentration for four congeners, and for the sum concentration of MeSO$_2$-CBs. The exposed pups displayed the highest median concentrations for four other congeners. The median, 75th percentile, and 100th percentile concentrations were the lowest for the control adults for all congeners and the sum concentration of MeSO$_2$-CBs.

The concentration and sample weight data for the individual samples from each exposure group are presented in **Appendices B1** through **B4**. A sample chromatogram is presented in **Appendix C**. Note that there was a high level of non-detections, or left-censored data, for certain congeners and/or sample groups in this data set. The percent censored data using the LOD as the cutoff is simply 100 minus the detection frequency reported in **Table 2.11** above. This amounts to 0 to 96% censoring, depending on the congener and/or the sample group examined. However, as mentioned in the previous paragraph, the LOQ was used as the cutoff for the concentration distribution data, so the percent censoring in this case is higher, from 11 to 100%. A common method for dealing with non-detects in environmental analysis is substituting a value such as 0.5 times the

LOD for all non-detects. However, it has been demonstrated that this method is inaccurate, particularly for highly censored data sets (Helsel 2006), and that there are other methods that can account for censored data and produce more reliable results (Helsel 2005). One of these methods is the non-parametric Kruskal-Wallis test, which was applied here because the data was skewed, as evidenced by the asymmetrical box plots for some congeners and/or sample groups. In order to apply the Kruskal-Wallis test to censored environmental data, all values below a threshold of interest (i.e. the LOQ) must be set to a single, arbitrary value lower than any of the detected concentrations. Applying this strategy to the sum $MeSO_2$-CB concentrations produced a significant P value of 0.0292 and a Kruskal-Wallis statistic of 9.004, indicating a significant difference between the medians of the four groups. However, when Dunn's Multiple Comparison test was applied, no differences in rank sum could be detected between any of the sample groups at a significance level of 0.05. Therefore, it can be concluded that there is a significant difference between the median of at least one sample group compared to the others, but it cannot be discerned which group(s) is (are) significantly different from the others using this post-hoc test. From visual inspection of the box plot in **Figure 2.26**, it appears that the control adult data set may be significantly lower than the other three groups, but this could not be confirmed. There were no significant differences among treatment groups for the individual congeners using the Kruskal-Wallis test.

Adipose tissue samples from these dogs were simultaneously extracted for the analysis of several other organohalogen contaminants, and significant

differences in both the individual congener and summed concentrations of PCBs were detected between the control and exposed dogs within each generation (Verreault *et al.* 2009a). Likewise, a significantly higher sum concentration of hydroxylated PCB metabolites was found in plasma samples from the exposed sledge dogs compared to controls (Verreault *et al.* 2008). However, there were no significant differences between the pups and the adults within each exposure group for PCBs in adipose tissue, and the authors concluded that the concentrations of these contaminants reach an equilibrium state early in life. There was a higher concentration of $MeSO_2$-CBs found in the exposed adults compared to the control adults in the current study, and a higher concentration in the exposed pups compared to the control pups, although these differences were not significant. Consistent with the results for PCBs, there was no obvious difference and no statistical between the exposed adults and exposed pups, however, there was a slightly higher concentration of methyl sulfone metabolites in the control pups compared to the control adults. This is an unusual situation, since the sum concentration of these contaminants was found to be 1.5 times lower in human cord serum compared to adult serum (Norén *et al.* 1996) and 6 times to 3 orders of magnitude lower in glaucous gull eggs (Verreault *et al.* 2006) and white tailed sea eagle eggs (Olsson *et al.* 1993), respectively, compared to the plasma of the mother birds. However, the sum $MeSO_2$-CB concentration found in the muscle tissue of 5-week old kits was similar to that in the mothers in a mink reproductive toxicity study (Lund *et al.* 1999). As mentioned previously, it was not known which samples were from offspring that were mature at study end and

which were still pre-weaning, and this may be a confounding factor in this comparison. In addition, the sample sizes were quite small and the percent censored data quite high in the control adult data set, so the higher concentration in the control pups is not thought to be meaningful.

The health effects of organic contaminants, including methyl sulfone PCBs, are of particular concern in sentinel Arctic species, such as the polar bear and Arctic fox, because biomagnification is amplified in these solely carnivorous predators due to the higher load of organic contaminants generally found in animal prey compared to plants. In addition, they eat mostly the blubber of their prey, which is the main tissue where most organic contaminants accumulate, due to the high energy content (Letcher *et al.* 1998). The circumpolar distribution and high level of organic contaminants accumulated in polar bears make them an excellent Arctic biomonitoring species (Sandala *et al.* 2004). However, studying large, free-ranging animals that must be sampled opportunistically makes it very difficult to control variables that could have a significant impact on the levels and effects of organic contaminants on their health, including age and gender (Gebbink *et al.* 2008a), seasonal variability (Dietz *et al.* 2004), physiological condition (Verreault *et al.* 2008), as well as diet, genetics, reproductive status, and metabolic capacity (Verreault *et al.* 2009a). For example, the concentrations of methyl sulfone PCBs detected in the adipose, brain and liver tissues of male polar bears were significantly less than those found in female bears, which was attributed to the ability of the females to unload a portion of their body burden to their young via trans-placental and lactational transfer (Gebbink *et al.* 2008a).

Recently, a multi-component study was conducted to determine the viability of using Greenland sledge dogs as a potential captive surrogate species for determining the effects of organic contaminants, including PCBs and hydroxylated PCB metabolites, in polar bear. It was found that exposed sledge dogs exhibited insufficient immune response associated with decreased gene expression of haptoglobin and fatty acid binding protein in liver (Sonne *et al.* 2007), decreased cellular immunity as determined by intradermal testing (Sonne *et al.* 2006a), alterations in haematological and urine clinical-chemical parameters, including increased urine glucose levels and decreased cholesterol, lactate dehydrogenase, creatinine kinase, and cortisol:creatinine ratio (Sonne *et al.* 2008a), and increased incidence of liver lesions, including granulomas, portal fibrosis, and mild bile duct hyperplasias (Sonne *et al.* 2008b). Similar observations have been reported in polar bears (Fisk *et al.* 2005, Kirkegaard *et al.* 2005, Sonne *et al.* 2006b, Sonne *et al.* 2005), indicating that organohalogen contaminants may potentially be affecting the health of these top Arctic predators and that the mechanisms of toxicity are similar to those in captive sledge dogs (Verreault *et al.* 2009b).

As an extension of this larger study, one of the goals of the current work was to measure and compare the congener patterns and concentrations of methyl sulfone PCB metabolites in the exposed dogs to those found in polar bears in previous studies. The most commonly detected congeners in the liver, brain, whole blood and adipose tissues of East Greenland polar bears (*Ursus maritimus*) were the *meta*- and *para*-isomers of MeSO$_2$-CBs 49, 64, 70, 87, 101 and 141, as

well as 4-MeSO$_2$-CB110, making up 60 to 86% of the sum concentration in these tissues (Gebbink *et al.* 2008b). Of these congeners, the most abundant in adipose tissue were 3′-/4′-MeSO$_2$-CB87 and 3′-/4′-MeSO$_2$-CB101, followed by 3′-/4′-MeSO$_2$-CB49, and 4-MeSO$_2$-CB110. The *meta-* and *para-*isomers of MeSO$_2$-CBs 52, 91, 132, 149 and 174 were also encountered, but at lower concentrations. Similar findings were reported in another study of East Greenland polar bears that examined whole blood and adipose tissue (Sandala *et al.* 2004). In the adipose tissue of bears sampled from across the western Arctic and Subarctic, the *meta-* and *para-*isomers of MeSO$_2$-CBs 87 and 101 were once again the most abundant congeners detected, comprising approximately 50% of the sum MeSO$_2$-CB concentration (Letcher *et al.* 1995). These congeners also dominated in the adipose tissue of Canadian polar bears (Wiberg *et al.* 1998). In a second, later study of the adipose tissue of polar bears across the western Arctic and Subarctic, 3′- and 4′-MeSO$_2$-CB101, 4′-MeSO$_2$-CB87, and 4-MeSO$_2$-CB149 were the most frequently detected congeners, accounting for 49% of the sum concentration of methyl sulfone PCBs in these samples (Verreault *et al.* 2005b). In the works of Letcher *et al.* 1995 and Wiberg *et al*. 1998, 4-MeSO$_2$-CB149 was also detected in relatively high abundance, along with 5-MeSO$_2$-CB149. In addition, the congener 4-MeSO$_2$-CB91 was detected in a higher relative abundance by Wiberg and colleagues and 4-MeSO$_2$-CB110 in lower relative abundance compared to the results presented by Gebbink *et al.* (2008b) and Sandala *et al*. (2004).These two congeners were not studied by Letcher and coworkers (1995), so comparisons could not be made with this study.

The current results demonstrate that the congener pattern found in Greenland sledge dog adipose tissue is comparable to that found in polar bears. The only glaring difference in the congener patterns between these two species is that 5-MeSO$_2$-CB91 and the *meta-* and *para-*substituted isomers of MeSO$_2$-CB174 were detected in polar bear but not in sledge dog. Smaller differences in the congener patterns are that 4-MeSO$_2$-CB52 was among the most frequently detected in sledge dog but was less commonly found in polar bear. Conversely, the *meta-* and *para-*substituted isomers of MeSO$_2$-CBs 64 and 141 were among the most frequently detected in polar bear but not in sledge dog. The *meta-*substituted isomers of MeSO$_2$-CBs 49, 132, 149, and 174 were all detected in polar bear, but the current method was not sensitive enough to detect these congeners at concentrations of up to 5000 ng/mL, so no comparisons could be made between data sets for these analytes. Also, the congener 3-MeSO$_2$-CB64 was not analyzed in the current work due to the fact that an analytical standard was not readily available. The minor differences found in MeSO$_2$-CB congener composition between these two species may be attributable to differences in PCB metabolism. Disparate congener patterns have also been reported between the adipose tissue and plasma, respectively, of sledge dogs and adult female polar bears for PCBs and their hydroxylated metabolites, and the authors stated that differences in metabolic activity and selectivity were likely the cause (Verreault *et al.* 2008).

In terms of absolute concentrations, sum MeSO$_2$-CB levels in the range of 432 ng/g lipid weight (Letcher *et al.* 1998) and 699 ng/g lipid weight (Sandala *et*

*al.* 2004) have been measured previously in Canadian and East Greenland polar

bears, respectively, with a range of 127 to 3920 ng/g lipid weight in the latter

study. Two studies of the geographical distribution of $MeSO_2$-CBs in polar bears

across the western Arctic and Subarctic, ranging from the Bering Sea to the

Greenland Sea and from the Chukchi Sea to Svalbard, determined sum

concentrations in the range of 138 to 633 ng/g lipid weight and 96 to 198 ng/g

lipid weight, respectively (Letcher *et al.* 1995, Verreault *et al.* 2005b). The lower

concentrations found by Verreault and coworkers (2005b) may be a function of

decreasing contaminant concentrations over the years between sampling periods

(1989 to 1991 versus 1996 to 2002). Conversely, the authors stated that it may be

a function of several confounding variables that could not be controlled, including

diet, nutritional and reproductive status, age, and sex ratio. In two other studies of

East Greenland polar bears, the mean sum concentrations were 455 ng/g wet

weight (Gebbink *et al.* 2008b)and 340 ng/g wet weight (Gebbink *et al.* 2008a).

The median sum $MeSO_2$-CB concentrations found in the current work were 82.1

and 99.5 ng/g in wet weight and 99.7 to 125 ng/g in lipid weight for the exposed

adults and pups, respectively. The median wet weight concentrations were quite a

bit lower than the mean concentration in East Greenland polar bears reported by

Gebbink *et al.* 2008a and b. The median lipid weight concentrations were similar

to those reported by Verreault *et al*. 2005b, but quite a bit lower than the

remaining polar bear studies expressing concentrations in lipid weight.

     Mean individual congener concentrations in the range of 20 to 70 ng/g

lipid weight have been presented for the most abundant congeners in polar bear

sampled from the Canadian Arctic (Wiberg *et al.* 1998). These values are higher than the median concentrations found here, which were in the range of 5 to 20 ng/g lipid weight for the highest concentration congeners in the exposed dogs. There are a number of different factors that could have contributed to this discrepancy in concentrations. Many of the variables that affect organohalogen contaminant concentrations in organisms, such as age, diet, and genetics (Verreault *et al.* 2009a), were controlled in the sledge study but could not be controlled (age, diet) or even known (diet, genetics) in the polar bear studies. In addition, although the exposed sledge dogs were fed minke whale blubber known to contain similar OC concentrations to East Greenland ringed seals (*Pusa hispida*), which are the main prey item of East Greenland polar bears, it should be noted that wild polar bears exhibit a more varied diet, sometimes feeding opportunistically on different species of seals and walruses, as well as on organs and tissues other than blubber (Verreault *et al.* 2008). This could certainly have contributed to the different concentrations and congener profiles observed. Another important factor is metabolic capacity. Once again, it is likely that these two species have different metabolic and clearance capacities for MeSO$_2$-CBs. Two comparative metabolism studies of MeSO$_2$-CBs have been carried out using rats, mice, and guinea pigs, and even among these different types of rodents, significant differences in metabolism have been observed (Haraguchi *et al.* 2005a, 2005b).

Due to problems with detection and co-elutions for several of the *meta*-substituted analytes, it was only possible to compare the concentrations of the

*meta* and *para* regioisomers of MeSO$_2$-CB70. In this case, the median concentration was slightly higher for the *para*-substituted congener for both the exposed adults and pups. Differences in concentrations between regioisomers have been observed previously in East Greenland polar bears. A small preference for the accumulation of the *meta*-isomer of MeSO$_2$-CB87 was observed in the liver, whereas a preference for *para*-isomer was observed in the brain, blood and adipose tissues (Gebbink *et al.* 2008b). In addition, analysis of the adipose tissue of Canadian polar bears revealed a higher abundance of the *para*-substituted isomers for the majority of the MeSO$_2$-CB congeners, including 4-MeSO$_2$-CB70 (Wiberg *et al.* 1998). The trend observed in the current work is therefore consistent with previous results. However, it would be desirable to improve the sensitivity of detection for the *meta*-substituted isomers so that comparisons could be made for other congeners, as well.

Although concentrations could not be calculated for the MeSO$_2$-CBs found in the sledge dog plasma samples, the congener pattern could still be compared to that of polar bear blood. The congeners 4-MeSO$_2$-CB 64, 4-MeSO$_2$-CB70, 3′-MeSO$_2$-CB87 + 4-MeSO$_2$-CB110, and 4-MeSO$_2$-CB149 were detected in sledge dog plasma, all of which are among the most commonly detected in polar bear blood, except for 4-MeSO$_2$-CB149, which is a lower abundance isomer. Clearly, there are a number of other isomers that were detected in polar bear blood but were not detected here. In addition to the factors listed above, the analysis of whole blood in polar bear versus blood plasma in sledge dog may have contributed to the different congener patterns in this case. Differences in the

concentrations and congener patterns of methyl sulfone PCB metabolites have been observed between the different lipoprotein fractions of human blood (Norén *et al.* 1999).

Finally, since several chiral congeners were quantifiable in the sledge dog adipose tissue samples, it was possible to calculate enantiomer fractions (EFs). The EF data is presented graphically in **Figure 2.27** on the following page and numerically in **Appendix D**. Note that EFs were only calculated when at least one of the enantiomers was present at a level exceeding the LOQ. As a result, no EF data is presented for the congener 5-MeSO$_2$-CB149, which was detected in one sample, but at a level below the LOQ. In cases where only one enantiomer was detected, EFs were calculated using the LOD as the signal for the non-detected enantiomer. This was necessary for the congeners 4-MeSO$_2$-CB91 and 4-MeSO$_2$-CB132, since only the first eluting enantiomer was detected for the former, and only the second eluting enantiomer was detected for the latter. Conversely, the EFs were nearly racemic for all but one sample for 4-MeSO$_2$-CB149. The EFs for the majority of the samples ranged from 0.522 to 0.562 for this congener, compared to a value of 0.518 ± 0.007 for the analytical standard. However, in one exposed pup sample, the EF was 0.989, and the second eluting enantiomer was not detected. In all samples, the first eluting enantiomer was the most abundant, but this is quite a large discrepancy and a little difficult to explain.  In contrast, all of the EFs calculated for 4′-MeSO$_2$-CB132 fell within a tight range from 0.001 to 0.006, although this congener was detected in fewer samples. Duplicate

**4-91**

**4'-132**

**4-149**

Legend:
- ■ Control Adults
- ▲ Control Pups
- ✕ Exposed Adults
- ○ Exposed Pups
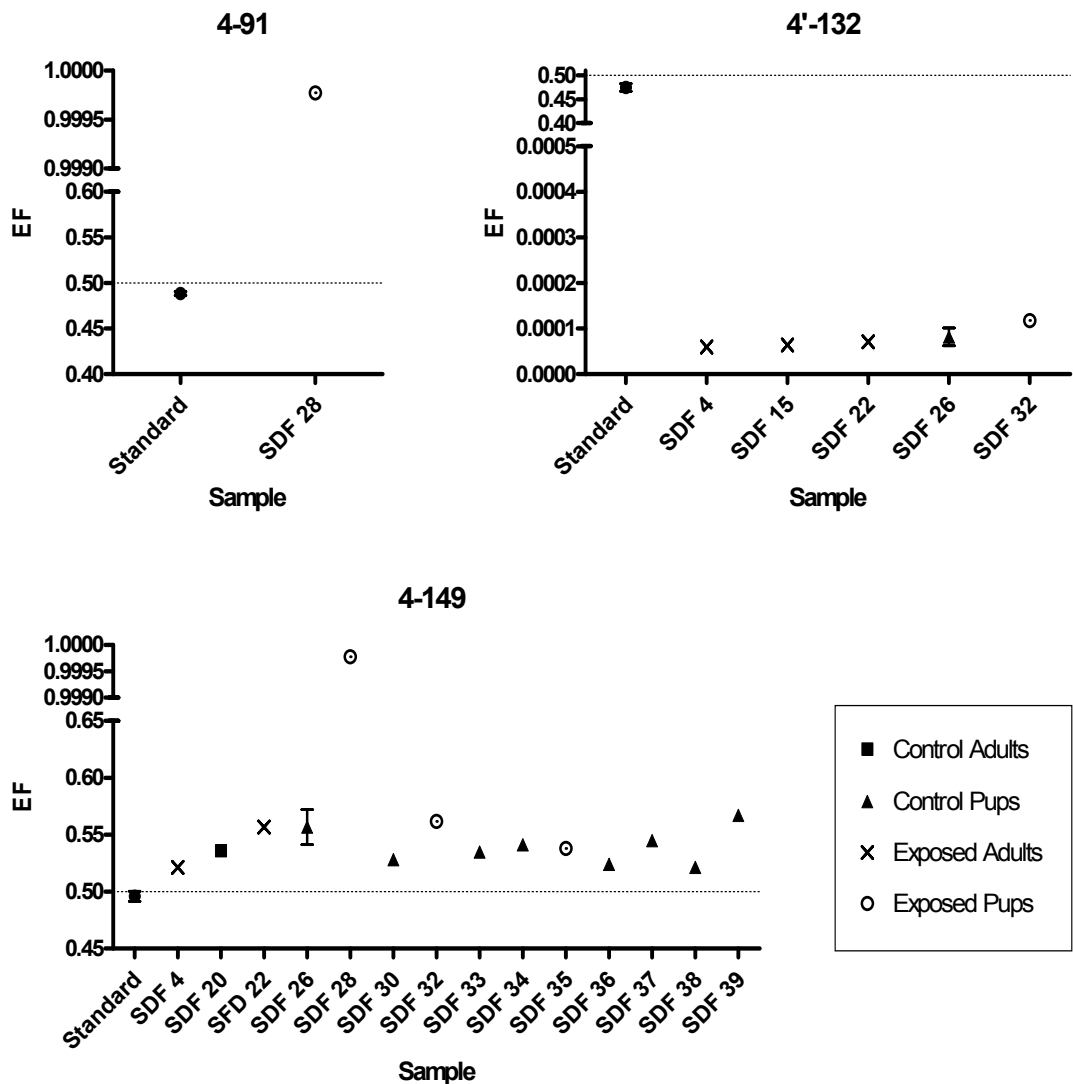
**Figure 2.27: Comparison of enantiomer fractions observed in analytical standards and in sledge dog fat samples**

*SDF: Sledge dog fat. Points with error bars are results of triplicate analyses for standards and duplicate measurements for samples. Error bars indicate maxima and minima, with average at the midpoint. Racemic EF is indicated with a dotted line. For points very near 0 or 1, one enantiomer was not detected, and its concentration was taken to be the limit of detection for EF calculation.*

measurements were performed for one sample (SDF 26), and the EFs were quite reproducible, as can been seen in **Figure 2.27**. As mentioned previously, less than 3% RSD in EF was observed upon repeated standard runs, and there were no significant matrix effects detected for any of the congeners or their enantiomers. Therefore, this result is not expected to be due to a lack of reproducibility in EF or matrix effects.

While it is common practice to verify enantiomer fractions using a different enantioselective stationary phase, this was not necessary in the current work because the EFs were all very near or very far from racemic. Methyl sulfone PCBs have not been analyzed in sledge dogs previously. However, chiral analysis of MeSO$_2$-CBs has been performed on the adipose tissue of polar bears and the blubber of ringed seals (*Phoca hispida*) from the Canadian Arctic (Wiberg *et al.* 1998), as well as the blubber, liver and lungs of grey seals (*Haliocherus grypus*) from the Baltic Sea (Larsson *et al.* 2004), the liver of harbor porpoises (*Phocoena phocoena*) from the Southern North Sea (Chu *et al.* 2003a), and the blubber of a seal (species unknown) from the Prague Zoo(Karásek *et al.* 2007). A comprehensive overview of the results of these studies is presented in **Section 1.3.4.2**. The results of the polar bear study and of the seal blubber studies will be the focus here.

In polar bear fat and ringed seal blubber, the most commonly detected chiral methyl sulfones were the *meta-* and *para-*isomers of MeSO$_2$-CBs 91, 132, and 149. This is similar to the results of the current work, where the *para-*isomers of these congeners were the most frequently detected, and 5-MeSO$_2$-CB149 was

detected in one sample. In polar bear and all of the seals species examined to date, a strong dominance of one enantiomer over the other was observed for all congeners detected. In fact, in polar bear, harbour porpoise, and grey seal, only one enantiomer was detected in many samples, as was the case in the current work. However, one difference between the results of the present study and those of Wiberg and colleagues is that nearly racemic EFs were observed for 4-MeSO$_2$-CB149 in the majority of the sledge dog samples, whereas one enantiomer dominated for this congener in polar bear. The authors estimated the enantiomer ratios (E1/E2) to be greater than 10 for 4-MeSO$_2$-CB91 and 4-MeSO$_2$-CB149 in polar bear. When expressed as enantiomer ratios (ERs) instead of EFs, the results of the current work agree well for the former congener (ER ~ 88) but not for the latter (ER ~ 1), assuming that the enantiomer elution order is the same between these methods. That being said, approximately racemic EFs have been observed for 4-MeSO$_2$-CB149 in the blubber of a seal raised in the Prague Zoo (Karásek *et al.* 2007). In the polar bear and ringed seal study, more extreme ERs were observed in the former compared to the latter, which the authors suggested implied that enantioselective metabolism was occurring in polar bear (Wiberg *et al.* 1998). Unfortunately, no samples of the minke whale blubber fed to the exposed sledge dogs in the current work were available for analysis. These would be imperative for drawing conclusions about enantioselective metabolism in sledge dogs, since the EFs of MeSO$_2$-CBs vary quite widely between different species of seal, as documented in the references given above.

## 2.3    Conclusions and future directions

It was demonstrated that the enantiomers of nine out of the ten environmentally relevant chiral methyl sulfone PCBs can be separated via enantioselective liquid chromatography with an amylose-based stationary phase. The current technique is an improvement over previous enantioselective GC methods both in terms of the number of chiral congeners separated and of total run time (Chu *et al.* 2003a, Ellerichmann *et al.* 1998). The use of an achiral pre-separation with a pyrenyl-ethyl silica stationary phase and of tandem mass spectral detection enabled the separation of most of the interfering isomers either by mass to charge ratio or retention time. Atmospheric pressure photoionization, which has not been applied to the analysis of PCB metabolites previously, proved to be an invaluable tool for the ionization of these contaminants. Good sensitivity was achieved for the *para*-substituted congeners and selected *meta*-substituted congeners. However, eight of the *meta*-substituted congeners of interest could not be quantified due to extremely poor response, a problem that has been encountered to a lesser extent in previous GC-MS methods (Letcher and Norstrom 1997). This remains the greatest weakness of this method, and potential strategies for increasing the overall sensitivity are presented below.

To the best of our knowledge, this is the first time that the metabolites of any organohalogen compounds, including PCBs, have been separated using pyrenyl ethyl silica, and the first time that this column has been used for on-line two-dimensional liquid chromatography. In addition, this is the first published report of this column being used with a normal phase solvent other than 100%

hexane, *n*-octane or isooctane, or at sub-ambient temperatures. As described in detail above, subtle changes in selectivity were obtained for the separation of MeSO$_2$-CBs by changing the solvents employed, the ratio of alkane and polar modifier, and the column temperature. For PCB separations, this stationary phase has mainly been used as a fractionation tool in the past (Concejero *et al.* 2001, Haglund *et al.* 1990a, 1990b, Jaouen-Madoulet *et al.* 2000, Ramos *et al.* 1999), but this work clearly demonstrates that under the appropriate conditions excellent selectivity between congeners can be achieved for the separation MeSO$_2$-CBs. It would be interesting to apply similar conditions to the separation of Aroclor mixtures of PCBs and to compare the results to previous 100% alkane separations.

It appears that MeSO$_2$-CBs are significantly more retained on the PYE stationary phase than their parent PCBs. This is expected since the highly electron withdrawing nature of the methylsulfonyl group (March 1992) would decrease electron density in the aromatic ring(s) and increase their affinity for the electron-donating stationary phase. As mentioned above, previous PCB separations on this column have been performed with 100% alkane, typically *n*-hexane. Unfortunately, there were problems with achieving column equilibration with this mobile phase in the current work, but one run was performed with a mobile phase of 99.5:0.25:0.25 hexanes:methanol:ethanol pumped at 0.5 mL/min at a column temperature of 25°C. Under these conditions, all of the chiral MeSO$_2$-CBs (from penta- to heptachlorinated) eluted between 26 and 41 minutes. Comparatively, a PCB separation previously performed on this column (same manufacturer and

column dimensions) at the same temperature and flow rate with a mobile phase of 100% hexane found that all of the PCB congeners (from penta-CB77 to octa-CB194) eluted in a time frame of 5 to 14 minutes (Ramos *et al.* 1999). This suggests that it should be possible to separate the parent PCBs from their $MeSO_2$-metabolites using this column. Indeed, if the mobile phase were switched to 100% hexane for the $MeSO_2$-CB separation, even more retention would be expected, so a time frame in excess of 12 minutes should exist between when the PCBs finish eluting and the $MeSO_2$-metabolites begin eluting. Current techniques for the isolation of the these metabolites from parent PCBs and other organohalogen contaminants in tissues involve several liquid-liquid extraction, as well as silica and Florisil open-column chromatography elution steps (Verreault *et al.* 2005a), as described in detail in **Section 2.2.3**. The amount of time required for this process is on the order of several hours and the total amount of solvent required approximately 250 mL, excluding that required for packing of the silica and Florisil columns, which could easily double this volume. Therefore, the possibility of fractionation using a single HPLC run amounting to less than 60 minutes and 30 mL of solvent is quite exciting and definitely merits further investigation.

A small increase in retention time, on the order of about 2 minutes for the last eluting peak, was noted over the course of the sample analyses. This may be attributable to build up of lipids and other biogenic material on the PYE guard cartridge, and possibly on the analytical column, since this stationary phase is notoriously sensitive to lipids (Concejero *et al.* 2001, Wells *et al.* 1995). For

future analyses, changing the guard cartridge in the PYE column every 50 samples is recommended to avoid this change in retention time and to avoid harm to the stationary phase of the analytical column.

This is, to our knowledge, the first report of a carbohydrate-based stationary phase being employed for the enantioselective separation of PCBs or their metabolites. Cyclodextrin-based stationary phases are typically the first choice for enantiomer separations of these types of contaminants (Haglund 1995, 1996a, 1996b, Hühnerfuss *et al.* 2002, Pham-Tuan *et al.* 2004, 2005, Reich and Schurig 1999). However, the present work demonstrates that excellent enantiomer separation can be achieved for the majority of the chiral $MeSO_2$-CB congeners using a Chiralpak AD/AD-H column. It would be interesting to apply this stationary phase to the separation of atropisomeric PCBs to see if similarly strong enantioselectivity could be achieved. Currently, the only methyl sulfone PCB congener that could not be separated was 5-$MeSO_2$-CB91, which has proven to be challenging to separate by enantioselective GC, as well. There are only two reports of successful enantioselective GC separations for this congener (Ellerichmann *et al.* 1998, Wiberg *et al.* 1998). Of the remaining isomers, only the enantiomers of 4-$MeSO_2$-CB149 were not baseline resolved, and unprecedented chromatographic distances between enantiomers of nearly 20 minutes (4′-$MeSO_2$-CB174) were observed for several isomers. It is possible to increase the separation between enantiomers beyond that presented in the final two dimensional chromatographic method in **Figure 2.22** by applying the optimal

conditions for each congener presented in **Table 2.9**. In this way, the enantiomers

of 4-MeSO$_2$-CB149 can be baseline resolved.

A potentially useful application for these enantiomer separations would be

the fractionation and collection of individual enantiomers for structural and

toxicokinetic studies. A strong preference for the accumulation of one enantiomer

over another has been observed in several tissues, but particularly in the liver, of

several organisms, including various species of seal (Chu *et al.* 2003a, Karásek *et

al.* 2007, Larsson *et al.* 2004, Wiberg *et al.* 1998), polar bears (Wiberg *et al.*

1998), and humans (Ellerichmann *et al.* 1998). In addition, it has been

demonstrated that enantioselective metabolism occurs for methyl sulfone PCBs in

rats (Hühnerfuss *et al.* 2003, Norström *et al.* 2006). Differential toxicity of the

enantiomers is therefore of great interest. Enantiomer specific toxicity testing has

not been carried out previously for methyl sulfone PCBs, but it has been shown

that the (+)-enantiomer of PCB 139 is a more potent inducer of aminopyrine *N*-

demethylase, aldrin epoxidase and cytochrome P450 enzymes (CYPs) than the

(-)-enantiomer or a racemic mixture in rat liver (Püttmann *et al.* 1989). Pure

enantiomers would be required to carry out similar studies for methylsulfonyl

PCBs.

Baseline resolution of enantiomers greatly simplifies fractionation by

enantioselective HPLC, as demonstrated for selected PCB congeners separated

using a Nucleodex β-PM column (Haglund 1995, 1996b). When baseline

enantioseparation is not achieved, fractions must typically be collected and re-

injected several times, which is a time consuming process. The present MeSO$_2$-

CB enantioseparations are therefore extremely desirable for the purpose of enantiomer isolation due to the extraordinary resolution achieved. This stationary phase is available in preparative HPLC dimensions, and the large distance between peaks would allow for the column to be overloaded without enantiomer peak overlap for many congeners, which would increase the yield per run and decrease the time required to achieve a desired amount of material (Haglund 1995, 1996b). Another attractive feature of this method is that the mobile phase is quite volatile, which would make switching the solvent for further testing straightforward. Note that the enantiomers of $MeSO_2$-CBs have previously been isolated using reversed phase HPLC on a Nucleodex β-PM column (Pham-Tuan *et al.* 2004, 2005). However, these workers found that the concentration of methyl sulfone PCBs that could be used was limited by the solubility of these compounds in methanol, which was also observed by Haglund (1995 and 1996a) for the isolation of PCB atropisomers. Another advantage of the current method is that the solubility of the $MeSO_2$-CBs is much higher in heptane than in methanol, so higher initial concentrations can be injected, leading to further savings in time.

An interesting phenomenon was observed upon introduction of selected achiral congeners onto the Chiralpak AD-H column in the current work. The compounds 5-$MeSO_2$-CB110 and 3′-$MeSO_2$-CB141, and possibly also 3′-$MeSO_2$-CB87, underwent slow on-column enantiomerization, resulting in two peaks with a plateau in between. Similar phenomena have been described previously for the separation of PCB 40 (Haglund 1996a) and of hindered naphthyl sulfones (Casarini *et al.* 1995, Villani and Pirkle 1995) on other chiral stationary phases.

The distance between the two peaks was observed to decrease and the height of the plateau between them to increase with increasing column temperature. In conjunction with computer modelling, these chromatograms could be used to calculated the enantiomerization barriers for these compounds using the method described by Wolf (2005). Briefly, after collection of chromatograms at various temperatures, computer simulations can be used to model the peaks in order to estimate the enantiomerization rate constant. An Eyring plot can then be produced and the enthalpy and entropy of enantiomerization calculated from the slope and intercept of the curve, respectively. Finally, the Gibbs free energy of enantiomerization can be calculated from these parameters.

The enantiomerization barriers of selected $MeSO_2$-CBs have been calculated previously using quantum calculations (Nezel *et al.* 1997). However, none of the congeners studied were of environmental relevance since they possessed *ortho*-methylsulfonyl substitution. Calculations of enantiomerization barriers for isomers of environmental concern therefore remain to be determined and are of fundamental interest. A nice data set of three chromatograms in which all conditions were kept constant except for temperature, which was varied over a range of 30°C, were acquired over the course of method development for 3′-$MeSO_2$-CB110, and this data is available upon request. In addition, it might be possible to apply this method to other congeners, particularly the ones with di-*ortho* substitution and *meta*-$MeSO_2$ substitution (i.e. 3′-$MeSO_2$-CB49, 3-$MeSO_2$-CB52, and 3′-$MeSO_2$-CB101), if the temperature of the separation can be further decreased. Sub-zero temperatures could be accomplished by submerging the

column in an appropriate solvent-dry ice bath along with approximately one meter of tubing to ensure that the entering mobile phase is equilibrated to the same temperature as the column (Villani and Pirkle 1995). Since the mobile phase used in this separation has a low melting point, there is no concern of it freezing at temperatures as low as -80°C. However, it should be noted that the minimum recommended column temperature is 0°C for Chiralpak AD-H, so it is possible that the stationary phase could be damaged and/or the separation compromised at sub-zero temperatures.

The biggest weakness of this method is that the sensitivity is poor for the majority of the *meta*-substituted congeners. A strategy that could be explored to increase the sensitivity for all compounds, including the *meta*-isomers, would be to experiment with different mixtures of dopants in order to improve ionization with either the krypton or the argon lamp. It has been demonstrated that the use of mixed dopants can lead to improved sensitivity compared to pure dopants. For example, a mixed dopant composed of 99.5:0.5 toluene:anisole gave superior results to either solvent alone for the analysis of PAHs using a krypton lamp (Itoh *et al.* 2006). In the present work, anisole led to an increase in ionization over the no dopant case, although not as significant as toluene. It is therefore possible that a mixture of anisole and toluene could be beneficial for the ionization of MeSO$_2$-CBs by APPI, particularly with the use of a krypton lamp and with a reversed phase solvent system.

Hybrid linear ion trap scans were investigated in an effort to improve the overall sensitivity. Although enhanced product ion scanning produced increased

signal-to-noise ratios for several congeners, the fragmentation efficiency for the *meta* congeners was still much lower than that of the *para* congeners. It is possible that the *meta* fragment ions are less stable and therefore lost more easily due to dissipation. One potential solution to this problem could be to change the excitation $q$-value during hybrid linear ion trap scanning. The $q$-value is typically set to a default value of 0.23 for the MS3 function in Analyst software, but it is possible to create a script to allow it to be changed by the user. This technique was applied to the quantitative analysis of clenbuterol in urine by researchers at Applied Biosystems/MDS Sciex, and they found that increased fragmentation efficiency could be achieved with decreased fragmentation time by increasing the $q$-value (Guna *et al.*). This strategy is particularly effective for compounds with optimal collision energies in excess of 35 eV during MRM scanning, as they tend to fragment less efficiently. Other than the hepta-chlorinated congeners, the optimal collision energy was equal to or greater than 35 eV for all of the target $MeSO_2$-CBs in this study. The authors also found that employing a higher $q$-value improved confinement of the fragment ions within the trap leading to an increase in sensitivity. It is possible that this could also help remediate the excessive noise that was problematic with the ion trap scans in the present work.

Application of this method to the analysis of sledge dog plasma and adipose tissue samples revealed some similarities and some differences in the congener patterns, concentrations and EFs of methyl sulfone PCBs compared to polar bears. There are a number of factors that are known to influence the accumulation of organic contaminants, including age, sex, diet, and metabolic

capacity, among others (Verreault *et al.* 2009a). These could have played a role in the observed differences between species, particularly since the since the latter two factors are difficult to determine for wild-caught polar bears. That being said, the sample size in the sledge dog study was quite small, and increasing the number of individuals would give more confidence in the results of these comparisons.

Two generations of offspring were incorporated into the sledge dog study design (Verreault *et al.* 2009a), however, it was not known which pups belonged to which generation for the current work. Knowing this information might make it possible to draw some conclusions with regards to maternal transfer of $MeSO_2$-CBs in sledge dogs. Grouping all of the pups together led to similar congener patterns compared to the mothers. While the mature pups would be expected to display a similar congener pattern to their mothers since they received the same diet post-weaning, this is not necessarily the case for the pre-weaning pups. Verreault and colleagues (2009a) found that the PCB congener patterns differed between the F1-MLK pups and their mothers, but not between the F1 pups and their mothers. On the other hand, non-selective maternal transfer has been indicated in studies of methyl sulfone PCBs in humans and mink, respectively (Linderholm *et al.* 2007, Lund *et al.* 1999). This would be an interesting point to resolve in future sledge dog investigations.

In the current work, only the adipose tissue and plasma of the sledge dogs were examined. However, there are a number of other tissues where methyl sulfone PCB metabolites accumulate and that would be useful to compare

221

between polar bears and sledge dogs. For example, the liver is known to be an important site of accumulation in polar bears (Gebbink *et al.* 2008a, Gebbink *et al.* 2008b). It is also a site of significant enantioselective and regioselective retention in several organisms (Chu *et al.* 2003a, Ellerichmann *et al.* 1998, Larsson *et al.* 2004). An interesting characteristic of polar bear physiology is that their livers contain abundant Ito cells, which function in the storage of vitamin A from their high fat diets (Gebbink *et al.* 2008a). It has been suggested that these cells may play a role in the accumulation of $MeSO_2$-CBs in polar bear liver (Letcher *et al.* 2000). This could be an important physiological difference between polar bears and sledge dogs that could lead to differences in the metabolism and accumulation of methyl sulfone PCBs. The lungs are another important tissue for methyl sulfone PCB accumulation, although these contaminants have not been measured in polar bear or sledge dog lungs to date. In humans, respiratory symptoms have been linked to methyl sulfone PCB toxicity in Yusho patients (Brandt and Bergman 1987). Whereas many organic contaminants have effects on immunity and on the levels and activities of drug-metabolizing enzymes, which have been examined previously in the context of the larger sledge dog study (Sonne *et al.* 2006a, Sonne *et al.* 2007, Verreault *et al.* 2009b, Verreault *et al.* 2009c), respiratory function may be a selective indicator of methyl sulfone PCB toxicity and would be worthwhile to investigate in these dogs.

# 3    Appendices

<u>Appendix A</u>: **Relative response factors for MeSO$_2$-CB analysis by LC-LC-APPI-MS-MS**

| Congener | Relative Response Factor (x10$^{-3}$) |
|---|---|
| 3'-49 | 0.006 |
| 4'-49 | 0.216 |
| 4-52 | 0.346 |
| 3-52 + 4-64 | 0.740 |
| 3-70 | 0.364 |
| 4-70 | 0.604 |
| 3'-87 + 4-110 | 0.804 |
| 4'-87 | 0.198 |
| E1+E2 5-91 | 0.354 |
| E1 4-91 | 0.574 |
| E2 4-91 | 0.570 |
| E1 3'-95 | 0.010 |
| E2 3'-95 | 0.010 |
| E1 4'-95 | 0.140 |
| E2 4'-95 | 0.156 |
| 3'-101 | 0.012 |
| 4'-101 | 0.498 |
| 5-110 | 0.328 |
| E1 4'-132 | 0.458 |
| E2 4'-132 | 0.468 |
| 3'-141 | 0.026 |
| 4'-141 | 0.614 |
| E1 4-149 | 0.412 |
| E2 4-149 | 0.452 |
| E1 4'-174 | 0.140 |
| E2 4'-174 | 0.168 |

## Appendix B1: Concentrations of MeSO$_2$-CBs in control adult sledge dog fat samples

*ND: Not Detected. Concentrations in italics are below the limit of quantitation and excluded from the sum concentration of MeSO$_2$-CBs.*

| Congener | Concentration (ng/g wet weight) | | | | | |
|---|---|---|---|---|---|---|
| | SDF 1 | SDF 2 | SDF 3 | SDF 8 | SDF 16 | SDF 20 |
| 4′-49 | ND | ND | ND | ND | ND | 5.6 ± 1.4 |
| 4-52 | ND | ND | ND | ND | ND | 6.6 ± 1.5 |
| 3-52 + 4-64 | ND | ND | ND | ND | ND | 9.0 ± 2.1 |
| 3-70 | ND | ND | ND | ND | ND | 7.7 ± 1.8 |
| 4-70 | ND | ND | ND | ND | ND | 10.4 ± 2.4 |
| 3′-87 + 4-110 | ND | ND | ND | ND | ND | 9.3 ± 2.2 |
| 4′-87 | ND | ND | ND | ND | ND | *3.61 ± 0.99* |
| E1+E2  5-91 | ND | ND | ND | ND | ND | ND |
| E1 4-91 | ND | ND | ND | ND | ND | ND |
| E2 4-91 | ND | ND | ND | ND | ND | ND |
| E1 4′-95 | ND | ND | ND | ND | ND | ND |
| E2 4′-95 | ND | ND | ND | ND | ND | ND |
| 4′-101 | ND | ND | ND | ND | ND | 7.0 ± 1.8 |
| 5-110 | ND | ND | ND | ND | ND | 6.6 ± 1.4 |
| E1 4′-132 | ND | ND | ND | ND | ND | ND |
| E2 4′-132 | ND | ND | ND | ND | ND | ND |
| 3′-141 | ND | ND | ND | ND | ND | ND |
| 4′-141 | ND | ND | ND | ND | ND | ND |
| E1 4-149 | ND | ND | ND | ND | ND | 9.3 ± 2.2 |
| E2 4-149 | ND | ND | ND | ND | ND | 8.0 ± 2.0 |
| E1 4′-174 | ND | ND | ND | ND | ND | ND |
| E2 4′-174 | ND | ND | ND | ND | ND | ND |
| Σ MeSO$_2$-CBs | ND | ND | ND | ND | ND | 79.4 ± 6.0 |
| *Sample mass (g)* | 1.60 | 1.60 | 1.69 | 1.49 | 1.61 | 1.59 |
| *% lipid* | 89.3 | 84.9 | 87.9 | 80.4 | 92.4 | 91.0 |

## Appendix B2: Concentrations of MeSO$_2$-CBs in control pup sledge dog fat samples

*ND: Not Detected. Concentrations in italics are below the limit of quantitation and excluded from the sum concentration of MeSO$_2$-CBs.*

| Congener | Concentration (ng/g wet weight) | | | | | | | | | |
| --- | --- | --- | --- | --- | --- | --- | --- | --- | --- | --- |
| | SDF 26 | SDF 29 | SDF 30 | SDF 31 | SDF 33 | SDF 34 | SDF 36 | SDF 37 | SDF 38 | SDF 39 |
| 4′-49 | 8.8 ± 2.2 | ND | 6.3 ± 1.6 | ND | 4.8 ± 1.2 | ND | ND | ND | ND | ND |
| 4-52 | 10.0 ± 2.2 | ND | 8.2 ± 1.8 | ND | 6.7 ± 1.5 | ND | ND | ND | ND | ND |
| 3-52 + 4-64 | 13.3 ± 3.1 | ND | 7.7 ± 1.8 | ND | 8.1 ± 1.9 | ND | ND | ND | ND | ND |
| 3-70 | 8.5 ± 2.0 | ND | 9.5 ± 2.2 | ND | 7.4 ± 1.7 | ND | ND | ND | ND | ND |
| 4-70 | 12.9 ± 2.9 | ND | 14.2 ± 3.2 | ND | 10.2 ± 2.3 | ND | ND | ND | ND | ND |
| 3′-87 + 4-110 | 10.9 ± 2.6 | ND | 10.2 ± 2.4 | ND | 9.5 ± 2.2 | ND | ND | ND | ND | ND |
| 4′-87 | *6.3 ± 1.6* | ND | 5.1 ± 1.3 | ND | 6.5 ± 1.7 | ND | ND | ND | ND | ND |
| E1+E2 5-91 | ND | ND | ND | ND | ND | ND | ND | ND | ND | ND |
| E1 4-91 | ND | ND | ND | ND | ND | ND | ND | ND | ND | ND |
| E2 4-91 | ND | ND | ND | ND | ND | ND | ND | ND | ND | ND |
| E1 4′-95 | ND | ND | ND | ND | ND | ND | ND | ND | ND | ND |
| E2 4′-95 | ND | ND | ND | ND | ND | ND | ND | ND | ND | ND |
| 4′-101 | 8.3 ± 2.1 | ND | 6.7 ± 1.7 | ND | 6.4 ± 1.6 | ND | ND | ND | ND | ND |
| 5-110 | 11.6 ± 2.5 | ND | 7.1 ± 1.5 | ND | 6.8 ± 1.5 | ND | ND | ND | ND | ND |
| E1 4′-132 | ND | ND | ND | ND | ND | ND | ND | ND | ND | ND |
| E2 4′-132 | 7.5 ± 1.7 | ND | ND | ND | *1.09 ± 0.26* | ND | ND | ND | ND | ND |
| 3′-141 | ND | ND | ND | ND | ND | ND | ND | ND | ND | ND |
| 4′-141 | ND | ND | ND | ND | ND | ND | ND | ND | ND | ND |
| E1 4-149 | 12.1 ± 2.8 | ND | 8.4 ± 2.0 | ND | 8.7 ± 2.0 | ND | ND | ND | ND | ND |
| E2 4-149 | 9.0 ± 2.2 | ND | 7.5 ± 1.9 | ND | 7.5 ± 1.9 | ND | ND | ND | ND | ND |
| E1 4′-174 | ND | ND | ND | ND | ND | ND | ND | ND | ND | ND |
| E2 4′-174 | ND | ND | ND | ND | ND | ND | ND | ND | ND | ND |
| Σ MeSO$_2$-CBs | 113.0 ± 8.0 | ND | 91.0 ± 6.7 | ND | 82.6 ± 6.0 | ND | ND | ND | ND | ND |
| *Sample mass (g)* | 1.59 | 1.54 | 1.45 | 1.50 | 1.54 | 1.34 | 1.58 | 1.63 | 1.56 | 1.52 |
| *% lipid* | 81.8 | 80.3 | 75.8 | 76.0 | 78.3 | 81.1 | 80.2 | 82.4 | 85.0 | 82.6 |

## Appendix B3: Concentrations of MeSO$_2$-CBs in exposed adult sledge dog fat samples

*ND: Not Detected. Concentrations in italics are below the limit of quantitation and excluded from the sum concentration of MeSO$_2$-CBs.*

| Congener | Concentration (ng/g wet weight) | | | | |
|---|---|---|---|---|---|
| | SDF 4 | SDF 12 | SDF 14 | SDF 15 | SDF 22 |
| 4′-49 | 6.5 ± 1.6 | ND | *3.70 ± 0.91* | *3.22 ± 0.79* | 12.4 ± 3.1 |
| 4-52 | ND | ND | ND | ND | 18.8 ± 4.1 |
| 3-52 + 4-64 | 9.9 ± 2.4 | 4.6 ± 1.1 | 3.94 ± 0.92 | 5.4 ± 1.26 | 70 ± 16 |
| 3-70 | 10.7 ± 2.5 | 8.2 ± 1.9 | 6.2 ± 1.5 | 8.1 ± 1.9 | 25.2 ± 5.9 |
| 4-70 | 11.1 ± 2.9 | 13.7 ± 3.1 | 9.7 ± 2.2 | 9.3 ± 2.1 | 60 ± 14 |
| 3′-87 + 4-110 | 12.2 ± 1.5 | 10.6 ± 2.5 | 7.3 ± 1.7 | 13.3 ± 3.1 | 68 ± 16 |
| 4′-87 | *5.9 ± 1.5* | *5.9 ± 1.5* | ND | *7.0 ± 1.8* | *9.7 ± 2.5* |
| E1+E2 5-91 | ND | ND | ND | ND | ND |
| E1 4-91 | *2.17 ± 0.57* | *1.83 ± 0.48* | ND | ND | *3.77 ± 0.99* |
| E2 4-91 | ND | ND | ND | ND | ND |
| E1 4′-95 | ND | ND | ND | ND | ND |
| E2 4′-95 | ND | ND | ND | ND | ND |
| 4′-101 | 23.9 ± 6.1 | 11.1 ± 2.8 | 9.8 ± 2.5 | 14.5 ± 3.7 | 73 ± 18 |
| 5-110 | ND | *1.84 ± 0.40* | ND | *1.75 ± 0.38* | 12.5 ± 2.7 |
| E1 4′-132 | ND | *2.84 ± 0.77* | ND | ND | ND |
| E2 4′-132 | 7.8 ± 1.8 | *2.26 ± 0.53* | *4.3 ± 1.0* | 7.5 ± 1.8 | 15.7 ± 3.7 |
| 3′-141 | *27.5 ± 6.0* | *26.5 ± 5.9* | ND | 38.4 ± 8.4 | *1.89 ± 0.41* |
| 4′-141 | ND | ND | ND | ND | ND |
| E1 4-149 | *5.3 ± 1.2* | *2.30 ± 0.54* | ND | *3.35 ± 0.80* | 28.0 ± 6.6 |
| E2 4-149 | ND | ND | ND | ND | 24.4 ± 6.0 |
| E1 4′-174 | ND | ND | ND | ND | ND |
| E2 4′-174 | ND | ND | ND | ND | ND |
| Σ MeSO$_2$-CBs | 82.1 ± 8.3 | 48.2 ± 5.4 | 36.9 ± 4.1 | 96.4 ± 10.3 | 407 ± 34 |
| *Sample mass (g)* | 1.59 | 1.48 | 1.54 | 1.54 | 1.59 |
| *% lipid* | 82.3 | 93.1 | 91.9 | 84.3 | 75.4 |

## Appendix B4: Concentrations of MeSO$_2$-CBs in exposed pup sledge dog fat samples

*ND: Not Detected. Concentrations in italics are below the limit of quantitation and excluded from the sum concentration of MeSO$_2$-CBs.*

| Congener | Concentration (ng/g wet weight) | | | |
| --- | --- | --- | --- | --- |
| | SDF 25 | SDF 28 | SDF 32 | SDF 35 |
| 4′-49 | *3.82 ± 0.94* | 3.30 ± 0.81 | 9.6 ± 2.4 | 9.2 ± 2.3 |
| 4-52 | ND | ND | 8.9 ± 2.0 | 11.4 ± 2.5 |
| 3-52 + 4-64 | 4.5 ± 1.1 | 4.08 ± 0.95 | 13.8 ± 3.2 | 14.1 ± 3.3 |
| 3-70 | 5.2 ± 1.2 | 5.8 ± 1.4 | 15.2 ± 3.6 | 13.2 ± 3.1 |
| 4-70 | 9.5 ± 2.2 | 8.6 ± 2.0 | 20.7 ± 4.7 | 20.2 ± 4.6 |
| 3′-87 + 4-110 | 9.2 ± 2.2 | 8.6 ± 2.0 | 18.8 ± 4.4 | 16.5 ± 3.9 |
| 4′-87 | *4.2 ± 1.1* | 4.28 ± 0.82 | *7.9 ± 2.1* | *13.7 ± 3.6* |
| E1+E2 5-91 | ND | ND | ND | ND |
| E1 4-91 | *1.76 ± 0.46* | 1.75 ± 0.46 | *1.82 ± 0.48* | ND |
| E2 4-91 | ND | ND | ND | ND |
| E1 4′-95 | ND | ND | ND | ND |
| E2 4′-95 | ND | ND | ND | ND |
| 4′-101 | 9.1 ± 2.3 | 8.1 ± 2.1 | 17.8 ± 4.5 | 11.1 ± 2.8 |
| 5-110 | ND | *1.00 ± 0.22* | 9.8 ± 2.1 | 7.7 ± 1.7 |
| E1 4′-132 | *1.63 ± 0.44* | *1.21 ± 0.33* | ND | ND |
| E2 4′-132 | *4.08 ± 0.96* | 3.35 ± 0.79 | 4.6 ± 1.1 | *2.35 ± 0.55* |
| 3′-141 | ND | 19.4 ± 4.2 | ND | ND |
| 4′-141 | ND | ND | ND | ND |
| E1 4-149 | *2.16 ± 0.51* | 2.28 ± 0.54 | 11.0 ± 2.6 | 14.0 ± 3.3 |
| E2 4-149 | *2.68 ± 0.66* | ND | 8.6 ± 2.1 | 12.0 ± 2.9 |
| E1 4′-174 | ND | ND | ND | ND |
| E2 4′-174 | ND | ND | ND | ND |
| Σ MeSO$_2$-CBs | 37.5 ± 4.2 | 69.6 ± 6.0 | 139 ± 10 | 129.3 ± 9.9 |
| *Sample mass (g)* | 1.55 | 1.51 | 1.36 | 1.01 |
| *% lipid* | 76.7 | 68.6 | 72.1 | 86.5 |

## Appendix C: Representative sledge dog fat sample chromatogram

*Sledge dog fat sample 22. Cosmosil 5-PYE connected in series with Chiralpak AD-H. Isocratic elution: 95:2.5:2.5 heptanes:methanol:ethanol. Flow rate 1.0 mL/min, temperature 12.5°C, 20 μL injection of sample dissolved in heptane. Diverter valve program: 0-14.6 min, position A; 14.6-23.8 min, position B; 23.8-91 min, position A. Extracted ion chromatograms. IS: internal standard, 3-MeSO$_2$-4-Me-2',3',4',5,5'-pentachlorobiphenyl.*
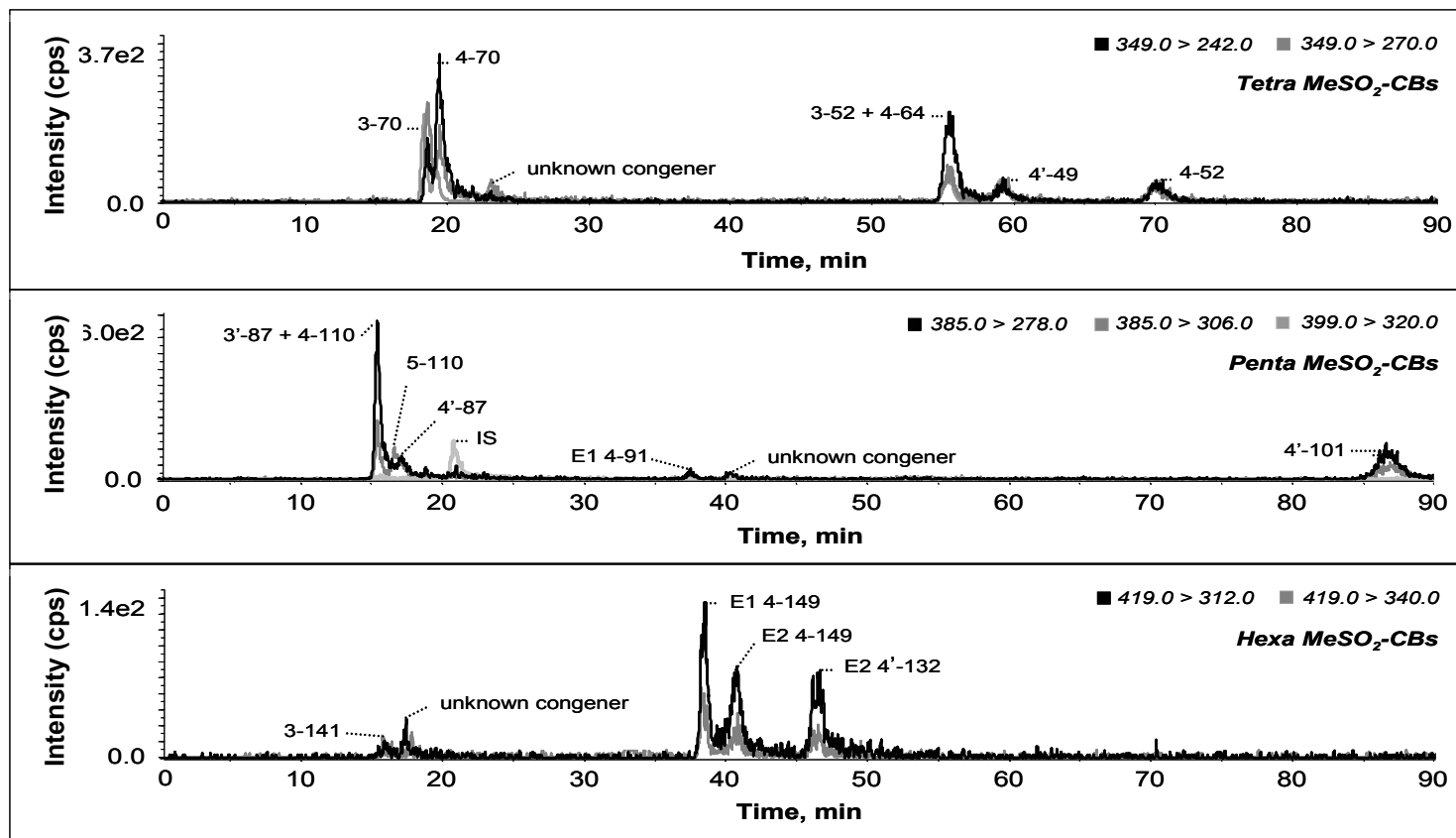
**Appendix D:** Enantiomer fractions of chiral $MeSO_2$-CB congeners detected in sledge dog fat samples

*For EFs very near 0 or 1, one enantiomer was not detected, and its concentration was taken to be the limit of detection.*
*[a] Average of duplicate measurements.*

| Exposure Group | Sample | Congener Enantiomer Fraction | | |
|---|---|---|---|---|
| | | 4-91 | 4-132 | 4-149 |
| Control Pups | SDF 26 | - | 0.004[a] | 0.558[a] |
| | SDF 30 | - | - | 0.529 |
| | SDF 33 | - | - | 0.536 |
| | SDF 34 | - | - | 0.542 |
| | SDF 36 | - | - | 0.525 |
| | SDF 37 | - | - | 0.545 |
| | SDF 38 | - | - | 0.522 |
| | SDF 39 | - | - | 0.567 |
| Exposed Pups | SDF 28 | 0.989 | - | 0.989 |
| | SDF 32 | - | 0.006 | 0.562 |
| | SDF 35 | - | - | 0.539 |
| Control Adult | SDF 20 | - | - | 0.537 |
| Exposed Adults | SDF 4 | - | 0.003 | - |
| | SDF 15 | - | 0.003 | 0.534 |
| | SDF 22 | - | 0.001 | - |

## 4        References

Afonso, C., Riu, A., Xu, Y., Fournier, F., and Tabet, J.-C., **2005**, "Structural characterization of fatty acids cationized with copper by electrospray ionization mass spectrometry under low-energy collision-induced dissociation", *Journal of Mass Spectrometry*, 40: 342-349.

Agency for Toxic Substances and Disease Registry, **2000**,*Toxicological Profile for Polychlorinated Biphenyls (PCBs)*, Department of Health and Human Services, Division of Toxicology/Toxicological Information Branch, Atlanta, GA, USA.

Annesley, T.M., **2003**, "Ion suppression in mass spectrometry", *Clinical Chemistry*, 49(*7*): 1041-1044.

Antignac, J.-P., de Wasch, K., Monteau, F., De Brabander, H., Andre, F., and Le Bizec, B., **2005**, "The ion suppression phenomenon in liquid chromatography-mass spectrometry and its consequences in the field of residue analysis", *Analytica Chimica Acta*, 529: 129-136.

Ariyoshi, N., Koga, N., Oguri, K., and Yoshimura, H., **1992**, "Metabolism of 2,4,5,2',4',5'-hexachlorobiphenyl with liver microsomes of phenobarbital-treated dog; the possible formation of PCB 2,3-arene oxide intermediate", *Xenobiotica*, 22(*11*): 1275-1290.

Ariyoshi, N., Yoshimura, H., and Oguri, K., **1993**, "Identification of *in vitro* metabolites of 2,4,6,2',4',6'-hexachlorobiphenyl from phenobarbital-treated dog liver microsomes", *Biological & Pharmaceutical Bulletin*, 16: 852-857.

Asher, B.J., D'Agostino, L.A., Way, J.D., Wong, C.S., and Harynuk, J.J., **2009**, "Comparison of peak integration methods for the determination of enantiomer fraction in environmental samples", *Chemosphere*, 75: 1042-1048.

Baarschers, W.H., and Krupay, B.W., **1973**, "Mass spectra of some sulfinate esters and sulfones", *Canadian Journal of Chemistry*, 51: 156-161.

Bakke, J.E., Bergman, Å., and Larsen, G.L., **1982**, "Metabolism of 2,4',5-trichlorobiphenyl by the mercapturic acid pathway", *Science*, 217(*4560*): 645-647.

Ballschmiter, K., and Zell, M., **1980**, "Analysis of polychlorinated biphenyls (PCBs) by glass capillary gas chromatography", *Fresenius Zeitschrift für Analytische Chemie*, 302: 20-31.

Balmér, K., Lagerström, P.-O., Persson, B.-A., and Schill, G., **1992**, "Reversed retention order and other stereoselective effects in the separation of amino alcohols on Chiralcel OD", *Journal of Chromatography*, 592: 331-337.

Basso, E., Marotta, E., Seraglia, R., Tubaro, M., and Traldi, P., **2003**, "On the formation of negative ions in atmospheric pressure photoionization conditions", *Journal of Mass Spectrometry*, 38: 1113-1115.

Berger, U., Herzke, D., and Sandanger, T.M., **2004**, "Two trace analytical methods for determination of hydroxylated PCBs and other halogenated phenolic compounds in eggs from Norwegian birds of prey", *Analytical Chemistry*, 76: 441-452.

Bergman, Å., Biessmann, A., Brandt, I., and Rafter, J., **1982a**, "Metabolism of 2,4',5-trichlorobiphenyl: Role of the intestinal microflora in the formation of bronchial-seeking methyl sulphone metabolites in mice", *Chemico-Biological Interactions*, 40: 123-131.

Bergman, Å., Brandt, I., Darnerud, P.O., and Wachtmeister, C.A., **1982b**, "Metabolism 2,2',5,5'-tetrachlorobiphenyl: Formation of mono- and bis-methyl sulphone metabolites with a selective affinity for the lung and kidney tissues in mice", *Xenobiotica*, 12(*1*): 1-17.

Bergman, Å., Brandt, I., Larsson, Y., and Wachtmeister, C.A., **1980a**, "Cysteine and methionine - Precursors of methyl sulphone metabolites of 2,4',5-trichlorobiphenyl in mice", *Chemico-Biological Interactions*, 31: 65-71.

Bergman, Å., Jansson, B., and Bamford, I., **1980b**, "Methylthio- and methylsulfonylpolychlorobiphenyls: Synthesis and studies of correlations between structure and fragmentation pattern on electron impact", *Biomedical Mass Spectrometry*, 7: 20-27.

Bos, S.J., van Leeuwen, S.M., and Karst, U., **2006**, "From fundamentals to applications: recent developments in atmospheric pressure photoionization mass spectrometry", *Analytical and Bioanalytical Chemistry*, 384: 85-99.

Bowie, J.H., and Stringer, M.B., **1985**, "Collision-induced dissociation of negative ions in the gas phase: [Aryl S]$^-$, [Aryl SO]$^-$ and [Aryl SO$_2$]$^-$", *Organic Mass Spectrometry*, 20(*2*): 138-142.

Brandt, I., and Bergman, Å., **1987**, "PCB methyl sulfones and related compounds: Identification of target cells and tissues in different species", *Chemosphere*, 16(*8/9*): 1671-1676.

Brandt, I., Bergman, Å., and Wachtmeister, C.A., **1976**, "Distribution of polychlorinated biphenyls: Structural requirements for accumulation in the mouse bronchial mucosa", *Experientia*, 32(*4*): 497-498.

Brandt, I., Darnerud, P.O., Bergman, Å., and Larsson, Y., **1982**, "Metabolism of 2,4',5-trichlorobiphenyl: Enrichment of hydroxylated and methyl sulphone metabolites in the uterine luminal fluid of pregnant mice", *Chemico-Biological Interactions*, 40: 45-56.

Brandt, I., Lund, J., Bergman, Å., Klasson-Wehler, E., Poellinger, L., and Gustafsson, J.-Å., **1985**, "Target cells for the polychlorinated biphenyl metabolite 4,4'-bis(methylsulfonyl)-2,2',5,5'-tetrachlorobiphenyl in lung and kidney", *Drug Metabolism and Disposition*, 13(*4*): 490-496.

Brodsky, J., and Ballschmiter, K., **1988**, "Reversed phase liquid chromatography of PCBs as a basis for the calculation of water solubility and log $K_{ow}$ for polychlorobiphenyls", *Fresenius Zeitschrift für Analytische Chemie*, 331: 295-301.

Brodsky, J., and Ballschmiter, K., **1989**, "Separation of polychlorinated benzenes (PCBzs) and biphenyls (PCBs) by reversed phase-liquid chromatography", *Fresenius Zeitschrift für Analytische Chemie*, 335: 817-825.

Bründl, A., and Buff, K., **1993**, "Partial purification and characterization of a rat liver polychlorinated biphenyl (PCB) binding protein", *Biochemical Pharmacology*, 45(*4*): 885-891.

Buser, H.-R., Zook, D.R., and Rappe, C., **1992**, "Determination of methyl sulfone-substituted polychlorobiphenyls by mass spectrometric techniques with application to environmental samples", *Analytical Chemistry*, 64: 1176-1183.

Cabrera, K., Jung, M., Fluck, M., and Schurig, V., **1996**, "Determination of enantiomerization barriers by computer simulation of experimental elution profiles obtained by high-performance liquid chromatography on a chiral stationary phase", *Journal of Chromatography A*, 731: 315-321.

Cai, S.-S., Hanold, K.A., and Syage, J.A., **2007a**, "Comparison of atmospheric pressure photoionization and atmospheric pressure chemical ionization for normal-phase LC/MS chiral analysis of pharmaceuticals", *Analytical Chemistry*, 79: 2491-2498.

Cai, S.-S., Short, L.C., Syage, J.A., Potvin, M., and Curtis, J.M., **2007b**, "Liquid chromatography-atmospheric pressure photoionization-mass spectrometry analysis of triacylglycerol lipids - Effects of mobile phases on sensitivity", *Journal of Chromatography A*, 1173: 88-97.

Cai, S.-S., and Syage, J.A., **2006**, "Atmospheric pressure photoionization mass spectrometry for analysis of fatty acid and acylglycerol lipids", *Journal of Chromatography A*, 1110: 15-26.

Cai, Y.X., Herold, D., McConnell, O., and Bach, A.C., **2005**, "THF as a new dopant for atmospheric pressure photoionization mass spectrometry and comparison to other existing dopants", *Abstracts of Papers of the American Chemical Society*, Abstract no. 229, p. U126.

Carroll, D.I., Dzidic, I., Horning, E.C., and Stillwell, R.N., **1981**, "Atmospheric Pressure Ionization Mass Spectrometry", *Applied Spectroscopy Reviews*, 17(*3*): 337-406.

Casarini, D., Lunazzi, L., Alcaro, S., Gasparrini, F., and Villani, C., **1995**, "Atropisomerism in hindered naphthyl sulfones investigated by dynamic NMR and dynamic HPLC techniques", *Journal of Organic Chemistry*, 60: 5515-5519.

Cass, Q.B., Lima, V.V., Oliveira, R.V., Cassiano, N.M., Degani, A.L.G., and Pedrazzoli, J.J., **2003**, "Enantiomeric determination of the plasma levels of omeprazole by direct plasma injection using high-performance liquid chromatography with achiral-chiral column-switching", *Journal of Chromatography B*, 798: 275-281.

Chen, J., Korfmacher, W.A., and Hsieh, Y., **2005**, "Chiral liquid chromatography-tandem mass spectrometric methods for stereoisomeric pharmaceutical determinations", *Journal of Chromatography B*, 820: 1-8.

Chiral Technologies Inc., **2001**, *Chiralpak AD-H Instruction Sheet*, West Chester, PA, USA.

Chu, S., Covaci, A., Haraguchi, K., and Schepens, P., **2002**, "Optimized separation and determination of methyl sulfone metabolites of polychlorinated biphenyls (PCBs) and p,p'-DDE in biota samples", *The Analyst*, 127: 1621-1626.

Chu, S., Covaci, A., Haraguchi, K., Voorspoels, S., van de Vijver, K., Das, K., Bouquegneau, J.-M., de Coen, W., Blust, R., and Schepens, P., **2003a**, "Levels and enantiomeric signatures of methyl sulfonyl PCB and DDE metabolites in livers of harbor porpoises (*Phocoena phocoena*) from the Southern North Sea", *Environmental Science & Technology*, 37: 4573-4578.

233

Chu, S., Covaci, A., Jacobs, W., Haraguchi, K., and Schepens, P., **2003b**, "Distribution of methyl sulfone metabolites of polychlorinated biphenyls and *p,p*'-DDE in human tissues", *Environmental Health Perspectives*, 111(*9*): 1222-1227.

Chu, S., Covaci, A., Van de Vijver, K., De Coen, W., Blust, R., and Schepens, P., **2003c**, "Enantiomeric signatures of chiral polychlorinated biphenyls atropisomers in liver of harbour porpoises (*Phocoena phocoena*) from the southern North Sea", *Journal of Environmental Monitoring*, 5: 521-526.

Chu, S., and Letcher, R.J., **2008**, "Analysis of fluorotelomer alcohols and perfluorinated sulfonamides in biotic samples by liquid chromatography-atmospheric pressure photoionization mass spectrometry", *Journal of Chromatography A*, 1215: 92-99.

Commission of the European Communities, The, **2002**, Decision 2002/657/EC: "Commission decision of 12 August 2002 implementing Council Directive 96/23/EC concerning the performance of analytical methods and the interpretation of results"; *Official Journal of the European Communities*, L 221: 8-36.

Concejero, M., Ramos, L., Jiménez, B., Gómara, B., Abad, E., Rivera, J., and González, M.J., **2001**, "Suitability of several carbon sorbents for the fractionation of various sub-groups of toxic polychlorinated biphenyls, polychlorinated dibenzo-*p*-dioxins and polychlorinated dibenzofurans", *Journal of Chromatography A*, 97: 227-237.

Covaci, A., Chu, S., Haraguchi, K., and Schepens, P., **2003**, "Distribution of methylsulfone metabolites of polychlorinated biphenyls and p,p'-DDE in human tissues", *Organohalogen Compounds*, 64: 45-48.

Creaser, C., and Al-Haddad, A., **1989**, "Fractionation of polychlorinated biphenyls, polychlorinated dibenzo-*p*-dioxins, and polychlorinated dibenzofurans on porous graphitic carbon", *Analytical Chemistry*, 61: 1300-1302.

D'Acquarica, I., Gasparrini, F., Pierini, M., Villani, C., and Zappia, G., **2006**, "Dynamic HPLC on chiral stationary phases: A powerful tool for the investigation of stereomutation processes", *Journal of Separation Science*, 29: 1508-1516.

Darnerud, P.O., Brandt, I., Klasson-Wehler, E., Bergman, Å., D'Argy, R., Dencker, L., and Sperber, G.O., **1986**, "3,3',4,4'-Tetrachloro[14C]biphenyl in pregnant mice: Enrichment of phenol and methyl sulphone metabolites in late gestational fetuses", *Xenobiotica*, 16(*4*): 295-306.

Davankov, V., **2006**, "Chirality as an inherent general property of matter", *Chirality*, 18: 459-461.

de Voogt, P., van Raat, P., and Rozemeijer, M., **1996**, "Methyl sulfonyl PCBs in cormorant chicks from The Netherlands", *Organohalogen Compounds*, 28: 517-521.

Debrauwer, L., Riu, A., Jouahri, M., Rathahao, E., Jouanin, I., Antignac, J.-P., Cariou, R., Le Bizec, B., and Zalko, D., **2005**, "Probing new approaches using atmospheric pressure photo ionization for the analysis of brominated flame retardants and their related degradation products by liquid chromatography-mass spectrometry", *Journal of Chromatography A*, 1082: 98-109.

Dietz, R., Riget, F.F., Sonne, C., Letcher, R.J., Born, E.W., and Muir, D.C.G., **2004**, "Seasonal and temporal trends in polychlorinated biphenyls and organochlorine pesticides in East Greenland polar bears (*Ursus maritimus*), 1990-2001", *Science of the Total Environment*, 331: 107-124.

Döbler, J., Peters, N., Larsson, C., Bergman, Å., Geidel, E., and Hühnerfuss, H., **2002**, "The absolute structures of separated PCB-methylsulfone enantiomers determined by vibrational circular dichroism and quantum chemical calculations", *Journal of Molecular Structure (Theochem)*, 586: 159-166.

Dzidic, I., Carroll, D.I., Stillwell, R.N., and Horning, E.C., **1975**, "Atmospheric pressure ionization (API) mass spectrometry: Formation of phenoxide ions from chlorinated aromatic compounds", *Analytical Chemistry*, 47(*8*): 1308-1312.

Eliel, E.L., and Wilen, S.H., **1994**, *Stereochemistry of Organic Compounds*, John Wiley & Sons, Inc., Hoboken, NJ, USA.

Ellerichmann, T., Bergman, Å., Franke, S., Hühnerfuss, H., Jakobsson, E., König, W.A., and Larsson, C., **1998**, "Gas chromatographic enantiomer separations of chiral PCB methyl sulfons and identification of selectively retained enantiomers in human liver", *Fresenius Environmental Bulletin*, 7: 244-257.

Euerby, M.R., and Petersson, P., **2003**, "Chromatographic classification and comparison of commercially available reversed-phase liquid chromatographic columns using principal component analysis", *Journal of Chromatography A*, 994: 13-36.

Fisk, A.T., de Wit, C.A., Waylan, M., Kuzyk, Z.Z., Burgess, N., Letcher, R., Braune, B., Norstrom, R., Polischuk Blum, S., Sandau, C., Lie, E., Larsen, H.J.S., Skaare, J.U., and Muir, D.C.G., **2005**, "An assessment of the toxicological significance of anthropogenic contaminants in Canadian arctic wildlife", *The Science of the Total Environment*, 351-352: 57-93.

Gaffney, M.H., Stiffin, R.M., and Wainer, I.W., **1989**, "The effect of alcoholic mobile phase modifiers on retention and stereoselectivity on a commercially available cellulose-based HPLC chiral stationary phase: An unexpected reversal in enantiomeric elution order", *Chromatographia*, 27(*1/2*): 15-18.

Gangl, E.T., Annan, M., Spooner, N., and Vouros, P., **2001**, "Reduction of signal suppression effects in ESI-MS using a nanosplitting device", *Analytical Chemistry*, 73: 5635-5644.

Gebbink, W.A., Sonne, C., Dietz, R., Kirkegaard, M., Born, E.W., Muir, D.C.G., and Letcher, R.J., **2008a**, "Target tissue selectivity and burdens of diverse classes of brominated and chlorinated contaminants in polar bears (*Ursus maritimus*) from East Greenland", *Environmental Science & Technology*, 42: 752-759.

Gebbink, W.A., Sonne, C., Dietz, R., Kirkegaard, M., Riget, F.F., Born E.W., Muir, D.C.G., and Letcher, R.J., **2008b**, "Tissue-specific congener composition of organohalogen and metabolite contaminants in East Greenland polar bear (*Ursus maritimus*)", *Environmental Pollution*, 152: 621-629.

Guerra, P., de la Torre, A., Martínez, M.A., Eljarrat, E., and Barceló, D., **2008**, "Identification and trace level determination of brominated flame retardants by liquid chromatography/quadrupole linear ion trap mass spectrometry", *Rapid Communications in Mass Spectrometry*, 22: 916-924.

Guna, M.M., Collings, B., and Le Blanc, J.C.Y., **2006**, "Extending MS[3] capabilities on a hybrid quadrupole linear ion trap", *54th American Society for Mass Spectrometry Conference on Mass Spectrometry and Allied Topics*, Conference poster # WP294, May 31, Seattle, Washington.

Hager, J.W., **2002**, "A new linear ion trap mass spectrometer", *Rapid Communications in Mass Spectrometry*, 16: 512-526.

Haglund, P., **1995**, "Isolation of PCB atropisomers for toxicological testing using chiral high-performance liquid chromatography", *Organohalogen Compounds*, 23: 35-40.

Haglund, P., **1996a**, "Enantioselective separation of polychlorinated biphenyl atropisomers using chiral high-performance liquid chromatography", *Journal of Chromatography A*, 724: 219-228.

Haglund, P., **1996b**, "Isolation and characterisation of polychlorinated biphenyl (PCB) atropisomers", *Chemosphere*, 32(*11*): 2133-2140.

Haglund, P., Asplund, L., Järnberg, U., and Jansson, B., **1990a**, "Isolation of mono- and non-ortho polychlorinated biphenyls from biological samples by electron-donor acceptor high performance liquid chromatography using a 2-(1-pyrenyl)ethyldimethylsilylated silica column", *Chemosphere*, 20(*7-9*): 887-894.

Haglund, P., Asplund, L., Järnberg, U., and Jansson, B., **1990b**, "Isolation of toxic polychlorinated biphenyls by electron donor-acceptor high-performance liquid chromatography on a 2-(1-pyrenyl)ethyldimethylsilylated silica column", *Journal of Chromatography*, 507: 389-398.

Hakala, K.S., Laitinen, L., Kaukonen, A.M., Hirvonen, J., Kostiainen, R., and Kotiaho, T., **2003**, "Development of LC/MS/MS methods for cocktail dose Caco-2 samples using atmospheric pressure photoionization and electrospray ionization", *Analytical Chemistry*, 75: 5969-5977.

Hanai, T., and Walton, H.F., **1977**, "Liquid chromatography of chlorinated biphenyls on pyrolytically-deposited carbon", *Analytical Chemistry*, 49(*13*): 1954-1958.

Hanold, K.A., Fischer, S.M., Cormia, P.H., Miller, C.E., and Syage, J.A., **2004**, "Atmospheric pressure photoionization. 1. General properties for LC/MS", *Analytical Chemistry*, 76: 2842-2851.

Hansen, A.S., Nielsen, T.G., Levinsen, H., Madsen, S.D., Thingstad, T.F., and Hansen, B.W., **2003**, "Impact of changing ice cover on pelagic productivity and food web structure in Disko Bay, West Greenland: a dynamic model approach", *Deep-Sea Research I*, 50: 171-187.

Haraguchi, K., Athanasiadou, M., Bergman, Å., Hovander, L., and Jensen, S., **1992**, "PCB and PCB methyl sulfones in selected groups of seals from Swedish waters", *Ambio*, 21(*8*): 546-549.

Haraguchi, K., Bergman, Å., Jakobsson, E., and Masuda, Y., **1993**, "Negative ion chemical ionization mass spectrometry in the analysis of polychlorinated biphenyl methyl sulphones", *Fresenius' Journal of Analytical Chemistry*, 347: 441-449.

Haraguchi, K., Kato, Y., Kimura, R., and Masuda, Y., **1998**, "Hydroxylation and methylthiolation of mono-*ortho*-substituted polychlorinated biphenyls in rats: Identification of metabolites with tissue affinity", *Chemical Research in Toxicology*, 11: 1508-1515.

Haraguchi, K., Kato, Y., Kimura, R., and Masuda, Y., **1999**, "Tissue distribution of methylsulfonyl metabolites derived from 2,2',4,5,5'-penta- and 2,2',3,4',5',6-hexachlorobiphenyls in rats", *Archives of Environmental Contamination and Toxicology*, 37: 135-142.

Haraguchi, K., Kato, Y., Koga, N., and Degawa, M., **2005a**, "Species differences in the tissue distribution of catechol and methylsulphonyl metabolites of 2,4,5,2',5'-penta- and 2,3,4,2',3',6-hexachlorobiphenyls in rats, mice, hamsters and guinea pigs", *Xenobiotica*, 35(*1*): 85-96.

Haraguchi, K., Kato, Y., Masuda, Y., and Kimura, R., **1997**, "Metabolism of 3,3',4,4'-tetrachlorobiphenyl via sulphur-containing pathway in rat: Liver-specific retention of methylsulphonyl metabolite", *Xenobiotica*, 27(*8*): 831-842.

Haraguchi, K., Koga, N., and Kato, Y., **2005b**, "Comparative metabolism of polychlorinated biphenyls and tissue distribution of persistent metabolites in rats, hamsters, and guinea pigs", *Drug Metabolism and Disposition*, 33: 373-380.

Haraguchi, K., Kuroki, H., and Masuda, Y., **1985**, "Toxicological evaluation of sulfur-containing metabolites of 2,5,2',5'-tetrachlorobiphenyl in rats", *Chemosphere*, 14(*11/12*): 1755-1762.

Haraguchi, K., Kuroki, H., and Masuda, Y., **1986**, "Determination of PCB-methylsulfone congeners in Yusho and control patients", *Chemosphere*, 15(*9-12*): 2027-2030.

Haraguchi, K., Kuroki, H., and Masuda, Y., **1987a**, "Determination of hydroxy methylsulfone metabolites of PCB in Yusho patients", *Chemosphere*, 16(*8/9*): 2033-2038.

Haraguchi, K., Kuroki, H., and Masuda, Y., **1987b**, "Synthesis of PCB methylsulfone: Some differences in mass and proton magnetic resonance spectroscopy", *Chemosphere*, 16(*10-12*): 2299-2313.

Harju, M.T., and Haglund, P., **1999**, "Determination of the rotational energy barriers of atropisomeric polychlorinated biphenyls", *Fresenius Journal of Analytical Chemistry*, 364: 219-223.

Harner, T., Wiberg, K., and Norstrom, R., **2000**, "Enantiomer fractions are preferred to enantiomer ratios for describing chiral signatures in environmental analysis", *Environmental Science & Technology*, 34(*1*): 218-220.

Hayen, H., and Karst, U., **2003**, "Strategies for the liquid chromatographic-mass spectrometric analysis of non-polar compounds", *Journal of Chromatography A*, 1000: 549-565.

Headley, J.V., Peru, K.M., Friesen, D.A., and Neu, T., **2001**, "Liquid chromatography-mass spectrometry and liquid chromatography-tandem mass spectrometry determination of *N*-methylpyrrolidinone in riverine biofilms", *Journal of Chromatography A*, 917: 159-165.

Heger, W., Schmahl, H.-J., Klug, S., Felies, A., Nau, H., Merker, H.-J., and Neubert, D., **1994**, "Embryotoxic effects of thalidomide derivatives in the non-human primate *Callithrix jacchus*. IV. Teratogenicity of µg/kg doses of the EM12 enantiomers", *Teratogenesis, Carcinogenesis, and Mutagenesis*, 14: 115-122.

Helsel, D.R., **2005**, *Nondetects and Data Analysis: Statistics for Censored Environmental Data*, John Wiley & Sons, Inc., Hoboken, NJ, USA.

Helsel, D.R., **2006**, "Fabricating data: How substituting values for nondetects can ruin results, and what can be done about it", *Chemosphere*, 65: 2434-2439.

Heneweer, M., van den Berg, M., de Geest, M., de Jong, P.C., Bergman, Å., and Sanderson, J.T., **2005**, "Inhibition of aromatase activity by methyl sulfonyl PCB metabolites in primary culture of human mammary fibroblasts", *Toxicology and Applied Pharmacology*, 202: 50-58.

Himmelsbach, M., Buchberger, W., and Reingruber, E., **2009**, "Determination of polymer additives by liquid chromatography coupled with mass spectrometry. A comparison of atmospheric pressure photoionization (APPI), atmospheric pressure chemical ionization (APCI), and electrospray ionization (ESI)", *Polymer Degradation and Stability*, 94: 1213-1219.

Hoekstra, P.F., Letcher, R.J., O'Hara, T.M., Backus, S.M., Solomon, K.R., and Muir, D.C.G., **2003**, "Hydroxylated and methylsulfone-containing metabolites of polychlorinated biphenyls in the plasma and blubber of bowhead whales (*Balaena mysticetus*)", *Environmental Toxicology and Chemistry*, 22(*11*): 2650-2658.

Höglund, P., Eriksson, T., and Björkman, S., **1998**, "A double-blind study of the sedative effects of the thalidomide enantiomers in humans", *Journal of Pharmacokinetics and Biopharmaceutics*, 26(*4*): 363-383.

Hovander, L., Linderholm, L., Athanasiadou, M., Athanansiadis, I., Bignert, A., Fängström, B., Kocan, A., Petrik, J., Trnovec, T., and Bergman, Å., **2006**, "Levels of PCBs and their metabolites in the serum of residents of a highly contaminated area in Eastern Slovakia", *Environmental Science & Technology*, 40: 3696-3703.

Hsieh, Y., Merkle, K., and Wang, G., **2003**, "Zirconia-based column high-performance liquid chromatography/atmospheric pressure photoionization tandem mass spectrometric analyses of drug molecules in rat plasma", *Rapid Communications in Mass Spectrometry*, 17: 1775-1780.

Hühnerfuss, H., Bergman, Å., Larsson, C., Peters, N., and Westendorf, J., **2003**, "Enantioselective transformation of atropisomeric PCBs or of their methylsulfonyl metabolites by rat hepatocytes?" *Organohalogen Compounds*, 62: 265-268.

Hühnerfuss, H., Peters, N., Döbler, J., Larsson, C., Bergman, Å., and Geidel, E., **2002**, "Enantioselective separation of chiral methylsulfonyl-PCB standards by preparative HPLC using methylated cyclodextrin phases", *Organohalogen Compounds*, 59: 287-290.

Ing-Lorenzini, K., Desmeules, J.A., Besson, M., Veuthey, J.-L., Dayer, P., and Daali, Y., **2009**, "Two-dimensional liquid chromatography-ion trap mass spectrometry for the simultaneous determination of ketorolac enantiomers and paracetamol in human plasma - Application to a pharmacokinetic study", *Journal of Chromatography A*, 1216(*3851-3856*).

Itoh, N., Aoyagi, Y., and Yarita, T., **2006**, "Optimization of the dopant for the trace determination of polycyclic aromatic hydrocarbons by liquid chromatography/dopant-assisted atmospheric-pressure photoionization/mass spectrometry", *Journal of Chromatography A*, 1131: 285-288.

Jansson, B., and Sundström, G., **1974**, "Mass spectrometry of the methyl ethers of isomeric hydroxychlorobiphenyls - Potential metabolites of chlorobiphenyls", *Biomedical Mass Spectrometry*, 1: 386-392.

Jaouen-Madoulet, A., Abarnou, A., Le Guellec, A.-M., Loizeau, V., and Leboulenger, F., **2000**, "Validation of an analytical procedure for polychlorinated biphenyls, coplanar polychlorinated biphenyls and polycyclic aromatic hydrocarbons in environmental samples", *Journal of Chromatography A*, 886: 153-173.

Jensen, S., and Jansson, B., **1976**, "Anthropogenic substances in seal from the Baltic: Methyl sulfone metabolites of PCB and DDE", *Ambio*, 5(*5-6*): 257-260.

Jerina, D.M., and Daly, J.W., **1974**, "Arene oxides: A new aspect of drug metabolism", *Science*, 185(*4151*): 573-582.

Job, G.E., Shvets, A., Pirkle, W.H., Kuwahara, S., Kosaka, M., Kasai, Y., Taji, H., Fujita, K., Watanabe, M., and Harada, N., **2004**, "The effects of aromatic substituents on the chromatographic enantioseparation of diarylmethyl esters with the Whelk-O1 chiral stationary phase", *Journal of Chromatography A*, 1055: 41-53.

Johansson, M., Larsson, C., Bergman, Å., and Lund, B.-O., **1998a**, "Structure-activity relationship for inhibition of CYP11B1-dependent glucocorticoid synthesis in Y1 cells by aryl methyl sulfones", *Pharmacology & Toxicology*, 83: 225-230.

Johansson, M., Nilsson, S., and Lund, B.-O., **1998b**, "Interactions between methylsulfonyl PCBs and the glucocorticoid receptor", *Environmental Health Perspectives*, 106(*12*): ??

Jörundsdóttir, H., Norström, K., Olsson, M., Pham-Tuan, H., Hühnerfuss, H., Bignert, A., and Bergman, Å., **2006**, "Temporal trend of bis(4-chlorophenyl) sulfone, methylsulfonyl-DDE and -PCBs in Baltic guillemot (*Uria aalge*) egg 1971-2001 - A comparison to 4,4'-DDE and PCB trends", *Environmental Pollution*, 141: 226-237.

Kaiser, K.L.E., **1974**, "On the optical activity of polychlorinated biphenyls", *Environmental Pollution*, 7: 93-101.

Karásek, L., Hajšlová, J., Rosmus, J., and Hühnerfuss, H., **2007**, "Methylsulfonyl PCB and DDE metabolites and their enantioselective gas chromatographic separation in human adipose tissues, seal blubber and pelican muscle", *Chemosphere*, 67: S22-S27.

Karlson, K., Ishaq, R., Becker, G., Berggren, P., Broman, D., and Colmsjö, A., **2000**, "PCBs, DDTs and methyl sulphone metabolites in various tissues of harbour porpoises from Swedish waters", *Environmental Pollution*, 110: 29-46.

Kato, Y., Haraguchi, K., Kawashima, M., Yamada, S., Isogai, M., Masuda, Y., and Kimura, R., **1995a**, "Characterization of hepatic microsomal cytochrome P-450 from rats treated with methylsulphonyl metabolites of polychlorinated biphenyl congeners", *Chemico-Biological Interactions*, 95: 269-278.

Kato, Y., Haraguchi, K., Kawashima, M., Yamada, S., Masuda, Y., and Kimura, R., **1995b**, "Induction of hepatic microsomal drug-metabolizing enzymes by methylsulphonyl metabolites of polychlorinated biphenyl congeners in rats", *Chemico-Biological Interactions*, 95: 257-268.

Kato, Y., Haraguchi, K., Shibahara, T., Shinmura, Y., Masuda, Y., and Kimura, R., **2000a**, "The induction of hepatic microsomal UDP-glucuronosyltransferase by the methylsulfonyl metabolites of polychlorinated biphenyl congeners in rats", *Chemico-Biological Interactions*, 125: 107-115.

Kato, Y., Haraguchi, K., Shibahara, T., Yumoto, S., Masuda, Y., and Kimura, R., **1999**, "Reduction of thyroid hormone levels by methylsulfonyl metabolites of tetra- and pentachlorinated biphenyls in male Sprague-Dawley rats", *Toxicological Sciences*, 48: 51-54.

Kato, Y., Haraguchi, K., Shibahara, T., Yumoto, S., Masuda, Y., and Kimura, R., **2000b**, "Reduction of serum thyroxine concentrations by methylsulfonyl metabolites of tetra-, penta- and hexachlorinated biphenyls in male Sprague-Dawley rats", *Chemosphere*, 40: 1233-1240.

Kato, Y., Haraguchi, K., Tomiyasu, K., Saito, H., Isogai, M., Masuda, Y., and Kimura, R., **1997**, "Structure dependent induction of CYP2B1/2 by 3-methylsulfonyl metabolites of polychlorinated biphenyl congeners in rats", *Environmental Toxicology and Pharmacology*, 3: 137-144.

Kauppila, T.J., and Bruins, A.P., **2005**, "Effect of the solvent flow rate on the ionization efficiency in atmospheric pressure photoionization-mass spectrometry", *Journal of the American Society for Mass Spectrometry*, 16: 1399-1407.

Kauppila, T.J., Kostiainen, R., and Bruins, A.P., **2004a**, "Anisole, a new dopant for atmospheric pressure photoionization mass spectrometry of low proton affinity, low ionization energy compounds", *Rapid Communications in Mass Spectrometry*, 18: 808-815.

Kauppila, T.J., Kotiaho, T., and Kostiainen, R., **2004b**, "Negative ion-atmospheric pressure photoionization-mass spectrometry", *Journal of the American Society for Mass Spectrometry*, 15: 203-211.

Kauppila, T.J., Kuuranne, T., Meurer, E.C., Eberlin, M.N., Kotiaho, T., and Kostiainen, R., **2002**, "Atmospheric pressure photoionization mass spectrometry. Ionization mechanism and the effect of solvent on the ionization of naphthalenes", *Analytical Chemistry*, 74: 5470-5479.

Kawano, S., Murata, H., Mikami, H., Mukaibatake, K., and Waki, H., **2006**, "Method optimization for the analysis of fullerenes by liquid chromatography/atmospheric pressure photoionization-mass spectrometry", *Rapid Communications in Mass Spectrometry*, 20: 2783-2785.

Kéki, S., Nagy, L., Kuki, Á., and Zsuga, M., **2008a**, "A new method for mass spectrometry of polyethylene waxes: The chloride ion attachment technique by atmospheric pressure photoionization", *Macromolecules*, 41: 3772-3774.

Kéki, S., Török, J., Nagy, L., and Zsuga, M., **2008b**, "Atmospheric Pressure Photoionization Mass Spectrometry of Polyisobutylene Derivatives", *Journal of the American Society for Mass Spectrometry*, 19: 656-665.

Kersten, H., Funcke, V., Lorenz, M., Brockmann, K.J., Benter, T., and O'Brien, R., **2009**, "Evidence of neutral radical induced analyte ion transformations in APPI and near-VUV APLI", *Journal of the American Society for Mass Spectrometry*, 20: 1868-1880.

Keski-Hynnilä, H., Kurkela, M., Elovaara, E., Antonio, L., Magdalou, J., Luukkanen, L., Taskinen, J., and Kostiainen, R., **2002**, "Comparison of electrospray, atmospheric pressure chemical ionization, and atmospheric pressure photoionization in the identification of apomorphine, dobutamine, and entacapone phase II metabolites in biological samples", *Analytical Chemistry*, 74: 3449-3457.

Kimata, K., Hosoya, K., Hiroaki, K., Tanaka, N., Barr, J.R., McClure, P.C., Patterson, D.G.J., Jakobsson, E., and Bergman, Å., **1997**, "Selectivity of electron-donor- and electron-acceptor-bonded silica packing materials for hydrophobic environmental contaminants in polar and non-polar eluents", *Journal of Chromatography A*, 786: 237-248.

King, R., Bofiglio, R., Fernandez-Metzler, Miller-Stein, C., and Olah, T., **2000**, "Mechanistic investigation of ionization suppression in electrospray ionization", *Journal of the American Society for Mass Spectrometry*, 11: 942-950.

Kirkegaard, M., Sonne, C., Leifsson, P.S., Dietz, R., Born, E.W., Muir, D.C.G., and Letcher, R.J., **2005**, "Histology of selected immunological organs in polar bear (*Ursus maritimus*) from East Greenland in relation to concentrations of organohalogen contaminants", *The Science of the Total Environment*, 341: 119-132.

Klasson-Wehler, E., Bergman, Å., Athanasiadou, M., Ludwig, J.P., Auman, H.J., Kannan, K., van den Berg, M., Murk, A.J., Feyk, L.A., and Giesy, J.P., **1998**, "Hydroxylated and methylsulfonyl polychlorinated biphenyl metabolites in albatrosses from Midway Atoll, North Pacific Ocean", *Environmental Toxicology and Chemistry*, 17(*8*): 1620-1625.

Kloepfer, A., Quintana, J.B., and Reemtsma, T., **2004**, "Operational options to reduce matrix effects in liquid chromatography-electrospray ionization-mass spectrometry analysis of aqueous environmental samples", *Journal of Chromatography A*, 1067: 153-160.

König, W.A., Bärbel, G., Hochmuth, D.H., Mlynek, C., and Hopf, H., **1994**, "Resolution of chiral [2.2]paracyclophanes by enantioselective gas chromatography", *Tetrahedron: Asymmetry*, 5(*3*): 347-350.

Krupčík, J., Májeková, M., Májek, P., Hrouzek, J., Benicka, E., Onuska, F., Sandra, P., and de Zeeuw, J., **1995**, "On the interconversion energy barriers obtained for atropisomers of some polychlorinated biphenyls by AM1 semiempirical quantum chemistry method and gas chromatography on a modified cyclodextrin stationary phase", *Fresenius' Journal of Analytical Chemistry*, 352: 696-698.

Lagalante, A.F., and Oswald, T.D., **2008**, "Analysis of polybrominated diphenyl ethers (PBDEs) by liquid chromatography with negative ion atmospheric pressure photoionization tandem mass spectrometry (LC/NI-APPI/MS/MS): application to house dust", *Analytical and Bioanalytical Chemistry*, 391: 2249-2256.

Lamprecht, G., Kraushofer, T., Stoschitzky, K., and Lindner, W., **2000**, "Enantioselective analysis of (*R*)- and (*S*)-atenolol in urine samples by a high-performance liquid chromatography column-switching setup", *Journal of Chromatography B*, 740: 219-226.

Larsen, G.L., Bergman, Å., Klasson-Wehler, E., and Bass, N.M., **1991**, "A methylsulfonyl metabolite of a polychlorinated biphenyl can serve as a ligand for fatty acid binding protein in rat intestinal mucosa", *Chemical-Biological Interactions*, 77: 315-323.

Larsen, G.L., Hakk, H., Larsson, C., and Bergman, Å., **1998**, "Interaction of 3-methylsulfonyl-2,2',4',5,5',6-hexachlorobiphenyl with mammalian carrier proteins", *Organohalogen Compounds*, 37: 345-349.

Larsen, G.L., Huwe, J.K., Bergman, Å., Klasson-Wehler, E., and Hargis, P., **1992**, "Methylsulfonyl metabolites of xenobiotics can serve as ligands for fatty acid binding proteins in chicken liver and intestinal mucosa", *Chemosphere*, 25(*7-10*): 1189-1194.

Larsson, C., Ellerichmann, T., Hühnerfuss, H., and Bergman, Å., **2002**, "Chiral PCB methyl sulfones in rat tissues after exposure to technical PCBs", *Environmental Science & Technology*, 36: 2833-2838.

Larsson, C., Norström, K., Athanansiadis, I., Bignert, A., König, W.A., and Bergman, Å., **2004**, "Enantiomeric specificity of methylsulfonyl-PCBs and distribution of bis(4-chlorophenyl) sulfone, PCB, and DDE methyl sulfones in grey seal tissues", *Environmental Science & Technology*, 38: 4950-4955.

Lenz, W., **1962**, "Thalidomide and congenital abnormalities", *The Lancet*, 279(*7219*): 45.

Letcher, R.J., Klasson-Wehler, E., and Bergman, Å., **2000**, "Methyl sulfone and hydroxylated metabolites of polychlorinated biphenyls" in *The Handbook of Environmental Chemistry*, Paasivirta, J., Ed., Springer-Verlag, Berlin, Germany, Vol. 3, Chap. 11, p. 315-359.

Letcher, R.J., Lemmen, J.G., van der Burg, B., Brouwer, A., Bergman, Å., Giesy, J.P., and Van den Berg, M., **2002**, "*In vitro* antiestrogenic effects of aryl methyl sulfone metabolites of polychlorinated biphenyls and 2,2-bis-(4-chlorophenyl)-1,1-dichloroethene on 17$\beta$-estradiol-induced gene expression in several bioassay systems", *Toxicological Sciences*, 69: 362-372.

Letcher, R.J., Li, H.X., and Chu, S.G., **2005**, "Determination of hydroxylated polychlorinated biphenyls (HO-PCBs) in blood plasma by high-performance liquid chromatography-electrospray ionization-tandem quadrupole mass spectrometry", *Journal of Analytical Toxicology*, 29: 1-8.

Letcher, R.J., and Norstrom, R.J., **1997**, "Electron capture/negative ionization mass spectrometric characteristics of bioaccumulating methyl sulfone-substituted polychlorinated biphenyls", *Journal of Mass Spectrometry*, 32: 232-240.

Letcher, R.J., Norstrom, R.J., and Bergman, Å., **1995**, "Geographical distribution and identification of methyl sulfone PCB and DDE metabolites in pooled polar bear (*Ursus maritimus*) adipose tissue from western hemisphere Arctic and Subarctic regions", *The Science of the Total Environment*, 160/161: 409-420.

Letcher, R.J., Norstrom, R.J., and Muir, D.C.G., **1998**, "Biotransformation versus bioaccumulation: Sources of methyl sulfone PCB and 4,4'-DDE metabolites in the polar bear food chain", *Environmental Science & Technology*, 32: 1656-1661.

Letcher, R.J., van Holsteijn, I., Drenth, H.-J., Norstrom, R.J., Bergman, Å., Safe, S., Pieters, R., and van den Berg, M., **1999**, "Cytotoxicity and aromatase (CYP19) activity modulation by organochlorines in human placental JEG-3 and JAR choriocarcinoma cells", *Toxicology and Applied Pharmacology*, 160: 10-20.

Leuthold, L.A., Grivet, C., Allen, M., Baumert, M., and Hopfgartner, G., **2004**, "Simultaneous selected reaction monitoring, MS/MS and MS$^3$ quantitation for the analysis of pharmaceutical compounds in human plasma using chip-based infusion", *Rapid Communications in Mass Spectrometry*, 18: 1995-2000.

Linderholm, L., Park, J.-S., Kocan, A., Trnovec, T., Athanasiadou, M., Bergman, Å., and Hertz-Picciotto, I., **2007**, "Maternal cord serum exposure to PCB and DDE methyl sulfone metabolites in eastern Slovakia", *Chemosphere*, 69: 403-410.

Loconto, P.R., **2006**, *Trace Environmental Quantitative Analysis: Principles, Techniques, and Applications*, 2nd Ed., Taylor & Francis, Boca Raton, FL, USA.

Lorenzen, K., Versluis, C., van Duijn, E., van den Heuvel, R.H.H., and Heck, A.J.R., **2007**, "Optimizing macromolecular tandem mass spectrometry of large non-covalent complexes using heavy collision gases", *International Journal of Mass Spectrometry*, 268: 198-206.

Lund, B.-O., Örberg, J., Bergman, Å., Larsson, C., Bergman, A., Bäcklin, B.-M., Håkansson, H., and Madej, A., **1999**, "Chronic and reproductive toxicity of a mixture of 15 methylsulfonyl-polychlorinated biphenyls and 3-methylsulfonyl-2,2-bis-(4-chlorophenyl)-1,1-dichloroethene in mink (*Mustela vison*)", *Environmental Toxicology and Chemistry*, 18(*2*): 292-298.

Lund, J., Brandt, I., Poellinger, L., Bergman, Å., Klasson-Wehler, E., and Gustafsson, J.-Å., **1984**, "Target cells for polychlorinated biphenyl metabolite 4,4'-bis(methylsulfonyl)-2,2',5,5'-tetrachlorobiphenyl. Characterization of high affinity binding in rat and mouse lung cytosol", *Molecular Pharmacology*, 27: 314-323.

Luosujärvi, L., Karikko, M.-M., Haapala, M., Saarela, V., Huhtala, S., Franssila, S., Kostiainen, R., Kotiaho, T., and Kauppila, T.J., **2008**, "Gas chromatography/mass spectrometry of polychlorinated biphenyls using atmospheric pressure chemical ionization and atmospheric pressure photoionization microchips", *Rapid Communications in Mass Spectrometry*, 22: 425-431.

Macleod, S.L., and Wong, C.S., **2010**, "Loadings, trends, comparisons, and fate of achiral and chiral pharmaceuticals in wastewaters from urban tertiary and rural aerated lagoon treatments", *Water Research*, 44: 533-544.

Maervoet, J., Covaci, A., Schepens, P., Sandau, C.D., and Letcher, R.J., **2004**, "A reassessment of the nomenclature of polychlorinated biphenyl (PCB) metabolites", *Environmental Health Perspectives*, 112(*3*): 291-294.

Mallet, C.R., Lu, Z., and Mazzeo, J.R., **2004**, "A study of ion suppression effects in electrospray ionization from mobile phase additives and solid-phase extracts", *Rapid Communications in Mass Spectrometry*, 18: 49-58.

March, J., **1992**, *Advanced Organic Chemistry: Reactions, Mechanisms and Structure*, 4th Ed., John Wiley & Sons, Inc., Hoboken, NJ, USA.

Marotta, E., Seraglia, R., Fabris, F., and Traldi, P., **2003**, "Atmospheric pressure photoionization mechanisms, 1. The case of acetonitrile", *International Journal of Mass Spectrometry*, 228: 841-849.

Martens-Lobenhoffer, J., Reiche, I., Tröger, U., Mönkemüller, K., Malfertheiner, P., and Bode-Böger, S.M., **2007**, "Enantioselective quantification of omeprazole and its main metabolites in human serum by chiral HPLC-atmospheric pressure photoionization tandem mass spectrometry", *Journal of Chromatography B*, 857: 301-307.

Marvin, C.H., Smith, R.W., Bryant, D.W., and McCarry, B.E., **1999**, "Analysis of high-molecular-mass polycyclic aromatic hydrocarbons in environmental samples using liquid chromatography-atmospheric pressure chemical ionization mass spectrometry", *Journal of chromatography A*, 863: 13-24.

Medvedovici, A., Sandra, P., Toribio, L., and David, F., **1997**, "Chiral packed column subcritical fluid chromatography on polysaccharide and macrocyclic antibiotic chiral stationary phases", *Journal of Chromatography A*, 785: 159-171.

Mei, H., Hsieh, Y., Nardo, C., Xu, X., Wang, S., Ng, K., and Korfmacher, W.A., **2003**, "Investigation of matrix effects in bioanalytical high-performance liquid chromatography/tandem mass spectrometric assays: application to drug discovery", *Rapid Communications in Mass Spectrometry*, 17: 97-103.

Mizutani, T., Yamamoto, K., and Tajima, K., **1978**, "Sulfur-containing metabolites of chlorobiphenyl isomers, a comparative study", *Journal of Agricultural and Food Chemistry*, 26(*4*): 862-866.

Morrissey, J.A., Bleackley, D.S., Warner, N.A., and Wong, C.S., **2007**, "Enantiomer fractions of polychlorinated biphenyls in three selected standard reference materials", *Chemosphere*, 66: 326-331.

Müller, A., Mickel, M., Geyer, R., Ringseis, R., Eder, K., and Steinhart, H., **2006**, "Identification of conjugated linoleic acid elongation and β-oxidation products by coupled silver-ion HPLC APPI-MS", *Journal of Chromatography B*, 837: 147-152.

Muth, P., Metz, R., Beck, H., Bolten, W.W., and Vergin, H., **1996**, "Improved high-performance liquid chromatographic determination of amoxicillin in human plasma by means of column switching", *Journal of Chromatography A*, 729(*1-2*): 259-266.

Nakanishi, Y., Shigematsu, N., Kurita, Y., Matsuba, K., Kanegae, H., Ishimaru, S., and Kawazoe, Y., **1985**, "Respiratory involvement and immune status in Yusho patients", *Environmental Health Perspectives*, 59: 31-36.

*New Scientist*, **1966**, "Report of a new chemical hazard", vol. 32, p. 612.

Newsome, W.H., and Davies, D., **1996**, "Determination of PCB metabolites in Canadian human milk", *Chemosphere*, 33(*3*): 559-565.

Nezel, T., Müller-Plathe, F., Müller, M.D., and Buser, H.-R., **1997**, "Theoretical considerations about chiral PCBs and their methylthio and methylsulfonyl metabolites being possibly present as stable enantiomers", *Chemosphere*, 35(*9*): 1895-1906.

Norén, K., Lundén, Å., Pettersson, E., and Bergman, Å., **1996**, "Methylsulfonyl metabolites of PCBs and DDE in human milk in Sweden, 1972-1992", *Environmental Health Perspectives*, 104(*7*): 766-772.

Norén, K., Weistrand, C., and Karpe, F., **1999**, "Distribution of PCB congeners, DDE, hexachlorobenzene, and methylsulfonyl metabolites of PCB and DDE among various fractions of human blood plasma", *Archives of Environmental Contamination and Toxicology*, 37: 408-414.

Norström, K., Eriksson, J., Haglund, J., Silvari, V., and Bergman, Å., **2006**, "Enantioselective formation of methyl sulfone metabolites of 2,2',3,3',4,6'-hexachlorobiphenyl in rat", *Environmental Science & Technology*, 40: 7649-7655.

Oda, Y., Asakawa, N., Yoshida, Y., and Sato, T., **1992**, "On-line determination and resolution of the enantiomers of ketoprofen in plasma using coupled achiral-chiral high-performance liquid chromatography", *Journal of Pharmaceutical and Biomedical Analysis*, 10(*1*): 81-87.

Okamoto, Y., and Kaida, Y., **1994**, "Resolution by high-performance liquid chromatography using polysaccharide carbamates and benzoates as chiral stationary phases", *Journal of Chromatography A*, 666: 403-419.

Olsson, A., Asplund, L., Helander, B., Bergman, Å., and Kylin, H., **1993**, "Isomer specific analysis of PCB and PCB methyl sulfones in eggs from white tailed sea eagle", *Organohalogen Compounds*, 14: 113-116.

Péhourcq, F., Jarry, C., and Bannwarth, B., **2001**, "Chiral resolution of flurbiprofen and ketoprofen enantiomers by HPLC on a glycopeptide-type column chiral stationary phase", *Biomedical Chromatography*, 15: 217-222.

Pérez, S., and Barceló, D., **2001**, "Determination of polycyclic aromatic hydrocarbons in sewage reference sludge by liquid chromatography-atmospheric-pressure chemical-ionization mass spectrometry", *Chromatographia*, 53: 475-480.

PerkinElmer Optoelectronics, **2008**, *PID Lamp Operation and Maintenance*, Salem, MA, USA.

Perrin, C., Vu, V.A., Matthjis, N., Maftouh, M., Massart, D.L., and Vander Heyden, Y., **2002**, "Screening approach for chiral separation of pharmaceuticals, Part I. Normal-phase liquid chromatography", *Journal of Chromatography A*, 947: 69-83.

Pham-Tuan, H., Larsson, C., Hoffmann, F., Bergman, Å., Fröba, M., and Hühnerfuss, H., **2004**, "Enantioselective semi-preparative HPLC separation of PCB metabolites and their absolute structures determined by electronic and vibrational circular dichroism", *Organohalogen Compounds*, 66: 398-403.

Pham-Tuan, H., Larsson, C., Hoffmann, F., Bergman, Å., Fröba, M., and Hühnerfuss, H., **2005**, "Enantioselective semipreparative HPLC separation of PCB metabolites and their absolute structure elucidation using electronic and vibrational circular dichroism", *Chirality*, 17: 266-280.

Pirkle, W.H., Koscho, M.E., and Wu, Z., **1996**, "High-performance liquid chromatography separation of the enantiomers of N-aryloxazolinones, N-aryl thiazolinones and their sulfur derivatives on a synthetic chiral stationary phase", *Journal of Chromatography A*, 726: 91-97.

Pratanata, I., Williams, L.R., and Williams, R.N., **1974**, "Carbon-oxygen bond formation in the mass spectra of aryl methyl sulphones", *Organic Mass Spectrometry*, 8: 175-178.

Püttmann, M., Mannschreck, A., Oesch, F., and Robertson, L., **1989**, "Chiral effects in the induction of drug-metabolizing enzymes using synthetic atropisomers of polychlorinated biphenyls (PCBs)", *Biochemical Pharmacology*, 38(*8*): 1345-1352.

Püttmann, M., Oesch, F., and Robertson, L.W., **1986**, "Characteristics of polychlorinated biphenyl (PCB) atropisomers", *Chemosphere*, 15(*9-12*): 2061-2064.

Raffaelli, A., and Saba, A., **2003**, "Atmospheric pressure photoionization mass spectrometry", *Mass Spectrometry Reviews*, 22: 318331.

Rafferty, J.L., Siepmann, J.I., and Schure, M.R., **2008**, "Molecular-level comparison of alkylsilane and polar-embedded reversed-phase liquid chromatography systems", *Analytical Chemistry*, 80: 6214-6221.

Ramos, L., Hernández, L.M., and González, M.J., **1999**, "Simultaneous separation of coplanar and chiral polychlorinated biphenyls by off-line pyrenyl-silica liquid chromatography and gas chromatography. Enantiomer ratios of chiral congeners", *Analytical Chemistry*, 71: 70-77.

Rauha, J.-P., Vuorela, H., and Kostiainen, R., **2001**, "Effect of eluent on the ionization efficiency of flavonoids by ion spray, atmospheric pressure chemical ionization, and atmospheric pressure photoionization mass spectrometry", *Journal of Mass Spectrometry*, 36: 1269-1280.

Reich, S., and Schurig, V., **1999**, "Enantiomerentrennung atropisomerer PCB mittels HPLC", *GIT Spezial Separation*, 19(*1*): 14-16.

Rhourri-Frih, B., Chaimbault, P., Claude, B., Lamy, C., André, P., and Lafosse, M., **2009**, "Analysis of pentacyclic triterpenes by LC-MS. A comparative study between APCI and APPI", *Journal of Mass Spectrometry*, 44: 71-80.

Risebrough, R.W., Rieche, P., Herman, S.G., Peakall, D.B., and Kirven, M.N., **1968**, "Polychlorinated biphenyls in the global ecosystem", *Nature*, 220: 1098-1102.

Robb, D.B., and Blades, M.W., **2005**, "Effects of solvent flow, dopant flow, and lamp current on dopant-assisted atmospheric pressure photoionization (DA-APPI) for LC-MS. Ionization via proton transfer", *Journal of the American Society for Mass Spectrometry*, 16: 1275-1290.

Robb, D.B., and Blades, M.W., **2006a**, "Atmospheric pressure photoionization for ionization of both polar and nonpolar compounds in reversed-phase LC/MS", *Analytical Chemistry*, 78: 8162-8164.

Robb, D.B., and Blades, M.W., **2006b**, "Factors affecting primary ionization in dopant-assisted atmospheric pressure photoionization (DA-APPI) for LC/MS", *Journal of the American Society for Mass Spectrometry*, 17: 130-138.

Robb, D.B., Covey, T.R., and Bruins, A.P., **2000**, "Atmospheric pressure photoionization: An ionization method for liquid chromatography-mass spectrometry", *Analytical Chemistry*, 72: 3653-3659.

Robb, D.B., Smith, D.R., and Blades, M.W., **2008**, "Investigation of substituted-benzene dopants for charge exchange ionization of nonpolar compounds by atmospheric pressure photoionization", *Journal of the American Society for Mass Spectrometry*, 19(*7*): 955-963.

Ross, M.S., Verreault, J., Letcher, R.J., Gabrielsen, G.W., and Wong, C.S., **2008**, "Chiral organochlorine contaminants in blood and eggs of glaucous gulls (*Larus hyperboreus*) from the Norwegian Arctic", *Environmental Science & Technology*, 42: 7181-7186.

Ross, M.S., and Wong, C.S., **2010**, "Comparison of electrospray ionization, atmospheric pressure photoionization, and anion attachment atmospheric pressure photoionization for the analysis of hexabromocyclododecane enantiomers in environmental samples", *Journal of Chromatography A*, 1217: 7855-7863.

Rousell, C., Del Rio, A., Pierrot-Sanders, J., Piras, P., and Vanthuyne, N., **2004**, "Chiral liquid chromatography contribution to the determination of the absolute structures of enantiomers", *Journal of Chromatography A*, 1037: 311-328.

Sandala, G.M., Sonne-Hansen, C., Dietz, R., Muir, D.C.G., Valters, K., Bennett, E.R., Born, E.W., and Letcher, R.J., **2004**, "Hydroxylated and methyl sulfone PCB metabolites in adipose tissue and whole blood of polar bear (*Ursus maritimus*) from East Greenland", *Science of the Total Environment*, 331: 125-141.

Sander, L.C., and Wise, S.A., **1993**, "Shape selectivity in reversed-phase liquid chromatography for the separation of planar and non-planar solutes", *Journal of Chromatography A*, 656: 335-351.

Schurig, V., Glausch, A., and Fluck, M., **1995**, "On the enantiomerization barrier of atropisomeric 2,2',3,3',4,6'-hexachlorobiphenyl (PCB132)", *Tetrahedron: Asymmetry*, 6(*9*): 2161-2164.

SeaSolve Software Inc., **2003**, *PeakFit v4 Users Guide*, Framingham, MA, USA.

Sears, L.J., and Grimsrud, E.P., **1989**, "Elimination of unexpected ions in electron capture mass spectrometry using carbon dioxide buffer gas", *Analytical Chemistry*, 81: 2523-2528.

Shen, J.X., Motyka, R.J., Roach, J.P., and Hayes, R.N., **2005**, "Minimization of ion suppression in LC-MS/MS analysis through the application of strong cation exchange solid-phase extraction (SCX-SPE)", *Journal of Pharmaceutical and Biomedical Analysis*, 37: 359-367.

Shigematsu, N., Ishimaru, S., Saito, R., Ikeda, T., Matsuba, K., Sugiyama, K., and Masuda, Y., **1978**, "Respiratory involvement in polychlorinated biphenyls poisoning", *Environmental Research*, 16: 92-100.

Short, L.C., Cai, S.-S., and Syage, J.A., **2007**, "APPI-MS: Effects of mobile phases and VUV lamps on the detection of PAH compounds", *Journal of the American Society for Mass Spectrometry*, 18: 589-599.

Smith, D.R., Robb, D.B., and Blades, M.W., **2009**, "Comparison of dopants for charge exchange ionization of nonpolar polycyclic aromatic hydrocarbons with reversed phase LC-APPI-MS", *Journal of the American Society for Mass Spectrometry*, 20: 73-79.

Snyder, L.R., **1978**, "Classification of the solvent properties of common liquids", *Journal of Chromatographic Science*, 16: 223-234.

Snyder, L.R., Kirkland, J.J., and Glajch, J.L., **1997**, *Practical HPLC Method Development*, 2nd Ed., John Wiley & Sons, Inc.,

Song, L., Wellman, A.D., Yao, H., and Bartmess, J.E., **2007**, "Negative ion-atmospheric pressure photoionization: Electron capture, proton transfer, and anion attachment", *Journal of the American Society for Mass Spectrometry*, 18: 1789-1798.

Sonne, C., Dietz, R., Kirkegaard, M., Letcher, R.J., Shahmiri, S., Andersen, S., Møller, P., Olsen, A.K., and Jensen, A.L., **2008a**, "Effects of organohalogen pollutants on haematological and urine clinical-chemical parameters in Greenland sledge dogs (*Canis familiaris*)", *Ecotoxicology and Environmental Safety*, 69: 381-390.

Sonne, C., Dietz, R., Larsen, H.J.S., Loft, K.E., Kirkegaard, M., Letcher, R.J., Shahmiri, S., and Møller, P., **2006a**, "Impairment of cellular immunity in West Greenland sledge dogs (*Canis familiaris*) dietary exposed to polluted minke whale (*Balaenoptera acutorostrata*) blubber", *Environmental Science & Technology*, 40: 2056-2062.

Sonne, C., Dietz, R., Leifsson, P.S., Born, E.W., Kirkegaard, M., Letcher, R.J., Muir, D.C.G., Riget, F.F., and Hyldstrup, L., **2006b**, "Are organohalogen contaminants a cofactor in the development of renal lesions in East Greenland polar bears (*Ursus maritimus*)?" *Environmental Toxicology and Chemistry*, 25(*6*): 1551-1557.

Sonne, C., Dietz, R., Leifsson, P.S., Born, E.W., Letcher, R.J., Kirkegaard, M., Muir, D.C.G., Riget, F.F., and Hyldstrup, L., **2005**, "Do organohalogen contaminants contribute to histopathology in liver from East Greenland polar bears (*Ursus maritimus*)", *Environmental Health Perspectives*, 113(*11*): 1569-1574.

Sonne, C., Fonfara, S., Dietz, R., Kirkegaard, M., Letcher, R.J., Shahmiri, S., Andersen, S., and Møller, P., **2007**, "Multiple cytokine and acute-phase protein gene transcription in West Greenland sledge dogs (*Canis familiaris*) dietary exposed to organic environmental pollutants", *Archives of Environmental Contamination and Toxicology*, 53: 110-118.

Sonne, C., Leifsson, P.S., Dietz, R., Kirkegaard, M., Jensen, A.L., Shahmiri, S., and Letcher, R.J., **2008b**, "Greenland sledge dogs (*Canis familiaris*) develop liver lesions when exposed to a chronic and dietary low dose of an environmental organohalogen cocktail", *Environmental Research*, 106: 72-80.

Stapleton, H.M., Letcher, R.J., and Baker, J.E., **2001**, "Metabolism of PCBs by the deepwater sculpin (*Myoxocephalus thompsoni*)", *Environmental Science & Technology*, 35: 4747-4752.

Straube, E.A., Dekant, W., and Völkel, W., **2004**, "Comparison of electrospray ionization, atmospheric pressure chemical ionization, and atmospheric pressure photoionization for the analysis of dinitropyrene and aminonitropyrene LC-MS/MS", *Journal of the American Society for Mass Spectrometry*, 15: 1853-1862.

Stringham, R.W., **2006**, "The use of polysaccharide phases in the separation of enantiomers", *Advances in Chromatography*, 44: 257-290.

Stripp, B.R., Lund, J., Mango, G.W., Doyen, K.C., Johnston, C., Hultenby, K., Nord, M., and Whitsett, J.A., **1996**, "Clara cell secretory protein: A determinant of PCB bioaccumulation in mammals", *American Journal of Physiology*, 271(*15*): L656-L664.

Takino, M., Yamaguchi, K., and Nakahara, T., **2004**, "Determination of carbamate pesticide residues in vegetables and fruits by liquid chromatography-atmospheric pressure photoionization-mass spectrometry and atmospheric pressure chemical ionization-mass spectrometry", *Journal of Agricultural and Food Chemistry*, 52: 727-735.

Theoret, J.J., **1962**, "Chronology of the Thalidomide Story", *Canadian Medical Association Journal*, 87: 981-982.

Trapp, O., Schoetz, G., and Schurig, V., **2001**, "Determination of enantiomerization barriers by dynamic and stopped-flow chromatographic methods", *Chirality*, 13: 403-414.

Tubaro, M., Marotta, E., Seraglia, R., and Traldi, P., **2003**, "Atmospheric pressure photoionization mechanisms. 2. The case of benzene and toluene", *Rapid Communications in Mass Spectrometry*, 17: 2423-2429.

Ulrich, E.M., Willett, K.L., Caperell-Grant, A., Bigsby, R.M., and Hites, R.A., **2001**, "Understanding enantioselective processes: A laboratory rat model for α-hexachlorocyclohexane accumulation", *Environmental Science & Technology*, 35: 1604-1609.

Valeur, A., Michelsen, P., and Odham, G., **1993**, "On-line straight-phase liquid chromatography/plasmaspray tandem mass spectrometry of glycerolipids", *Lipids*, 28(*3*): 255-259.

Van De Steene, J.C., Mortier, K.A., and Lambert, W.E., **2006**, "Tackling matrix effects during development of a liquid chromatographic-electrospray ionisation tandem mass spectrometric analysis of nine basic pharmaceuticals in aqueous environmental samples", *Journal of Chromatography A*, 1123: 71-81.

Verboven, N., Verreault, J., Letcher, R.J., Gabrielsen, G.W., and Evans, N.P., **2008**, "Maternally derived testosterone and 17β-estradiol in the eggs of Arctic-breeding glaucous gulls in relation to persistent organic pollutants", *Comparative Biochemistry and Physiology, Part C*, 148: 143-151.

Verreault, J., Dietz, R., Sonne, C., Gebbink, W.A., Shahmiri, S., and Letcher, R.J., **2008**, "Comparative fate of organohalogen contaminants in two top carnivores in Greenland: Captive sledge dogs and wild polar bears", *Comparative Biochemistry and Physiology, Part C*, 147: 306-315.

Verreault, J., Letcher, R.J., Muir, D.C.G., Chu, S., Gebbink, W.A., and Gabrielsen, G.W., **2005a**, "New organochlorine contaminants and metabolites in plasma and eggs of glaucous gulls (*Larus hyperboreus*) from the Norwegian Arctic", *Environmental Toxicology and Chemistry*, 24(*10*): 2486-2499.

Verreault, J., Letcher, R.J., Sonne, C., and Dietz, R., **2009a**, "Dietary, age and trans-generational effects on the fate of organohalogen contaminants in captive sledge dogs in Greenland", *Environment International*, 35: 56-62.

Verreault, J., Letcher, R.J., Sonne, C., and Dietz, R., **2009b**, "*In vitro* metabolism and of polychlorinated biphenyls and cytochrome P450 monooxygenase activities in dietary-exposed Greenland sledge dogs", *Comparative Biochemistry and Physiology, Part C*, 150: 91-100.

Verreault, J., Maisonneuve, F., Dietz, R., Sonne, C., and Letcher, R.J., **2009c**, "Comparative hepatic activity of xenobiotic-metabolizing enzymes and concentrations of organohalogens and their hydroxylated analogues in captive Greenland sledge dogs (*Canis familiaris*)", *Environmental Toxicology and Chemistry*, 28(*1*): 162-172.

Verreault, J., Muir, D.C.G., Norstrom, R., Stirling, I., Fisk, A.T., Gabrielsen, G.W., Derocher, A.E., Evans, T.J., Dietz, R., Sonne, C., Sandala, G.M., Gebbink, W., Riget, F.F., Born, E.W., Taylor, M.K., Nagy, J., and Letcher, R.J., **2005b**, "Chlorinated hydrocarbon contaminants and metabolites in polar bears (*Ursus maritimus*) from Alaska, Canada, East Greenland, and Svalbard: 1996-2002", *The Science of the Total Environment*, 351-352: 369-390.

Verreault, J., Skaare, J.U., Jenssen, B.M., and Gabrielsen, G.W., **2004**, "Effects of organochlorine contaminants on thyroid hormone levels in Arctic breeding glaucous gulls, *Larus hyperboreus*", *Environmental Health Perspectives*, 112(*5*): 532-537.

Verreault, J., Villa, R.A., Gabrielsen, G.W., Skaare, J.U., and Letcher, R.J., **2006**, "Maternal transfer of organohalogen contaminants and metabolites to eggs of Arctic-breeding glaucous gulls", *Environmental Pollution*, 144: 1053-1060.

Viglino, L., Aboulfadl, K., Prévost, M., and Sauvé, S., **2008**, "Analysis of natural and synthetic estrogenic endocrine disruptors in environmental waters using online preconcentration coupled with LC-APPI-MS/MS", *Talanta*, 76: 1088-1096.

Villani, C., and Pirkle, W.H., **1995**, "Chromatographic resolution of the interconverting stereoisomers of hindered sulfinyl and sulfonyl naphthalene derivatives", *Tetrahedron: Asymmetry*, 6(*1*): 27-30.

Voet, D., and Voet, J.G., **2004**, *Biochemistry*, 3rd Ed., John Wiley & Sons, Inc., Hoboken, NJ, USA.

Wang, G., Hsieh, Y., and Korfmacher, W.A., **2005**, "Comparison of atmospheric pressure chemical ionization, electrospray ionization, and atmospheric pressure photoionization for the determination of cyclosporin A in rat plasma", *Analytical Chemistry*, 77: 541-548.

Wang, T., Chen, Y.W., and Vailaya, A., **2000**, "Enantiomeric separation of some pharmaceutical intermediates and reversal of elution orders by high-performance liquid chromatography using cellulose and amylose tris(3,5-dimethylphenylcarbamate) derivatives as stationary phases", *Journal of Chromatography A*, 902: 345-355.

Wania, F., and Mackay, D., **1993**, "Global fractionation and cold condensation of low volatility organochlorine compounds in polar regions", *Ambio*, 22(*1*): 10-18.

Weistrand, C., and Norén, K., **1997**, "Methylsulfonyl metabolites of PCBs and DDE in Human Tissues", *Environmental Health Perspectives*, 105(*6*): 644-649.

Wells, D.E., Echarri, I., and McKenzie, C., **1995**, "Separation of planar organic contaminants by pyrenyl-silica high-performance liquid chromatography", *Journal of Chromatography A*, 718: 107-118.

Wenda, C., and Rajendran, A., **2009**, "Enantioseparation of flurbiprofen on amylose-derived chiral stationary phase by supercritical fluid chromatography", *Journal of Chromatography A*, 1216: 8750-8758.

Wiberg, K., Letcher, R., Sandau, C., Duffe, J., Norstrom, R., Haglund, P., and Bidleman, T., **1998**, "Enantioselective gas chromatography/mass spectrometry of methylsulfonyl PCBs with application to marine mammals", *Analytical Chemistry*, 70: 3845-3852.

Wilke, C.R., and Chang, P., **1955**, "Correlation of diffusion coefficients in dilute solutions", *A.I.Ch.E. Journal*, 1(*2*): 264-270.

Will, S., and Leipertz, A., **1997**, "Viscosity of liquid *n*-heptane by dynamic light scattering", *International Journal of Thermophysics*, 18(*6*): 1339-1354.

Wolf, C., **2005**, "Stereolabile chiral compounds: Analysis by dynamic chromatography and stopped-flow methods", *Chemical Society Reviews*, 34: 595-608.

Wong, C.S., Garrison, A.W., and Foreman, W.T., **2001**, "Enantiomeric composition of chiral polychlorinated biphenyl atropisomers in aquatic bed sediment", *Environmental Science & Technology*, 35: 33-39.

Yamada, M., Suga, M., Waki, I., Sakamoto, M., and Morita, M., **2005**, "Continuous monitoring of polychlorinated biphenyls in air using direct sampling APCI/ITMS", *International Journal of Mass Spectrometry*, 244: 65-71.

Yang, C., and Henion, J., **2002**, "Atmospheric pressure photoionization liquid chromatographic-mass spectrometric determination of idoxifene and its metabolites in human plasma", *Journal of Chromatography A*, 970: 155-165.

ZirChrom Separations, Inc., **2004**, *Reversed-Phase Method Development Guide*, Anoka, MN, USA.